



**University of
Leicester**

Opioids
and a
Neuro-Vascular-Immune Axis

John Parry Williams BSc (Hons), MBChB, FRCA

University Department of Cardiovascular Sciences
(Pharmacology and Therapeutics Group)
Division of Anaesthesia Critical Care & Pain Management
University Leicester

Thesis Submitted for the Degree of Doctor of Philosophy
July 2008

Opioids and a Neuro-vascular-immune Axis

John Parry Williams

Opioid-based agents represent the cornerstone of analgesia in modern clinical practice. Additionally however opioids produce a range of unwelcome side-effects including immunomodulation. It has been suggested that this immunomodulation may result either as a direct effect of opioids on circulating immune cells or via a central action. Meanwhile studies show that classical opioid receptors are up-regulated in peripheral inflammation, while endogenous opioids are released from circulating immune cells producing local analgesia. Expression of opioid receptors on immune cells however remains contentious.

This thesis has made a significant contribution to understanding the interaction between opioids and a neurovascular-immune axis by employing radioligand binding, flow cytometry and polymerase chain reaction techniques to make a systematic and detailed examination of the expression of the classical opioid receptors (MOP, DOP and KOP) and the non-classical opioid receptor (NOP) and the precursor for its endogenous ligand N/OFQ (ppN/OFQ) in the peripheral blood mononuclear cells (PBMCs) of healthy volunteers. Using these techniques we have shown (1) that naïve human PBMCs do not express classical opioid receptors, (2) that PCR techniques support the view that PBMCs do express gene transcripts for NOP and ppN/OFQ.

In an additional clinical study during a profound vascular insult we have used quantitative PCR and radioimmunoassay techniques to follow the expression of the opioid receptors and native N/OFQ throughout a septic episode in patients admitted to the intensive care unit (ICU). Here we report for the first time an elevation in plasma N/OFQ concentration in non-survivors of sepsis requiring ICU admission, 3.0 [2.5 – 5.0]pg ml⁻¹ in non-survivors *vs.* 1.0 [1.0 – 2.5]pg ml⁻¹ in survivors (p=0.028). Similarly we are first in reporting an elevation in plasma N/OFQ following major abdominal surgery in septic patients.

These findings lead us to suggest an amendment to the previously proposed neuroimmune axis to include the N/OFQ-NOP system.

Acknowledgements

I'd like to thank the following people who have helped me with support, in many differing ways, over the past six years.

Firstly, thank-you to the people from within the Division of Anaesthesia Critical Care and Pain Management; Tim Barnes, Stuart Gold, Chris Hebbes, Emma Johnson, Anton Leonard, Paul Maslowski, John McDonald, Ed Pallett, Jim Strupish and Jon Thompson who all provided invaluable help, advice and humour on a daily basis.

Many thanks to Tiago Duarte, for his tutoring and suggestions with PCR.

Tom Cote from the Uniformed Services University of the Health Sciences, Bethesda, MD, USA, who provided antibodies for fluorescent staining.

I'd also like to thank Manjinder and the rest of my family, for the patience and encouragement that they have shown during a very long "couple of weekends writing up".

Thanks are also due to the research staff of the University of Leicester, who have always greeted my inquiries and requests for assistance with interest, enthusiasm and help. Apologies to anyone I have forgotten.

Finally two people have been instrumental in making this project work, Prof. Rowbotham for making sure that it could happen and Prof. Lambert for making it happen, many thanks.

CONTENTS

List of Abbreviations	v
I. List of Figures	vii
II. List of Tables	xiii
III. Publications, presentations, prizes and grants	xiv
1. Introduction	1
1.1 The evolution of opioid analgesics	1
1.2 The classical physiology of pain transmission and opioid action	2
1.3 Opioid receptors and their endogenous ligands	7
1.4 Peripheral opioid receptors and the neuroimmune system	11
1.5 The NOP/NOFQ opioid system	17
1.6 Aims	18
2. Materials and Methods	20
2.1 Cell lines	20
2.1.1 Materials	20
2.1.2 Chinese hamster ovary cells	20
2.1.3 Leukaemic cell lines	21
2.1.4 Human neural cells	22
2.1.5 Venous blood/peripheral mononuclear cells	22
2.1.6 Stimulated upregulation of opioid receptor gene expression	24
2.2 Radioligand binding	25
2.2.1 Materials for radioligand binding	25
2.2.2 Saturation binding assays	26
2.2.3 Competition binding assays	31
2.2.4 GTP γ [³⁵ S] binding assays	33
2.3 Radioimmunoassay	37
2.3.1 Materials	37
2.3.2 N/OFQ radiimmunoassay	37
2.4 Immunofluorescent staining	39
2.4.1 Materials	39
2.4.2 Direct and confocal immunofluorescent staining	39
2.4.3 Flow cytometry	46
2.5 Polymerase chain reactions	52
2.5.1 Materials	52

2.5.2	Endpoint PCR	53
2.5.3	Quantitative PCR	64
2.6	Data Analysis	69
3.	MOP Receptor Expression in Peripheral Immune Cells	70
3.1	Background	70
3.2	Radioligand binding studies	72
3.2.1	Results: Saturation binding experiments	72
3.2.2	Results: Competition binding experiments	75
3.3	Fluorescent binding studies	77
3.3.1	Results: Fluorescent staining for direct and confocal microscopy	77
3.3.2	Results: Immunofluorescent staining for flow cytometry	79
3.3.3	Results: Fluorescent-naloxone staining for flow cytometry	83
3.4	Polymerase chain reaction	86
3.4.1	Results: Endpoint polymerase chain reactions	86
3.4.2	Results: Quantitative polymerase chain reactions	101
3.4.3	Results: Stimulated upregulation of MOP gene expression	103
3.5	Discussion	105
4.	DOP and KOP Receptor Expression in Peripheral Immune Cells	111
4.1	Background	111
4.2	Polymerase chain reaction	113
4.2.1	Results: DOP primers, Endpoint PCR	114
4.2.2	Results: DOP Primers, Quantitative PCR	120
4.2.3	Results: KOP Primers, Endpoint PCR	122
4.2.4	Results: KOP Primers, Quantitative PCR	127
4.3	Discussion	129
5.	NOP Receptor Expression in Peripheral Immune Cells	131
5.1	Background	131
5.2	Radioligand binding studies	133
5.2.1	Results: Saturation binding experiments	133
5.2.2	Results: GTP γ [³⁵ S] competitive binding assays	137
5.3	Polymerase chain reactions	139
5.3.1	Results: Endpoint PCR	141
5.3.2	Results: Quantitative PCR	149

5.4 Stimulated Upregulation of NOP Receptor Gene Expression	152
5.4.1 Results: Stimulated Expression of NOP	152
5.4 Discussion	154
6. Opioid Signalling in Peripheral Immune Cells During Sepsis	157
6.1 Background	157
6.2 Primer design and optimisation	160
6.2.1 Methods: Housekeeping Primer Optimisation	163
6.2.2 Results: Housekeeping Primer Optimisation	164
6.3 Patient selection and tissue collection	171
6.4 Plasma and RNA preparation from blood	174
6.4.1 RNA extraction	174
6.4.2 Plasma isolation and radioimmunoassay	175
6.5 Results	176
6.5.1 Patient characteristics	176
6.5.2 RNA expression	177
6.5.3 Quantitative PCR	181
6.5.4 Peptide radioimmunoassay	186
6.6 Discussion	190
7. Discussion	196
7.1 Summary of main findings	196
7.1.1 MOP receptor expression	196
7.1.2 DOP/KOP receptor expression	196
7.1.3 NOP receptor expression	197
7.1.4 Opioid signalling and sepsis	197
7.2 MOP receptor expression	198
7.3 DOP/KOP receptor expression	205
7.4 NOP receptor expression	207
7.5 Opioid signalling and sepsis	209
7.6 Concluding statement	211

Appendix I: Protein Assay	212
Appendix II: Ethics committee approval 7218: Investigation into the presence of opioid receptors on human immune cells before and after treatment <i>in vitro</i> with a variety of mediators of inflammation	213
Appendix III: Ethics committee approval 7233: Observational study of urotensin II levels in patients with severe sepsis	219
Appendix IV: Ethics committee amendment 7233	226
Bibliography	229

I List of Abbreviations

5-HT	5-Hydroxy Tryptamine (Serotonin)
ACTH	Adrenocorticotrophic Hormone
AIDS	Acquired Immune Deficiency Syndrome
APACHE II	Acute Physiology and Chronic Health Evaluation II
APC	Antigen Presenting Cell
ATP	Adenosine Triphosphate
BSA	Bovine Serum Albumin
cAMP	Cyclic Adenosine Monophosphate
CD	Cluster of Differentiation
cDNA	complimentary Deoxyribonucleic Acid
cGMP	Cyclic Guanosine Monophosphate
CHO	Chinese Hamster Ovary
CNS	Central Nervous System
CRH	Corticotrophin Releasing Hormone
CVS	Cardiovascular System
DEPC	Diethylpyrocarbonate
DNA	Deoxyribonucleic Acid
dNTP	Deoxyribonucleotide Triphosphate
DOP	Delta opioid receptor
dpm	Disintegrations Per Minute
DTT	Dithiothreitol
EDTA	Ethylenediaminetetraacetic acid
EGTA	Ethyleneglycol-bis(2-aminoethylether)-N,N,N',N'-tetraacetic Acid
FACS	Fluorescence Activated Cell Sorting
FBS	Fetal Bovine Serum
FCS	Fetal Calf Serum
FITC	Fluorescein Isothiocyanate
GABA	γ -aminobutyric Acid
GCS	Glasgow Coma Scale
gDNA	genomic Deoxyribonucleic Acid
GDP	Guanosine Diphosphate
GTP	Guanosine Triphosphate
GTP γ S	Guanosine 5' $[\gamma$ -thio]triphosphate
HEPES	N-(2-Hydroxyethyl)piperazine-N'-(2-ethanesulphonic acid)
HPA	Hypothalamic-Pituitary-Adrenal axis
i.c.v	intracerebroventricularly
ICAM-1	Intercellular Adhesion Molecule-1
IgG	Immunoglobulin G
IQR	Inter Quartile Range
IUPHAR	International Union of Pharmacology
KOP	Kappa opioid receptor
LC	Locus Ceruleus
MACS	Magnetic Activated Cell Sorting

MEM	Minimal Essential Medium
MFI	Mean Fluorescence Intensity
MOFS	Multiple Organ Failure Syndrome
MOP	Mu opioid receptor
MOPS	3-(N-Morpholino)-propanesulfonic acid
mRNA	messenger Ribonucleic Acid
MuLV	Murine Leukaemia Virus
N/OFQ	Nociceptin/Orphanin FQ
NMDA	N-Methyl-D-Aspartate
NO	Nitric Oxide
NOP	Nociceptin opioid receptor
NRM	Nucleus Raphe Magnus
NRPG	Nucleus Reticularis Paragigantocellularis
NSB	Non-Specific Binding
OP1	Delta opioid receptor
OP2	Kappa opioid receptor
OP3	Mu opioid receptor
ORL ₁	Opioid Like Receptor-1
PAG	Periaqueductal Grey
PBMC	Peripheral Blood Mononuclear Cell
PBS	Phosphate Buffered Saline
PCR	Polymerase Chain Reaction
PEI	Polyethylenimine
POMC	Proopiomelanocortin
QPCR	Quantitative Polymerase Change Reaction
RIA	Radioimmuno Assay
RNA	Ribonucleic Acid
RPMI	Roswell Park Memorial Institute media
rRNA	ribosomal Ribonucleic Acid
SEM	Standard Error of the Mean
SG	Substantia Gelatinosa
SIRS	Systemic Inflammatory Response Syndrome
SOFA	Sequential Organ Failure Assessment
TAE	Tris-acetate-EDTA
Taq	Thermus Aquaticus
TFA	Trifluoroacetic Acid
TNF- α	Tumour Necrosis Factor- α
Tris-HCl	Tris(hydroxymethyl)aminomethane Hydrochloride

II List of Figures

Figure 1.1 Laminae of the dorsal horn with areas and associated nerve fibres listed	3
Figure 1.2 Ascending pain pathway	4
Figure 1.3 Gate control by descending inhibitory fibres	4
Figure 1.4 Descending inhibitory pathways	6
Figure 1.5. Effect of opioid agonist/receptor coupling on G-protein	9
Figure 1.6 A schematic drawing showing N/OFQ modulation of nociceptive transmission	10
Figure 1.7 Mechanism of the peripheral action of endogenous opioids on peripheral receptors	13
Figure 1.8 Possible immunological sites of opioid action	16
Figure 2.1 Isolation of peripheral blood mononuclear cells from blood	24
Figure 2.2 The Langmuir absorption isotherm	27
Figure 2.3 Isotherm plots for total and non-specific binding	28
Figure 2.4 Semi-logarithmic plot of log drug concentration vs. specific binding	29
Figure 2.5 G-protein coupled receptor and intracellular events following agonist binding	34
Figure 2.6 Semi-logarithmic dose response curve expected when log [ligand] is plotted against stimulation factor	35
Figure 2.7 Excitation emission spectra for a fluorochrome	41
Figure 2.8 Schematic of the arrangement for a direct fluorescence microscope	42
Figure 2.9 Region of the MOP receptor to which primary antibodies bind	44
Figure 2.10 Schematic of a flow cytometer	47
Figure 2.11 Flow cytometer gating I	48
Figure 2.12 Flow cytometer gating II	48
Figure 2.13 Flow cytometer gating III	49
Figure 2.14 Diagram of region of primer amplification	54
Figure 2.15 Amplification steps in polymerase chain reaction amplification of an initial template	55
Figure 2.16 Typical 3% agarose PCR gel stained with ethidium bromide	56
Figure 2.17 Graph showing the correlation between weight of the amplicon and distance moved through a 3% agarose gel	57
Figure 2.18 Diagram of primer binding to template DNA across an intron	58
Figure 2.19 Schematic showing the process of amplification and probe cleavage during QPCR with a <i>TaqMan</i> [®] probe system	65
Figure 2.20 Schematic showing the different number of cycles required to be completed before fluorescence rises above the detection threshold	66
Figure 3.1 Saturation Binding of [³ H]-Diprenorphine to CHO _{hMOP} cells	72
Figure 3.2 Saturation Binding of [³ H]-Diprenorphine to L1210 (mouse thymoma cells) cells	73
Figure 3.3 Saturation Binding of [³ H]-Diprenorphine to CEMx174 cells	

(B/T lymphocyte cell hybridoma)	73
Figure 3.4 Saturation Binding of [³ H]-Diprenorphine to Raji cells (human B-lymphocytic cell line)	74
Figure 3.5 Saturation Binding of [³ H]-Diprenorphine to peripheral blood mononuclear cells	74
Figure 3.6 Mean of competition displacement assays of [³ H]-diprenorphine with CHO _{hMOP} cells by naloxone and fluorescent-naloxone	76
Figure 3.7 Confocal image image of immunofluorescent staining of CHO _{hMOP} cells with primary NHQLENLEAETAPLP and Secondary FITC	78
Figure 3.8 Staining of CHO _{hMOP} cells with FITC secondary alone	78
Figure 3.9 Confocal image of immunofluorescent staining of peripheral blood mononuclear cells with primary NHQLENLEAETAPLP and Secondary FITC	78
Figure 3.10 Staining of PBMC's with FITC secondary alone	78
Figure 3.11 Confocal image of immunofluorescent staining of CHO _{hMOP} cells with primary VIAKALITIPETTFQ and Secondary FITC	79
Figure 3.12 Staining of CHO _{hMOP} cells with FITC secondary alone	79
Figure 3.13 Confocal image of immunofluorescent staining of PBMC's with primary VIAKALITIPETTFQ and Secondary	79
Figure 3.14 Staining of peripheral blood mononuclear cells with FITC secondary alone	79
Figure 3.15 Mean Fluorescent Intensity shift for CHO _{hMOP} cells with PBS primary FITC 1:250 secondary	80
Figure 3.16 MFI shift for CHO _{hMOP} cells, with NHQLENLEAETAPLP primary 1:200 and FITC secondary 1:250	80
Figure 3.17 MFI shift for CHO _{hMOP} cells with VIAKALITIPETTFQ primary 1:200 primary and FITC 1:250 secondary	80
Figure 3.18 MFI shift for CHO _{hMOP} cells, with normal rabbit serum primary 1:200 and FITC secondary 1:250	80
Figure 3.19 MFI shift for Jurkat cells with NHQLENLEAETAPLP primary 1:200 and FITC 1:250 secondary	81
Figure 3.20 MFI shift for Jurkat cells, with normal rabbit serum primary 1:200 and FITC secondary 1:250	81
Figure 3.21 MFI shift for CHO _{hMOP} with IgG primary 1:200 and FITC 1:250 secondary	81
Figure 3.22 MFI shift for CHO _{hMOP} cells, with 1414 primary 1:200 and FITC secondary 1:250	81
Figure 3.23 MFI shift for CHO _{hMOP} with 1414 primary 1:200 GST-C50 blocking agent and FITC 1:250 secondary	81
Figure 3.24 MFI shift for PBMC's with 1414 primary 1:200 and FITC 1:250 secondary	82
Figure 3.25 MFI shift for PBMC's, with IgG primary 1:200 and FITC secondary 1:250	82
Figure 3.26 MFI shift for CHO _{hMOP} cells with 1404 primary 1:200 and FITC 1:250 secondary	82

Figure 3.27 MFI shift for CHO _{hMOP} cells, with IgG primary 1:200 and FITC secondary 1:250	82
Figure 3.28 MFI shift for CHO _{hMOP} cells with PBS alone	84
Figure 3.29 MFI shift for CHO _{hMOP} cells, fluorescent-naloxone staining 3 X 10 ⁻⁶ M	84
Figure 3.30 MFI shift for PBMC cells with fluorescent-naloxone at low concentration 1 X 10 ⁻¹⁰ M alone	84
Figure 3.31 MFI shift for PBMC cells with fluorescent-naloxone at high concentration 1 X 10 ⁻⁷ M alone	84
Figure 3.32 Semi-logarithmic plot of normalised MFI shift for CHO _{hMOP} cells with fluorescent-naloxone concentration	85
Figure 3.33 Position of primer pairs MOP1, MOP2 and MOP3 on the gDNA sequence	87
Figure 3.34 Position of MOP1 primer pairs on the gDNA sequence, expected position of MOP3 primer pairing on cDNA and the position of MOP 3+1 primer pairs on gDNA	88
Figure 3.35 Annealing gradient for MOP1 primers used with cDNA from CHO _{hMOP} cells	89
Figure 3.36 PCR gel for venous blood and CEM x 174 gDNA with MOP1 primers	90
Figure 3.37 PCR gel for CEM x 174 gDNA with MOP1 and MOP2 primers	92
Figure 3.38 PCR gel for MOP2 primers with a variety of templates	92
Figure 3.39 PCR gel for MOP2 primers with Raji cDNA templates	93
Figure 3.40 PCR gel for MOP2 primers with SHSY5Y and CHO _{hMOP} as template	93
Figure 3.41 Annealing gradient for MOP3 primers used with cDNA and gDNA SH-SY5Y I	94
Figure 3.42 Annealing gradient for MOP3 primers used with cDNA and gDNA SH-SY5Y II	95
Figure 3.43 Annealing gradient for MOP3+1 primers used with cDNA from SH-SY5Y	96
Figure 3.44 PCR gel for MOP3+1 primers with SH-SY5Y gDNA and cDNA as template	97
Figure 3.45 PCR gel for MOP3+1 primers with SH-SY5Y cDNA as template reverse transcribed (RT+) and non-reverse transcribed (RT-)	98
Figure 3.46 PCR gel for MOP3+1 primers with a variety of different templates both reverse transcribed (RT+) and non-reverse transcribed (RT-)	99
Figure 3.47 PCR from two gels for MOP3+1 primers cDNA from the PBMC's of ten healthy male volunteers	100
Figure 3.48 RNA integrity gel for the RNA extracted from the PBMCs of 10 healthy volunteers	100
Figure 3.49 QPCR using <i>TaqMan</i> ® Gene expression assay for MOP receptor with cDNA from whole venous blood with CHO _{hMOP} cells as positive control	101
Figure 3.50 QPCR using <i>TaqMan</i> ® Gene expression assay for MOP receptor with cDNA from PBMCs with CHO _{hMOP} cells as positive control curve	102
Figure 3.51 PCR gel for MOP2 primers with cDNA from Raji cells TNF treated and not treated	103
Figure 3.52. Survival of U937 cells treated and not treated with 30 pg/ml of TNF α and 1 μ g of cycloheximide after twenty-four hours	104
Figure 3.53 PCR gel analysis I from <i>Kraus et al (2003) Mol Pharmacol 64: 876-84</i>	109

Figure 3.54 PCR gel analysis II from <i>Kraus et al (2003) Mol Pharmacol 64: 876-84</i>	109
Figure 4.1 PCR Annealing gradient for DOP1 primers with cDNA from CHO _{hDOP} cells	115
Figure 4.2 PCR Annealing gradient for DOP1 primers with gDNA from venous blood cells	116
Figure 4.3 PCR Annealing gradient for DOP1 primers with gDNA CEMx174 cells	116
Figure 4.4 PCR Annealing gradient for DOP2 primers with cDNA from CHO _{hDOP} cells	117
Figure 4.5 PCR gel analysis DOP2 primers with cDNA from Raji cells or CHO _{hDOP}	118
Figure 4.6 PCR gel analysis DOP2 primers with cDNA from PBMCs or CHO _{hDOP}	119
Figure 4.7 PCR gel analysis DOP2 primers with cDNA from whole venous blood or CHO _{hDOP}	119
Figure 4.8 QPCR using <i>TaqMan</i> [®] Gene expression assay for DOP, cDNA from CHO _{hDOP} cells and from PBMCs	120
Figure 4.9 QPCR using <i>TaqMan</i> [®] Gene expression assay for DOP, cDNA from CHO _{hDOP} cells and from whole venous blood	121
Figure 4.10 PCR Annealing gradient for KOP1 primers with cDNA from CHO _{hKOP} cells	123
Figure 4.11 PCR Annealing gradient for KOP2 primers with cDNA from CHO _{hKOP} cells	124
Figure 4.12 PCR gel analysis KOP2 primers with cDNA from Raji cells and CHO _{hKOP}	125
Figure 4.13 PCR gel analysis KOP2 primers, cDNA from PBMCs and CHO _{hKOP}	125
Figure 4.14 PCR gel analysis KOP2 primers with cDNA from venous blood and CHO _{hKOP}	126
Figure 4.15 QPCR using <i>TaqMan</i> [®] Gene expression assay for KOP receptor with cDNA from CHO _{hKOP} cells and PBMCs	127
Figure 4.16 QPCR using <i>TaqMan</i> [®] Gene expression assay for KOP receptor with cDNA from CHO _{hKOP} cells and whole blood	128
Figure 5.1 Binding of ³ H-N/OFQ to CHO _{hNOP} cells	133
Figure 5.2 Semi-logarithmic plot ³ H-N/OFQ vs specific binding in CHO _{hNOP} cells	134
Figure 5.3 ³ H-N/OFQ vs radioactive decay expressed as mass of protein in PBMCs	135
Figure 5.4 Log [³ H-N/OFQ] vs DPM specific binding in PBMCs and CHO _{hNOP}	135
Figure 5.5 Log [³ H-N/OFQ] vs radioactive decay expressed as binding per mass of protein in Raji cells	136
Figure 5.8 Semi-logarithmic plot log [N/OFQ] vs stimulation factor in CHO _{hNOP} cells	137
Figure 5.9 Semi-logarithmic plot log [N/OFQ] vs DPM in Raji cells, GTP γ [³⁵ S] binding assay	138
Figure 5.10 Semi-logarithmic plot log [N/OFQ] vs DPM in PBMCs cells, GTP γ [³⁵ S] binding assay	138
Figure 5.11 PCR Annealing gradient for NOPR1 receptor primers using cDNA from PBMCs	141
Figure 5.12 PCR Annealing gradient for NOPP1, cDNA from PBMCs	142
Figure 5.13 PCR Annealing gradient for NOPP2, cDNA from venous blood	142
Figure 5.14 PCR gel analysis NOP1 primers with cDNA from SH-SY5Y cells	143
Figure 5.15 PCR gel analysis NOP1 primers with cDNA from Raji and CHO _{hNOP} cells	144
Figure 5.16 PCR gel analysis NOP1 primers cDNA from PBMCs ten healthy volunteers	145

Figure 5.17 PCR gel analysis NOP1 primers with cDNA from the venous blood of five healthy volunteers and SH-SY5Y cells	146
Figure 5.18 PCR gel analysis NOPP1, with cDNA from the PBMCs of ten healthy volunteers	147
Figure 5.19 PCR gel analysis NOPP1 primers with cDNA from PBMCs of six healthy volunteers and Raji cells	147
Figure 5.20 PCR gel analysis NOPP1 primers with cDNA from Raji and SHSY5Y cells	148
Figure 5.21 QPCR using <i>TaqMan</i> [®] Gene expression assay for NOP receptor with cDNA from SH-SY5Y cells and from PBMCs	149
Figure 5.22 QPCR using <i>TaqMan</i> [®] Gene expression assay for NOP receptor with cDNA from SH-SY5Y cells and from venous blood	150
Figure 5.23 QPCR using SYBR green for NOP peptide (NOPP2) with cDNA from PBMCs	151
Figure 5.24 PCR gel analysis NOP1 primers with cDNA Raji, SH-SY5Y cells and CEM gDNA with and without TNF- α	153
Figure 6.1 PCR Annealing gradient for B2M primers with cDNA from whole venous blood	164
Figure 6.2 PCR Annealing gradient for EF1A primers, cDNA from whole venous blood	165
Figure 6.3 PCR Annealing gradient for PPIB primers with cDNA from whole venous blood	165
Figure 6.4 PCR Annealing gradient for UBC primers, cDNA from whole venous blood	166
Figure 6.5 PCR Annealing gradient for YWHAZ primers, cDNA from whole venous blood	166
Figure 6.6 PCR Annealing gradient for NOPP2 primers with cDNA from whole venous blood	167
Figure 6.7 QPCR C _t values for a range of forward and reverse primer concentration combinations between 100nM and 300nM for four target genes	168
Figure 6.8 QPCR Dissociation curves for B2M, EF1A, HPRT, PPIB, YWHAZ and NOPP2	169
Figure 6.9 RNA extracted from whole septic blood before and after DNA eradication	177
Figure 6.10 Correlation of RNA extracted from septic white cells and total white cell count	178
Figure 6.11 RNA integrity bands for RNA extracted from septic blood samples	179
Figure 6.12 RNA integrity gel for the RNA extracted from the PBMCs of 10 healthy volunteers	180
Figure 6.13 QPCR plot for two control samples SH-SY5Y and septic blood cDNA with B2M primers	182
Figure 6.14 QPCR plot for two control samples SH-SY5Y and septic blood cDNA with EF1A primers	182
Figure 6.15 QPCR plot for two control samples SH-SY5Y and septic blood cDNA with YWHAZ primers	183
Figure 6.16 QPCR plot for two control samples CHO _{DOP} cDNA and septic blood cDNA with DOP primers	184
Figure 6.17 QPCR plot for two control samples CHO _{KOP} cDNA and septic blood cDNA with KOP primers	184
Figure 6.18 QPCR plot for two control samples SH-SY5Y and septic blood cDNA	

with MOP primers	185
Figure 6.19 QPCR plot for two control samples SH-SY5Y and septic blood cDNA	
with NOP primers	185
Figure 6.20 Standard curve for radioimmuno assay with N/OFQ peptide	186
Figure 6.21 Plasma N/OFQ concentrations in critically ill patients with SIRS	
on admission to the intensive care unit	189
Figure 6.22 Plasma N/OFQ concentrations in major gastrointestinal post-operative patients	
and non-postoperative patients on admission to the intensive care unit	189
Figure 7.1 Opioid action on the HPA	200
Figure 7.2 Mechanism of the peripheral action of endogenous opioids on peripheral receptors	202
Figure 7.3 Mechanism hapten initiation of an immune response	204

III List of Tables

Table 1.1 Names given to the three classical opioid receptors	7
Table 1.2 The four opioid receptors and the endogenous opioid ligands acting upon them	10
Table 2.1 Components of Saturation Binding Assay	31
Table 2.2 Components of Competition Binding Assay	33
Table 2.3 Components of GTP γ [³⁵ S] Binding Assay	36
Table 2.4 Components of radioimmunoassay for N/OFQ peptide	38
Table 2.5 Position, homology to human amino acid sequence of MOP receptor and position of binding of primary antibodies	43
Table 2.6 Components required for polymerase chain reaction	62
Table 2.7 Components used for QPCR with <i>Taqman</i> [®] probes	68
Table 2.8 Components used for QPCR with SYBR green probes	68
Table 3.1 Summary of presence of MOP receptor, using a MOP agonist by cell type with radioligand binding	75
Table 3.2 Calculated pK _i values for naloxone and fluorescent-naloxone	76
Table 3.3 Summary of fluorescent binding to a variety of cell types	83
Table 3.4 Primer pairings used in standard gel based PCR for MOP transcripts	88
Table 4.1 Primer pairings used in standard gel based PCR for DOP transcripts	114
Table 4.2 Primer pairings used in standard gel based PCR for KOP transcripts	122
Table 5.1 Primer pairings used in standard gel based PCR for NOP and prepronociceptin transcripts	140
Table 5.2 Calculated nociceptin receptor and prepronociceptin primer pair combinations optimized annealing temperatures and amplicon sizes	143
Table 6.1 Primer pairings used in quantitative PCR for housekeeping gene transcripts	162
Table 6.2 Housekeeping genes and their functions	162
Table 6.3 Amplification efficiency for housekeeping gene primer pairs with amplification linearity	170
Table 6.4 SOFA scores for physiological parameters	173
Table 6.5 Characteristics of patients admitted to ITU with sepsis	176
Table 6.6 Correlations of N/OFQ concentration with markers of illness severity on day 1 ITU	187
Table 6.7 Plasma concentrations of N/OFQ measured serially in critically ill patients with SIRS	187
Table 6.8 Mode of death of patients who died in hospital within 30 days of admission to the intensive care unit	188

IV Publications, presentations, prizes and grants arising from this thesis

Full papers

1. **Williams JP**, Thompson JP, McDonald J, Barnes TA, Cote T, Rowbotham DJ, Lambert DG. (2007) Human peripheral blood mononuclear cells express nociceptin/orphanin FQ, but not mu, delta, or kappa opioid receptors. *Anesthesia Analgesia*. Oct;105(4):998-1005
2. **Williams JP**, Thompson JP, Rowbotham DJ, Lambert DG (2008) Human peripheral blood mononuclear cells produce pre-pro-nociceptin/orphanin FQ mRNA. *Anesthesia and Analgesia*. Mar;106(3):865-6
3. **Williams JP**, Thompson JP, Young S, Gold S, McDonald J, Rowbotham DJ, Lambert DG. (2008) Nociceptin and urotensin-II concentrations in critically ill patients with sepsis. *British Journal of Anaesthesia*. 100:810-4.

Reviews/Editorials

1. Lambert DG, **Williams JP**, and Thompson JP (2007) Opioids and the neuroimmune axis. *Hirosaki Medical Journal* 59:(suppl) S109-S118
2. **Williams JP**, Lambert DG. (2005) Opioids and the neuroimmune axis. *Br J Anaesth*. 94:3-6
3. **Williams JP**.(2008) Basic opioid pharmacology. *Reviews in Pain BPS*.1(2):2-5.

Abstracts

1. **Williams JP**. Cote TE. Thompson J. Rowbotham DJ. Lambert DG. (2004) Do Peripheral Blood Mononuclear Cells Express MOP Receptors? A Preliminary Study. *Anaesthetic Research Society Meeting Aberdeen April 2004*
2. **Williams JP**, McDonald J, Thompson J, Rowbotham DJ and Lambert DG. (2005) Human peripheral blood mononuclear cells express the mRNA encoding for the nociceptin peptide and its receptor. *Anaesthetic Research Society Meeting Leicester Nov. 2005*
3. **Williams JP**, Gold SJ, McDonald J, Young SP, Thompson J and Lambert DG. (2006) Does nociceptin peptide concentration change during the course of a critical episode? *Anaesthetic Research Society Meeting Dundee 2006*

Presentations

1. **Williams JP.** Opioid receptors and peripheral blood mononuclear cells. *Leicester-Ferrara collaboration meeting.* Leicester (2005)

Prizes

1. Winner of the Anaesthetic Research Society prize 2003/2004 for:
Williams JP. Cote TE. Thompson J. Rowbotham DJ. Lambert DG. (2004) Do Peripheral Blood Mononuclear Cells Express MOP Receptors? A Preliminary Study. *Anaesthetic Research Society Meeting* Aberdeen April 2004
2. Winner of the Royal College of Anaesthetists Jubilee Medal 2003/2004 for:
Williams JP. Cote TE. Thompson J. Rowbotham DJ. Lambert DG. (2004) Do Peripheral Blood Mononuclear Cells Express MOP Receptors? A Preliminary Study. *Anaesthetic Research Society Meeting* Aberdeen April 2004

Grants

1. **Dr JP Williams,** Prof DG Lambert and Dr JP Thompson £9,196 Investigation into changes in endogenous opiates and receptors on PBMC during the course of a septic episode. *British Journal of Anaesthesia/Royal College of Anaesthetists Research Grant* 2004

Chapter 1:

Introduction

1.1 The evolution of opioid analgesics.

Opioid based analgesic agents have in one form or another been used by man to control pain for thousands of years. Of these preparations morphine is now considered the archetypal opioid analgesic to which all other painkillers are compared. During the last century considerable progress has been made into understanding the mechanism and sites of action of opioids. This has led to the availability of newer opioid analgesics possessing a range of different pharmacodynamic and -kinetic profiles to morphine (*Eguchi 2004*). Despite this evolution in drug design, improved understanding of opioid pharmacology and an increased knowledge of endogenous opioid physiology, the exact impact of exogenous opioids and much of the pharmacology of endogenous opioid ligand/receptor systems remains unclear. In tandem with this adequate pain control remains difficult for some patients in clinical practice, which may be compounded by the adverse effects of opioids including tolerance (*Collett 1998, 2001*) and dependence (*Borgland 2001, Harrison et al 1998*). Additionally, though scientific research has led to an appreciation of the mechanisms of action of opioids in neural tissue (mainly of central origin), little is known about the peripheral effects and distribution of endogenous opioids and their receptors, or the effect endogenous and exogenous opioids may have upon these systems. In particular our understanding of the effect of opioid action and immune cell function has been limited, with only recently an appreciation of the link between pain and the immune system being realised (*Bidlack 2000, Brack et al 2003, Cabot et al 2001, Fiset et al 2003 & 2004, Mousa et al 2004*). It now seems clear that opioids exert some form of immunomodulatory action within man. A wealth of scientific evidence supports this view, opioid medications have deleterious effects upon the immune function of some of the patients to which they are given (*Manfredi et al 1993, McCarthy et al 2001b, Mellon et al 1999, Morgan 1996, Roy et al 2001, Yeager et al 1995*) and it seems that endogenous opioid delivery is, at least partially, controlled by immunocompetent cells (*Jessop et al 2002, Mousa et al 2004, Rittner et al 2001, Stefano et al 1998*). This data comes from studies on both patient populations, and also from *in vitro* and *in vivo* laboratory experiments.

1.2 The classical physiology of pain transmission and opioid action.

In order to treat pain effectively in a clinical setting and appreciate the action of opioids it is first necessary to have a degree of understanding of the physiology of pain transmission and opioid action. The experience of pain is usually associated with the initial stimulation of naked nerve endings attached to small diameter primary afferent peripheral nerve fibres (primary afferent neurones), by mechano-thermal or more commonly chemical stimuli (e.g. the long-lived pain following thermal burns is chemically stimulated). Information is then conveyed from the periphery to the CNS via two types of nociceptive nerve fibres designated A- δ and C. A- δ fibres are 2-5 μm diameter myelinated fibres, which respond primarily to mechanical stimuli (high threshold mechanoreceptors **Figure 1.1**) and transmit impulses at a rate of 4-30 m.s^{-1} to the dorsal horn of the spinal cord. They synapse mainly in lamina I and V of the dorsal horn and are responsible for producing sharp, well-defined pain. C fibres are 0.4-1.2 μm diameter unmyelinated fibres (polymodal nociceptors) with a conduction velocity of 0.5 - 2.5 m.s^{-1} (*Despopoulos & Silbernagl 2003*). These fibres respond to chemical, mechanical and thermal stimuli, synapse in lamina I and II of the dorsal horn and are responsible for producing pain, which is dull and poorly localised. Chemical stimulation of polymodal nociceptors is caused by the release of a number of pro-algesic mediators, (5-HT, ATP, potassium ions, prostaglandins, kinins, and leucotrienes), which activate local mechanisms and facilitate transmission through the primary afferent neuron (*Berne & Levy 1996, Ganong 2005*).

In the dorsal horn, primary afferent neurones synapse with dorsal horn neurones. Many of these neurones then ascend in the antero-lateral side of the cord as the spinothalamic tract following decussation at the corresponding segment of the spinal cord. Most pass through the brain stem to the thalamus, and then relay to three cortical areas, somatosensory areas I and II and the cingulate gyrus, where the impulses are recognised as painful **Figure 1.2**. (*Ganong 2005*).

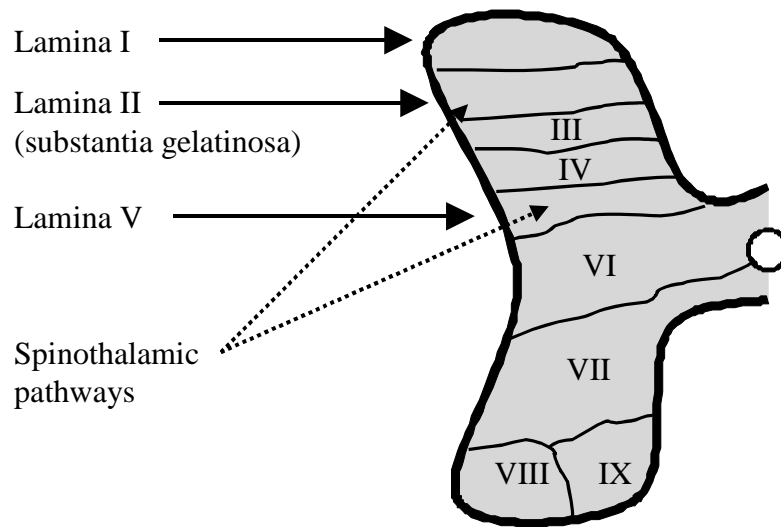


Figure 1.1

Laminae of the dorsal horn with areas and associated nerve fibres listed (*Adapted from Ganong 2005*).

- C and A δ -fibres terminate mainly in the superficial laminae (I & II) of the dorsal horn
- Some terminate deeper, laminae V
- In laminae I and V they synapse with 2nd order nociceptive afferents
- In lamina II they synapse onto cell bodies of inhibitory interneurons
- Inhibitory interneurons act to inhibit transmission between primary and 2nd order nociceptive afferents
- Both noxious and non-noxious primary afferents synapse onto the cell bodies of the substantia gelatinosa

Descending inhibitory control and the activation of A β mechanoreceptors as they pass through the dorsal horn may modulate nociceptive impulses **Figure 1.3**. This is achieved via increased activity within the inhibitory neurones of the substantia gelatinosa (lamina II of the dorsal horn), which is in turn caused by the activation of the neuronal pathways mentioned above. Melzak originally proposed this “gate control” of pain in 1965 (*Melzak et al 1965*).

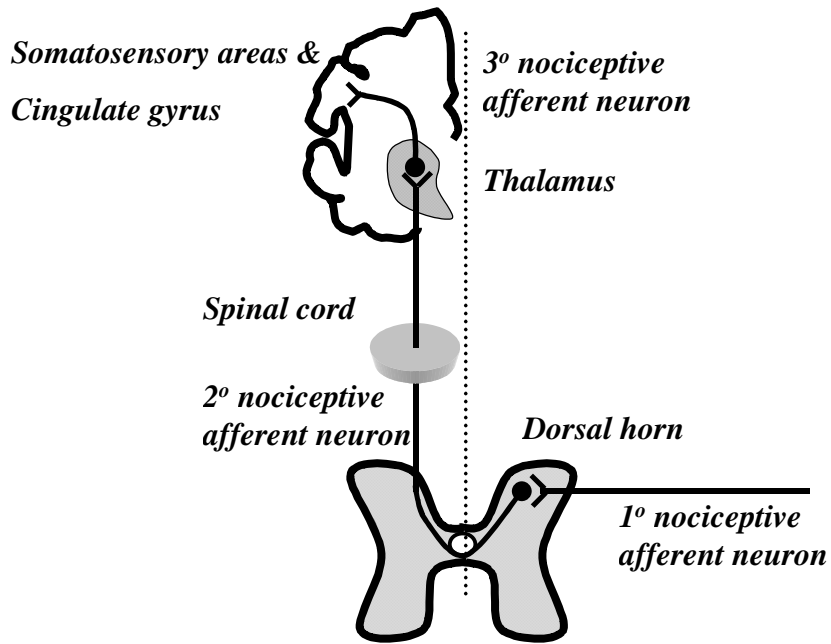


Figure 1.2
Ascending pain pathway, showing primary, secondary and tertiary nociceptive afferents finally synapsing in the cortex.

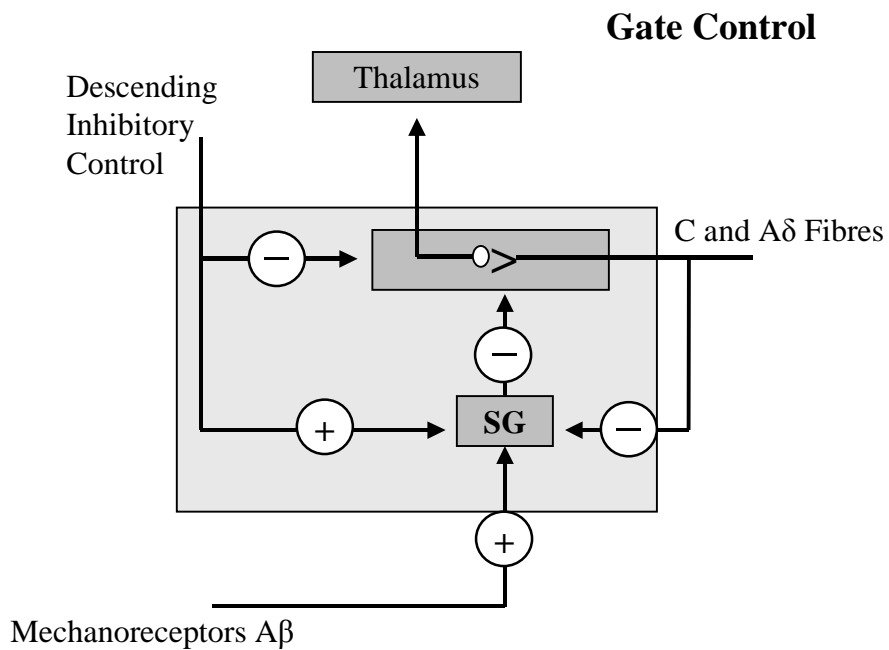


Figure 1.3
Gate control by descending inhibitory fibres and A β mechanoreceptors acts to inhibit nociceptive transmission by an excitatory action on inhibitory neurones in the substantia gelatinosa (SG) (Adapted from Rang et al 2007).

Pain sensation is modified physiologically in a number of ways. Tissue damage leads to a decrease in local pH and changes in nociceptor function, which then amplify

transmission of painful impulses to the spinal cord (primary hyperalgesia). This also permits previously non-noxious stimuli to be perceived as painful (allodynia) and causes reflex release of 5-HT, histamine and substance P leading to widening of the receptive field, so that impulses from adjacent non-injured tissue are perceived as painful (secondary hyperalgesia). Repeated transmission of noxious impulses to the spinal cord increases its responsiveness to further noxious stimuli (the wind-up phenomenon) and facilitates transmission of pain signals to the brain (*Jensen et al 2003*). Neurotransmitters involved in these phenomena include glutamate, N-methyl-D-aspartate (NMDA), kinins and substance P. If allowed to persist, permanent changes in spinal cord neurones and impulse transmission occur (long-term potentiation) to exacerbate pain sensation (*Jensen et al 2003, Loeser et al 2001*).

A number of descending impulses inhibit transmission through lamina II of dorsal horn (the substantia gelatinosa) (**Figure 1.4**), including stimulation of large diameter afferent fibres and descending pathways from the periaqueductal grey area via the nucleus raphe magnus. These are affected by opioid ligands and by α_2 adrenergic pathways through the locus ceruleus (LC). In particular, the substantia gelatinosa and periaqueductal grey are rich in endogenous opioids (β -endorphins and enkephalins) and opioid receptors. Structures shaded grey within **Figure 1.4** contain opioid receptors and ligands (*Rang et al 2007*).

While both exogenous and endogenous opioids can exert a direct inhibitory effect upon the substantia gelatinosa and peripheral nociceptive afferent neurones, which reduces nociceptive transmission from the periphery, they may also act indirectly by stimulating descending inhibitory pathways via their excitatory action on neurones within the periaqueductal grey (PAG) and nucleus reticularis paragigantocellularis (NRPG). Stimulation of these inhibitory neurones leads to greater neuronal traffic through the nucleus raphe magnus (NRM) increasing stimulation of 5-HT and enkephalin containing neurons which connect directly with the substantia gelatinosa of the dorsal horn, resulting in a reduction in nociceptive transmission from the periphery to the thalamus. These mechanisms result in the analgesic effects commonly seen following the administration of opioid analgesic agents (*Rang et al 2007*).

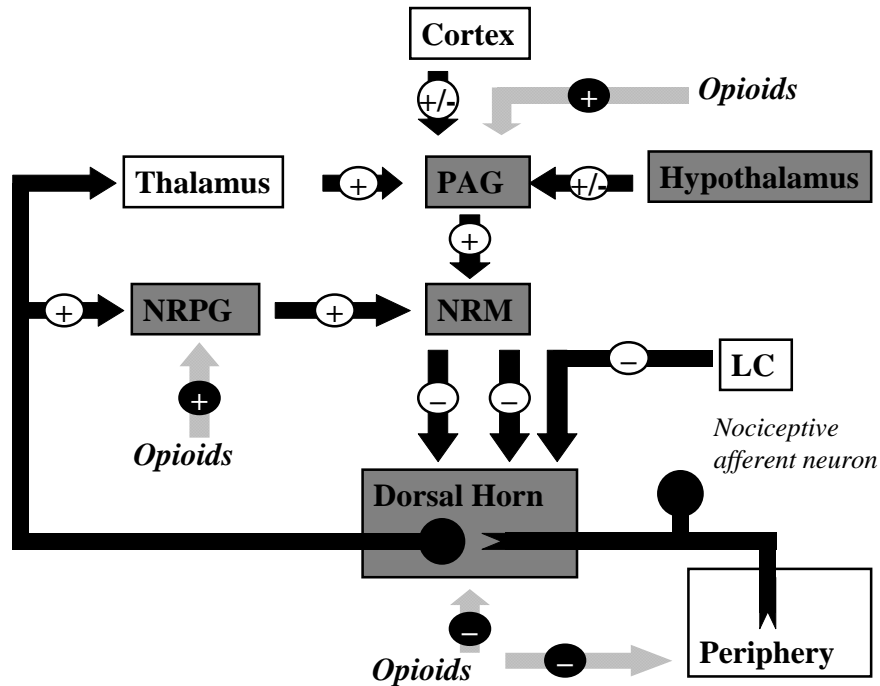


Figure 1.4

Descending inhibitory pathways. Areas in grey show the sites of action of endogenous and exogenous opioid (Adapted from Rang *et al* 2007).

PAG = Periaqueductal grey

NRPG = Nucleus reticularis
paragigantocellularis

NRM = nucleus raphe magnus

LC = Locus ceruleus

The complexity of pain physiology means that it can be treated using a number of different strategies. For example non-steroidal anti-inflammatory agents reduce pain produced locally at the site of injury by limiting the production of prostaglandins from arachidonic acid by the enzyme cyclo-oxygenase, while local anaesthetic agents can be used to stop transmission from peripheral afferent fibres by preventing voltage-dependent increases in sodium ion conductance (Calvey & Williams 1997). Local anaesthetic agents may be administered via a variety of routes (from subcutaneous infiltration to nerve, plexus, epidural and/or spinal blockade). Conversely opioids produce centrally-mediated analgesia by actions at spinal and supraspinal CNS opioid receptors, but may also act at peripheral opioid receptors (Stein *et al* 2000 & 2003). Several other agents have also been used in clinical practice (e.g. clonidine, ketamine, tricyclic antidepressants etc) for their analgesic properties, and may be useful as adjunctive therapy or in particular scenarios as they act at specific sites within the pain pathway (Jensen *et al* 2003). However of these, opioid-based agents, and morphine in particular, are considered to be the mainstay of analgesic therapy.

1.3 Opioid receptors and their endogenous ligands.

Both endogenous and exogenous opioid ligands act upon opioid receptors of which there are classically three subtypes. These receptors are all G-protein coupled, and were originally named mu (after morphine its most commonly recognised exogenous ligand), delta (after vas deferens the tissue within which it was first isolated) and kappa (after the first ligand to act at this receptor ketocyclazocine). In 1996 the International Union of Pharmacology (IUPHAR) renamed the receptors OP1 (the delta receptor), OP2 (the kappa receptor) and OP3 (the mu receptor). In 2000 this nomenclature was again changed to DOP, KOP and MOP, and this remains the current classification (*Cox et al 2000*). **Table 1.1** outlines these changes. (During the rest of this thesis the 2000 IUPHAR classification of DOP, KOP and MOP has been used). All three of the classical opioid receptors are distributed widely within the central nervous system and to a lesser extent throughout the periphery, occupying sites within the vas deferens, knee joint, gastrointestinal tract, heart and immune system amongst others (*Harrison et al 2000*).

Pre-cloning	Post-cloning	IUPHAR 1996	IUPHAR 2000
δ	DOR	OP1	DOP
κ	KOR	OP2	KOP
μ	MOR	OP3	MOP

Table 1.1

Names given to the three classical opioid receptors, including the current IUPHAR classification. All are naloxone sensitive

Three pro-hormone precursors provide the main source of endogenous opioid ligands acting upon the classical opioid receptors. Proenkephalin is cleaved to form met-enkephalin and leu-enkephalin which will act upon the DOP receptor, dynorphin A and B are derived from prodynorphin and are agonists at the KOP receptor, while proopioidmelanocortin (POMC) is the parent compound for β -endorphin, an agonist at the MOP receptor, though it is capable of displaying agonist activity at all three

classical opioid receptors (*McDonald et al 2005*). Two further endogenous peptides act as agonists at the MOP receptor, endomorphin 1 and 2, but as of yet no precursor has been identified.

Opioid ligands may mediate their action by either direct or indirect inhibition of the transmission of a peripheral nociceptive stimulus. However with all of these receptors common cellular responses follow receptor activation. Binding of an opioid ligand to a G-protein coupled opioid receptor on the extracellular portion of the receptor causes interaction with a G-protein of the i/o class. The α subunit of the G-protein exchanges its bound GDP molecule with intracellular GTP. This then allows the α -GTP complex to dissociate away from the $\beta\gamma$ complex. Both of these complexes (α -GTP and $\beta\gamma$) are then free to interact with target proteins. In the case of opioid receptor binding, this results in the inhibition of adenylate cyclase, causing a reduction in intracellular cAMP levels (*Corbett et al 2006, Rang et al 2007*). Additionally these complexes interact with a number of ion channels, producing activation of potassium conductance and an inhibition of calcium conductance. The net effect of these changes is of a reduced intracellular cAMP, a hyperpolarisation of the cell and for neuronal cells a reduction in neurotransmitter release **Figure 1.5**.

In 1994 a fourth G-protein coupled opioid like receptor was found and subsequently named the nociceptin receptor (NOP) (*Bunzow et al 1994, Mollereau et al 1994*). Rapidly after this discovery came the isolation from brain extracts of its endogenous ligand nociceptin/orphanin FQ (N/OFQ) (*Meunier et al 1995, Reinscheid et al 1995*). This endogenous ligand is similarly derived from a precursor compound, in this instance from the polypeptide precursor pre-pro-nociceptin. Whilst the N/OFQ/NOP system is naloxone insensitive, it is a G-protein coupled receptor system that shares a degree of homology with the known amino acid sequences of classical opioid receptors. Pre-pro-nociceptin also encodes for nocistatin the endogenous physiological antagonist at the NOP receptor, which reverses the effects of N/OFQ while not binding with the NOP receptor, and N/OFQ-2 whose actions are largely unknown (*Florin et al 1997, Okuda-Ashitaka et al 2000*). At a cellular level N/OFQ acts to produce similar actions to those described for the classical opioid receptors above. Consequently this is often referred to as a non-classical opioid receptor. The four opioid receptors and the endogenous opioid ligands acting upon them are shown in **Table 1.2**.

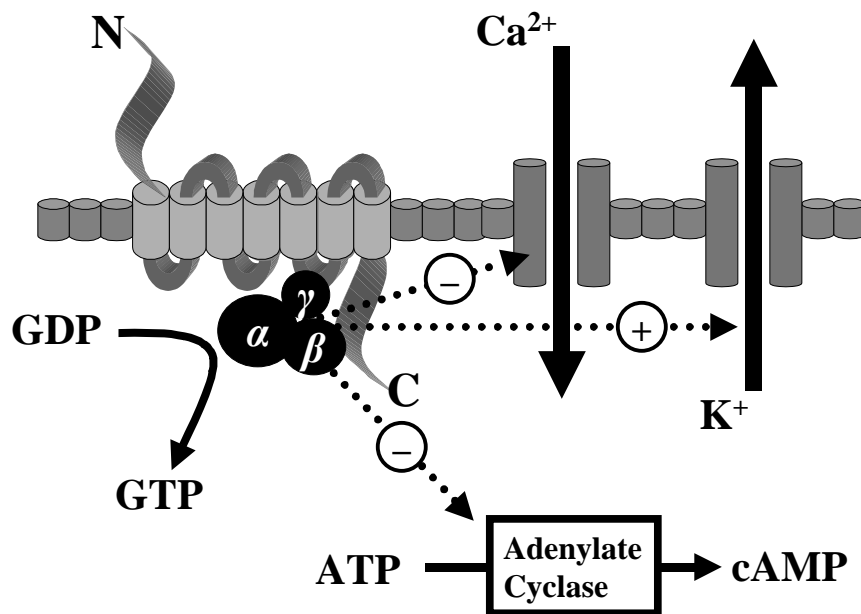


Figure 1.5.
Effect of opioid agonist/receptor coupling on G-protein and consequent intracellular effects.

However in laboratory studies N/OFQ has shown varied effects dependent upon the tissue into which it is released. Spinally, N/OFQ peptide has been shown to produce analgesia or hyperalgesia, dependent upon the administered concentration, and allodynia. However when administered intracerebroventricularly (i.c.v), it is thought to produce a pronociceptive antianalgesic effect (*Calo et al 2000*). It is thought that this pronociceptive effect may be due to an inhibition of endogenous opioid tone. The finding that blockade of the nociceptin peptide/NOP receptor system causes potentiation of the effects of both exogenous and endogenous opioids, lends credence to this theory. It has been hypothesised that N/OFQ achieves these supraspinal antiopioid effects by inhibition of primary off cells within the NRM, which would normally induce analgesia via activation of the descending inhibitory pathways **Figure 1.6** (*Pan et al 2000*). While MOP opioid agonists elicit analgesia centrally by inhibiting inhibitory ON GABAergic cells in the NRM, which normally themselves inhibit descending antinociceptive pathways, NOP agonists not only inhibit these cells, but also have a more profound direct inhibitory effect on the descending antinociceptive OFF cells. This mechanism proposed by *Pan* in 2000 could account for the supraspinal pronociceptive characteristics seen with N/OFQ.

Precursor	Opioid Peptide	Receptor
Pro-enkephalin	[Met]-enkephalin [Leu]-enkephalin	DOP
POMC	β -Endorphin	MOP
Unknown	Endomorphin-1 Endomorphin-2	
Pro-dynorphin	Dynorphin-A Dynorphin-B	KOP
Prepro-nociceptin	Nociceptin (N/OFQ) N/OFQ-2 <i>Nocistatin</i>	NOP

Table 1.2

The four opioid receptors and the endogenous opioid ligands acting upon them. Nocistatin is a physiological antagonist for N/OFQ.

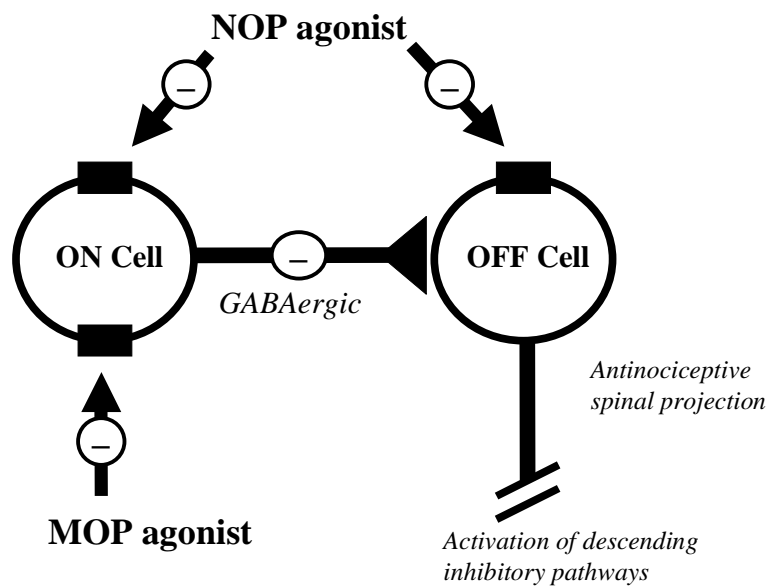


Figure 1.6 A schematic drawing showing N/OFQ modulation of nociceptive transmission within the nucleus raphe magnus (Pan et al 2000).

1.4 Peripheral opioid receptors and the neuroimmune system

Over the past ten years our understanding of the peripheral actions of the neuroimmune system has increased dramatically. These advances have allowed us a greater understanding of the mechanisms behind the presentation of peripheral opioid receptors to sites of inflammation and the delivery of endogenous opioids to these sites.

Much of this basic scientific research has been accomplished using small animal models of inflammation. These studies have helped to elucidate the effects of local inflammation on the immune system's ability to deliver endogenous opioids and their receptors to the site of a standardised discrete inflammatory insult (often Freund's complete adjuvant, a water-in-oil emulsion with dead mycobacterial organisms), and hence produce a degree of antinociception (*Mousa et al 2001 & 2004*).

Experiments show that rats killed up to twenty-four hours after an inoculation of Freund's complete adjuvant into a hind paw, show an increased expression of MOP opioid receptors in the ipsilateral lumbar dorsal root ganglia, with an absence of increase in similar receptors in the central nervous system. This up regulation of MOP can be observed by both immunochemical staining of histological specimens, and radioligand-binding experiments, carried out on dorsal root ganglia cell suspensions (*Shaqura et al 2004*).

However early infiltration of MOP agonists into the inflamed paw, within two hours of initial insult, produces little analgesia as judged by standard behavioural tests used in animal models of pain. This suggests a limited expression of MOP on primary afferent neurones in the periphery during the early stages following an inflammatory insult. Additional studies carried out at ninety-six hours after administration of Freund's complete adjuvant, again utilising similar imaging techniques, do provide evidence for an increased expression of MOP on peripheral nerve terminals, in inflamed compared to non-inflamed tissue (*Mousa et al 2001*). At four days receptor up regulation can also be seen within laminae I and II of the lumbar dorsal horn. Administration of MOP agonists into the inflamed paws of experimental animals at this time has been found to elicit significant degrees of long-lived analgesia in behavioural tests, when compared to matched controls receiving saline injection, or MOP agonists injected into non-inflamed paws (*Zollner et al 2003*).

These findings coupled with studies investigating the trafficking of receptors from the dorsal root ganglia to the periphery by a number of investigators, strongly suggests that MOP receptors are synthesised in the dorsal root ganglia in response to inflammation, prior to transport along intra-axonal microtubules to peripheral sensory neurons. Here they are incorporated into the membranes of neurones and take up a functional role, capable of binding to endogenous and exogenous opioid receptor ligands where they may elicit analgesia when stimulated.

In tandem with this increase in expression of peripheral opioid receptors, circulating immunocompetent cells are attracted to the site of inflammation by the action of local chemokines. In the initial hours following an inflammatory insult the sequestration of immunocytes consists primarily of granulocytes, with an accumulation of monocytes and macrophages over the next ninety-six hours, and finally an increased concentration of activated T-lymphocytes following the first four days of inflammation (*Brack et al 2003*).

Sections of rat paw taken from animals subjected to an inflammatory insult preserved in fixative and then immunofluorescently stained, show not only increased infiltration of white cells into inflamed tissue, but also enhanced intracellular staining of endogenous MOP agonists (β -endorphin, endomorphin-1 and endomorphin-2) within immune cells (*Rittner et al 2001*). Differential staining of this tissue confirms that the initial cellular infiltration is by granulocytes followed by mononuclear cells and finally T-lymphocytes. This follows the order of response expected for a typical non-specific inflammatory reaction. These findings can be replicated with flow cytometric analysis of cell suspensions taken from inflamed paws, and additionally in the case of β -endorphin by radioimmuno-assay of cell suspensions. Analysis of inflamed paw tissue indicates that the concentration of endogenous opioids within the inflamed tissue rises in parallel with increases in white cell recruitment. Additionally blockade of a range of adhesion molecules (L-selectin, integrins $\alpha 4$ and $\beta 2$ and intercellular adhesion molecule-1 (ICAM-1)) involved in the passage of immune cells through the endothelium to inflamed tissue, results in a limitation of immune cell numbers at the site of inflammation, as would be expected, and also a reduction in endogenous opioids at that site (*Likar et al 2004, Machelska et al 1998, 2002 & 2004*).

Full-length messenger RNA transcripts for POMC have also been found in immune cells indicating expression of the gene coding for β -endorphin. Collectively these

findings suggest immunocytes are capable of synthesising and presenting endogenous opioids to sites of inflammation (*Mousa et al 2004*).

Moreover behavioural studies in animals with locally induced inflammation indicate that sympathetic stimulation causes release of opioids from immunocytes into the surrounding tissue. This stimulation can be induced in the laboratory either by local infiltration directly into inflamed tissue of α and/or β -adrenergic ligands, or by subjecting an animal to a physiological challenge (commonly a cold water swim test), known to activate the sympathetic nervous system. In both cases increased local concentrations of endogenous opioids result, yielding comparatively greater degrees of analgesia in inflamed compared to non-inflamed tissue. These effects can be reversed by the local infiltration of sympatholytic drugs (*Binder et al 2004*).

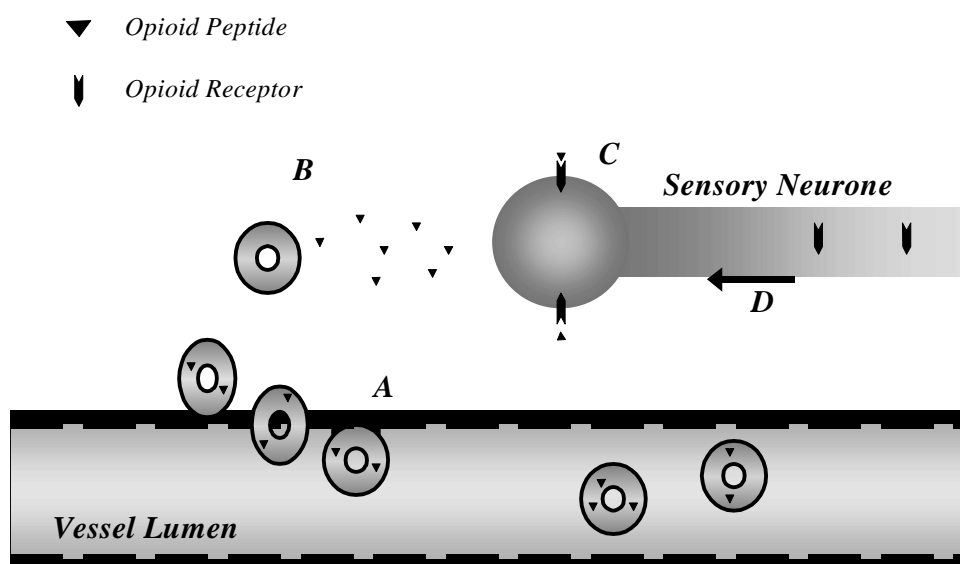


Figure 1.7

Mechanism of the peripheral action of endogenous opioids on peripheral receptors.

- A.** Adhesion molecules on both vascular endothelium and immune cells are up regulated, allowing passage of immune cells through the endothelium into the surrounding inflamed tissue. Immunocytes contain endogenous opioid peptides.
- B.** In response to sympathetic stimulation immune cells release endogenous opioid peptides into the inflamed tissue.
- C.** The released opioid peptides then bind to opioid receptors on peripheral sensory neurones.
- D.** Opioid receptors newly synthesised in the dorsal root ganglia in response to inflammation are trafficked to the periphery where they are presented at the neuronal membrane.

Collectively these findings provide a clear and coherent argument for the release of immune cell-derived opioids upon sympathetic stimulation, acting on peripheral opioid receptors, which have recently been up-regulated in the face of local

inflammation, **Figure 1.7**. Activated immune cells not only migrate to sites of inflammation and release opioid peptides, where they provide local analgesia, but are also implicated in providing an anti-inflammatory action at the site of inflammation. In part this is thought to be achieved by a direct action of the released opioid peptides, and additionally by the liberation of enkelytin, a naturally occurring antibacterial peptide (*Stefano et al 1998*).

These findings coupled with the contention by some researchers that much of the effect of both centrally and peripherally administered opioids is in fact peripheral in nature, leads to a new perspective on the neuroimmune axis (*Stein et al 2003*). It is now possible to postulate an intriguing connection between pain and the immune system, in which peripheral opioid peptides released by immune cells act upon receptors newly trafficked to the site of inflammation along peripheral neurones (*Brack et al 2003, Cadet et al 2001*).

If this paradigm were proven to be correct it opens the possibility for a range of novel therapeutic options by which the neuroimmune system could be manipulated. This could provide not only effective analgesia without many of the adverse central effects of the currently available opioid drugs, but also give new insight into the natural cellular physiological response to inflammation. Though unfortunately at this moment in time there is little evidence to support a clinically advantageous effect of endogenous opioids in the control of inflammatory pain, a number of studies support the opinion that exogenous opioid drugs administered peripherally can produce analgesia, in clinically relevant scenarios, by their action on peripherally-expressed opioid receptors. Perhaps more exciting however, is the potential for manipulation of the immune system to provide a means of endogenous opioid delivery.

While a body of evidence supports the involvement of immune cells in the delivery of endogenous opioid ligands, it is also recognised that the exogenous administration of opioid drugs can have profound and possibly deleterious effects upon the immune system itself. The site of the effect of these administered opioids on the immune system is however highly contentious. Three possible sites of action have been postulated; opioids acting directly upon the classical opioid receptors of peripheral immune cells, acting upon non-classical opioid receptors of peripheral immune cells, or an indirect action through their effects on the hypothalamic-pituitary-adrenal axis (*McCarthy et al 2001b, Mellon et al 1998, Patrini et al 1996, Saurer et al 2004*). It

seems likely that both direct and indirect effects may be working simultaneously,

Figure 1.8.

Though laboratory based research has consistently provided some evidence for the presence of both of the classical opioid receptors DOP and KOP on peripheral immune cells and immune cell lines in man (*Bidlack 2000*), with functional, binding and molecular biological studies, opinion over the existence of MOP receptors (the receptor mediating the majority of the effects of all clinically significant opioid medications) on immune cells is divided and highly controversial. As early as 1983 *Mehrishi and Mills* were claiming radioligand-binding studies showed evidence for the presence of MOP on lymphocytes (*Mehrishi et al 1983*). Since then further investigations using flow cytometry coupled with fluorescent staining (*Beck et al 2002, Caldrioli et al 1999, Lang et al 1995*) and molecular biological techniques (*Cadet et al 2001, Chuang et al 1995b, Suzuki et al 2000*) have purported to show MOP receptors on peripheral immune tissue. However these results have been difficult to reproduce in different laboratories and doubt has been cast over some of the experimental methods used. More recently data from experiments in which the administration of different cytokines to immune cell lines and lymphocytes cultured in suspension has suggested that though the MOP receptor is not expressed under basal conditions in man, certain stimuli encountered during an inflammatory response may cause up regulation. *Hollt's* team suggest that the administration of the cytokine TNF- α with or without the adjunct cycloheximide can induce immunocytes to express MOP receptors within 6 hours (*Kraus et al 2001 & 2003*). Clearly if these results were to be confirmed by others they would have far reaching implications, particularly in the fields of anaesthesia and intensive care medicine where opioids are commonly administered to patients suffering from sepsis or the systemic inflammatory response syndrome.

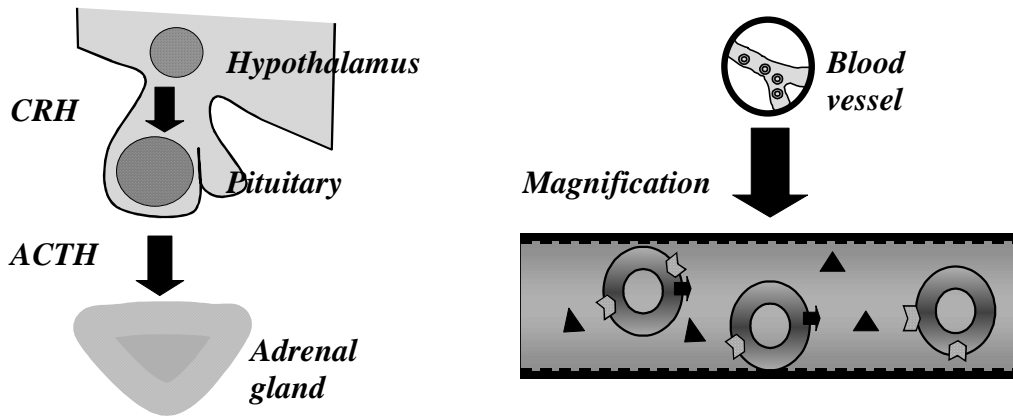


Figure 1.8
Possible immunological sites of opioid action.

- ▲ Endogenous opioid ligand
- ◩ Classical opioid receptor
- ▲ Non-classical opioid receptor
- ◉ White blood cell

Figure 1.8 shows the postulated sites of opioid ligand action, which could result in immune effects. The left side of the schematic shows the hypothalamic-pituitary-adrenal axis, with corticotrophin releasing hormone (CRH) and adrenocorticotrophic hormone (ACTH) shown in bold. Opioid ligands acting anywhere along this axis could have indirect effects on immune system function. The right hand side of the schematic shows white cells in a magnified blood vessel, displaying both classical and non-classical opioid receptors, which upon stimulation by free circulating opioid ligands could exert a direct immunological effect upon the cells.

1.5 The NOP/NOFQ Opioid System

Most of the work linking the immune system and the endogenous opioid ligand/receptor systems has so far centred on the classical opioids MOP, DOP and KOP. NOP/NOFQ has also been shown to have a range of effects beyond the central nervous system upon many other tissue and physiological systems, including the immune system.

If administered centrally N/OFQ produces an increase in parasympathetic tone and a reduction in sympathetic outflow, with attendant falls in blood pressure, heart rate and renal sympathetic nerve activity (*Malinowska et al 2002*). However even though peripherally administered N/OFQ cannot pass the blood brain barrier, N/OFQ still has the potential to cause a dose-dependent decrease in blood pressure and heart rate when administered intravenously to rodents (*Giuliani et al 1997, Hashiba et al 2003, Madeddu et al 1999*). These effects are naloxone insensitive as are its analgesic and pronociceptive effects, but can be reversed by NOP antagonists. Interestingly the administration of NOP antagonists has no effect upon the basal blood pressure and heart rate, giving rise to questions regarding the cardiovascular function of N/OFQ in the resting state. Larger peripheral arterioles greater than 100 μm in diameter have a degree of sympathetic innervation upon which N/OFQ could directly exert a vasodilatory effect upon the microcirculation. Smaller arterioles (<30 μm in diameter) however are under limited neurogenic control and rely instead on local intrinsic mediators to alter their tone. N/OFQ has been shown to cause a direct vasodilatation of these smaller arterioles independent of neurally mediated mechanisms, when added directly to either *in vivo* or *in vitro* preparations of small arterioles from rodents. Again this effect is not reversed by naloxone and is independent of classical opioid receptor activation. The mechanisms by which N/OFQ achieves this vasodilatation following direct administration are uncertain, though it is known not to be mediated via NO, K_{ATP} channels or prostaglandins. Mast cells release histamine in response to N/OFQ, which could account for the dilatation of small arterioles seen with N/OFQ (*Bucher 1998, Champion et al 1998 & 1997, Chen et al 2002*). Comparable to the classical opioid receptor-peptide systems N/OFQ has also been shown to exert effects upon the inflammatory system, not only through effects on vascular compliance, but also through its actions associated with peripheral immune cells (*Fiset et al 2003, Serhan et al 2001*).

1.6 Aims.

The initial drive to study MOP receptors on lymphocytes was to develop a working laboratory system with which to observe MOP opioid receptor changes in a peripheral and easily harvested clinical sample following administration of clinically significant opioids and to equate this to the central effects of opioid administration. It was hoped that this would enable central desensitisation to be modelled from peripheral blood samples. A number of groups have previously demonstrated the presence of MOP receptors on human leukocytes using a range of techniques (*Cadet et al 2001, Caldrioli et al 1999, Chuang et al 1995b, Mehrishi et al 1983*) including radioligand binding, immunofluorescence and reverse transcription PCR. These findings are however contentious with a body of opinion challenging this point of view (*Kraus et al 2003, Madden et al 2001, Pampusch et al 1998, Vidal et al 1998*). We have imitated these experiments in an attempt to identify MOP receptors.

The presence of DOP, KOP and NOP receptors on peripheral immune cells similarly remains controversial. The same range of experiments used in an attempt to identify MOP receptors has therefore also been employed to detect DOP, KOP and NOP receptors on naive peripheral immune cells.

Previous studies have also suggested that MOP receptors though not present in immunocytes in the resting state may be expressed after the administration of a number of inflammatory cytokines. Recent research has also made it increasingly apparent that the peripheral as well as central nervous system plays a significant role in immunological responses at both a cellular and sub-cellular level. Peripheral opioid receptors on immunocompetent cells within solid organs and the blood, and the opioid receptor ligands coupled to these receptors, whether delivered from distant sites or by immunocytes themselves are mechanisms by which these effects may be mediated. More particularly N/OFQ/NOP has also been associated with immuno-modulation in a number of investigations (*Fiset et al 2003, Meunier 1997 & 2000, Serhan et al 2001*). Taken together these findings if confirmed have important implications for the practice of clinical medicine and anaesthesia and critical care medicine in particular.

The aims of this thesis are therefore:

- To attempt to identify MOP receptors on peripheral blood mononuclear cells and immortalised immune cells in the naïve state, utilising a range of complementary experimental techniques including radioligand binding, endpoint PCR, quantitative PCR and immunofluorescent staining.
- To repeat these experiments with peripheral immune cells and immune cell lines following administration of the tumour necrosis factor- α and cycloheximide.
- To duplicate these investigations in an attempt to identify DOP, KOP and NOP receptors in similar cells and cell lines. Additionally in the case of NOP, this thesis attempts to find evidence for the expression of the gene encoding for prepronociceptin (the precursor of N/OFQ and nocistatin), by PCR techniques.
- To follow changes in expression of the genes encoding for all of these opioid receptors and prepronociceptin in the peripheral blood mononuclear cells of patients during a septic episode necessitating admission to the Leicester Royal Infirmary Intensive Care unit, using quantitative PCR techniques.

Chapter 2:

Materials and Methods

2.1 Cell lines

A variety of cells, tissue and cell lines reflecting the evolution of this thesis, from *in vitro* experimentation to *ex vivo* observation of opioid receptors and endogenous opioids, were used in the assays described below. All cell lines were available from within the University of Leicester Department of Anaesthesia or University of Leicester apart from CEM x174 cells, which were purchased from the Centralised Facility for AIDS Reagents sponsored by the UK Medical Research Council in Potters Bar, Herts. All cells not directly donated from volunteers or clinical samples were cultured at 37°C in 5% carbon dioxide with humidified air.

2.1.1 Materials

Dulbecco's MEM, Fischer's Medium, Foetal Calf Serum, Fungizone, Gentecin, Glutamine, HAM-F12, Hygromycin B, Penicillin/Streptomycin, RPMI, Trypsin/EDTA – *Invitrogen Ltd, UK*
Tumor Necrosis Factor- α (recombinant *E. coli*), Cycloheximide – *Calbiochem, UK*
Ficoll-Paque Plus - *Amersham Pharmacia Biotech, UK*
Harvest Buffer – 154mM NaCl, 10mM HEPES, 1.71 mM EDTA (pH 7.4 with NaOH)

2.1.2 Chinese hamster ovary cells

Chinese hamster ovary cells, transfected with and stably expressing human MOP, DOP, KOP or NOP (CHO_{hMOP/DOP/KOP} or CHO_{hNOP}), were used as the experimental model for optimising imaging techniques for human opioid receptors prior to work on neural cell lines, leukaemic cell lines and *ex vivo* tissue or cells.

CHO_{hMOP/DOP/KOP} cell stocks were maintained in HAM-F12 supplemented with 10% FCS, penicillin (100 IU/ml), streptomycin (100 μ g/ml) and fungizone (2.5 μ g/ml). CHO_{hNOP} cells were cultured in Dulbecco's MEM / HAM-F12 (50/50) supplemented with 5% FCS, penicillin (100 IU/ml), streptomycin (100 μ g/ml) and fungizone (2.5 μ g/ml). In order to maintain the opioid receptor plasmid that these cells had been transfected with stock cultures were further supplemented with geneticin (400 μ g/ml)

MOP/DOP/KOP or 200µg/ml NOP). NOP stock culture media was further supplemented with hygromycin B (200µg/ml), to maintain for expression of a reporter gene not used in this study.

To propagate cells, cells were harvested by first discarding any excess media. 5ml of trypsin/EDTA was then added to the confluent flask and allowed to stand in the incubator at 37°C, 5% CO₂ for 5 minutes. Gentle agitation then allowed the cells to be readily detached from the culture vessel surface, whereupon a small volume of fresh media was added to neutralise the trypsin. The resulting cell suspension was centrifuged at 1500 rpm (437g) for 2 minutes (Heraeus Instruments Labofuge 400R). The supernatant was discarded and the resulting cell pellet used to seed new culture flasks. If cells were to be used for experimental purposes, harvest buffer was used in place of trypsin.

2.1.3 Leukaemic cell lines

Four different human immune cell lines (CEMx174, Raji, U937 and Jurkat E6.1) and one murine immune cell line (L1210) were cultured to provide a ready source of easily available tissue to work with.

L1210	Murine leukaemic cell line.
U937	Human Caucasian histiocytic lymphoma. Derived from the malignant cells drained from a pleural effusion in a 37 year-old Caucasian man.
CEMX174	Fusion product of human B-cell and T-cell line.
Jurkat E6.1	Human leukaemic T-cell lymphoblast
Raji	Human Negroid Burkitts lymphoma B-cell line.

The CEM X174 cells differ from the three other human cell lines by virtue of being synthetically manufactured. These cells express both B and T cell markers in addition to CD4, and are a fusion product of a human B-cell (721.174) and T-cell line (CEM) purchased from the Centralised Facility for AIDS Reagents sponsored by the UK Medical Research Council in Potters Bar, Herts. Previous reports had suggested the presence of MOP receptors on these cells (*Chuang et al 1995b, Suzuki et al 2000*). Raji, Jurkat and U937 leukaemic cell lines each represent a class of mononuclear cell found in man.

During immunofluorescent staining of the MOP receptor using primary and secondary antibodies a mouse lymphoblastic cell line L1210 was additionally used. It was thought it may display MOP receptors, though not human in nature, its amino acid sequence was sufficiently close to the human sequence to warrant investigation of the primary antibodies available.

L1210 cells were cultured in Fischer's media supplemented with 10% FCS and containing 2mM glutamine, penicillin (100 IU/ml), streptomycin (100µg/ml) and fungizone (2.5µg/ml). CEM X174, Raji, Jurkat and U937 cells were grown in RPMI 1640 with 10% FCS and containing 2mM glutamine, penicillin (100 IU/ml), streptomycin (100µg/ml) and fungizone (2.5µg/ml).

Following propagation leukaemic cell lines were either centrifuged for 2 minutes at 1500 rpm (437g), the supernatant discarded and the cell pellet used to seed further flasks or for experimental procedures. All of these cell lines grew in clumps at elevated cell densities, a finding most noticeable with the CEMX174 cells. For this reason and to maintain cell vigour flasks were passaged on average every 72-96 hours.

2.1.4 Human neural cells

SH-SY5Y cells, are a human neuroblastoma cell line derived from a sub-line of a bone marrow line (SK-N-SH), known to display MOP and NOP receptors and were therefore used as a model for the central effects of opioids (*Prather et al 1994, and unpublished data*).

SH-SY5Y cells were cultured in HAM-F12/Dulbecco's MEM (50/50) containing 10% FCS, penicillin (100 IU/ml), streptomycin (100µg/ml) and fungizone (2.5µg/ml).

These cells contain no transfected plasmid and therefore did not require specific stock media to ensure against loss of genetic material. Cells were generally used when approximately 80% confluent. To propagate cells, or prior to their use in experiments, cells were harvested in a similar manner to transfected CHO cells as described above. Cells were passaged every 72-96 hours.

2.1.5 Venous blood/peripheral blood mononuclear cells

Peripheral blood mononuclear cells (PBMCs) were isolated from venous blood drawn from healthy volunteers, from within the Department of Anaesthesia, Critical Care

and Pain Management, University Hospitals of Leicester. Investigators wore protective gloves and the skin over the puncture site was first cleaned with a sterile swab prior to taking any blood samples. After venepuncture with a 21G green needle blood was aspirated into a 9-ml monovette tube pre-filled with EDTA to stop coagulation. The local ethics committee gave approval for this study (*Appendix II*).

PBMCs were then separated from the extracted blood. To achieve this blood was first diluted with phosphate buffered saline (PBS) at room temperature in a 1:1 ratio. The PBS had earlier been brought to room temperature. Using 30 ml sterilins for the separation, “blood” was then carefully layered over Ficoll-Paque Plus (Amersham Biosciences) in the ratio 3ml of Ficoll to 4 ml of blood, **Figure 2.1**. Care was taken not to mix the diluted blood and Ficoll. The resulting solution was then centrifuged at 400g for 30 minutes at 18-20 °C. This caused the granulocytes and erythrocytes to sediment through the Ficoll into a pellet at the base of the sterilin, and left a layer of lymphocytes and platelets above the Ficoll, but beneath the now cell depleted plasma phase. The PBMCs were then easily removed via pipette. This PBMC rich solution was now diluted with at least 3 volumes of PBS and centrifuged for 10 minutes at 100g and 4°C, yielding a cell pellet, which was immediately placed on ice and used in a variety of assays **Protocol 2.1**. If required venous blood was used directly in assays with no prior separation.

1. Venepuncture to EDTA tube
2. Dilute blood 1:1 with PBS
3. Layer over Ficoll-Paque (3ml:4ml Ficoll:blood)
4. Centrifuge 400g, 30 mins at 18-20°C
5. Remove PBMC layer
6. Dilute with x3 PBS
7. Centrifuge 100g, 10 mins at 4°C
8. Remove pellet

Protocol 2.1

Extraction of peripheral blood mononuclear cells from venous blood

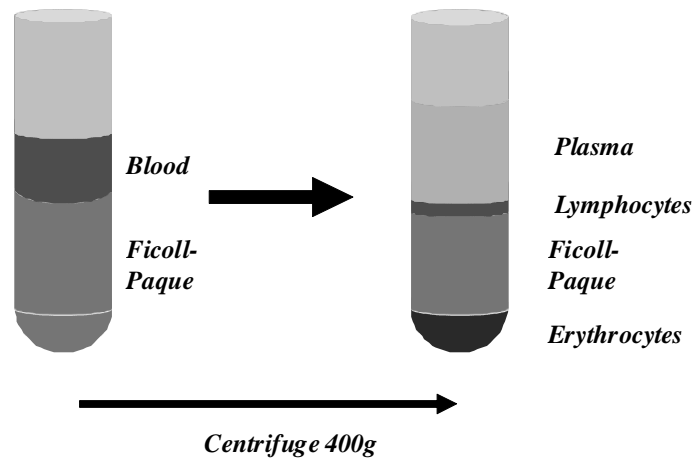


Figure 2.1
Isolation of peripheral blood mononuclear cells from blood by ficoll density sedimentation.

PBMCs were occasionally kept in culture by suspending in RPMI supplemented with 2mM glutamine, penicillin (100 IU/ml), streptomycin (100 μ g/ml) and fungizone (2.5 μ g/ml). These cells were placed in the incubator at 37°C with 5% CO₂.

2.1.6 Stimulated Upregulation of opioid receptor gene expression

Raji cells were also cultured in the presence of TNF α in an attempt to mimic the inflammatory conditions of sepsis in vitro. Previous reports had provided some evidence using PCR techniques that opioid receptors may be expressed following stimulation by inflammatory mediators in polymorphonuclear cells and B-lymphocytes (*Kraus et al 2001 & 2003*). Cells were also grown in media containing TNF α and cycloheximide in order to assess the effect of TNF α on cell viability and to verify the stimulatory effects of TNF α .

Raji cells were cultured in standard media as previously described in two 75cm² flasks (37°C, 5% CO₂). Twenty hours prior to harvesting 100-200 pg/ml of TNF α was added to one of the flasks. A second flask acted as a negative control with no addition of inflammatory mediators. RNA was then harvested and converted to cDNA using standard techniques described below **Protocols 2.4-2.6**. U937 cells grown in culture with 30pg/ml of TNF α and 1 μ g/ml of cycloheximide over a similar time frame were used to evaluate the effect of TNF α on cell viability.

2.2 Radioligand Binding

2.2.1 Materials for Radioligand Binding

General:

Magnesium Sulphate, Potassium Hydroxide, Sodium Hydroxide, Trifluoroacetic acid, TRIS-HCl, HiSafe3 Optiphase Safe, Whatman G/F B filters, Folin's reagent – *Fisher Scientific UK Ltd, UK*

Sodium Chloride, PEI, BSA, DTT, EDTA, EGTA, GDP, GTP γ S, HEPES, Amastatin, Bestatin, Captopril, Phosphoamidon, Bacitracin – *Sigma*

Radio and Fluorescently Labelled Compounds:

[³H]-Diprenorphine, GTP γ [³⁵S] – *PerkinElmer Life Sciences Inc. USA, (now GE Health Care)*

[leucyl-³H]N/OFQ, – *Amersham*

Fluorescent-Naloxone – *Invitrogen*

Buffer Composition:

Harvest Buffer – 154mM NaCl, 10mM HEPES, 1.71 mM EDTA (pH 7.4 with NaOH)

Saturation/Competition Binding Assay Wash Buffer– 50mM TRIS-HCl, 5mM MgSO₄ (pH 7.4 with NaOH)

Saturation/Competition Binding Assay Buffer – 0.5% w/v BSA in wash buffer

GTP γ [³⁵S] Homogenisation Buffer – 50mM TRIS HCl, 200 μ M EGTA (pH 7.4 with NaOH)

GTP γ [³⁵S] Assay Buffer – 100mM NaCl, 50mM TRIS-HCl, 1mM MgCl₂, 200 μ M EGTA (pH 7.4 with NaOH)

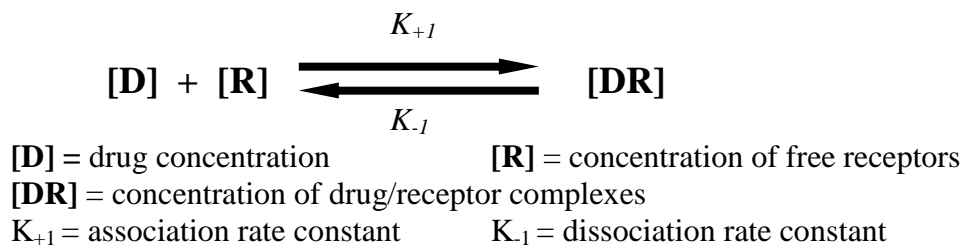
GTP γ [³⁵S] Radiolabel Buffer – 50mM TRIS-HCl, 10mM DTT (pH 7.4 with NaOH)

2.2.2 Saturation Binding Assay

Theory

The interaction of a drug or ligand with a receptor can be thought to have two component parts, firstly the binding of the drug to the receptor and secondly the action the drug has upon that receptor. Binding assays enable the description of the first component of this interaction, while functional assays can be used to investigate the second, namely the consequences of the drug binding to the receptor.

The binding of a ligand to its receptor can be modeled by using the following equation:



A drug, [D], binds to its receptor, [R], to become the drug-receptor complex, [DR]. This reaction proceeds in this direction at a rate K₊₁[D][R], while the rate of dissociation of the drug-receptor complex is determined by the formula K₋₁ [DR]. If this system is at equilibrium then these two rates are equal and,

$$K_{+1}[D][R] = K_{-1} [DR]$$

K_d is the equilibrium dissociation rate constant for this drug-receptor interaction. It is given the value K_d such that at the point where association to the receptor by the drug is equivalent to its dissociation from the receptor,

$$K_d = K_{+1}[D][R] = K_{-1} [DR]$$

This equation can be rewritten to read,

$$K_d = K_{-1}/ K_{+1} = [D][R] / [DR]$$

If 50% of the receptors are occupied by drug then the number of occupied receptors (i.e.50%) is equal to the number of unoccupied receptors (again 50%). In this instance,

$$[R] = [DR]$$

This allows the above equation relating K_d to K_{-1}/K_{+1} to be simplified to read,

$$K_d = [D]$$

This value is frequently used in pharmacology to give an indication of the affinity of a drug for a particular receptor. Another value commonly quoted in experiments exploring the binding of drugs to receptors is the B_{max} , expressed as a mass of the radiolabel bound per mg of tissue. This value like the K_d is dependent upon the binding and kinetic properties of the drug-receptor interaction, but unlike the K_d the actual amount of tissue available for drug binding will also change the absolute amount of drug bound. The units for B_{max} will compensate for this. These two values, the K_d and the B_{max} can also be derived from a graphical representation of a drug's binding to a receptor in the form of a Langmuir absorption isotherm which plots concentration of drug against the amount of drug specifically bound to the receptor, as shown below, *Figure 2.2* (Bylund *et al* 1993, Kenakin 2006).

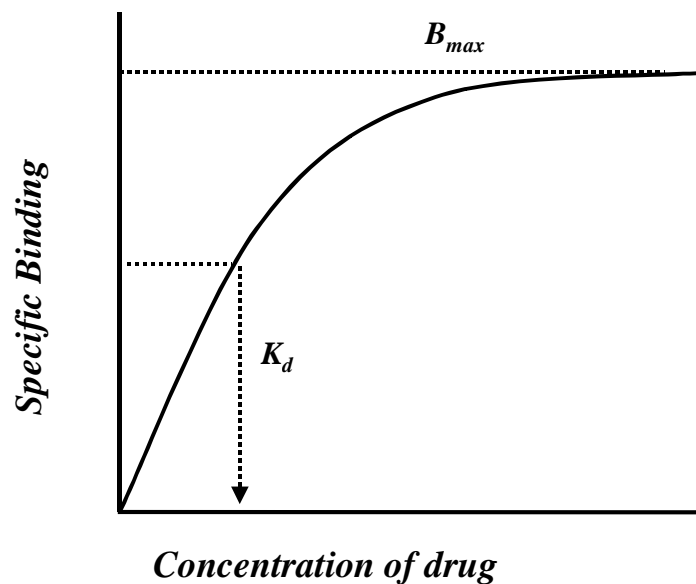


Figure 2.2
The Langmuir absorption isotherm.

In practice specific binding is calculated by subtracting non-specific binding of the radioligand from the total binding, where non-specific binding is the binding of the

radioligand to the cell membrane in a non ligand-receptor fashion. A value for non-specific binding is obtained by the addition of an excess of non-radiolabelled ligand (preferably an antagonist), which will occupy all of the receptor sites due to its molar excess, but will not be able to occupy all of the non-specific sites to which the radiolabelled ligand may attach, **Figure 2.3**.

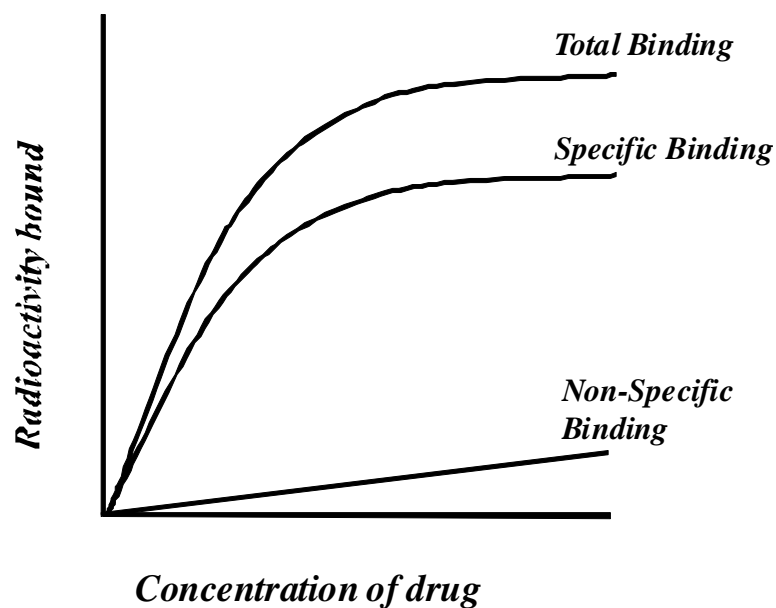


Figure 2.3. Isotherm plots for total and non-specific binding from which the third plot of specific binding can be calculated by simple subtraction of non-specific binding from total binding.

More commonly however the Langmuir isotherm is represented as a semi-logarithmic plot, in which the $\log [D]$ (the log of the drug concentration) is plotted against the specific binding, **Figure 2.4**. From this plot the negative log of K_d can be found, pK_d . This value is commonly used in pharmacology to give an indication of the binding affinity of a drug for a receptor.

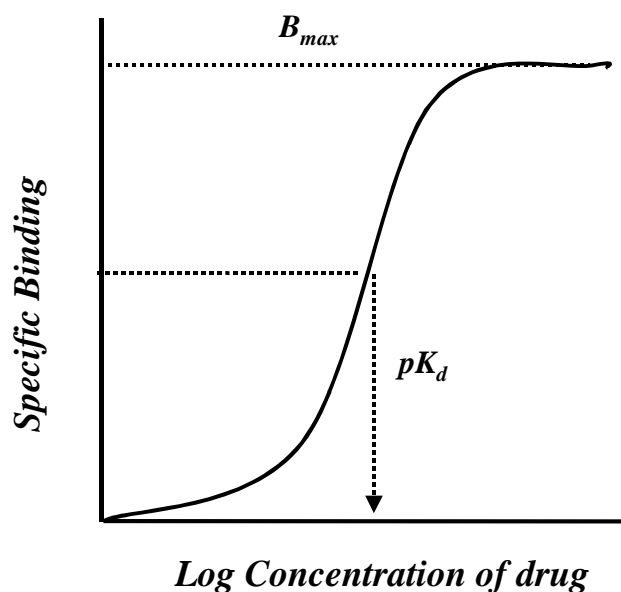


Figure 2.4. Semi-logarithmic plot of log drug concentration vs. specific binding, from which B_{max} and pK_d can be calculated.

Saturation binding studies are a form of experiment used to explore the binding properties of a drug to a specific receptor. Interpretation of this type of experiment relies on an understanding of the equations and principles discussed above, commonly using the Langmuir isotherm and semi-logarithmic plots to calculate values for pK_d , K_d and B_{max} . In this type of experiment increasing concentrations of a radiolabelled drug known to bind to a specific receptor are added to a cell membrane suspension. A point of saturation will occur when all the receptors in question are occupied by that radioligand. Following the washing away of any excess unbound radioligand, assay of the bound radioligand gives the total binding of the radioligand to the receptor and membrane, subtraction of non-specific binding (NSB) giving specific binding.

Method

Cells grown in a monolayer (CHO_{hMOP}, CHO_{hNOP} and SH-SY5Y) were harvested using harvest buffer and gentle agitation. The resulting cell suspensions were then centrifuged at 1500 rpm for two minutes to form a cell pellet. Cell pellets were re-suspended in wash buffer to “clean” the cells, centrifuged once more and finally re-suspended in an appropriate volume of assay buffer.

Immunocompetent cell lines grew in suspension. Cell pellets were therefore collected under centrifugation (1500rpm, 2min) and initially re-suspended in PBS to remove any excess media and cell debris. Peripheral blood mononuclear cells (PBMCs) were isolated as described above and washed in PBS prior to use. Whole blood was used intact.

Once harvested cells were homogenised by the action of an Ultra Turrax homogeniser applied for ten seconds followed by six consecutive short bursts. The membrane preparation was then centrifuged at 13,500 rpm for 10 minutes at 4°C. This process was carried out a maximum of three times for cultured cells, but only once for PBMCs as low cell yields were anticipated. The membrane suspension was re-suspended in a minimal volume of wash buffer and was then ready for use in subsequent radioligand binding experiments. The protein content of this suspension was calculated by using the method described by *Lowry et al* in 1951 (*Lowry et al 1951, Appendix D*).

The membrane suspension produced was diluted to the desired concentration for saturation binding assay. Total binding was calculated by adding 100µl volumes of membrane, containing up to ~1mg of protein for immunocytes and 50µg for CHO cells, to a range of concentrations of [³H]-Diprenorphine (1pM-2nM), (a radiolabelled non-selective classical opioid receptor antagonist) or radiolabelled N/OFQ, [*leucyl*-³H]-N/OFQ (2pM-2nM). This volume was made up to 1ml by the addition of binding assay buffer and a cocktail of peptidase inhibitors (amastatin, bestatin, captopril and phosphoramidon 10µM each). The mixture was then incubated for 1 hour at room temperature. **Table 2.1** shows the volumes of reagents added to each of the tubes in this reaction. A range of total binding reactions would be produced as differing concentrations of radiolabelled compound were used.

Tube Label	Binding Buffer	Radiolabelled compound	Naloxone	Membranes
Total	700	200	-	100
NSB	500	200	200	100

Table 2.1

Components of Saturation Binding Assay (volumes are in μl .)

Non-specific binding (NSB) was calculated for the classical opioid receptors in an almost identical manner, with the only exception being the addition of Naloxone (an unlabelled classical opioid receptor antagonist) at a final concentration of 10^{-6}M prior to the incubation for 1 hour. For NOP binding NSB was determined in the presence of an excess ($10\mu\text{M}$) of unlabelled N/OFQ. The reaction was terminated in both instances by vacuum filtration through glassfibre filters (Whatman GF/B) soaked in 0.5% polyethylenimine (PEI), using a Brandel vacuum harvester, trapping bound radioactivity. The filters were cut out and placed in scintillation vials to which 4.5ml of Optiphase safe scintillation fluid was added. After an eight-hour delay to allow for extraction the vials were counted for three minutes each using a scintillation counter (Packard 1900TR).

2.2.3 Competition Binding Assays

Theory

Saturation binding experiments can be used to calculate some of the binding properties of novel therapeutic agents and molecular probes that are unlabelled. Additionally it is a useful technique for calculating receptor number and density on various tissues and cell lines. Though saturation-binding studies are clearly a useful way to determine some of the properties of a drug, it is not always possible to produce or acquire commercially a radiolabelled form of a drug. In this instance competition-binding studies (also known as displacement binding studies) can be used.

In competition assays an increasing concentration of non-radiolabelled ligand is added to a receptor-ligand system, which contains a known fixed concentration of a radiolabelled ligand. As the concentration of unlabelled ligand increases the radioligand species will be displaced from the receptor site. From this experiment the concentration of unlabelled ligand, which displaces 50% of the radioligand can be determined. This value is called the IC_{50} for the non-radiolabelled ligand, and is dependent upon three factors:

- The affinity of the competing ligand for the receptor (i.e. the non radiolabelled ligand)
- The concentration of the radiolabelled ligand
- The affinity of the radiolabelled ligand for the receptor, its K_d

The IC_{50} is a measure of the affinity of the non-radio labelled ligand for the receptor. From the IC_{50} the K_i can be calculated, where K_i is an estimation of the concentration of ligand required to occupy 50% of the receptors in the absence of the radiolabeled ligand. It is therefore an approximation of the K_d calculated from a standard saturation-binding assay. The Cheng-Prusoff equation is used to calculate the K_i for a ligand from the derived IC_{50} value, while correcting for the mass of radiolabel used and its K_d for the receptor under investigation. By quoting K_i it is understood that this is a value derived from a displacement binding study (*Cheng et al 1973, Kenakin 2006*).

Cheng-Prusoff equation:

$$K_i = IC_{50} / (1 + [Ligand]/K_d)$$

IC_{50} = IC_{50} of competing non-radio labelled ligand

[Ligand] = concentration of radio labelled ligand

K_d = equilibrium dissociation constant of radio labelled ligand

Method

Competition binding experiments were performed in order to determine the binding properties of fluorescent-naloxone and assess its potential as a fluorescent probe. Hence in these experiments fluorescent-naloxone or naloxone were used as the displacing ligand and [3H]-Diprenorphine as the displaced radiolabelled compound (at a fixed concentration of 0.5nM). CHO_{hMOP} cells (~50 μ g of membrane protein) were added to a total reaction volume of 0.5ml of which 100 μ l was membrane preparation prepared as for a saturation-binding assay **Table 2.2**. Naloxone was added in excess where appropriate in order to displace any radiolabel from receptor sites, only leaving non-specific binding to be assayed in these reactions. Increasing concentrations of naloxone/fluorescent-naloxone (10^{-5} - 10^{-12} M) were added. Competition binding reactions were terminated by vacuum filtration, using a Brandel harvester, through

Whatman G/F-B filters treated with 0.5% polyethylenimine (PEI) to reduce NSB. Filter bound radioactivity was quantified by liquid scintillation spectroscopy.

Tube Label	Binding Buffer	[³ H]-Diprenorphine [0.5nM]	Naloxone	Displacer	Membranes
Total	300	100	-	-	100
NSB	200	100	100	-	100
Displacer	200	100	-	100	100

Table 2.2.
Components of Competition Binding Assay (volumes in μ l).

2.2.4 GTP γ [³⁵S] Binding Assay

Theory

Another radiolabelled binding assay, which can be used to probe for receptor function, is the GTP γ [³⁵S] binding assay. This type of assay measures agonist stimulated binding of radiolabelled GTP, GTP γ [³⁵S]. There may be signal amplification in this assay such that activation of a low density of receptors might be detected (*Berger et al 2000, Kenakin 2006*).

When an agonist binds to a G-protein coupled receptor there are conformational changes in the G-protein. The α subunit of the receptor exchanges GDP for GTP, this in turn causes the G-protein itself to dissociate into two functional units. The first of these consists of the original α subunit of the G-protein now bound to the GTP molecule, while the second is made up of a β and γ subunit complex. These subunits then exert effects upon the ion channels of the cell membrane and act to alter the rate of conversion of ATP to cAMP, **Figure 2.5**.

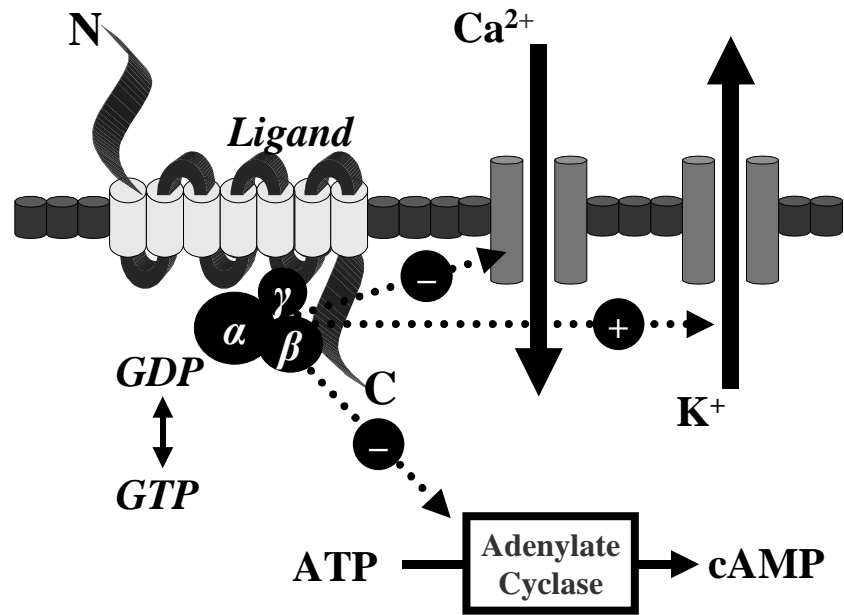


Figure 2.5.
G-protein coupled receptor and intracellular events following agonist binding.

Normally the α subunit (which has intrinsic GTPase activity) would then convert the GTP bound to it back into GDP, thus allowing the system to return to its basal state. However if the GTP is exchanged for a non-hydrolysable sulphur-containing analogue, $GTP\gamma S$, this system will remain in the active state with the α subunit unable to hydrolyse this GTP analogue. If a radiolabel is incorporated into the $GTP\gamma S$ in the form of $GTP\gamma [^{35}S]$ then a radiolabelled binding assay can be performed. Usually the data from this type of experiment is then expressed as a stimulation factor using the equation below.

$$\text{Stimulation factor} = \frac{dpm(\text{sample}) - dpm(\text{NSB})}{dpm(\text{total}) - dpm(\text{NSB})}$$

Plots of the stimulation factors and log of the concentration of the ligand in question will yield a sigmoid concentration-response curve from which maximal stimulation or efficacy (E_{\max}) and potency (pEC_{50}) can be calculated, **Figure 2.6.**

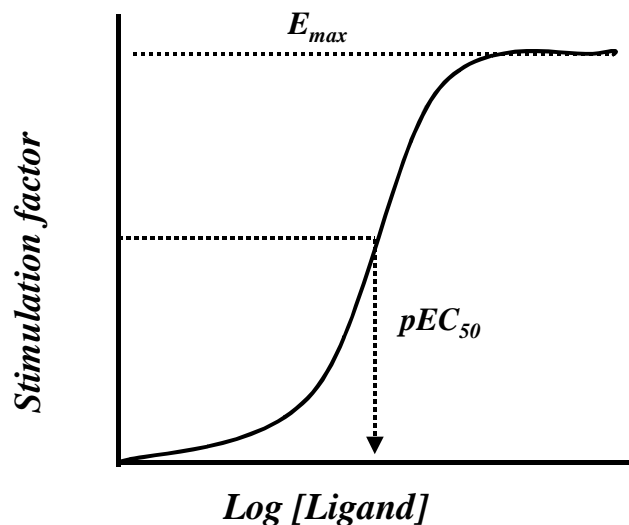


Figure 2.6. Shows the semi-logarithmic dose response curve expected when \log [ligand] is plotted against stimulation factor. E_{max} and pEC_{50} are also marked.

Method

The $GTP\gamma$ [^{35}S] binding assay was used to look for NOP expression on immune cells. Cells were harvested as previously described washed in harvest buffer and homogenized. Membrane homogenates were then prepared in $GTP\gamma$ [^{35}S] assay buffer (≈ 2 ml with no BSA). Following determination of protein concentration in this solution the homogenate was further diluted using $GTP\gamma$ [^{35}S] assay buffer to a final concentration, which would yield between 50 and 150 μg of membrane protein per tube in the assay. Homogenates were incubated with serial dilutions of N/OFQ in the presence of 150pM $GTP\gamma$ [^{35}S], 0.1% BSA, 5 μM GDP, 10 μM peptidase inhibitors and 150 μM bacitracin. The addition of 10 μM $GTP\gamma S$ allowed NSB to be calculated. CHO_{hNOP} cells were used as a positive control. These cells showed a high level of opioid receptor expression and so only 20 μg of protein was required per tube. Additionally 100 μM of GDP was added rather than the 5 μM used with the immunocompetent cells. This favours optimal stimulation factor at the expense of “absolute” counts bound.

In all instances these assays were incubated for 1-hour at 30°C with gentle agitation after which time they were harvested by vacuum filtration to dry Whatman GF/B

filters. Radioligand bound was determined after an 8-hour extraction in Optiphase safe by scintillation counting. **Table 2.3** details the volumes of each reagent used in the reactions.

Content (μl)	Assay buffer	BSA	Bacitracin	PI	GDP	GTPγ [³⁵S]	GTPγS	N/OFQ	Memb.
Total	220	20	20	20	20	100	-	-	100
NSB	200	20	20	20	20	100	20	-	100
Ligand	200	20	20	20	20	100	-	20	100

Table 2.3. Components of GTP γ [³⁵S] Binding Assay, all volumes in μ l (assay volume 500 μ l)

2.3 Radioimmunoassay

2.3.1 Materials

Nociceptin/Opioid Receptor-Like (ORL₁) Peptide (Orphanin FQ) RIA Kit – *Phoenix Pharmaceuticals, Ltd, USA*

Acetonitrile, Trifluoroacetic acid – Sigma

Aprotonin, Calbiochem, UK

2.3.2 N/OFQ radioimmunoassay

Theory

To measure the plasma concentration of peptides a radioimmuno-assay was employed. A radioimmunoassay is a competitive assay, which relies on a known concentration of ¹²⁵Iodine radiolabelled peptide being present within the assay reaction. ¹²⁵I-peptide competes with an unknown concentration of peptide, isolated from the samples of interest, for binding to a limited quantity of antibody specific to the peptide. Greater concentrations of peptide extracted from a sample will lead to lower binding of ¹²⁵I-peptide to the antibody. By producing a standard curve for ¹²⁵I-peptide binding to antibody in the presence of known concentrations of unlabelled peptide, concentrations of peptide in unknown samples can be calculated (*Cowley et al 2005*). Samples are analysed using a γ -counter. Following extraction of plasma from blood, samples can be analysed for peptide at the same time as a standard curve is produced. In this thesis it has been used to follow changes in the plasma concentration of N/OFQ during a septic episode in patients requiring admission to the Leicester Royal Infirmary Intensive Care unit.

Method

Blood was collected into 10 ml Monovette tubes (*Sarstedt, Leicester, UK*) pre-filled with EDTA to prevent coagulation. Aprotonin, 0.6 TIU ml⁻¹, was then added. Tubes were mixed thoroughly and immediately placed on ice. To isolate plasma from whole blood, blood was centrifuged at 3000g for 10 minutes at 4°C and the supernatant carefully removed. These samples were then stored at –70°C prior to use. Following thawing plasma was acidified with an equal amount of 1% trifluoroacetic acid (TFA) in water. This was thoroughly mixed and centrifuged at 1500g for 20 minutes at 4°C. The supernatant from this process was then retained. At the same time a separation

column containing 200mg of C-18 was prepared by washing with 1ml of 60% acetonitrile in 1% TFA once and then 3mls of 1% TFA 3 times. After this preparation of the column the plasma solution from which the peptides were to be isolated was loaded onto the column. The column was then slowly washed through with 1% TFA 3mls three times and then the peptides were eluted from the column by washing through and collecting 3mls of 60% acetonitrile. In this instance the eluent contains nociceptin peptide (N/OFQ). The eluent was then dried at room temperature under a vacuum. Peptides were stored at -20°C until required. For use in a radioimmunoassay dried samples were dissolved in 250 μl of radioimmuno assay (RIA) buffer (*Phoenix Pharmaceuticals*; composition proprietary information). Tube contents were made up as below in **Table 2.4**.

Radioimmuno assay reactions were performed as below:

- Add 200 μl of RIA buffer to each NSB tube
- Add 100 μl of RIA buffer to each total binding tube
- Add 100 μl of sample to each sample and standard tube
- Then add 100 μl of primary antibody (rabbit anti-peptide) to sample, standard and total binding tubes
- Vortex, cover and allow to stand for 24 hours
- Add 100 μl of ^{125}I -N/OFQ to each tube
- Vortex, cover and allow to stand for 24 hours
- Add 100 μl of goat anti-rabbit IgG serum to each tube
- Add 100 μl of normal rabbit serum to each tube
- Vortex and allow to stand for 90min at room temperature
- Add 500 μl of RIA buffer to each tube
- Centrifuge all tubes at 3,000rpm for 20 mins 4°C
- Remove supernatant and assay pellet for ^{125}I content using γ -counter (Packard-Cobra)

Tube Label	RIA Buffer	Primary antibody	Sample	^{125}I -N/OFQ	Goat anti-rabbit IgG serum	Normal rabbit serum
Total	100	100	-	100	100	100
NSB	200	-	-	100	100	100
Sample	-	100	100	100	100	100

Table 2.4. Volume of components added to radioimmunoassay for N/OFQ peptide. (Volumes in μl)

2.4 Immunofluorescent Staining

2.4.1 Materials

Anti-Rabbit IgG FITC Conjugate Antibody (secondary antibody), Formaldehyde, Glycerol, Hanks Buffer Tablets, Sodium Azide, Polylysine, Saponin, Triton X-100, Trypan Blue, Wright-Geisma Stain - *Sigma*

Mu-opioid receptor Rabbit Polyclonal Antiserum – *Oncogene, USA*

Rabbit anti-mu opioid receptor Polyclonal Antibody (primary antibodies NHQLENLEAETAPLP and VIKALITIPETTFQ) - *Chemicon Ltd, USA*

Polyclonal Affinity purified mu-opioid Receptor Antibodies 1404/1414 (primary antibodies) - *Uniformed Services University, Bethesda, USA*

GST-C50 & GST N61 mu-opioid receptor Blocking Agents - *Uniformed Services University, Bethesda, USA*

2.4.2 Direct and Confocal immunofluorescent staining

Theory

Immunofluorescent staining relies upon the labelling of a particular region of a cell with a fluorescent antibody and allows this area to be imaged with the use of a fluorescent microscope. For example cells expressing a surface antigen of interest can be stained with a fluorescein-conjugated antibody and then imaged. This technique has been utilised to study the presence of opioid receptors on CHO cells transfected with human opioid receptors and PBMCs. The antigen in which we are interested may be demonstrated by either a direct immunofluorescent stain, or by indirect staining. In direct staining the antibody bound to the antigen is itself fluorescent, while with indirect staining a secondary fluorescent antibody is conjugated to a primary antibody, which has first been bound to the antigen of interest. During all immunofluorescent staining experiments an indirect staining procedure was used.

As well as the differences in fluorescent staining, antibodies differ in their mode of production. There are two different production methods, giving either monoclonal or polyclonal antibodies. Monoclonal antibodies are selective for only one antigen, and are produced by utilising a technique first described in 1975 by Georges Kohler and Cesar Milstein (*Alberts et al 2002, Kohler et al 1975*). B-cells are harvested from the spleen of a mouse immunised several days before with the antigen of interest. These cells are then immortalised by fusion with a myeloma cell line (fusion of B-cells with

myeloma cells tends to give rise to a stable cell line). Addition of selection media ensures the survival of only the hybridoma cells. Fused cells are then cultured at such low concentrations that culture wells contain only one original hybridoma cell, such that each well contains only one antibody. Each particular well/antibody is then screened for the presence of antibody activity to the original antigen used for immunisation. In this way antibodies highly selective for the antigen in question can be produced.

In contrast polyclonal antibodies are produced by the purification of blood taken from an individual animal injected multiple times with the specific antigen to be investigated. This technique is simpler and less costly than the production of monoclonal antibodies, but gives a mixture of antibodies that may be reactive to various portions of the antigen in question. Polyclonal primary antibodies were used during the immunofluorescent staining experiments described.

After staining of cells using one of the techniques described above cells were imaged using either direct fluorescence microscopy, confocal microscopy or flow cytometric analysis. To accomplish this all of these imaging techniques require that the fluorescent moiety or fluorophore bound to the cell is capable of absorbing light at one wavelength and emitting it at another. Imaging of any fluorophore relies on the fluorophore shifting the wavelength of incident light directed upon it to the lower energy level of the emitted light, *Figure 2.7*. In this way the specific binding of antibody (or other binding moiety) to cell antigen (receptor) can be imaged. During all of the immunofluorescent staining experiments described below fluorescein was used as the fluorescent dye, either coupled to a secondary antibody or bound directly to the opioid ligand in question.

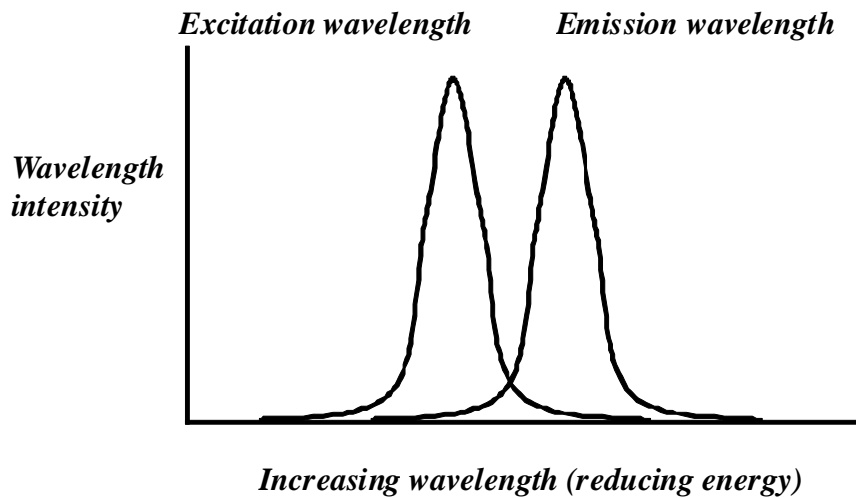


Figure 2.7.
Excitation emission spectra for a fluorophore.

Direct fluorescent microscopy uses a similar optical arrangement to a normal light microscope, however in addition it contains two barrier filters. The first of these ensures that only one wavelength of light reaches the sample to be investigated, while the second makes sure that only emitted light of the wavelength of interest reaches the viewing eyepiece, **Figure 2.8**.

Though this allows the stained antigenic regions of the cell to be visualised it unfortunately also provides information not only from the point of focus of the microscope, but in addition from areas out of focus within the three-dimensional structure. Unless very thin tissue specimens can be prepared this invariably produces a blurred image. Confocal microscopy is one form of microscopy that can overcome this problem. This technique utilises a laser set at the specific wavelength of the absorption characteristics of the fluorophore under investigation. In addition emitted light must pass through a pinhole prior to it being incident at a photo detector. This guarantees that only the image in focus will be detected. As the confocal laser passes over and through the specimen in question a sharp three-dimensional image can then be built up.

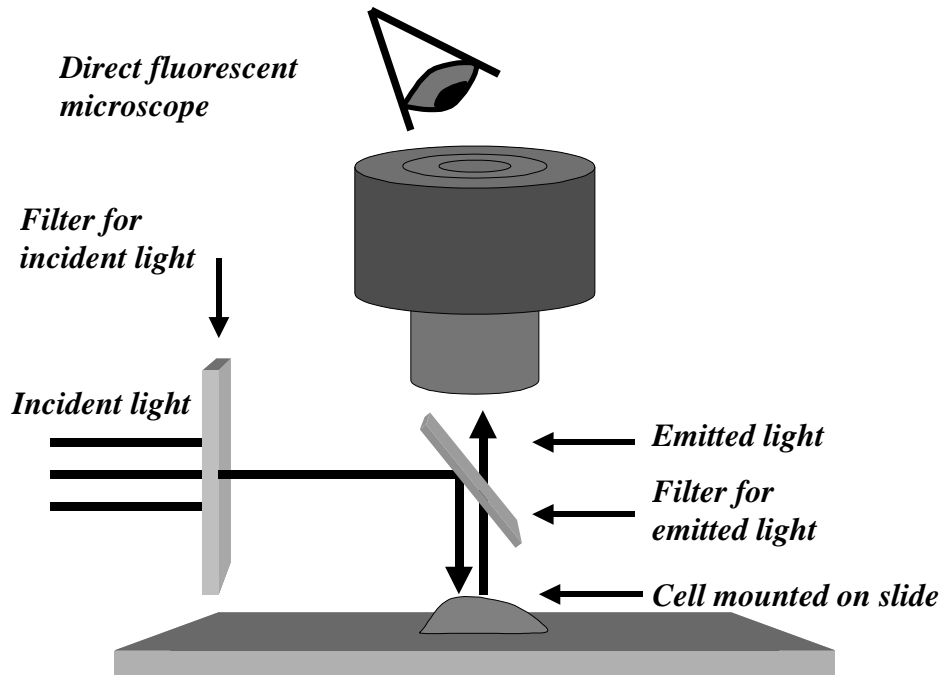


Figure 2.8.
Schematic of the arrangement for a direct fluorescence microscope.

Method

Four different polyclonal primary antibodies were used to probe for the MOP receptor on CHO_{hMOP} cells and immune cells. The antibodies are summarised in **Table 2.5**, while **Figure 2.9** gives a graphic representation of the sites of primary antibody binding. Two of these antibodies were commercially acquired, and two were provided by *T Cote* (*Chalecka-Franaszek et al 2000*) from the Department of Pharmacology, Uniformed Services University in Bethesda, Maryland USA. All four were raised in rabbits.

NHQLENLEAETAPLP, the first antibody to be used was commercially acquired and raised against the final fifteen amino acids of the MOP receptor of the rat. This region has 100% homology with the carboxyl terminal, an intracellular part of the receptor of the human MOP receptor. VIKALITIPETTFQ the second antibody used shows a 93% homology with the human MOP receptor in the region of the third extra cellular loop. This antibody was originally raised in the rabbit against rat MOP antigen.

The two primary antibodies provided by *T Cote* were numbered 1404 and 1414. 1404 was directed against the amino acids numbered 10-70 at the N-terminal of the receptor in rat and shows limited homology (about 75%) with the amino acid sequence in humans. 1414 was directed against the carboxyl terminal of the MOP receptor in rat

and corresponds to the last 50 amino acids (351-401) in man. Though raised versus rat antigen it has over 90% homology to the human receptor in this region. Both 1404 and 1414 are affinity purified, limiting the amount of contaminating antibodies. Two blocking agents GST-N61 to be used with 1404, and GST-C50 to be used with 1414 were also supplied. These compounds adhere to the regions of the receptor that the primary antibodies in question have been raised against, and so prevent binding of the primary antibody, thus allowing confirmation of specific binding.

Antibody	Amino acids to which 1^o raised	Target portion of receptor	Homology to sequence of hMOP
NHQLENLEAETAPLP	387-401	Carboxyl terminal	100%
VIKALITIPETTFQ	301-316	Third extra cellular loop	93%
1404	10-70	N-terminal	75%
1414	351-401	Carboxyl terminal	>90%

Table 2.5

Antibody, position and homology to human amino acid sequence of rat MOP receptor antibodies.

The secondary antibody used with all of the primary antibody stains described above was an anti-rabbit secondary developed in sheep. In a similar fashion to the *Cote* primary antibodies it was affinity purified. Fluorescein-isothiocyanate was the fluorescent moiety conjugated to the secondary antibody, giving maximal excitation and emission spectra at 488nm and 530nm respectively.

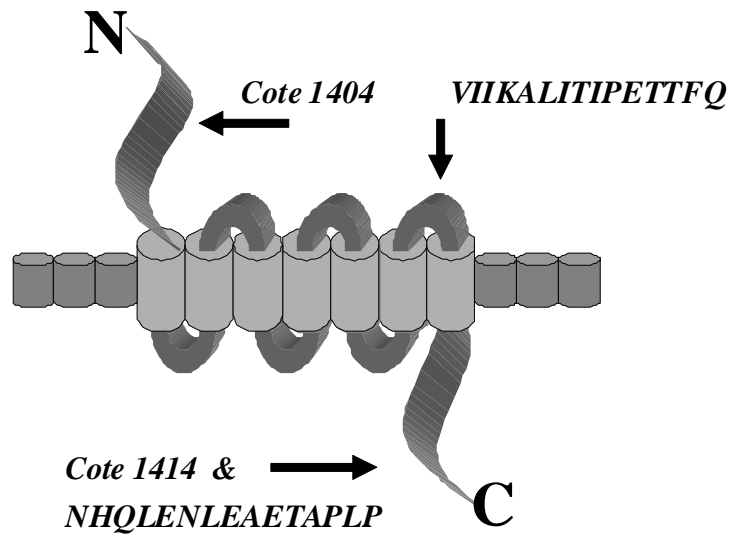


Figure 2.9.
Region of the MOP receptor to which primary antibodies bind.

In addition to immunofluorescent staining of the MOP receptor, fluorescent-naloxone was used to directly stain the receptor. It was hoped that the receptor could be stained utilizing techniques that were familiar from earlier work with radioligand binding experiments. Fluorescent-naloxone contains a large organic side chain (the fluorescent moiety) which naloxone does not, because of this a series of competition-binding studies were undertaken as described above to elucidate fluorescent-naloxone's binding characteristics at the MOP receptor.

CHO_{hMOP} cells were grown adhered to cover slips or microscope slides, stained and imaged. However PBMCs as non-adherent cells needed to be attached to slides. To achieve this venous blood was initially collected into an EDTA tube in a standard manner as described previously, before isolation of PBMCs by Ficoll sedimentation the venous blood was re-suspended in Hanks buffer solution or PBS containing 0.02% sodium azide solution to prevent cycling of the cell. Following this PBMCs were extracted as described above. First coating the cover slip in polylysine, and then allowing the cells to sediment onto it achieved adhesion of PBMCs to cover slips. The cover slip was then washed carefully by bathing in PBS. Once adhered to slides the cells were fixed by soaking in 3% formaldehyde in PBS, preventing any further cellular activity or receptor cycling within the cell. Slides were then washed in PBS

and stained first with a primary antibody and later, following a further PBS wash, with the secondary antibody. This was again followed by a PBS wash, after which the slide was mounted, ready for imaging, in glycerol:PBS 50:50 solution, **Protocol 2.2**.

1. Extract peripheral blood mononuclear cells from venous blood.
2. Dry 20µl of polylysine onto slide.
3. Allow 20 µl of PBMC preparation to sediment for at least one hour onto slide.
4. Wash x3 for 10 minutes in PBS.
5. Fix with 3% formaldehyde in PBS for 10 minutes at room temperature.
6. Wash x3 for 10 minutes in PBS.
7. Cover PBMCs in 20 µl of primary antibody at desired concentration (1:10 – 1:100), and incubate for 20 hours at 4°C.
8. Wash x3 for 10 minutes in PBS.
9. Cover PBMCs in 20 µl of secondary antibody at 1:160 concentrations and incubate for 20 hours at 4°C.
10. Wash x3 for 10 minutes in PBS.
11. Mount with glycerol:PBS 50:50.

Protocol 2.2.

Immunofluorescent Staining prior to direct/confocal microscopy

Concentration ranges of primary and secondary antibodies were taken from the manufacturer's literature. In all instances a variety of concentrations and combinations of concentrations for primary and secondary antibodies were attempted to optimise immunofluorescent staining.

A number of variations on this basic protocol were used in an effort to improve the immunofluorescent staining. The first of these was the addition of a permeabilisation step, which was thought, might improve the access of the primary antibody NHQLENLEAETAPLP to the intracellular carboxyl terminal of the MOP receptor against which it is raised. Incubating cells for 10 minutes with Triton X 0.1 % or Saponin 0.1%, before staining achieved this permeabilisation. Another incubation step was also used with 10% Foetal Calf Serum for 20 hours prior to staining to reduce non-specific binding. A wide range of variations in length of time of primary and secondary antibody staining, from 1 hour to 24 hours each were also employed in an attempt to improve staining.

For preparations, which were to undergo direct fluorescent staining with fluorescent-naloxone, cells were adhered to microscopy slides or glass cover slips as described above. Fluorescent staining was performed on ice by the addition of fluorescent-naloxone directly onto the slide (no primary stain was required). Excess fluorescent-

naloxone was washed away after 20 minutes by gentle rinsing with PBS. Non-specific binding (NSB) was recorded by the addition of naloxone (non-fluorescently labelled) in excess. Slides were imaged on ice by direct fluorescent microscopy, this technique unfortunately did not lend itself to imaging via confocal microscopy.

2.4.3 Flow Cytometry

Theory

Flow cytometry provides another means for the imaging of fluorochromes whether they are immunofluorescent stains or fluorescently labelled ligands. This procedure is commonly used in clinical practice for not only counting particular cell types as in white cell differentials and full blood counts, but also for the identification of a range of surface and intracellular markers that may be of clinical importance. After labeling with a fluorescent probe cells were resuspended in phosphate buffered saline. In the flow cytometer labelled cells were allowed to fall under the influence of gravity in a fine stream passing through a laser beam. At the same time this column of cells and carriage medium is surrounded by a concentric column of sheath fluid, normally of the same composition as the physiological buffer in which the cells are suspended. This column of fluid prevents the cells under investigation from passing out of the fluid column within which they are travelling. The laser beam is set at an energy level capable of causing excitation of the fluorophore, while a photo detector set beyond the stream of cells records the emission spectra from the cells, **Figure 2.10** (*Alberts et al 2002, Shapiro 1995*).

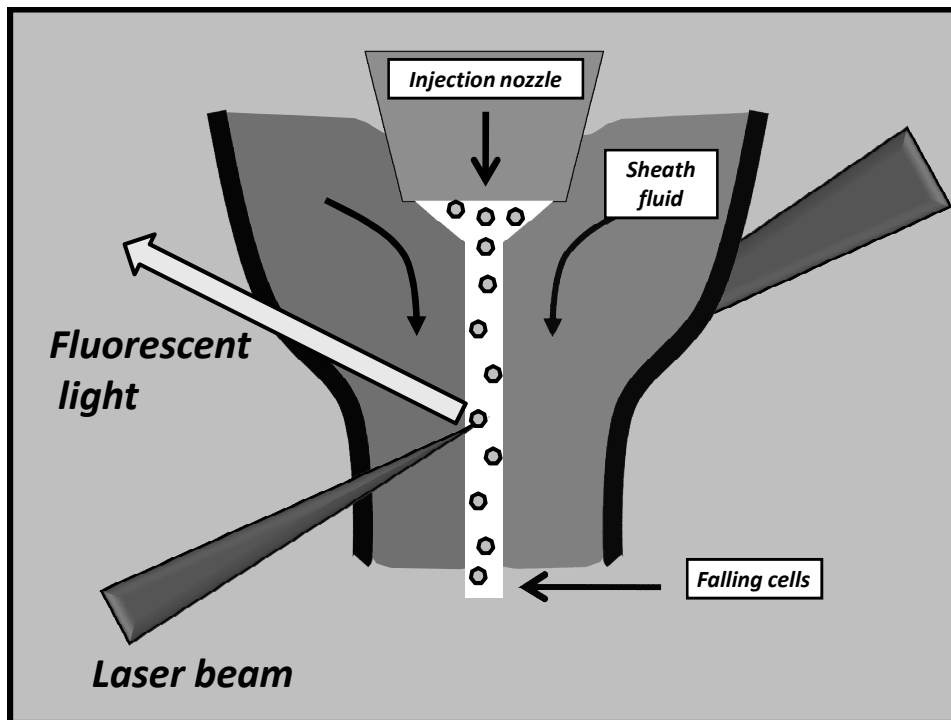


Figure 2.10. Schematic of a flow cytometer. Cells fall under gravity within the column of sheath fluid, through a laser beam causing excitation of the fluorescent particles.

In addition to the shift in wavelength of the incident light, the cell through which it passes also deflects the light in its path of transit. The degree of deflection in the forward plane is termed forward scatter and is dependent upon the size of the cell imaged, while the degree of scatter in a plane 90° to the forward plane is called side scatter and relates to the size of the cell, its surface topography and internal complexity. This allows a flow cytometer to differentiate one cell type from another. This bivariate or scattergram display can be gated to investigate only the cell type of interest. In **Figure 2.11** below cells within the R3, R4 or R5 gates could be investigated.

After this initial step the flow cytometer is calibrated with a negative unstained sample. However even this control sample will possess a degree of background fluorescence, therefore the flow cytometer is calibrated such that the control samples background fluorescence falls within the first decade log of the fluorescence intensity axis, **Figure 2.12**.

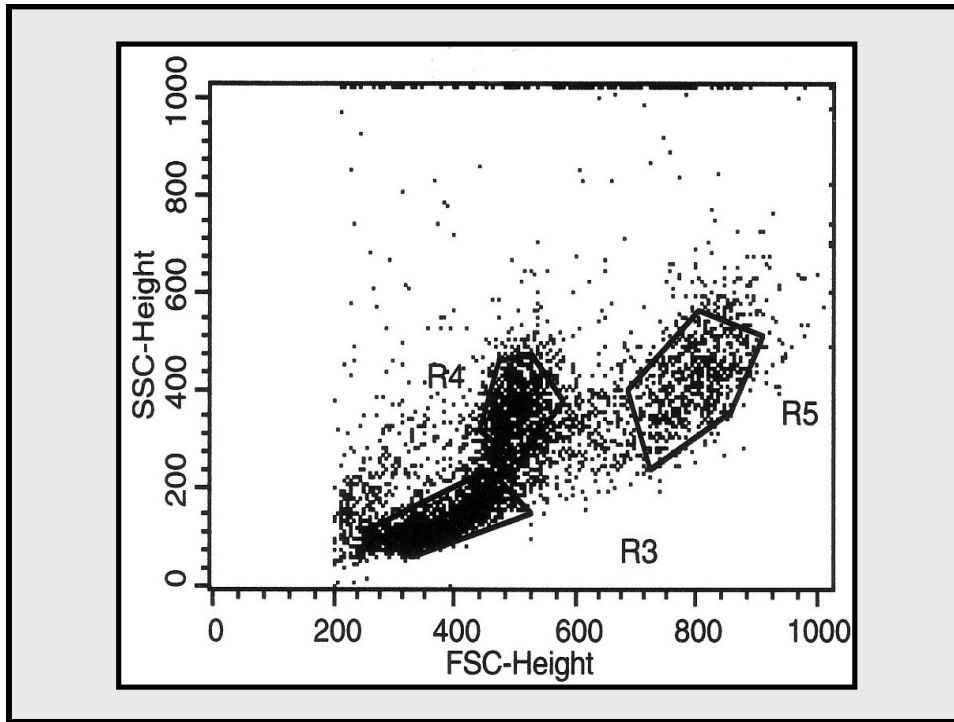


Figure 2.11.

The flow cytometer is used to concentrate (gate) on one particular cell type. In the above example this could be cells within the gates R3, R4 or R5. FSC=forward scatter, SSC= side scatter.

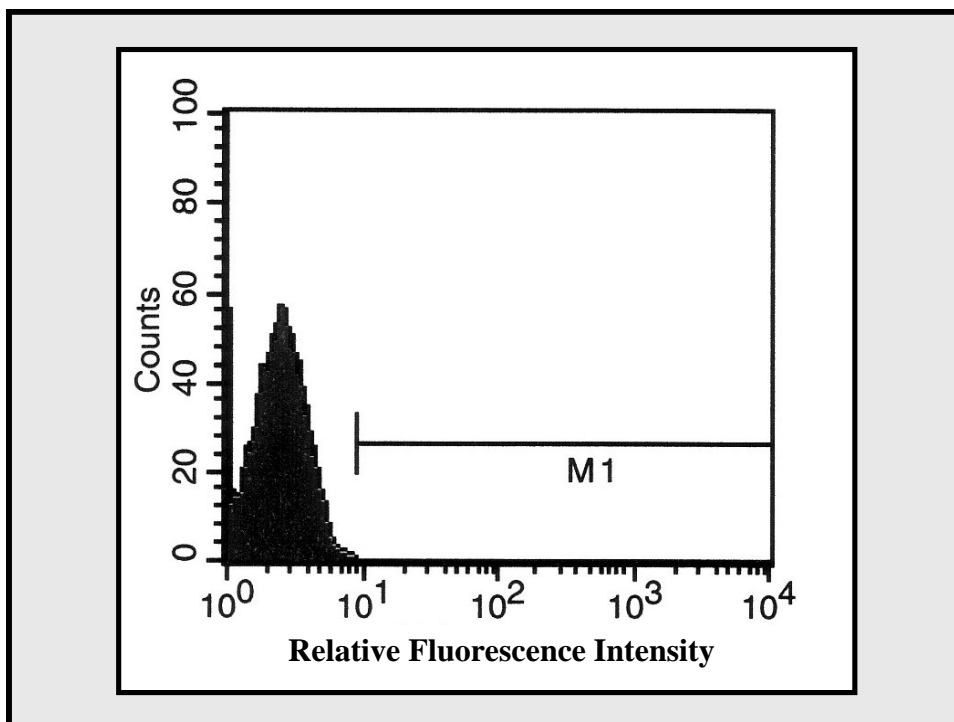


Figure 2.12.

The M1 gate of the flow cytometer is the set to read only 5% of the background fluorescence from the negative control.

The gate (M1 in *Figure 2.12*) is then adjusted until less than 5% of the background fluorescence lies within the fluorescence intensity values that it encompasses. If the sample is now stained with a fluorescent antibody there will be an increase in the relative fluorescence intensity and the histogram will move up the log scale and further into the gate M1, *Figure 2.13*. The degree of this shift in fluorescence is called the mean fluorescence intensity shift (MFI), and is an indication of the amount of fluorophore bound. By running the appropriate controls, specific antibody binding can be differentiated from non-specific binding of the antibody and the fluorescence intensity used to give an indication of the degree of specific antibody binding.

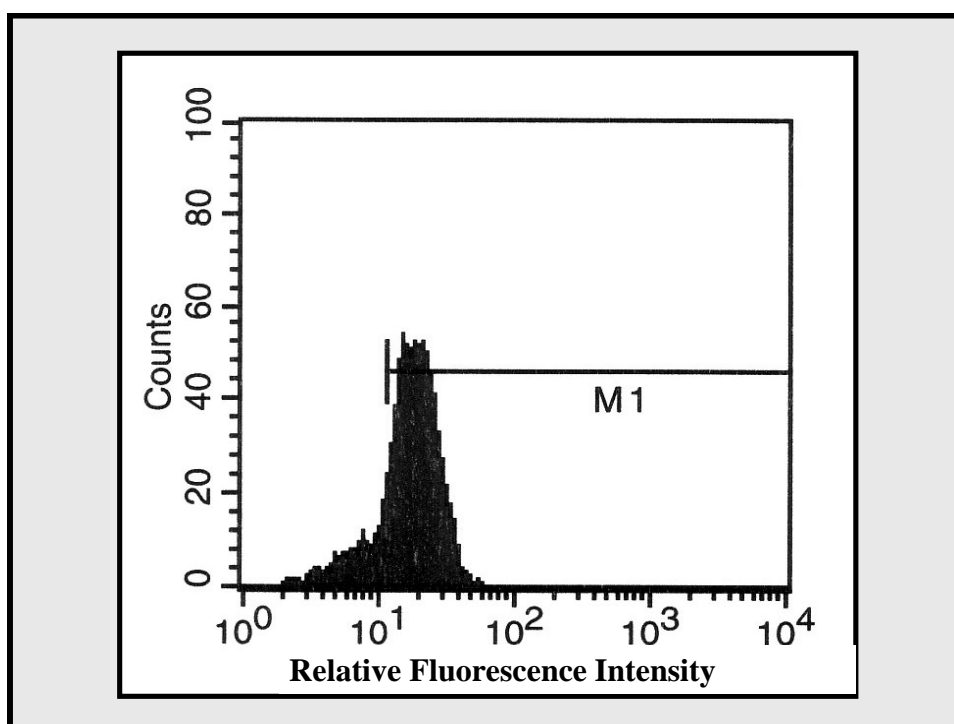


Figure 2.13.

This plot shows the shift rightward in the relative fluorescence intensity following staining of the sample with a fluorescent probe.

As has been stated above flow cytometry is widely used as a tool in clinical medicine, in laboratory investigations it has an advantage over confocal and direct fluorescent microscopy in its rapidity and ease of use. Samples do not need to be mounted on slides or adhered to surfaces, and so run less risk of degradation associated with prolonged laboratory preparations.

Method

When utilising flow cytometry to image opioid receptors all four available primary antibodies described above and fluorescent μ -naloxone were employed for staining of CHO_{hMOP} cells or PBMCs. In addition Jurkat, Raji and L1210 cells were also stained with the commercially available primary antibody NHQLENLEAETAPLP.

Cells needed to be in suspension before being passed through the flow cytometer. Recombinant adherent cells needed to be harvested (as described above in radiolabelled binding techniques) and re-suspended before staining. CHO_{hMOP} cells were though passed through a 21-gauge needle following harvesting in order to break-up any remaining large clumps of cells.

Non-specific staining was recorded by the omission of the primary antibody. Additionally flow cytometry was run with normal rabbit serum (for both commercially available polyclonal antibodies) or affinity purified IgG (for 1414 and 1404 antibodies) in the place of the primary antibody in question. This acted as a negative control and allowed confidence that the original media in which the primary antibody was suspended or produced within was not acting as a primary antibody and binding non-specifically in its own right. Immunofluorescent staining required that two staining steps were performed in the dark, both at room temperature. Similar concentrations of primary (1:10-1:100) and secondary (1:160) antibody to direct/confocal staining were employed, but only 30 minutes were allowed to elapse for the cells to be stained. Where required cells were permeabilised as described previously.

Direct staining with fluorescent-naloxone was carried out on ice in the dark for 30 minutes, followed by washing in PBS or Hanks buffer solution at 4°C, **Protocol 2.3**. Non-specific binding was accomplished by the addition of unlabelled naloxone in excess (10µM). Cell suspensions were passed through a Becton-Dickenson or Coulter flow cytometer for analysis. In the case of fluorescent-naloxone ice-cold PBS was used as sheath fluid to limit the possibility of dissociation of fluorescent-naloxone from the receptor. Mean fluorescent intensity shift was taken as a measure of both total and non-specific binding.

1. 100µl of cells suspended in Hanks buffer added to 900µl of F-Naloxone of varying concentrations (10^{-11} – 10^{-6} M).
2. Incubate in the dark for 30 minutes on ice.
3. Transfer to ice cold environment.
4. Wash on ice twice with Hanks buffer or PBS both ice cold (Centrifuge 1500rpm for 4 minutes).
5. Leave on ice prior to FACS analysis.
6. For Non-Specific Binding as above but incubate with F-Nal varying concentrations (10^{-11} – 10^{-6} M) plus Naloxone 1×10^{-5} M.

Protocol 2.3.

Fluorescent –Naloxone Stain for flow Cytometric analysis.

2.5 Polymerase Chain Reactions

2.5.1 Materials

RNA Extraction

TRI-reagent (BD,LS), Chloroform, Isopropanol, 100% Molecular Biology Grade Ethanol, Acetic Acid, Molecular Biology Grade Water, Tris HCl - *Sigma*

DNase Treatment

TURBO DNA free Kit (DNase (2U.ml⁻¹), DNase Inactivation Reagent, 10x Turbo DNase Buffer, Nuclease Free Water) – *Ambion, UK*

Reverse Transcription

Gene Amp RNA PCR Kit (Murine Leukaemia Virus (MuLV, 50U.μl⁻¹), RNase Inhibitor (20U.μl⁻¹), dNTP's (10mM), MgCl₂ (25mM), Oligo d(T)₁₆ (50μM), 10x Reverse Transcriptase Buffer) - *Applied BioSystems, UK*

Gel based Endpoint PCR

JumpStart Taq Readymix, PCR 100bp Low Ladder - *Sigma*

DNA Gel Loading Buffer, 10x – *Eppendorf, UK*

Agarose – *BioPur, UK*

Primers (100μM, stored at 20μM -20°C) – *Various*

Ethidium Bromide, 50x TAE Buffer (2M Tris-Acetate, 50 mM EDTA, pH 8.3) – *Fisher*

RNA Integrity Gels

MOPS buffer (200 mM MOPS, 50 mM Sodium acetate, 10 mM EDTA, pH 7.0), 37% Formaldehyde, Formamide, RNA Sample Loading Buffer, - *Sigma*

Quantitative PCR

2x SYBR Green Jumpstart Taq Readymix - *Sigma*

TaqMan® Gene expression assays (Hs00538331_m1, Hs00175127_m1, Hs00168570_m1 and Hs00173471_m1) – *Applied BioSystems*

2.5.2 Endpoint PCR

Theory

The techniques of radioligand binding and fluorescence microscopy described above provide mechanisms for imaging receptors on cell lines of interest. However in many of the cells investigated in this thesis receptor density was not of sufficiently high number for these imaging techniques to prove useful, or the tissue type investigated did not lend itself to investigation by these means. In both of these scenarios polymerase chain reaction (PCR) was used to look for the genetic code for the receptor. This allowed data to be acquired regarding receptor and peptide presence, both at the genomic level, with data obtained about the deoxyribonucleic acid (DNA) sequence present within a particular cell, or to study the expression of the genomic message through the messenger ribonucleic acid (mRNA) signal for a particular cellular product.

Every cell within an organism contains the complete genomic (DNA) message for that particular organism, however each type of cell will synthesize a range of proteins and associated cellular products that are dissimilar from the products of another cell type within the same organism (such that a human skeletal muscle cell will produce the proteins actin and myosin, which are involved in muscle contraction but not prolactin a protein produced in the anterior pituitary and associated with lactation. This is despite both cells containing the exact same genomic DNA sequence.). To accomplish this each cell type converts only certain particular parts of the genomic message into mRNA, which will then itself in turn be translated into the protein of interest. By utilising the techniques described below for the isolation of the RNA message from DNA and the amplification of this message by PCR, it is possible to investigate the presence of not only the genomic DNA message, but also the expression and conversion of this message to mRNA in cells (a disadvantage of this is that the magnitude of change in mRNA expression is not necessarily the same as the change in the protein produced in the cell). As PCR methods incorporate amplification steps of the genomic or mRNA message in the order of a billion fold, the presence of receptors and their peptides on and in cells with only very low expression can be found. Investigation of these cell types would not be amenable to the conventional imaging techniques of radioligand binding and fluorescence microscopy.

PCR was first used in 1983 by Kary Mullis, a scientific advance for which he later received a Nobel Prize (*Galley et al 1999, Saiki et al 1986*). When any cell replicates

the whole genome must be faithfully copied, this initially requires the conversion of the original double stranded DNA into single DNA strands. The enzyme DNA polymerase then acts upon these single strands of DNA to bind deoxyribonucleotides and construct a complementary sequence for the single DNA strand. In the human body this occurs at 37°C and with a very high degree of fidelity. Two major advances made PCR possible. The first of these was the discovery of a heat stable DNA polymerase enzyme from *Thermus Aquaticus* (Taq DNA polymerase) isolated from hot springs. This allowed the repeated and rapid replication of DNA strands at high temperatures at which human DNA polymerase is not stable. The second advance was the production of precise and efficient thermal cyclers, capable of heating and cooling to specific temperatures at rapid rates.

To perform PCR two sets of DNA oligonucleotide primers are designed to compliment the DNA sequence. These oligonucleotides are short portions of the DNA code, which have been chemically synthesised to exactly match a small portion of the parent DNA molecule and to bound the area of the genetic code that is of interest,

Figure 2.14.

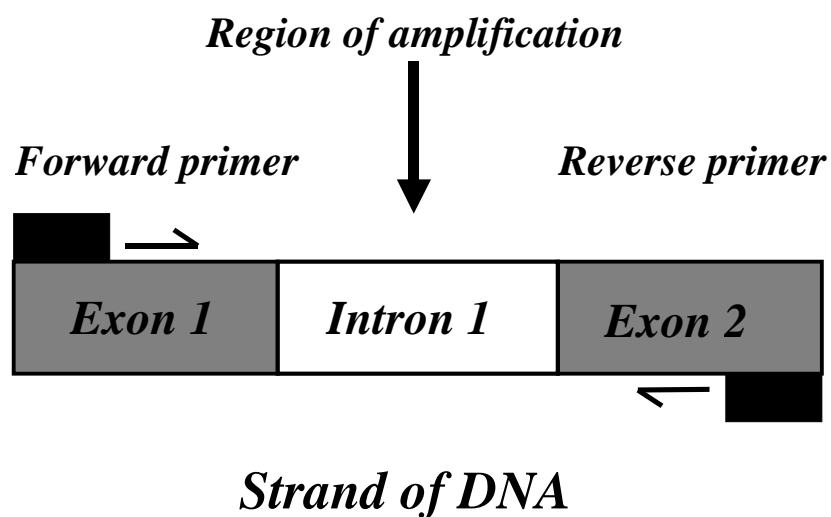


Figure 2.14.

Schematic diagram showing the region of amplification. Arrows show direction of primer movement. The region between the two primers is amplified.

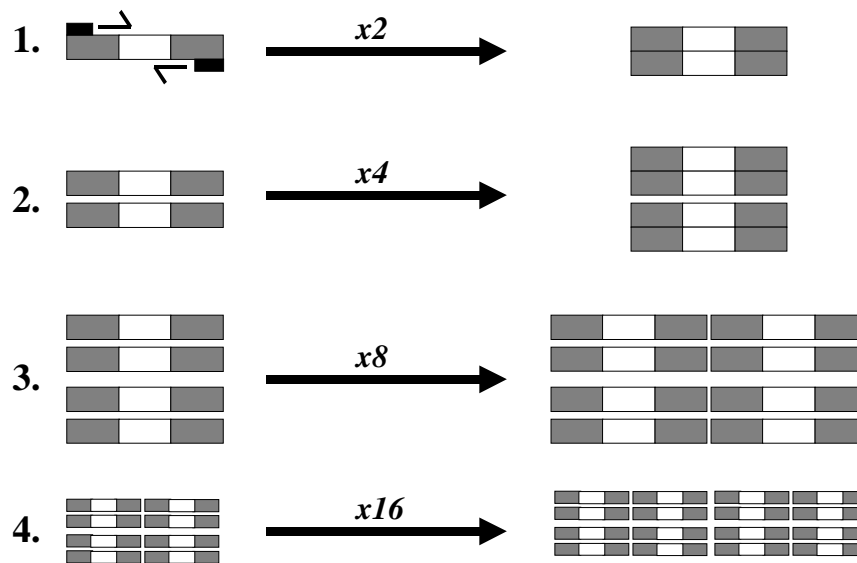


Figure 2.15. Amplification steps in polymerase chain reaction amplification of an initial template.

Figure 2.15 Step 1 shows the initial annealing of primers to a piece of single stranded DNA and subsequent elongation of a new complimentary strand of DNA. Steps 2-4 then show additional amplification of the DNA product, illustrating the rapid increase in DNA product after only 4 cycles of PCR.

The amplified DNA product can then be imaged, by allowing it to migrate through an agarose gel containing ethidium bromide. The ethidium bromide binds to the DNA and can be visualised by exposure to an ultraviolet light. By comparison to a DNA ladder of known mass run on the same agarose gel, a mass for the amplicon can be calculated, and compared to the expected mass from knowledge of the DNA or RNA sequence of interest and the positions of the primers used.

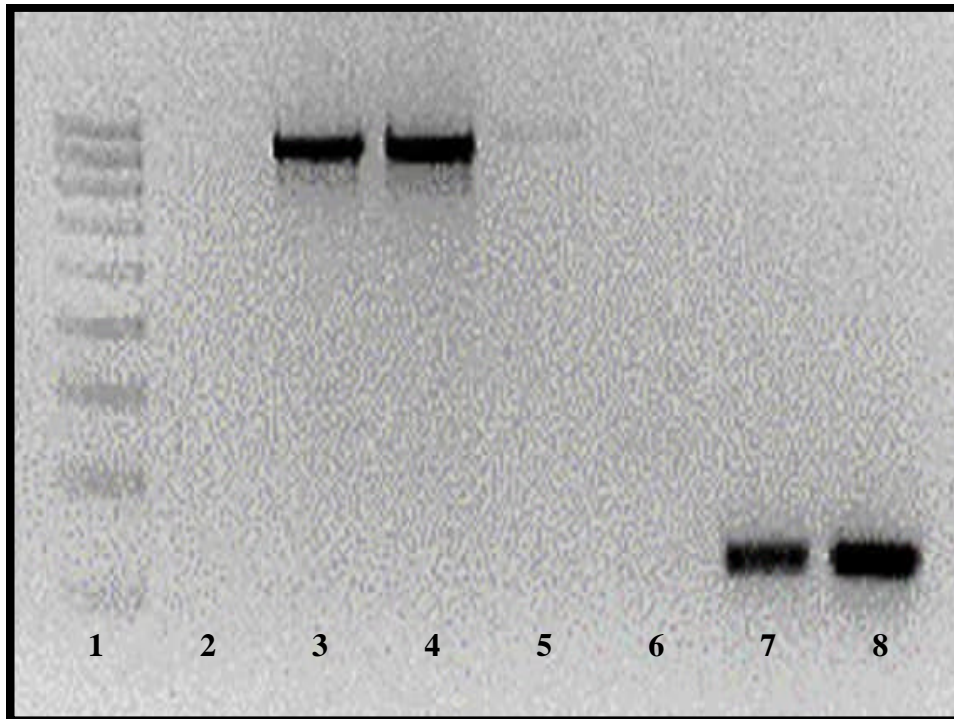


Figure 2.16.
Typical 3% agarose PCR gel stained with ethidium bromide.

Figure 2.16. is an example of an agarose gel stained with ethidium bromide. To the left hand side of the gel is a DNA ladder which decreases in size by 100 base pairs from the top of the gel to the bottom, such that the first band corresponds to a weight of 1000 base pairs the second band 900 base pairs, the third 800 base pairs and so on. PCR amplification products are seen in the third, fourth, seventh and eighth lanes. The products in lanes three and four have weights between 900 and 1000 base pairs, while those in lanes seven and eight have weights of between 300 and 200 base pairs.

Below **Figure 2.17** graphically shows the relationship between distance travelled by a PCR amplicon and its weight in base pairs. As can be seen from this image, as the amplicon becomes smaller and so lighter its transit distance through the agarose gel increases in a logarithmic fashion.

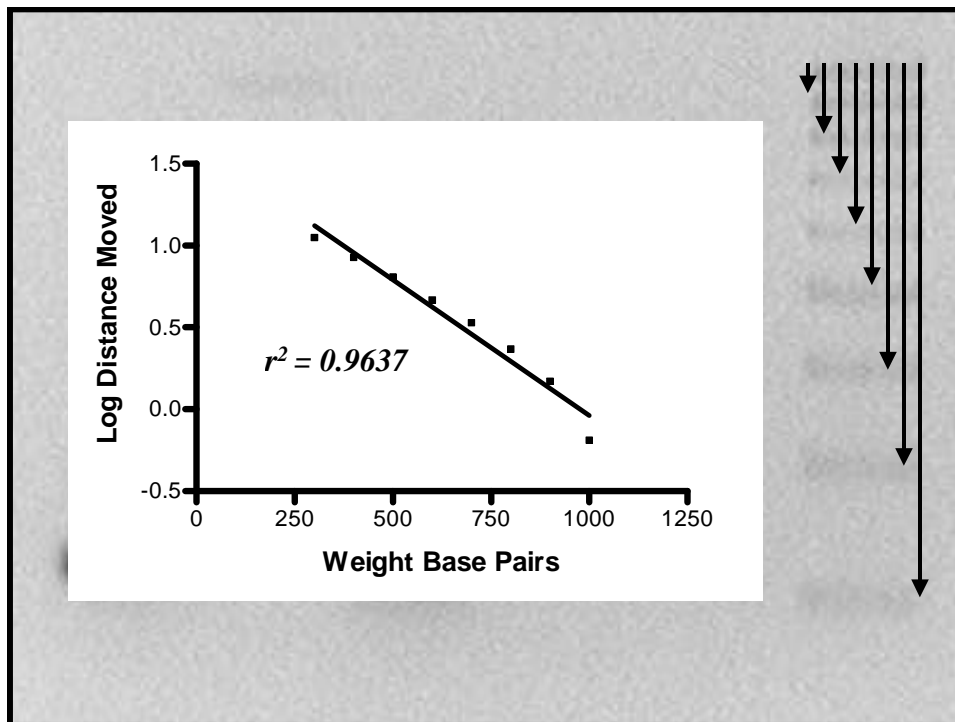


Figure 2.17.

This graph shows the correlation between weight of the amplicon and the distance moved through the 3% agarose gel. Heavier amplicons move less far than lighter amplicons and this relationship has an inverse logarithmic relationship.

The above provides a description of an experimental technique that is frequently used to investigate the genome in living cells. PCR and molecular biological technologies can also supply information about changes in the level of expression of a particular part of the genetic code in varying states and physiological conditions within a cell. The DNA in any cell contains the basic code from which all elements of that cell can be constructed as described above. mRNA can be isolated from a cell by the use of a phenol/chloroform extraction technique and converted to its complementary DNA (cDNA) by the action of a reverse transcription enzyme, these are usually retroviral in origin (*Chomczynski 1993*). The cDNA copy can then be used for further downstream PCR reactions. This provides a powerful technique whereby the immediate precursor of any proteins of interest, RNA, can be amplified, imaged and possibly quantified, so giving information about levels of expression of the genetic code. There is however no guarantee that the presence of RNA at the intracellular level relates to receptor expression at the cell membrane.

The chemical composition of RNA differs subtly from that of DNA, however a more substantial difference between the two lies in the absence of introns from the RNA sequence. This difference in the make up of DNA and RNA can be utilised in PCR to

differentiate the two. DNA contains areas of the genome, which code for the production of proteins, these are called exons, but also large sequences of DNA called introns lie between the exons and seem to code for nothing, **Figure 2.18 A**. The RNA sequence on the other hand is composed solely of exons, the introns rapidly being discarded after RNA is produced, **Figure 2.18 B**. If primers are chosen to sit on different exons then the product from amplification of pieces of DNA will be longer than that from RNA, as the introns in the DNA will be included in the portion of genetic code that the Taq polymerase acts upon. Often the intron will be of such a significant length that the DNA message will fail to be amplified and only the RNA message will be found. In this way any residual genomic DNA left in the sample following conversion of RNA to cDNA can either be ignored or discounted from the final agarose gel analysis.

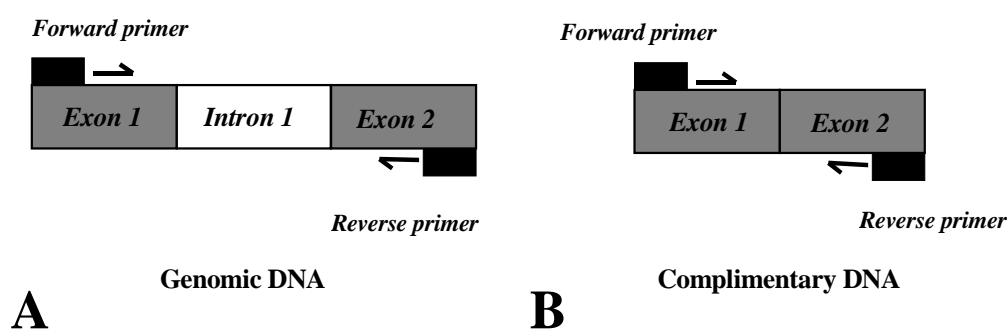


Figure 2.18.
 Diagram of primer binding to template DNA across an intron

Clearly an important consideration in PCR is to make sure that only the region of DNA we are interested in is amplified. To ensure this primer pairs must be carefully designed for PCR to effectively and accurately amplify the region of interest. Primers are made so that they will hybridise to the two different strands of DNA, and are termed sense and antisense primers, giving amplification of the DNA in convergent directions; this results in only one homogenous type of amplicon. A variety of primers have been used to look at opioid receptors and their peptide ligands in *in vitro* cell lines, *ex vivo* cells and *ex vivo* tissue from both man and rodents. However all of the primers used to look for opioid receptor expression in man were initially verified, and experimental conditions optimised in Chinese hamster ovary cells transfected with and stably expressing the receptor in question, before use in human cells and cell

lines. Experimental conditions for the primers for the human NOP peptide were optimised in *ex vivo* tissue, as no cell model was available.

When designing primers it is desirable that the primer has the following characteristics:

- The primer should be between 18-24 base pairs in length.
- The 5' end and central regions should be high in GC residues.
- However the 3' region should not be rich in GC residues.
- Complementary sequences and mismatches of the 3' end should be avoided.
- 40-60% of the residues should be GC in nature.
- The potential to form an internal secondary structure should be avoided.
- The T_M , melting temperature, of the primers should preferably be close in value, only about 5°C apart.

The melting temperature describes the temperature at which half of the primer is present in its duplex form with the complementary sequence. This will dictate the annealing temperature for the system. High annealing temperatures mean higher specificity while lower temperatures give more efficient annealing. Annealing temperatures are set 5°C beneath the T_M as a rule of thumb. The T_M can be calculated from the structure of the primer concerned either by using a simple formula, which looks at the nucleotides of the primer, or more accurately by a calculation called the nearest neighbour calculation. This takes into account not only the nucleotide content of the primer but also the order in which the nucleotides are arranged (*Innis et al 1990*).

Method

A variety of RNA extraction kits are commercially available, and though these gave high yields and purity of RNA from cultured cells in a relatively short time, they provide lower yields and poor quality returns from the smaller quantities of PBMCs and blood which were available. Therefore though more laborious a phenol/chloroform extraction technique was favoured over the commercially produced kits. Using this technique cells are lysed in a phenol/guanidine thiocyanate solution (TRI Reagent, *Sigma*), addition of chloroform then results in three phases, the aqueous phase which contains RNA. This is extracted and precipitated by mixing with isopropanol and then ethanol. Different grades of TRI-Reagent were used for different types of tissue. If cell number allows and RNA yield is expected to be high a second phenol/chloroform extraction step was included to improve purity. **Protocol 2.4** below summarises this technique.

1. Perform in RNase clean fume hood.
2. Add 1ml of TRI-reagent to pelleted cells and mix. Allow to stand at room temp. for 5 minutes.
3. To this mixture add 200 μ l of chloroform. (Note should be stored in dark/ corrodes plastic). Mix thoroughly by vortexing for 2 mins until milky solution produced. Allow to stand for 3+ minutes at room temperature.
4. Centrifuge at 13000rpm for 15 mins. At 4 °C.
5. Remove upper aqueous layer and transfer this to a clean RNase free 2.5ml Eppendorf tube.
6. Add 500 μ l of TRI-reagent followed by 100 μ l of chloroform.
7. Again mix thoroughly by vortexing for 2 mins.
8. Allow to stand at room temp. for 3 mins.
9. Centrifuge at 13000rpm for 15 mins. At 4 °C.
10. Remove upper aqueous layer and transfer this to a clean RNase free 2.5 ml Eppendorf tube.
11. Add 500 μ l of isopropanol and mix.
12. Leave to stand for 10 mins. At room temp.
13. Centrifuge at 13000rpm for 10 mins. At 4 °C.
14. Discard supernatant and re-suspend pellet in 1 ml of 70% ethanol. (Very difficult to get pellet to re-suspend).
15. Centrifuge at 13000rpm for 15 mins. At 4 °C.
16. Discard supernatant and air-dry pellet.
17. Re-suspend in appropriate volume of PCR grade water or Tris-EDTA. (approx. 30-100 μ l).

Protocol 2.4.

Extraction of RNA from cellular matter using a trireagent/chloroform technique.

If RNA was extracted from whole blood rather than a cellular component of blood a similar extraction was followed. Initially however 0.75ml of TRI-reagent BD (*Sigma*) and 20 μ l of 5N acetic acid was added for each 0.2ml of blood. 200 μ l of chloroform was then used per 0.75ml of TRI-BD used. RNA extracted from cells was either stored at -70°C or immediately converted to cDNA using an available kit (MuLV, *Applied BioSystems*). This reaction was performed in the presence of a mixture of deoxyribonucleoside triphosphates, reaction buffer, magnesium chloride and random sequence oligonucleotides. **Protocol 2.5** describes the reagents and methods used when employing the reverse transcription kit for the production of cDNA from RNA. In most instances a negative control was also produced with the reverse transcriptase omitted.

Protocol 2.5.

A maximum mass of 2 μ g of RNA was reverse transcribed in a preparation consisting of: MuLV (50U. μ l⁻¹), RNase inhibitor (20U. μ l⁻¹), dNTP's (10mM), MgCl₂ (25mM), Oligo d(T)₁₆ (50 μ M), RT buffer and RNA with a final volume of 20 μ l. Reactions were incubated for 10 min at 25 $^{\circ}\text{C}$, 30 min at 44 $^{\circ}\text{C}$ and finally 2 min at 99 $^{\circ}\text{C}$. cDNA samples were stored at -20°C prior to further analysis.

In certain experiments genomic DNA caused contamination of the extracted RNA, it was therefore necessary to add an additional step in the extraction of the RNA to eradicate the gDNA prior to RNA reverse transcription to cDNA. This was achieved by using a commercially available DNase kit (*Ambion TurboDNase*®) **Protocol 2.6.**

Protocol 2.6.

RNA was treated with DNase in a reaction comprising a maximum of 10 μ g of RNA, with 1 μ l of TurboDNase, 5 μ l reagent buffer and molecular biology grade water to a total reaction volume 50 μ l. Reactions were incubated for 30 min at 37 $^{\circ}\text{C}$. The reaction was then terminated by the addition of 5 μ l of DNase inactivator at room temperature for 2 min. This mixture was then centrifuged at 10,000g at room temperature for 1.5 min and the supernatant removed and stored at -20°C .

Protocol 2.7 was followed for standard endpoint PCR, with **Table 2.6** giving the components of the PCR mastermix. Different primers required different cycling

profiles. In a 50 μ l reaction mix 2-4 μ l of template was added and run for between 30-40 PCR cycles. Optimal annealing temperatures and times, if not known, were found by running new primers at from 5 $^{\circ}$ C below their melting temperatures and at a gradient of temperatures. An Eppendorf Mastercycler Gradient was used for all of the thermal cycling reactions.

Reagent	Volume
Water	105 μ l
JumpStart Taq Readymix	125 μ l
Forward Primer (10 μ M)	5 μ l
Reverse Primer (10 μ M)	5 μ l
Total	240 μ l (48 μ l per run)

Table 2.6.
Components required for polymerase chain reaction.

1. 48 μ l of mastermix aliquoted into PCR tubes	
2. 2 μ l of cDNA or gDNA template added to each tube	
3. PCR reaction mix heated in thermal cycler	
4. 95 $^{\circ}$ C 3 min	
5. 95 $^{\circ}$ C 20sec	
6. 64 $^{\circ}$ C 30sec	} 35 cycles
7. 72 $^{\circ}$ C 30sec	
8. 72 $^{\circ}$ C 10 min	
9. 4 $^{\circ}$ C Hold	

Protocol 2.7.
Example of regime for endpoint PCR

19 μ l of each PCR amplicon was then added to 1 μ l of DNA loading buffer (Sigma) and this mixture pipetted into one of the wells of a 3% agarose gel made in 1% TAE buffer containing 5 μ l/100ml of ethidium bromide. This gel was submerged in 1% TAE buffer in an electrophoretic cell, and run at approximately 100V for 45 minutes. Gels were imaged using an UV light illuminator. A DNA ladder was run concurrently with the PCR amplicons to give some indication of amplicon length.

1. Prepare 200 ml of 10× MOPS buffer (200 mM MOPS, 50 mM Sodium acetate, 10 mM EDTA, pH 7.0) using DEPC-H₂O, autoclave and store at room temperature in the dark.
2. Prepare 500 ml of 1× formaldehyde gel running buffer:
 - 50 ml 10× MOPS buffer
 - 10 ml 37% formaldehyde (FA)
 - 440 ml DEPC-H₂O
3. Prepare a 1.2 % formaldehyde gel:
 - dissolve 0.6 g agarose in 5 mL 10× MOPS buffer and 45 mL DEPC-H₂O
 - heat to melt
 - cool to ~65 C
 - add 900 ul 37% formaldehyde and mix well (perform this inside a fume hood, do not breathe FA vapours)
 - pour onto gel support
 - prior to running the gel, equilibrate in 1× FA gel running buffer for > 30 min.
4. Prepare samples & run gel:
 - add RNA (1.5-3 µg) to 1.2 µl 10× MOPS buffer, 1.7 µl formaldehyde, 5 µl formamide and DEPC-H₂O up to 10 µl
 - heat to 65 °C for 5 minutes
 - add 2 ul of 6x loading dye solution and load on gel
 - run gel at 5 V/cm for approximately 40 minutes inside a fume hood (do not breathe FA vapours)
 - stain gel in 0.5 ug/ml EtBr for 15 minutes
 - destain in DEPC-H₂O for > 1 hour
 - visualise under UV.

Protocol 2.8.

Protocol for the formaldehyde gel analysis of RNA integrity.

Extracted RNA from cells was also analysed by biophotometry to ensure RNA quality and elucidate quantity. ($A_{260/280}$ values exceeding 1.7 were generally obtained). Further analysis using electrophoretic RNA denaturing integrity gels was also undertaken, ***Protocol 2.8.*** Clear ribosomal bands at 18S and 28S, confirming that RNA had been extracted were sought.

2.5.3 Quantitative PCR

Theory

The standard endpoint PCR methods described above can be usefully employed to provide the investigator with a straightforward answer as to whether a particular gene is expressed or not. However though visual calculation of amplicon density and comparison to a known quantity of reference material can and have been used to allow inferences to be made regarding the relative abundance of a gene, endpoint PCR is generally considered to be a less powerful tool for following changes in gene expression. Quantitative polymerase chain reactions (QPCR) are more commonly used to follow this type of variation and in this thesis QPCR has been used in conjunction with endpoint PCR to look for variations in gene expression.

The main difference between endpoint PCR and QPCR is that QPCR provides information after each amplification cycle allowing for incremental increases in amplicon production to be seen. Its quantitative nature also allows for comparison of the starting amount of template of interest to a known standard. This can be used to give some insight into the original mass of template and how it changes in a variety of settings. A number of chemistries can be used to achieve this comparison, however in the experiments described below either a SYBR green fluorescence system or *TaqMan*[®] probes have been used. SYBR green is a dye that binds to double-stranded DNA, which is added to the reaction mixture. Upon the formation of double stranded DNA SYBR green will bind to the DNA and emit a strong fluorescent signal. Therefore greater and greater fluorescence is observed after each progressive amplification cycle. A disadvantage of this type of quantification is however the non-specific nature of the binding of SYBR green to any double stranded DNA present. Therefore the production of dimeric primer compounds, other double stranded amplification products or contaminating genomic DNA needs to be minimised.

Another way to study changes in amplicon production during QPCR is to use a hydrolysis probe technique such as *TaqMan*[®]. Rather than following the production of double stranded DNA by direct binding of a fluorescent probe this system looks at the polymerase chain reaction itself. In addition to the traditional forward and reverse primers of endpoint PCR, hydrolysis probe reactions rely on a third primer, which binds downstream to the forward primer. This probe labeled as the *TaqMan*[®] probe in **Figure 2.19** contains two fluorophores, one at either end of the probe. A reporting

fluorophore sits at the 5' end, while a quencher fluorophore is attached to the 3' end. In the resting state the quencher fluorophore absorbs the reporters fluorescence. During the amplification cycle the probe is however displaced and hydrolysed. The free reporter fluorophore is now, without the close presence of the quencher, allowed to fluoresce freely. Each subsequent amplification cycle will release more reporter dye and lead to greater fluorescence, **Figure 2.19**.

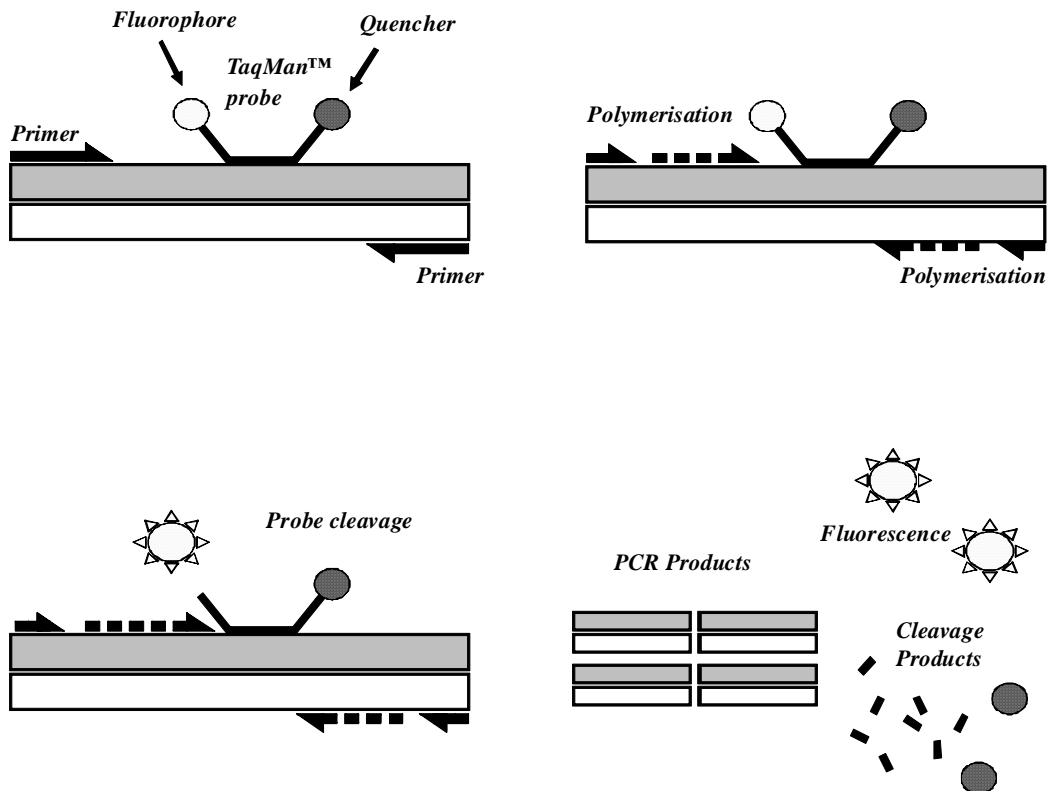


Figure 2.19. Schematic showing the process of amplification and probe cleavage during QPCR with a *TaqMan*® probe system.

Both of these techniques provide a mechanism for following the change in amplicon production during QPCR cycle on cycle. However each QPCR system will provide its own background fluorescence. Any emission from either SYBR green or *TaqMan*® probes will only be recordable once this background has been exceeded. This level of detection is referred to as the threshold line and the amplification cycle at which this occurs the cycle threshold or C_T , **Figure 2.20**.

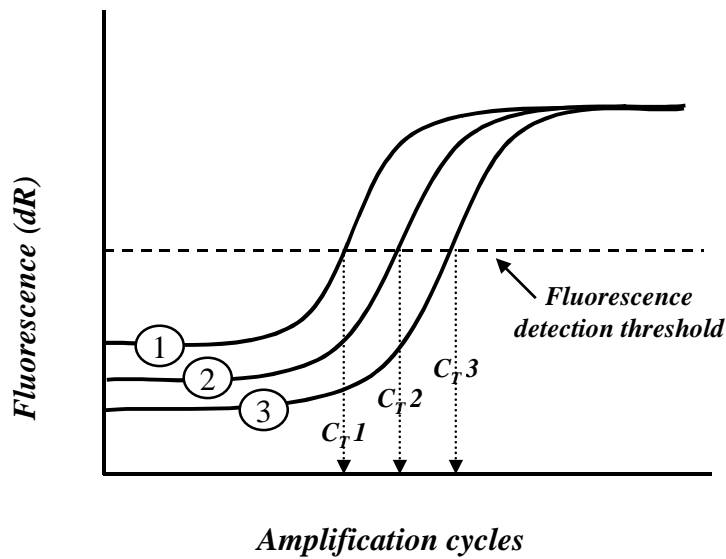


Figure 2.20.

Schematic showing the different number of cycles required to be completed before fluorescence rises above the detection threshold, with varying amounts of starting template. Plot 1 has the greatest amount of template and so fluorescence rises above the detection level at the lowest number of cycles, while plot 3 has the lowest initial template mass and so requires the greatest number of amplification cycles to pass the detection threshold.

It is assumed that there is a linear relationship between the amount of DNA present and fluorescence and that amplification is one hundred percent efficient between cycles. If these two criteria are met then it is possible to compare the initial amounts of cDNA used in differing QPCR reactions by recording the C_T values for each reaction. A higher C_T value will relate to a lower initial starting mass of DNA. **Figure 2.20** shows a schematic of a QPCR amplification plot with differing amounts of initial DNA copy. Sample 1 has the highest number of DNA copies and so reaches the threshold level in the least number of amplification cycles (the lowest C_T value).

QPCR can give absolute values for the amount of starting DNA if compared against a known amount of DNA. However more commonly the abundance of DNA of a gene of interest is compared to the abundance of a reference gene, or housekeeping gene. This approach requires that the housekeeping gene be expressed at a consistent level between states of interest (such as inflammatory conditions and non-inflamed states). Though this technique will not allow for the absolute quantity of starting DNA to be calculated it can be used to semi-quantitatively track changes in the expression of genes in which we are interested over a variety of conditions (*Bustin 2000, Bustin et al 2005, Dheda et al 2004, Hoorfar et al 2004*).

Method

Quantitative real time PCR (QPCR) reactions were run using a commercially available *TaqMan*[®] Gene expression assay from Applied Biosystems or using primers designed in house and SYBR green fluorescence probes. cDNA from PBMCs and venous blood samples from healthy volunteers and various CHO transfected cell lines and SH-SY5Y cells (as positive controls) were used as templates. cDNA was extracted from these cells using **Protocols 2.4-2.6** described above.

QPCR reactions using *TaqMan*[®] Gene expression assays were performed using the following thermal profile,

- 95°C for 10 minutes
- 40 cycles of 95°C (15s) then 60°C (1 min)

Protocol 2.9.

SYBR green based expression assays had the below thermal profile,

- 95°C 10 minutes
- 40 cycles of 95°C (30s), 57°C (1 min), 72°C (30s)
- 95°C (1min)
- 55°C hold

Protocol 2.10.

QPCR reactions were performed using a Stratagene Mx4000 machine and inbuilt software. Assays were capable of differentiating gDNA from cDNA by virtue of primers being located on different exons. A deflection from the baseline before the 35th cycle of amplification was considered significant for QPCR. The *TaqMan*[®] Gene expression assay was purchased as a ready optimized pre-formulated assay (20x mix) containing 2 unlabelled PCR primers (900nM each final concentration) and 1 FAM[™] dye labelled *TaqMan*[®] probe (250nM final concentration). This mixture only required the addition of MgCl₂ (final concentration 4mM), cDNA and water. The Taq polymerase used in SYBR green QPCR came as a complete reaction mix to which only cDNA, water and forward and reverse primers needed to be added. A ninety-six well plate was typically used for analysis with components of each well as listed in **Table 2.7 & 2.8** dependent on analysis technique employed.

Component	Volume (µl)
<i>TaqMan</i> ® Universal PCR Master Mix	25
<i>TaqMan</i> ® Gene expression assay x20	2.5
MgCl ₂	4
cDNA	X
H ₂ O	18.5-X
Total volume	50

Table 2.7.

Components used for QPCR with *TaqMan*® probes.

Component	Volume (µl)
SYBR green PCR Master Mix	12.5
Forward primer	2
Reverse primer	2
cDNA	X
H ₂ O	8.5-X
Total volume	25

Table 2.8.

Components used for QPCR with SYBR green probes.

2.6 Data Analysis

All data in this thesis are expressed as mean \pm standard error of the mean (sem), from n experiments performed as single points or as duplicates. All curve fitting was performed using *GraphPad PRISM V3.0* (San Diego). Where appropriate differences in binding affinity were compared using Student's t -test (*GraphPad PRISM V3.0*) with $P \leq 0.05$ being significant.

For saturation and displacement binding assays results were analysed using *GraphPad PRISM V3.0* to show saturation curves and sigmoid binding curve. From these values B_{\max} and K_D were derived. In displacement curves, IC_{50} values were calculated using the Cheng-Prusoff equation, as described above. For $GTP\gamma[^{35}S]$ assays results were presented as maximal stimulation of binding (E_{\max}) and potency (pEC_{50}).

For the analysis of plasma N/OFQ concentration in septic patients numerical data are presented as medians (interquartile range) unless otherwise stated. Comparisons between patient groups were made using the Mann-Whitney test. Tests of correlation were made using the two-tailed Spearman rank test. A p value < 0.05 was considered to be statistically significant.

Chapter 3:

MOP Opioid Receptor Expression in Peripheral Immune Cells

3.1 Background

The initial drive to study MOP receptors on lymphocytes was to develop a working laboratory system with which to observe changes in MOP opioid receptor. This would allow a peripheral and easily harvested clinical sample to be obtained following administration of clinically significant opioids and equated to the central effects of opioid administration. Additionally it was hoped that changes in MOP receptor density and expression on immunocompetent cells could be equated to the depression in immune cell function commonly reported in the literature, upon administration of opioid-based analgesic agents.

Previous studies suggested that MOP receptors were present on the cell surface of a range of white blood cells in man and significantly were also present on peripheral blood mononuclear cells (PBMCs) (*Cadet et al 2001, Caldrioli et al 1999, Chuang et al 1995b, Mehrishi et al 1983*). MOP receptors have been reported on these cells using a variety of experimental techniques, radioligand binding, immunofluorescent staining and binding of fluorescently labelled ligands. In addition the ribonucleic acid (RNA) encoding for the MOP receptor has been reported on PBMCs using techniques employing the extraction of RNA and conversion to the more stable cDNA using reverse transcription polymerase chain reactions. It was hoped that these experimental methods could provide not only evidence of the presence of MOP receptors on leukocytic cell lines but could also be used to look for quantitative changes of the receptor on these cells and of the RNA message.

In tandem with the analysis of PBMCs from blood donated by healthy volunteers, a variety of human leukaemic and neural cell lines were also investigated. Cell lines provided a readily available easily harvested source of human immune and neural cells to be studied. It was thought that if changes in MOP receptor concentration and number could be followed on leukaemic cells after opioid administration and that these variations correlated with comparable changes in neural cell lines, then similarly changes in MOP receptor number on PBMCs from clinical samples after opioid administration may indicate central changes in MOP receptor number in vivo. This would then allow for a technique whereby analysis of peripheral MOP receptor

number would allow for comment on central MOP receptor up or down regulation. Changes in MOP receptor expression on immunocompetent cells within the periphery are also of interest in their own right, with a possible connection between opioid administration and immune function being recorded in a number of previous studies.

The aims of this chapter are therefore:

- To undertake a series of radioligand binding experiments to look for MOP receptor expression on a variety of immune cell lines and peripheral blood mononuclear cells and whole venous blood extracted from healthy male volunteers.
- To characterise fluorescent-naloxone through a series of radioligand binding experiments prior to its uses as a direct fluorescent probe at classical opioid receptors.
- To employ a range of primary and secondary antibodies directed against the MOP receptor in an attempt to fluorescently stain this receptor for direct and confocal imaging and flow cytometric analysis. To repeat these investigations using fluorescent-naloxone (characterised above) as a direct imaging probe at all of the classical opioid receptors. To use these techniques to image the MOP receptor on immune cells and immune cell lines.
- To optimise the techniques of endpoint and quantitative PCR to look for the expression of the MOP gene in CHO_{hMOP} cells, and then to use these techniques in immune cells immune cell lines and whole venous blood in the naïve state.
- To use the techniques of PCR to look for upregulation of the MOP receptor on immune cells and immune cell viability following stimulation with the cytokines TNF- α and cycloheximide.

In all of these investigations Chinese hamster ovary cells stably transfected with the human MOP receptor and SH-SY5Y cells were used as positive controls.

3.2 Radioligand Binding Studies

3.2.1 Results: Saturation binding experiments

Binding of [³H]-Diprenorphine to CHO_{hMOP} cells is well documented (*Harrison et al 1999, Hirota et al 2000*). This experiment was performed three times as a positive control.

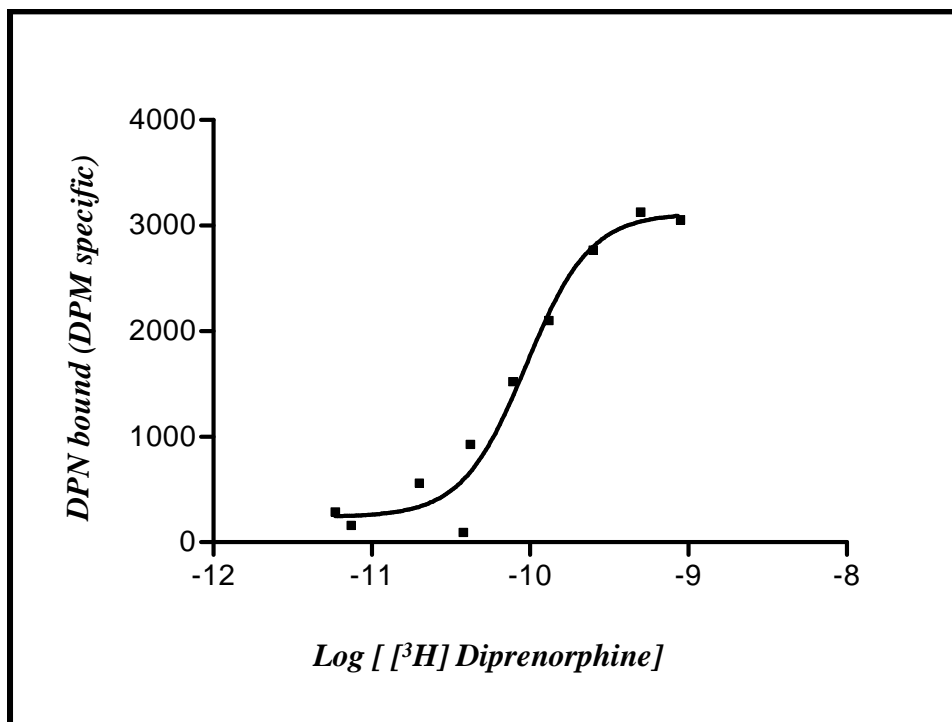


Figure 3.1 Saturation Binding of [³H]-Diprenorphine (DPN) to CHO_{hMOP} cells (example of one) showing typical sigmoid dose response with increasing concentrations of ligand.

There was a typical sigmoid semi-logarithmic curve of ligand-receptor binding in each instance. (An example of this is shown in **Figure 3.1**). Note not only the characteristic sigmoid plot but also the much higher binding compared to the immunocompetent cell lines shown below. A $pK_D = 9.92 \pm 0.11$ ($n=3$) was calculated from the experiments using CHO_{hMOP} cells.

Saturation binding assays were also performed on a range of immunocompetent cells using [³H]-Diprenorphine as the radioligand (**Figures 3.2-3.5**).

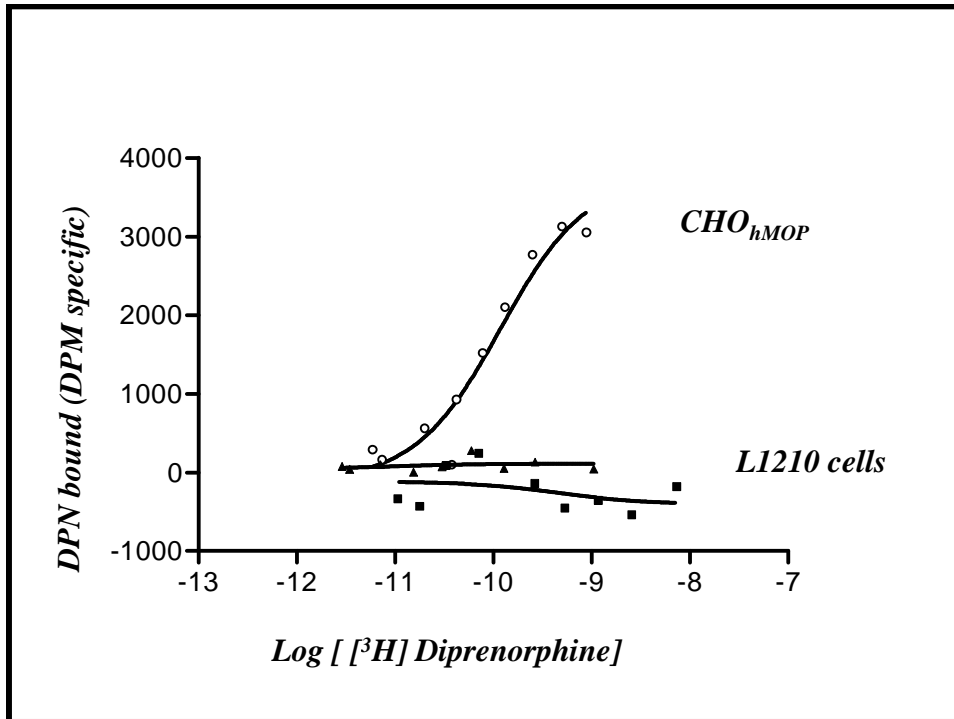


Figure 3.2 Saturation Binding of [³H]-Diprenorphine (DPN) to L1210 (mouse thymoma cells) cells n=2. No obvious binding is present. Single CHO_{hMOP} shown as control.

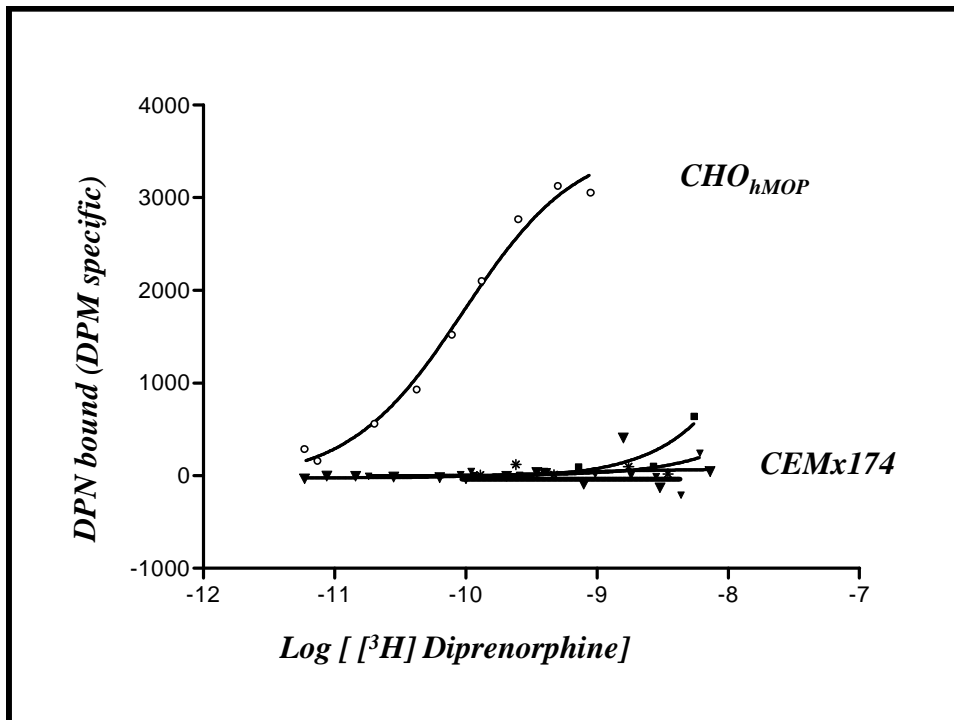


Figure 3.3 Saturation Binding of [³H]-Diprenorphine (DPN) to CEMx174 cells (B/T lymphocyte cell hybridoma) n=5. No binding present. Single CHO_{hMOP} shown as control.

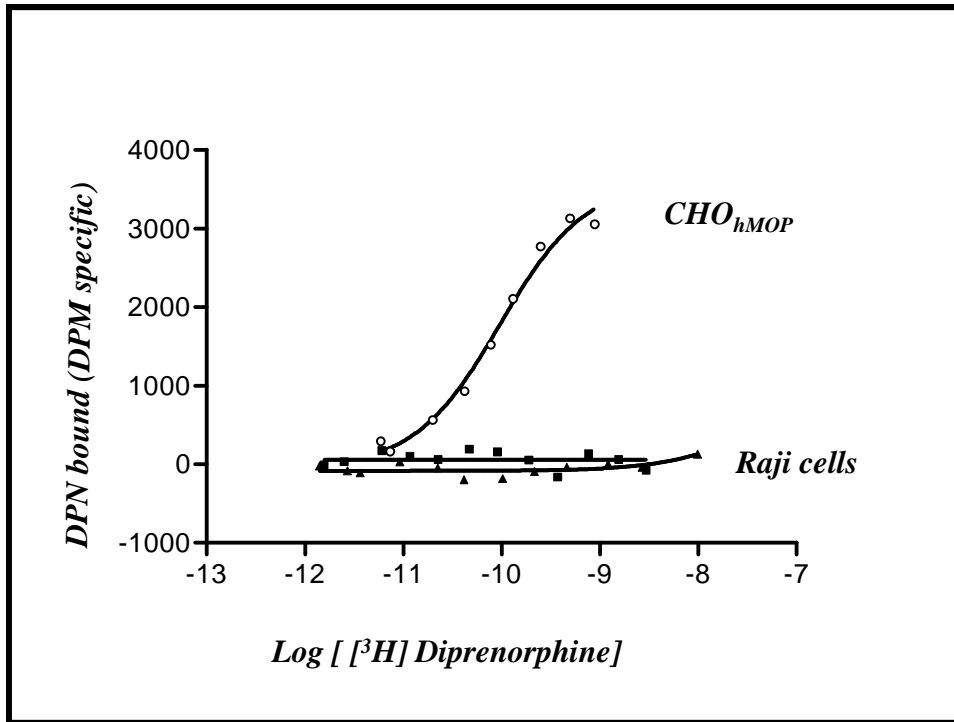


Figure 3.4 Saturation Binding of $[^3\text{H}]$ -Diprenorphine (DPN) to Raji cells (human B-lymphocytic cell line) $n=2$. No binding present. Single CHO_{hMOP} shown as control.

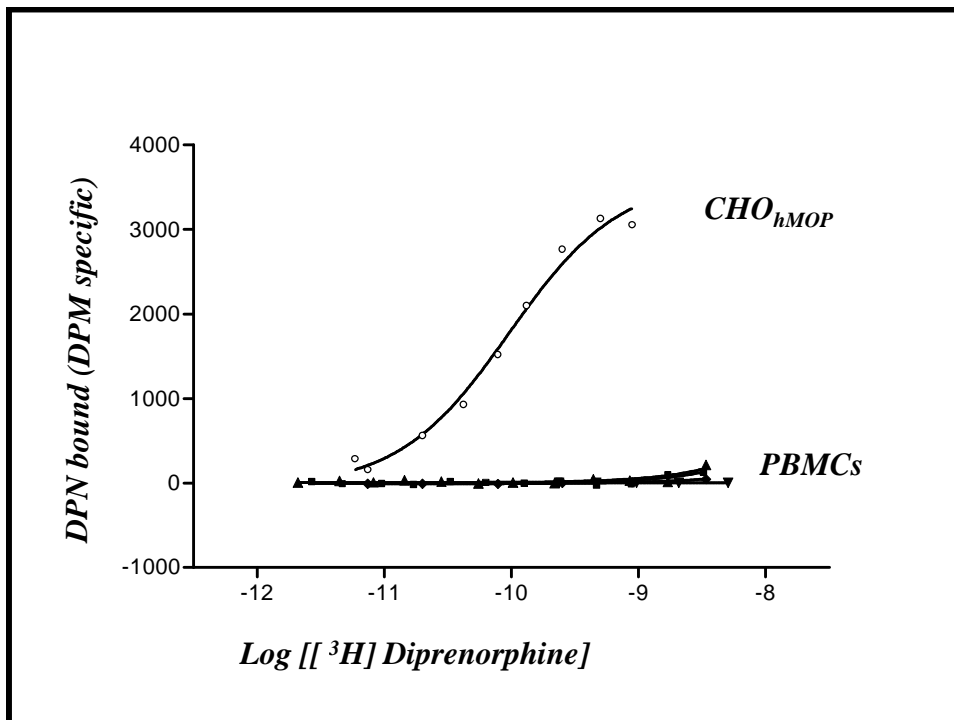


Figure 3.5 Saturation Binding of $[^3\text{H}]$ -Diprenorphine (DPN) to peripheral blood mononuclear cells $n=4$. No binding present. Single CHO_{hMOP} shown as control.

Table 3.1 summaries the findings of the above saturation binding experiments by cell type.

Cell Type	MOP receptor present	Estimated max Counts bound/mg	n
CHO _{hMOP}	Yes	~ 61000	3
L1210	No	~ 3000	2
CEMx174	No	~ 850	5
Raji	No	~ 650	2
PBMCs	No	~ 200	4
Whole blood	No	N/A	2

Table 3.1 Summary of presence of MOP receptor, using a non-selective opioid antagonist (³H]-Diprenorphine), by cell type with radioligand binding. Protein calculation using the Lowry technique was not possible for whole blood.

3.2.2 Results: Competition binding assays

A series of competition binding assays were undertaken in CHO_{hMOP} cells, using [³H]-Diprenorphine as the radioligand with naloxone and fluorescent-naloxone as displacing agents. **Figure 3.6** shows the plots obtained for both naloxone and fluorescent-naloxone displacing [³H]-Diprenorphine from the MOP receptors on CHO_{hMOP} cell membranes. Both naloxone and fluorescent-naloxone cause a concentration dependent displacement of [³H]-Diprenorphine. The addition of a fluorescent moiety to naloxone causes a 10-fold reduction in its binding affinity at the human MOP receptor, although fluorescent-naloxone still has a favourable binding profile.

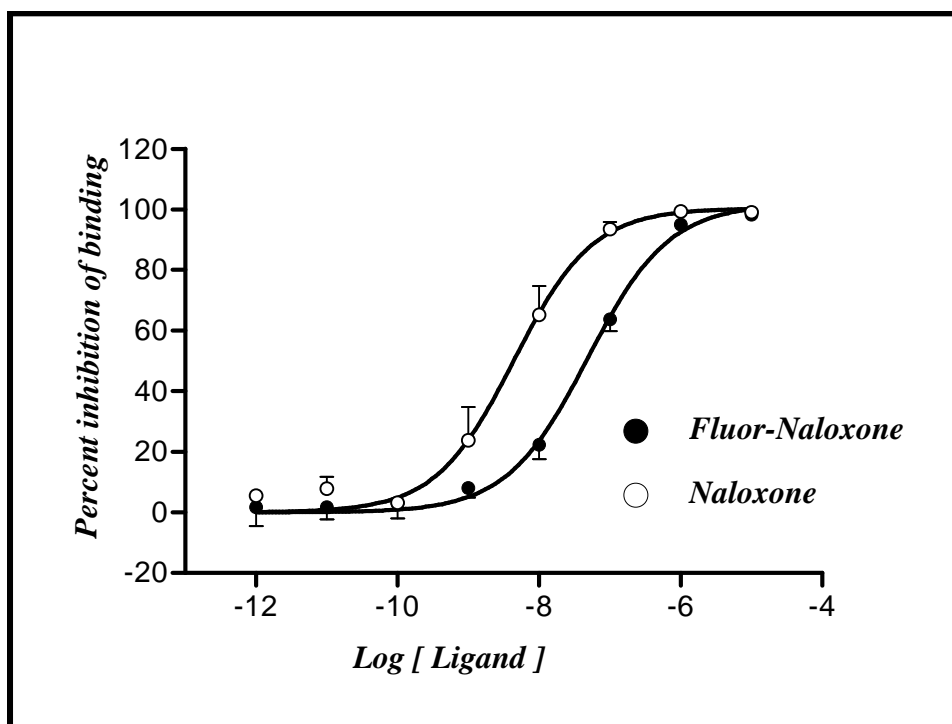


Figure 3.6 Mean of competition displacement assays of [³H]-Diprenorphine with CHO_{hMOP} cells by naloxone (n=3) and fluorescent-naloxone (n=5).

Values for the pK_i for both naloxone and fluorescent-naloxone were calculated (**Table 3.2**) using the measured pK_D of 9.92±0.11 determined for [³H]-Diprenorphine and employing the Cheng-Prusoff equation (*Cheng et al 1973*).

Compound	pK _i
Naloxone	9.34 ± 0.25
Fluorescent-Naloxone	8.19 ± 0.05

Table 3.2 Calculated pK_i values for naloxone and fluorescent-naloxone (SEM).

3.3 Fluorescent Staining

3.3.1 Results: Fluorescent staining for direct and confocal microscopy

PBMCs and CHO_{hMOP} cells were stained with both of the commercially available primary antibodies. Though total staining was frequently bright and clear it was no greater than the non-specific stain seen with just application of the secondary fluorescent antibody, **Figures 3.7-3.14**. This was true regardless of whether CHO_{hMOP} cells or PBMCs were the cells being imaged. Neither direct fluorescent microscopy nor use of confocal microscopy changed this lack of specific staining of the image in any way.

Figures 3.7 & 3.8 show confocal images of the immunofluorescent staining of CHO_{hMOP} cells with and without primary antibody NHQLENLEAETAPLP, though with FITC secondary stain in both cases. No clear staining of MOP receptors is seen.

Figures 3.9 & 3.10 similarly show confocal pictures with and without primary antibody NHQLENLEAETAPLP and FITC secondary stain is used in both, these images are taken with peripheral blood mononuclear cells.

As discussed in the methods section a range of concentrations of primary and secondary stains were used, this also did not alter the difference between total and non-specific staining, with no clear MOP receptor staining. These experiments were repeated 10 times for PBMCs and 4 times for CHO_{hMOP} cells.

Figures 3.11 & 3.12 show confocal images of the immunofluorescent staining of CHO_{hMOP} cells with and without the second commercially available primary antibody VIKALITIPETTFQ though with FITC secondary stain in both cases. As with NHQLENLEAETAPLP primary no clear staining of MOP receptors is seen.

Figures 3.13 & 3.14 show confocal images of the immunofluorescent staining of PBMC cells with and without the second commercially available primary antibody VIKALITIPETTFQ, with FITC secondary stain in both cases. No specific staining for the MOP receptors is seen.

Similar results were obtained when fluorescent-naloxone was used to directly stain CHO_{hMOP} cells adhered to glass cover slips or PBMCs sedimented onto cover slips. This technique proved difficult for both types of cells with a direct staining of cells by fluorescent-naloxone being carried out as a one step procedure on ice

No specific staining was seen with this technique, and cells were only imaged by the use of direct fluorescent-microscopy (not shown).

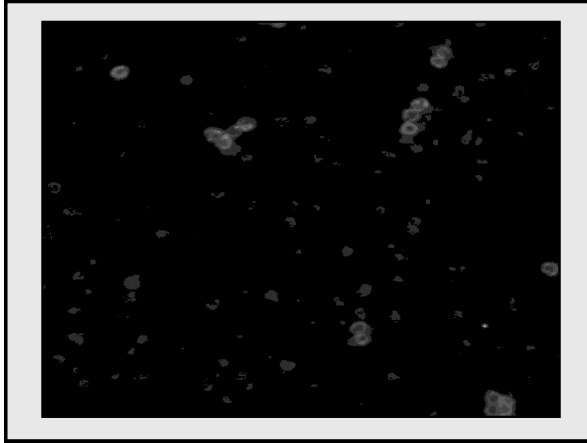


Figure 3.7

Figure 3.7 shows a confocal image of immunofluorescent staining of CHO_{hMOP} cells With Primary NHQLENLEAETAPLP and Secondary FITC (n=4). **Figure 3.8** staining of CHO_{hMOP} cells with FITC secondary alone (n=4) as non-specific binding. There is no obvious difference in fluorescence between the two preparations.

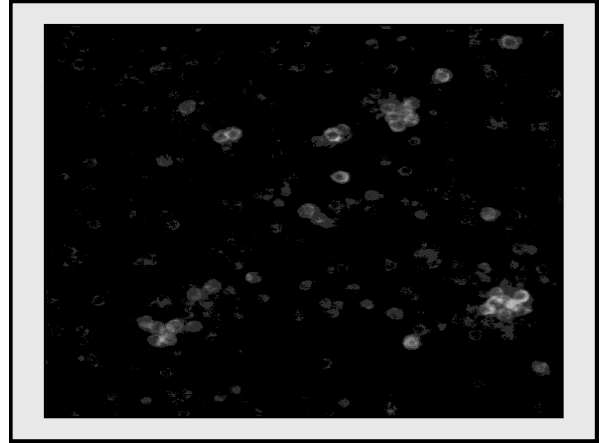


Figure 3.8

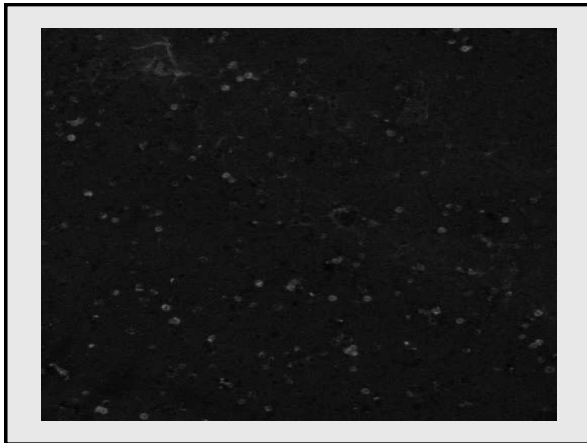


Figure 3.9

Figure 3.9 shows a confocal image image of immunofluorescent staining of peripheral blood mononuclear cells with primary NHQLENLEAETAPLP antibody and secondary stain FITC (n=10). **Figure 3.10** staining of PBMCs with FITC secondary alone (n=10) as non-specific binding. There is no obvious difference in fluorescence between the two preparations.

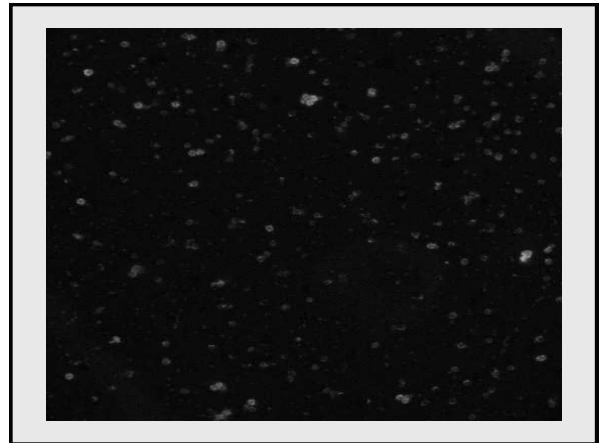


Figure 3.10

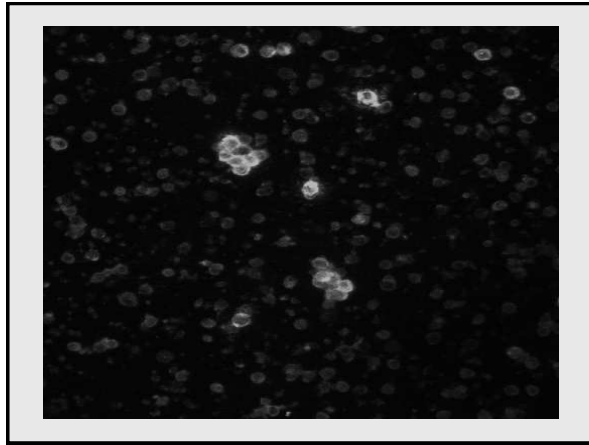


Figure 3.11

Figure 3.11 shows a confocal image of immunofluorescent staining of CHO_{hMOP} cells with the primary antibody VIIKALITIPETTFQ and secondary stain FITC (n=7). **Figure 3.12** staining of CHO_{hMOP} cells with FITC secondary alone (n=7) as non-specific binding. There is no obvious difference in fluorescence between the two preparations.

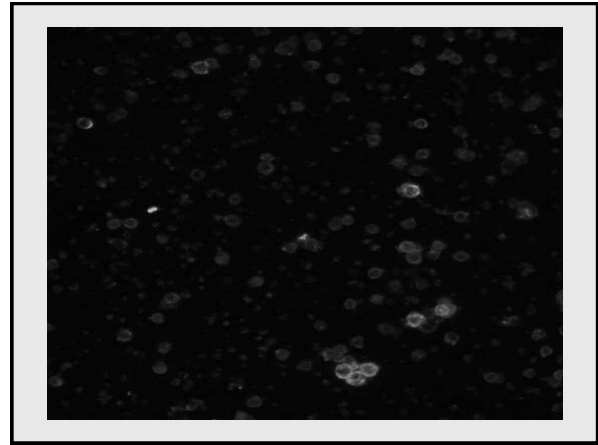


Figure 3.12

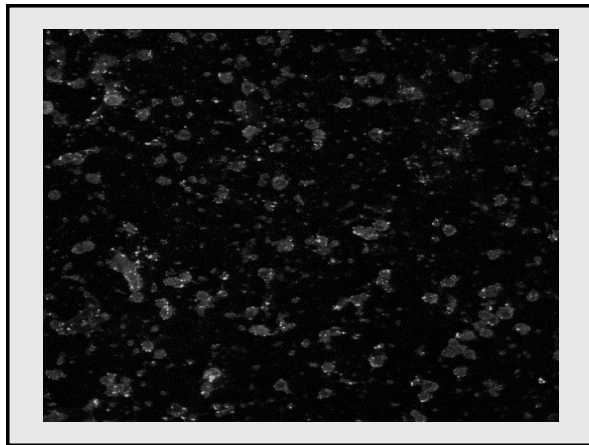


Figure 3.13

Figure 3.13 shows a confocal image image of immunofluorescent staining of PBMCs with the primary antibody VIIKALITIPETTFQ and secondary FITC (n=4). **Figure 3.14** staining of peripheral blood mononuclear cells with FITC secondary alone (n=4) as non-specific binding. There is no obvious difference in fluorescence between the two preparations.

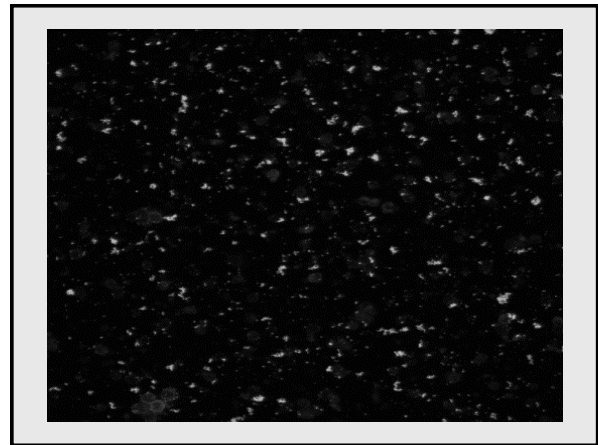


Figure 3.14

3.3.2 Results: Immunofluorescent staining for flow cytometry

With both permeabilised and non-permeabilised cells the two commercially available primary antibodies, NHQLENLEAETAPLP and VIIKALITIPETTFQ showed significant shifts in mean fluorescence intensity **Figures 3.15 - 3.17**. This was most pronounced with the CHO_{hMOP} cells. However if normal rabbit serum was used in place of the primary antibody then this shift in mean fluorescence intensity was just as marked, **Figure 3.18**. This suggests that the normal rabbit serum is acting as an effective primary antibody binding to immunocompetent or CHO_{hMOP} cells and that primary antibody binding is not necessarily at the MOP receptor.

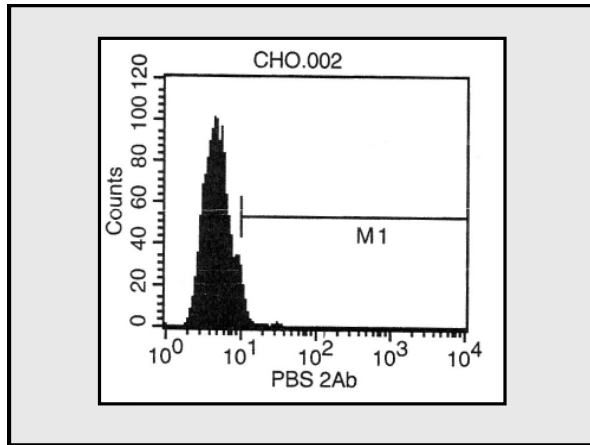


Figure 3.15

MFI shift for CHO_{hMOP} cells with PBS primary FITC 1:250 secondary, **Figure 3.15** shows no rightward shift. **Figure 3.16** shows MFI for CHO_{hMOP} cells, with NHQLENLEAETAPLP primary 1:200 and FITC secondary 1:250 (n=4), displays rightward shift.

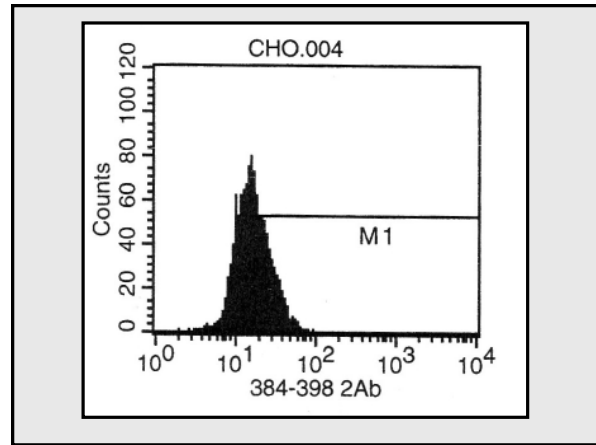


Figure 3.16

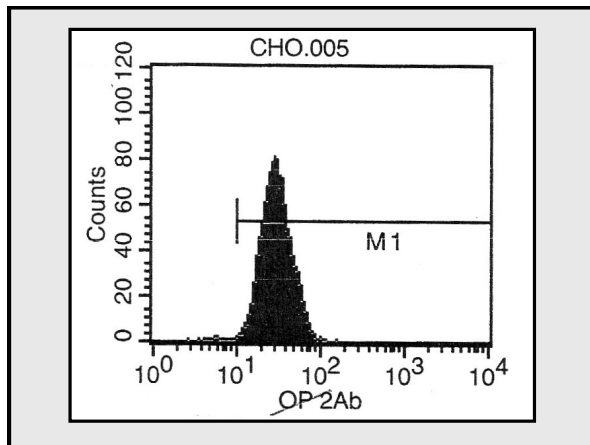


Figure 3.17

MFI shift for CHO_{hMOP} cells with VIKALITIPETTFQ primary 1:200 primary and FITC 1:250 secondary, **Figure 3.17** shows rightward shift. However **Figure 3.18** shows MFI for CHO_{hMOP} cells, with normal rabbit serum primary 1:200 and FITC secondary 1:250 (n=4), also displaying rightward shift.

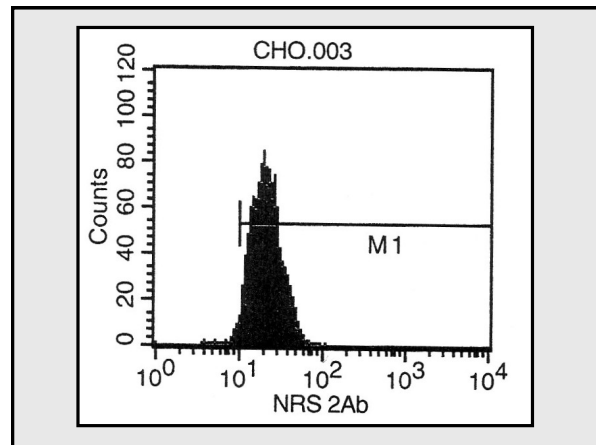


Figure 3.18

A range of primary antibody concentrations were used from 1:100 – 1:1000. Additionally neither of the immunocompetent cell lines Raji cells and Jurkat cells or whole human blood, produced significant changes in fluorescence when coupled with either of these two commercially available primary antibodies, examples of this are given in **Figures 3.19 & 3.20**.

The affinity purified Cote primary antibody 1414 did however show a significant rightward shift of the mean fluorescence intensity peak in CHO_{hMOP} cells when analysed by flow cytometry as shown in **Figures 3.21 – 3.22**. This followed permeabilisation of the cells as 1414 is directed intracellularly against the carboxyl end

of the receptor. This fluorescence was reversed by the addition of GST-C50, the blocking agent for the receptor, **Figure 3.23**. Suggesting that 1414 binds the receptor.

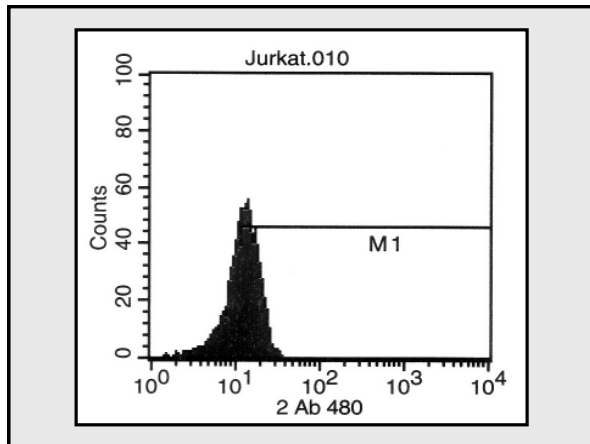


Figure 3.19

MFI shift for human lymphocytic cell line (Jurkat cells) with NHQLENLEAETAPLP primary 1:200 and FITC 1:250 secondary, **Figure 3.19** shows no rightward shift (n=2). However **Figure 3.20** shows MFI for Jurkat cells, with normal rabbit serum primary 1:200 and FITC secondary 1:250 (n=2), displaying rightward shift.

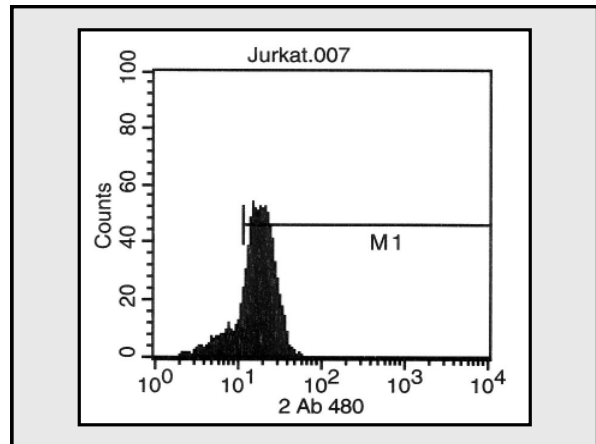


Figure 3.20

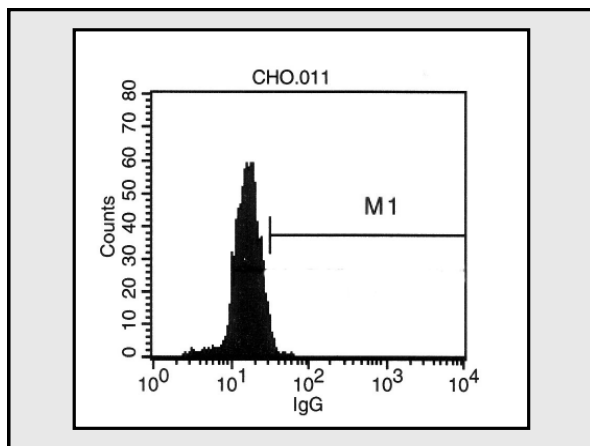


Figure 3.21

MFI shift for CHO_{hMOP} with IgG primary 1:200 and FITC 1:250 secondary (n=2), **Figure 3.21** shows no rightward shift. However **Figure 3.22** shows MFI for CHO_{hMOP} cells, with 1414 primary 1:200 and FITC secondary 1:250, displaying rightward shift (n=4).

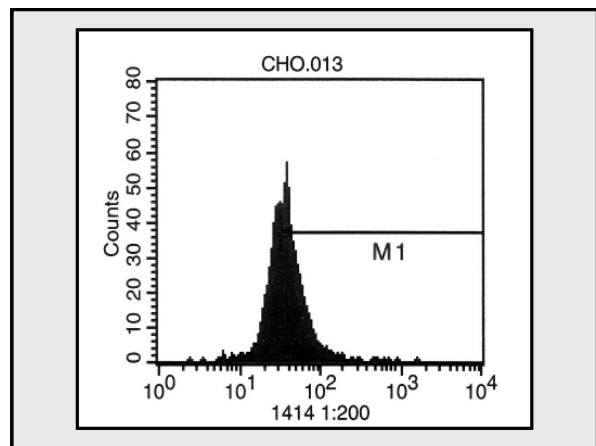


Figure 3.22

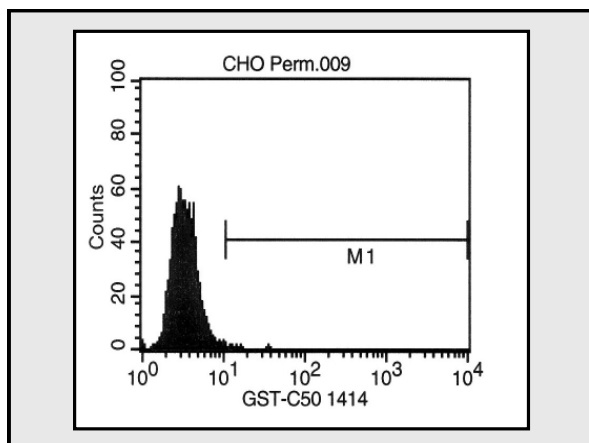


Figure 3.23 MFI shift for CHO_{hMOP} with 1414 primary 1:200 GST-C50 blocking agent and FITC 1:250 secondary (n=2).

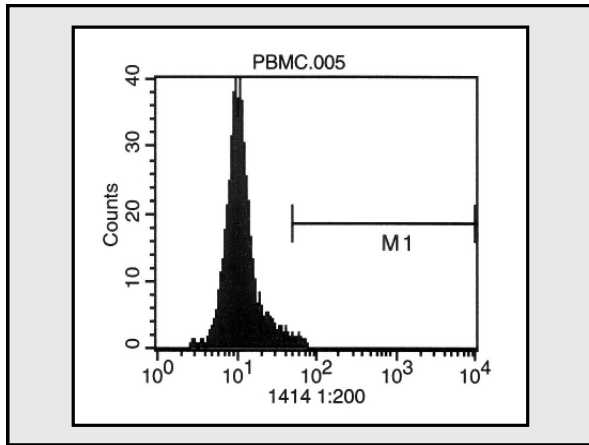


Figure 3.24

Mean Fluorescent Intensity shift for PBMCs with 1414 primary 1:200 and FITC 1:250 secondary (n=4), **Figure 3.24** shows no rightward shift. **Figure 3.25** shows MFI for PBMCs, with IgG primary 1:200 and FITC secondary 1:250 (n=2), displaying no rightward shift.

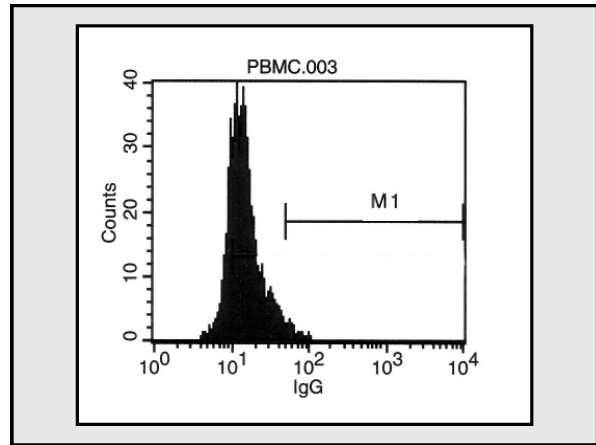


Figure 3.25

However when applied to permeabilised peripheral blood mononuclear cells as shown in **Figures 3.24 & 3.25** the Cote primary antibody 1414 produces no shift in mean fluorescent intensity, suggestive of no MOP receptor binding.

The second Cote antibody 1404 did not show a shift in mean fluorescent intensity however when added to permeabilised or non-permeabilised CHO_{hMOP} cells **Figures 3.26 & 3.27** in this example permeabilised cells.

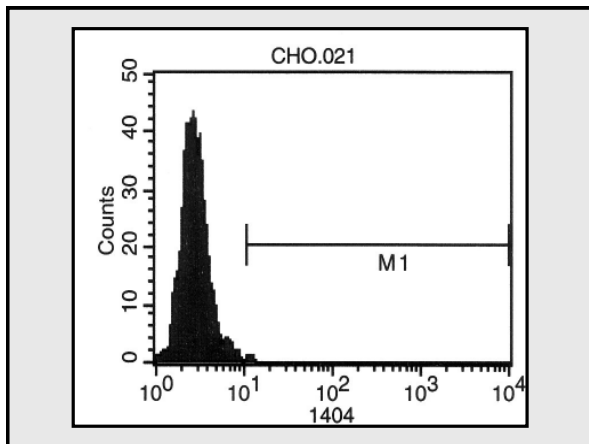


Figure 3.26

Mean Fluorescent Intensity shift for CHO_{hMOP} cells with 1404 primary 1:200 and FITC 1:250 secondary (n=4), **Figure 3.26** shows no rightward shift. **Figure 3.27** shows MFI for CHO_{hMOP} cells, with IgG primary 1:200 and FITC secondary 1:250 (n=2), displaying no rightward shift. In these experiments CHO_{hMOP} cells were permeabilised.

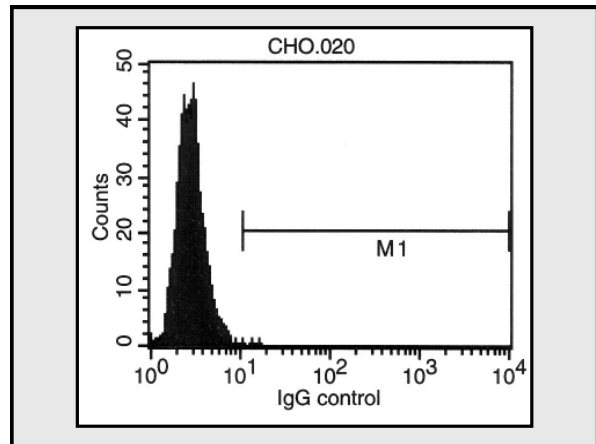


Figure 3.27

3.3.3 Results: Fluorescent-naloxone staining for flow cytometry

A range of concentrations of fluorescent-naloxone were incubated with CHO_{hMOP} cells and PBMCs prior to being analysed by flow cytometry in accordance with the **Protocol 2.3**. Flow cytometry was performed five times with PBMCs and a total of seven times with CHO_{hMOP} cells. **Figures 3.28 and 3.29** show typical flow cytometry plots produced for fluorescent-naloxone binding to CHO_{hMOP} cells, with increasing shift in MFI at increasing concentrations of fluorescent-naloxone. While **Figures 3.30 & 3.31** show no change in MFI shift when increasing concentrations of fluorescent-naloxone are added to PBMCs.

This gave a concentration-dependent and saturable increase in normalised mean fluorescence intensity shift for CHO_{hMOP} cells yielding a $pK_D = 7.69 \pm 0.38$ **Figure 3.32**. This compares favourably with the pK_i of 8.19 ± 0.05 calculated from displacement binding experiments for fluorescent-naloxone with [³H]-Diprenorphine, with no statistically significant difference between the two.

The mean fluorescence intensity shift (MFI) for CHO_{hMOP} cells and PBMCs was compared at a single concentration of fluorescent-naloxone (1×10^{-7} M) inset **Figure 3.32**. At this concentration of fluorescent-naloxone there is a significant shift in mean fluorescent intensity for the CHO_{hMOP} cells, but not for the PBMCs suggesting MOP receptors are present on CHO_{hMOP} cells, and that flow cytometric analysis using fluorescent-naloxone can detect this but that MOP receptors are not present on PBMCs. **Table 3.3** below summarises the attempted binding of the five different fluorescent probes to the cells and cell lines used within this project.

Binding of fluorescent label suggesting MOP receptor present					
Cell Type	NHQLLENLEAETAPLP	VIKALITIPETTFQ	Cote 1414	Cote 1404	F-Naloxone
PBMCs	No	No	No	No	No
CHO _{hMOP}	No	No	Yes	No	Yes
Jurkat	No	No	N/A	N/A	N/A
Whole blood	No	No	N/A	N/A	N/A
Raji	No	No	N/A	N/A	N/A

Table 3.3 Summary of fluorescent binding to a various cell types. N/A = not available.

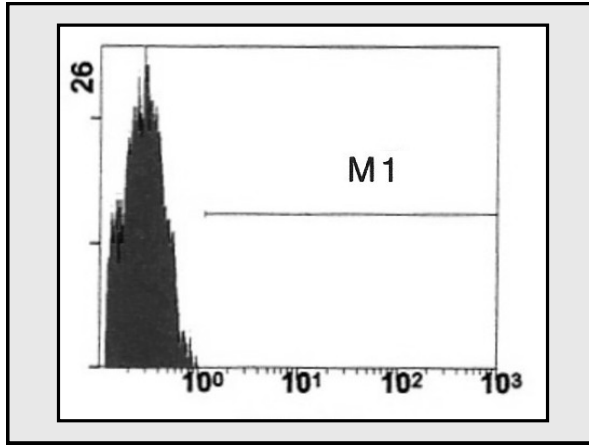


Figure 3.28

MFI shift for CHO_{hMOP} cells with PBS alone (n=2), **Figure 3.28** shows no rightward shift. **Figure 3.29** shows MFI for CHO_{hMOP} cells, fluorescent-naloxone staining 3×10^{-6} M (n=7), displaying appreciable rightward shift.

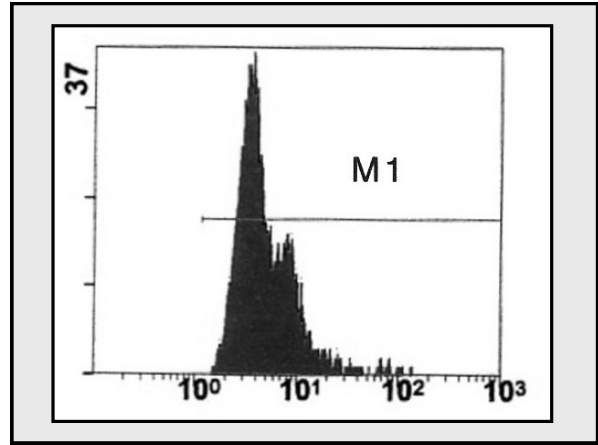


Figure 3.29

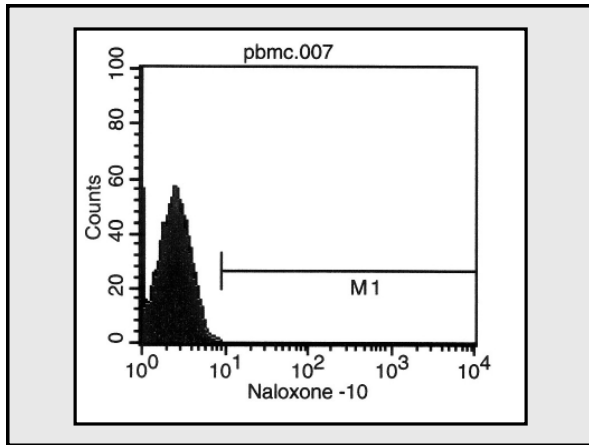


Figure 3.30

MFI shift for PBMC cells with fluorescent-naloxone at low concentration 1×10^{-10} M (n=5), **Figure 3.30** shows no rightward shift. **Figure 3.31** similarly shows no rightward shift for PBMC cells at higher fluorescent-naloxone concentrations (1×10^{-7} M).

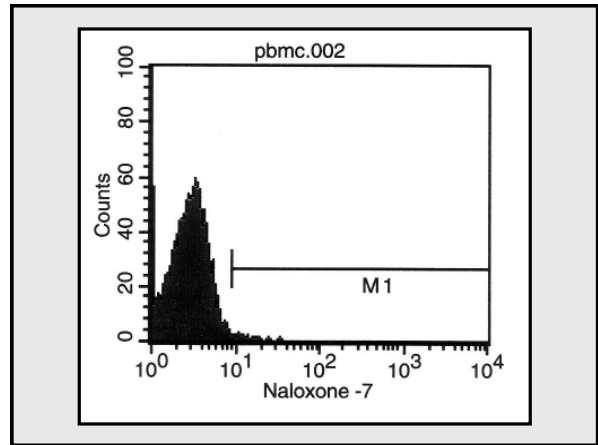


Figure 3.31

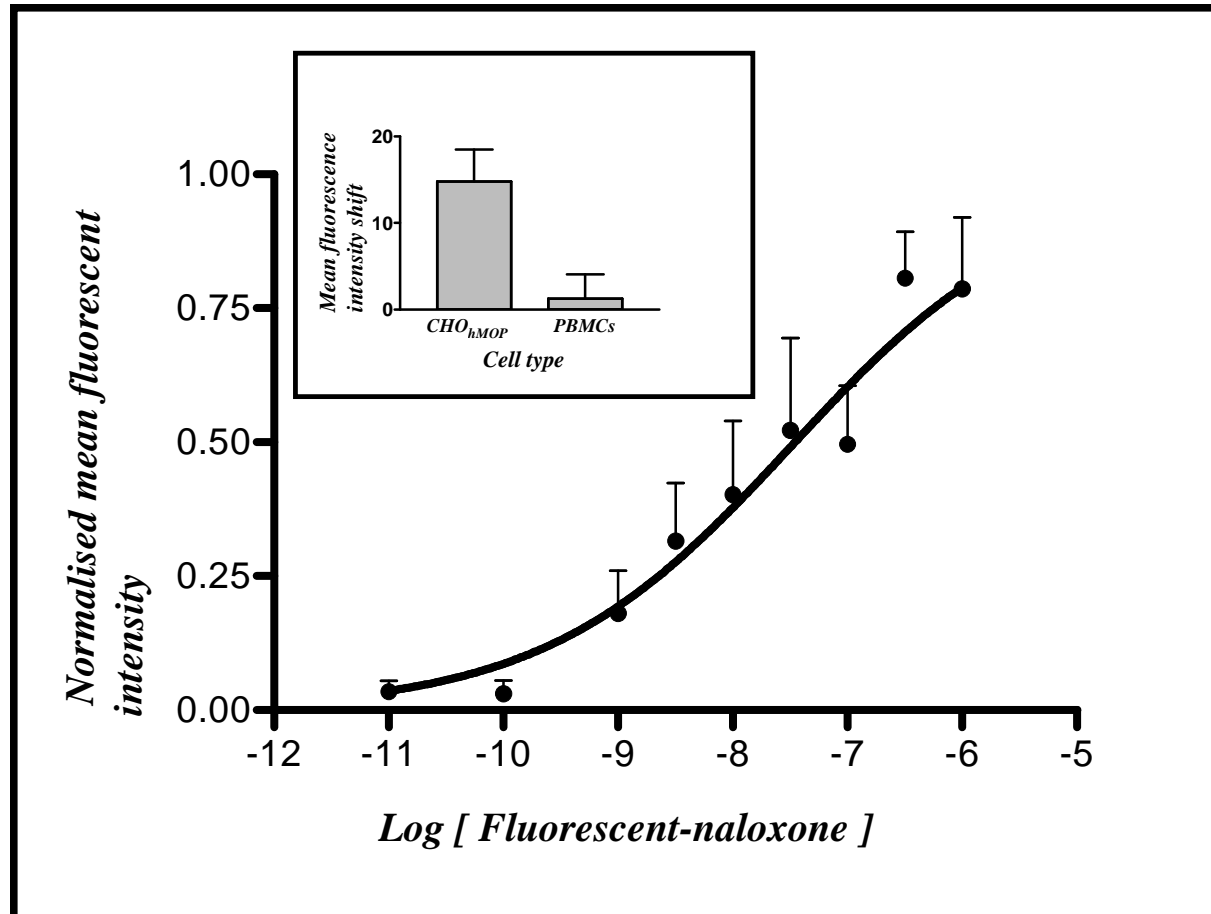


Figure 3.32

Semi-logarithmic plot of normalised MFI with SEM for n=7 CHO_{hMOP} cells, against fluorescent-naloxone concentration. MFI - shift for CHO_{hMOP} cells and PBMCs compared at a fluorescent-naloxone concentration of 1×10^{-7} M, inset, shows limited MFI for PBMCs (n=5) compared to CHO_{hMOP} cells.

3.4 Polymerase chain reaction

3.4.1 Results: Endpoint polymerase chain reactions

A wide range of human MOP receptor primer pairs have been used in the literature to look for the presence of MOP receptors on PBMCs and other tissue. However many of these primer pairs bind to sequences found only on one exon and no individual primer recognized sequences that span an exon-exon boundary, therefore giving no specificity for cDNA as opposed to gDNA. Therefore in addition to the primers identified from the literature new sets of primers were also designed.

The first set of primer pairs to be used in PCR reactions looking for the human MOP receptor were designed to anneal to two portions of exon 3, and were situated 91 base pairs apart. They were 5'-TCCAACCTGGTACTGGGAAA-3,' the forward primer, and 5'-GTCCATAGCACACGGTAATGATG-3,' the reverse primer. They correspond to bases 887-906 and 956-978 respectively of the human MOP receptor mRNA sequence accession No. gi-4505514. These two primers were known as MOP1F and MOP1R, they showed melting temperatures (T_M) of 51.6°C and 55°C based on percentage GC content. Originally they were produced for use in real time PCR and hence produce a small amplicon.

A second set of primers was taken from the literature (*Suzuki et al 2000*). The primers were, 5'-GGTACTGGGAAAACCTGCTGAAGATCTGTG-3', MOP2F, and 5'-GGTCTCTAGTGTCTGACGAATTCGAGTGG-3', MOP2R, corresponding to base pairs 895-924 and 1306-1335 respectively. The primers yielded a PCR amplicon of 440 base pairs in length. Like the MOP1 primers both of the MOP2 primers anneal to portions of the DNA sequence on exon 3, and so similarly alone cannot differentiate gDNA from cDNA. These primers had T_M values of 63°C and 63°C. **Figure 3.33** gives a schematic representation of the positions of MOP1 or MOP2 primers relative to the genomic DNA sequence of the MOP receptor.

MOP3 primers were, like MOP1 primers, designed in house. They were chosen so that the forward primer would sit on exon 2 while the reverse primer sat across the exon 2-3 boundary, as shown in **Figure 3.34**. The sequences were 5'-AAAATTATCAATGTCTGCAACTGGAT-3' for MOP3F and 5'-TATGGAACCTTGCCTGTATTTTGTT-3' for MOP3R. They correspond to bases 771-

796 and 839-863 of the mRNA sequence. Though the primers are 26 base pairs and 25 base pairs in length the amplicon they produce is only 92 base pairs long, and so acceptable for QPCR. They have T_M values of 51.5°C and 52.6°C As MOP3R anneals to two exons there should be no amplification of genomic DNA during PCR, as the reverse primer should fail to anneal to the intron of the gDNA separating these two exons.

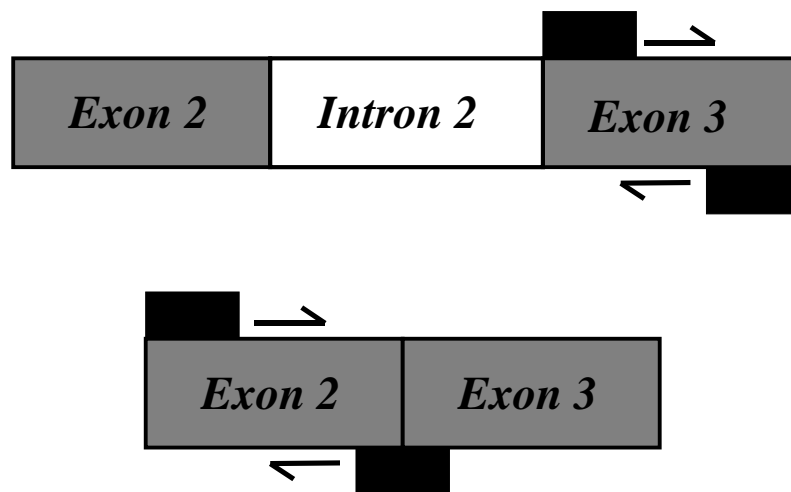


Figure 3.33

The figure shows the position of primer pairs MOP1 and MOP2 upper image on the gDNA sequence (black boxes) and the position of MOP3 primer pairs in the lower image.

During many of the following investigations MOP3F was coupled with MOP1R to produce a primer pair of similar T_M , which would give a PCR amplicon of 207 base pairs in length if cDNA was amplified and 980 if gDNA were amplified. This provided a means of differentiating genomic DNA and its RNA message. **Figure 3.34** gives a schematic relationship of MOP1 MOP3 and MOP3+1 primer pairs. The primer pairings described above are summarised in **Table 3.4**.

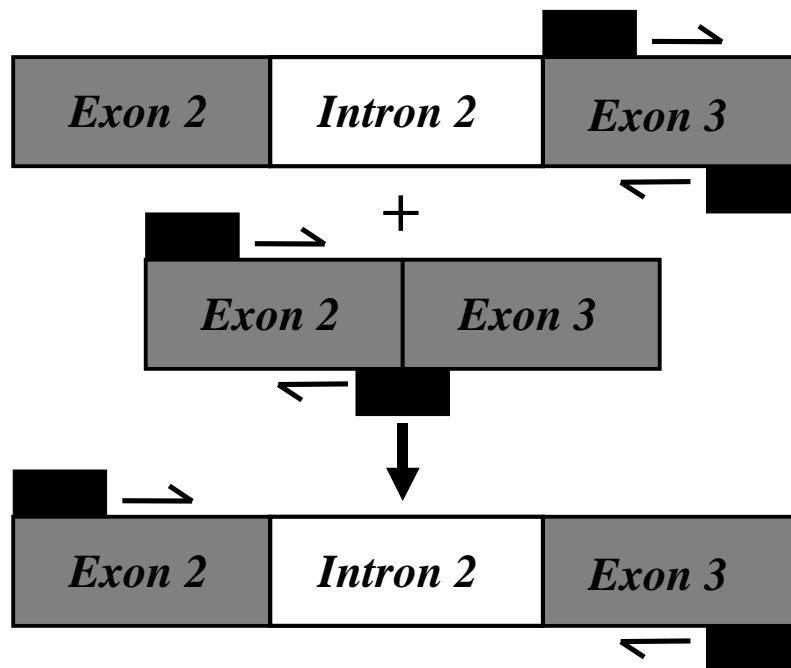


Figure 3.34

The figure shows the position of MOP1 primer pairs on the gDNA sequence (black boxes) of the MOP receptor in the upper figure. The middle figure shows the expected position of the MOP3 primer pairing on cDNA while the lower figure shows the position of the MOP 3+1 primer pairs on gDNA.

Primer Name	Sequence	mRNA Position	Amplicon size
MOP1F	5'-TCCAACCTGGTACTGGGAAA-3'	887-906	91
MOP1R	5'-GTCCATAGCACACGGTAATGATG-3'	956-978	91*
MOP2F	5'-GGTACTGGGAAAACCTGCTGAAGATCTGTG-3'	895-924	440
MOP2R	5'-GGTCTCTAGTGTTCTGACGAATTCGAGTGG-3'	1306-1335	440
MOP3F	5'-AAAATTATCAATGTCTGCAACTGGAT-3'	771-796	92*
MOP3R	5'-TATGGAACCTTGCCTGTATTTTGTT-3'	839-863	92

Table 3.4. Human MOP Receptor Primers. *Gives amplicon of 207bp or 980bp in MOP3F/MOP1R combination.

Results:

All of the MOP receptor primer pairs described above were used to screen for MOP receptors in the cells, cell lines and tissue samples used in this study.

MOP1

Initial studies showed that the MOP1 primer pair functioned best at an annealing temperature of 53°C *Figure 3.35*, producing a PCR amplicon that could be visualised by gel electrophoresis at 91 base pairs.

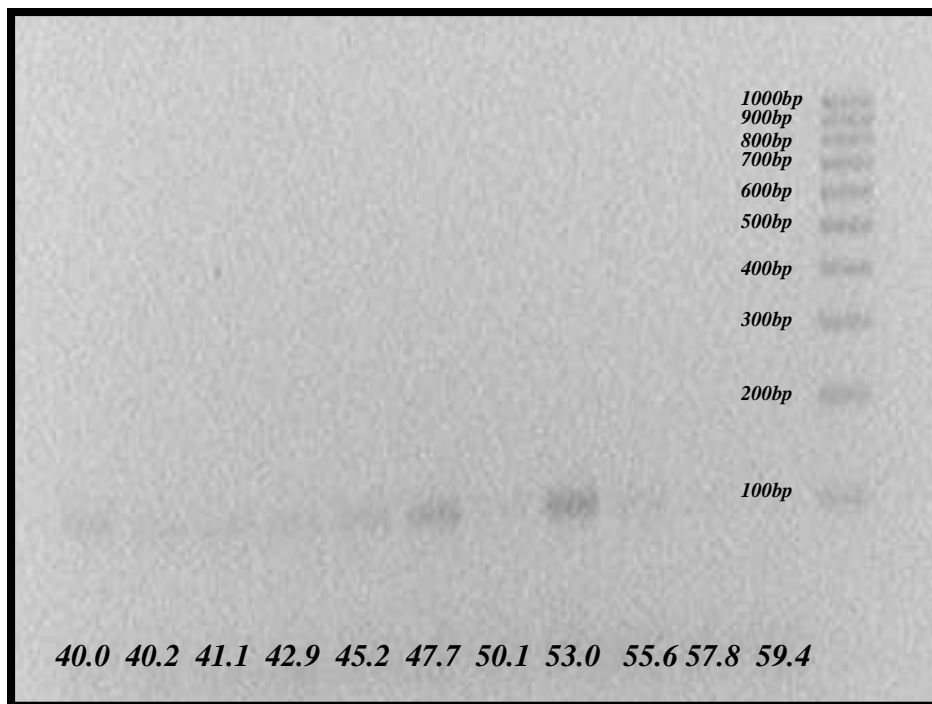


Figure 3.35

Annealing gradient for MOP1 primers used with cDNA from CHO_{hMOP} cells. All temperatures shown along the lower border are in degrees centigrade. Product is seen at the expected amplicon length of 91 base pairs strongest at 53°C. The weight ladder to the right ranges from 1000 base pairs to 100 base pairs in 100 base pair increments.

This 91 base pair amplicon was found to be present following PCR reaction with cDNA produced from not only CHO_{hMOP} cells, but also the neuroblastoma cell line SH-SY5Y and gDNA from CEMX174 cells and venous blood, *Figure 3.36*.

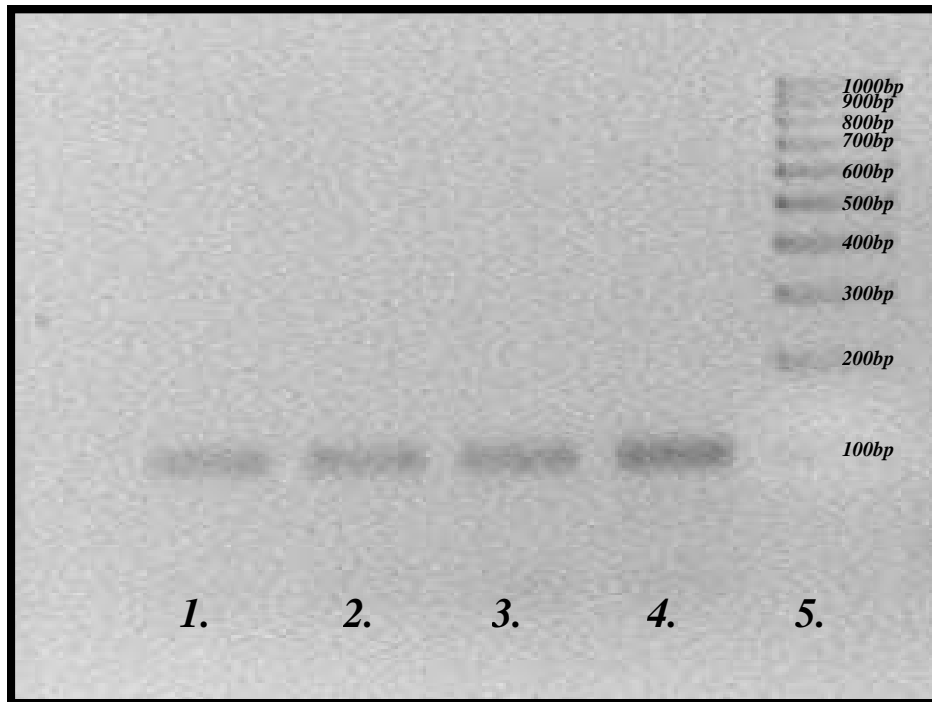


Figure 3.36

PCR gel for venous blood gDNA lane 1 and CEM x 174 gDNA lanes 2-4 with MOP1 primers. Product is seen at the expected amplicon length of 91 base pairs in lanes 1-4. The weight ladder in lane 5 ranges from 1000 base pairs to 100 base pairs in 100 base pair increments.

However as stated above this combination of primers rests on only one exon and therefore can amplify genomic DNA as well as cDNA. Additionally, as is seen in the figures above, only a faint band on gel analysis can be seen due to its short length. For these reasons it was infrequently used.

MOP2

Throughout many of the earlier PCR reactions carried out in this study MOP2 primer pairs were the primers of choice, they gave a good clear consistent band on gel analysis at 440 base pairs in length, much clearer than the bands produced when using the MOP1 primers as shown in **Figure 3.37**. Previous optimisation by *Chuang et al* had indicated an optimal annealing temperature of 64°C, this was used in all experiments with MOP2 primers. In a similar fashion to the MOP1 primers, product was seen with MOP2 in CHO_{hMOP}, CEMx174, SH-SY5Y, **Figure 3.38**, and Raji cells, **Figure 3.39**.

Unfortunately similarly to the MOP1 primers, primers annealed to regions of DNA on the same exon allowing for amplification of genomic DNA. Hence the amplicon could be genomic or cDNA in nature. By improving the original RNA extracted to give a higher purity with lower gDNA contamination, and by using an additional DNA eradication step, **Protocol 2.6**, prior to conversion to cDNA it was possible to remove much of the contaminating gDNA. However bands for gDNA were still seen despite using this eradication step. **Figure 3.40** shows PCR products following MOP2 reaction with cDNA derived from SH-SY5Y cells in the first four lanes or from CHO_{hMOP} cells in lanes 5-8. Despite the treatment with DNA eradicating compounds prior to reverse transcription, faint amplicons can be seen in lanes 2,4,6 and 8, suggesting that some gDNA is still present post eradication step. A DNA eradication step potent enough to remove all of the genomic DNA from RNA samples derived from immunocompetent cell also removed the small amount of RNA that could possibly have encoded for the MOP receptor in these cells.

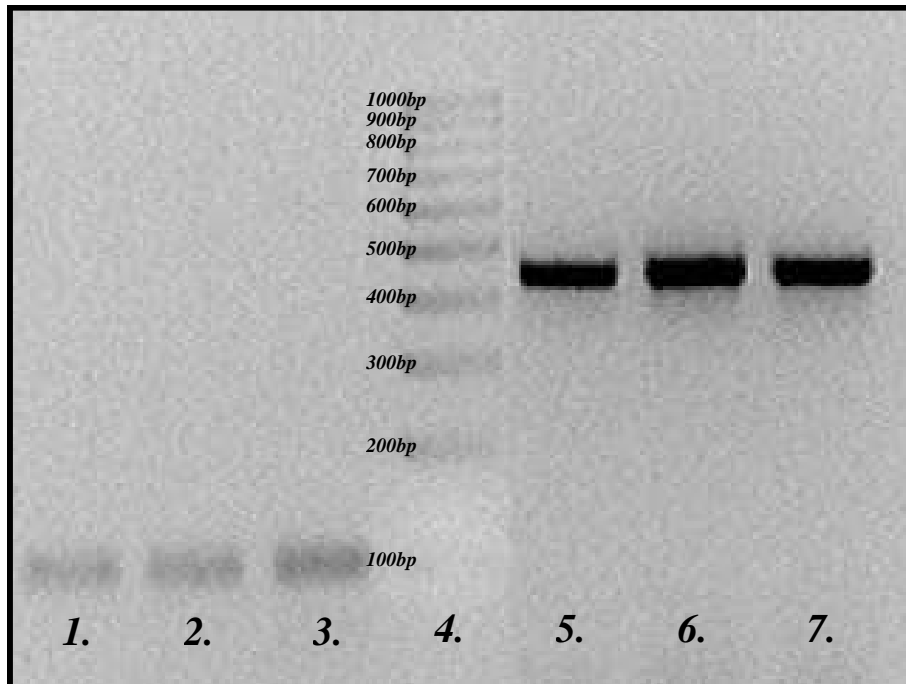


Figure 3.37 PCR gel for CEM x 174 gDNA with MOP1 primers, lanes 1-3, and MOP2 primers, lanes 5-7. Product is seen at the expected amplicon length of 91 base pairs in lanes 1-3, while lanes 5-7 show an amplicon at 440 base pairs as expected.. The weight ladder in lane 4 ranges from 1000 base pairs to 100 base pairs in 100 base pair increments. MOP2 clearly gives more easily discernible band on gel analysis lanes 5-7.

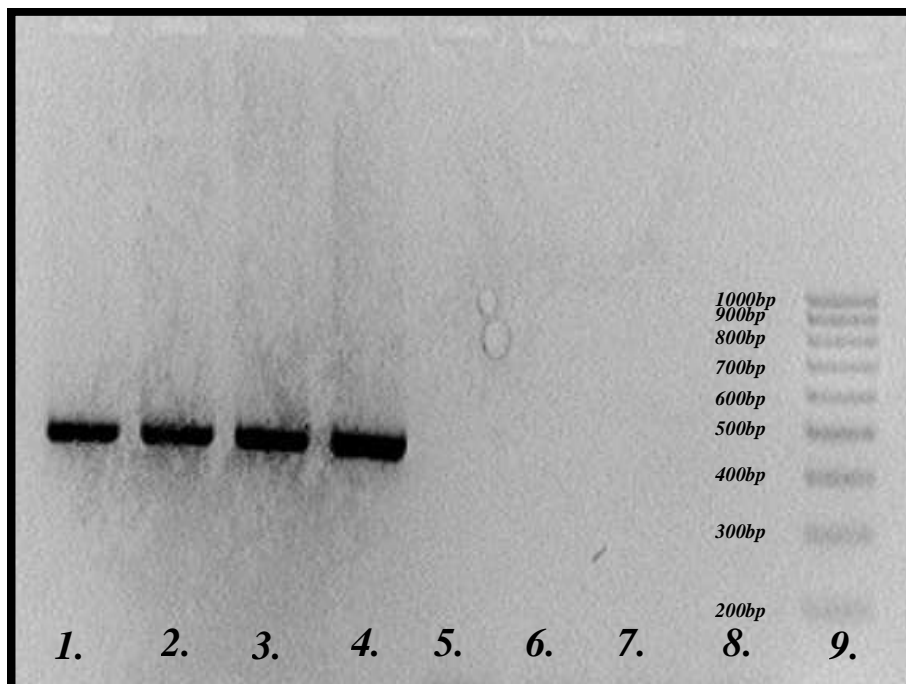


Figure 3.38 PCR gel for MOP2 primers with a variety of templates. lanes 1 CEM gDNA, lane 2 CHO_{hMOP} cDNA, lane 3 SH-SY5Y cDNA reverse transcribed, lane 4 SH-SY5Y cDNA non-reverse transcribed, lane 5-8 blank, ladder lane 9. Product is seen at the expected amplicon length of 440 base pairs in lanes 1-4. The weight ladder in lane 9 ranges from 1000 base pairs to 200 base pairs in 100 base pair increments.



Figure 3.39 PCR gel for MOP2 primers with Raji cDNA templates. Lanes 1 negative control, lane 2 Raji cDNA reverse transcribed, lane 3 Raji cDNA non-reverse transcribed, lane 4 negative control, ladder lane 5. Product is seen at the expected amplicon length of 440 base pairs in lanes 2 and 3 despite no RT step in lane 3.

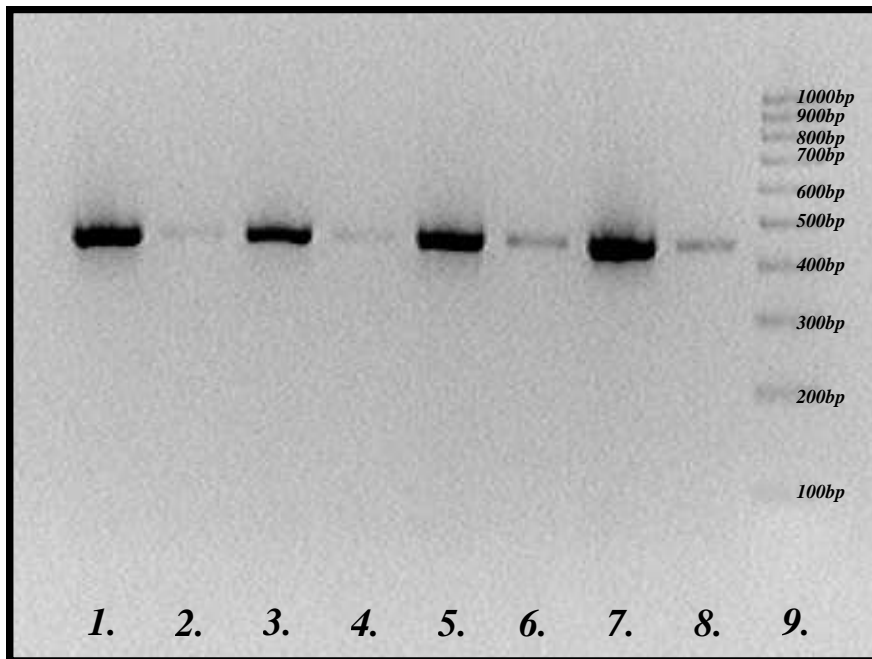


Figure 3.40 PCR gel for MOP2 primers with SHSY5Y and CHO_{hMOP} as template. Lane 1 SH-SY5Y cDNA RT+, DNase +, lane 2 SH-SY5Y cDNA RT-, lane 3 SH-SY5Y cDNA RT+, DNase -, lane 4 SH-SY5Y cDNA RT-, DNase-, lane 5 CHO_{hMOP} cDNA RT+, DNase +, lane 6 CHO_{hMOP} cDNA RT-, DNase +, lane 7 CHO_{hMOP} cDNA RT+, DNase -, lane 8 CHO_{hMOP} cDNA RT-, DNase -. Ladder lane 9. Product is seen in each lane at the expected amplicon length of 440 base pairs. Amplicons are fainter in the non-RT lanes but still present. DNA eradication has no effect upon amplicon intensity.

MOP3

Due to the shortcomings of the previous two primer pairs a third MOP receptor probe was developed. This primer pair was designed to bind sequences on different exons, the forward primer on exon 2 and the reverse on the exon 2-3 boundary. Theoretically it was therefore an ideal primer pair for the investigation of cDNA for the MOP receptor particularly in real time PCR experiments. Unfortunately it was found that the MOP3 primers amplified gDNA as well as annealing to cDNA **Figure 3.41**.

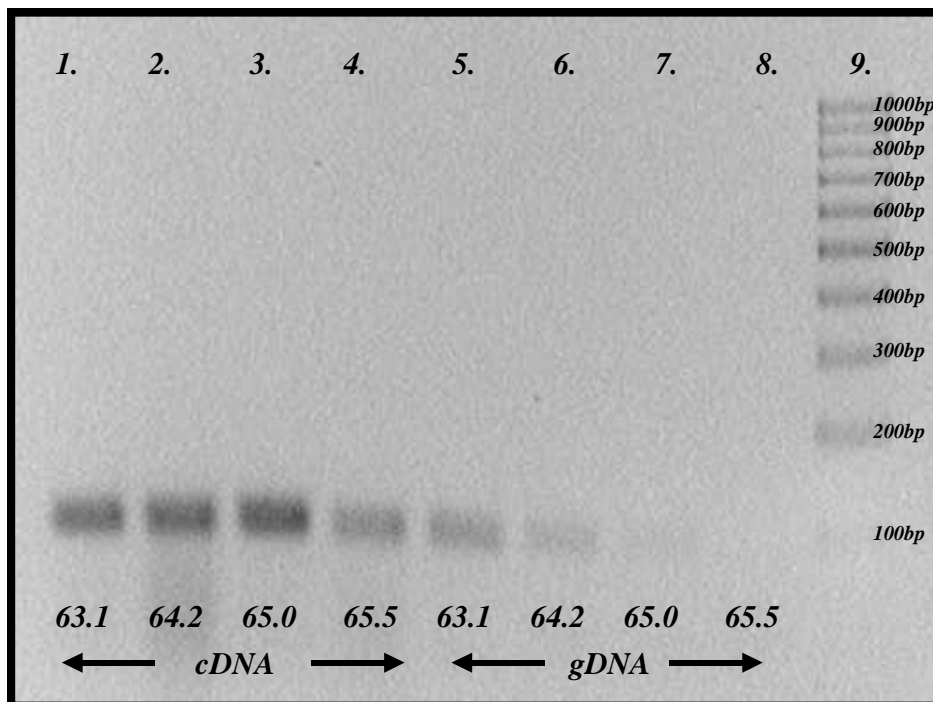


Figure 3.41

Annealing gradient for MOP3 primers used with cDNA from SH-SY5Y lanes 1-4 and gDNA SH-SY5Y lanes 5-8. Ladder lane 9. All temperatures shown along the lower border are in degrees centigrade. Product is seen at the expected amplicon length of 92 base pairs strongly in the first 4 lanes indicating strong binding to cDNA. However an amplicon is still seen at 65°C with gDNA. The weight ladder to the right ranges from 1000 base pairs to 100 base pairs in 100 base pair increments.

As can be seen from the above image of an agarose gel the cDNA from RT+ (reverse transcribed) produces stronger bands when compared to the gDNA from RT- (non-reverse transcribed), however even at 65°C bands are still faintly visible for the gDNA. To increase the specificity of the primer for the exon 2-3 junction the annealing temperature was gradually raised in a series of experiments. Unfortunately though the

annealing temperature for binding to cDNA was consistently higher than for gDNA there was no reliability as to the exact temperature at which this would happen. This can be seen in **Figure 3.42** where gDNA will not produce an amplicon at an annealing temperature of 63.1°C, despite this being a temperature at which it had previously annealed to the MOP3 primer pair, **Figure 3.41**. This primer pair was therefore not used further in PCR investigations of the MOP receptor.

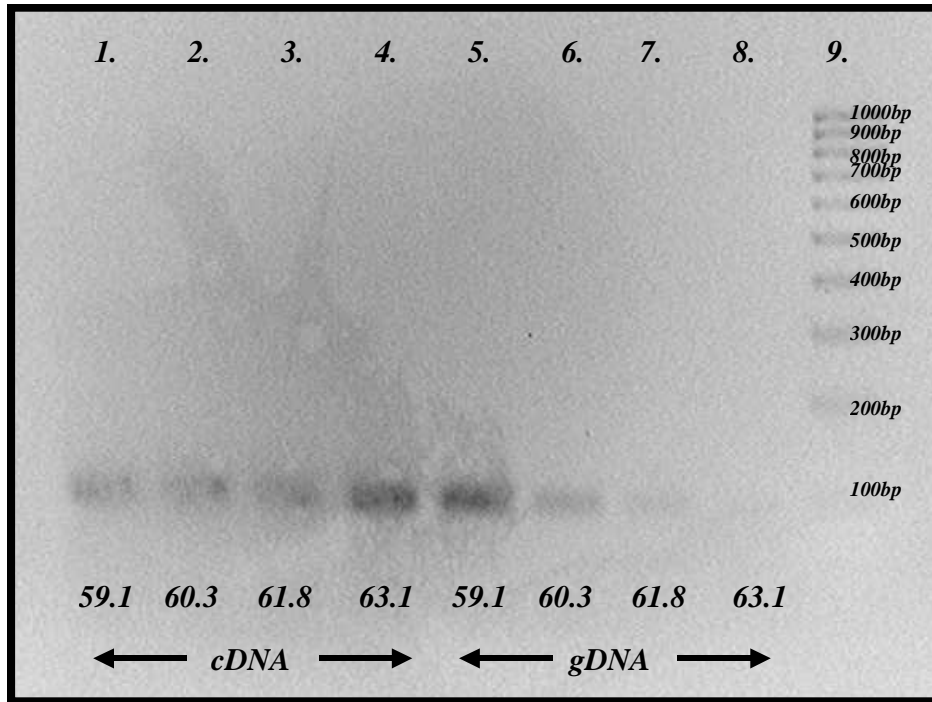


Figure 3.42

Annealing gradient for MOP3 primers used with cDNA from SH-SY5Y lanes 1-4 and gDNA SH-SY5Y lanes 5-8. Ladder lane 9. All temperatures shown along the lower border are in degrees centigrade. Product is seen at the expected amplicon length of 92 base pairs strongly in the first 4 lanes again indicating strong binding to cDNA but at lower temperatures than previously. However an amplicon is seen at 59.1 and 60.3°C with gDNA. Now though no amplicon is seen at 63.1°C with gDNA. The weight ladder to the right ranges from 1000 base pairs to 100 base pairs in 100 base pair increments.

MOP3+1

It was realised that if the forward primer from MOP3 was coupled with the reverse primer from MOP1 then primers sitting on different exons could be used to differentiate cDNA and gDNA. These primers were also chosen for the proximity of their melting points 51.5 and 55°C an annealing gradient experiment using SH-SY5Y cDNA showed the optimal annealing temperature to be 50.7°C, **Figure 3.43**, which was used in future PCR reactions with this primer combination. They give a cDNA amplicon of 207bp length and a gDNA amplicon of 980bp length.

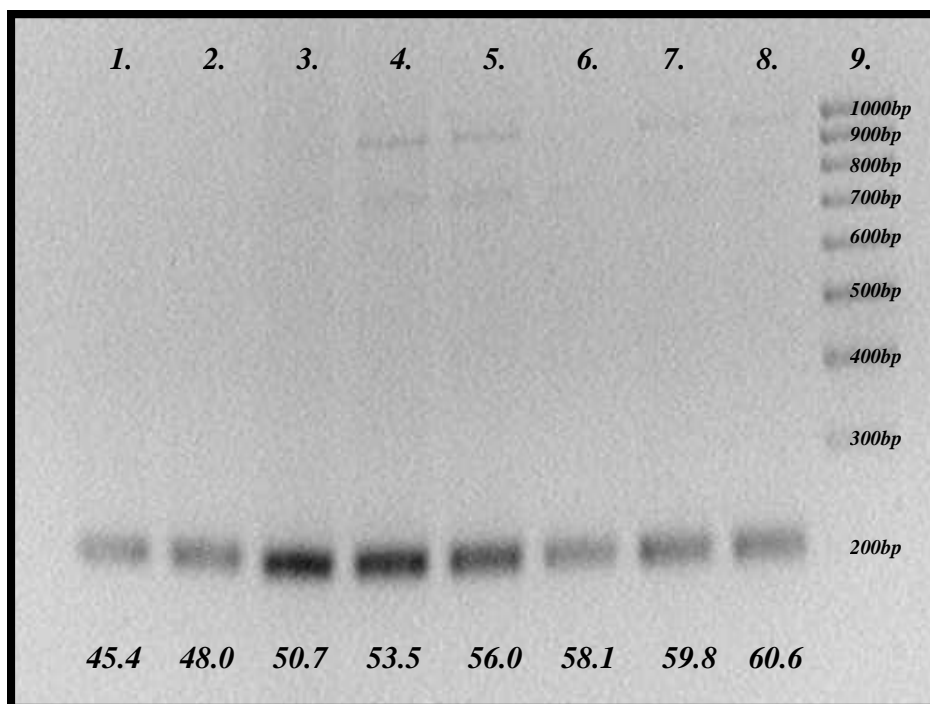


Figure 3.43

Annealing gradient for MOP3+1 primers used with cDNA from SH-SY5Y lanes 1-8. Ladder lane 9. All temperatures shown along the lower border are in degrees centigrade. Product is seen at the expected amplicon length of 207 base pairs strongly in all 8 lanes indicating strong binding to cDNA. There is however some faint contamination by genomic DNA in lanes 4 and 5. The weight ladder to the right ranges from 1000 base pairs to 200 base pairs in 100 base pair increments.

PCR of this primer pair at 50.7°C with gDNA from CEMx174 cells and cDNA from SH-SY5Y cells showed the ability of the product to discriminate between cDNA and gDNA for the MOP receptor, **Figure 3.44**. The ladder is only faintly visible in lane 9, however the gDNA from CEMx174 cells gives a clear 980bp band and cDNA from SH-SY5Y

cells a band at 207bp. SH-SY5Y RT- lanes 3+4 show no gDNA contamination as well as no cDNA band as expected.

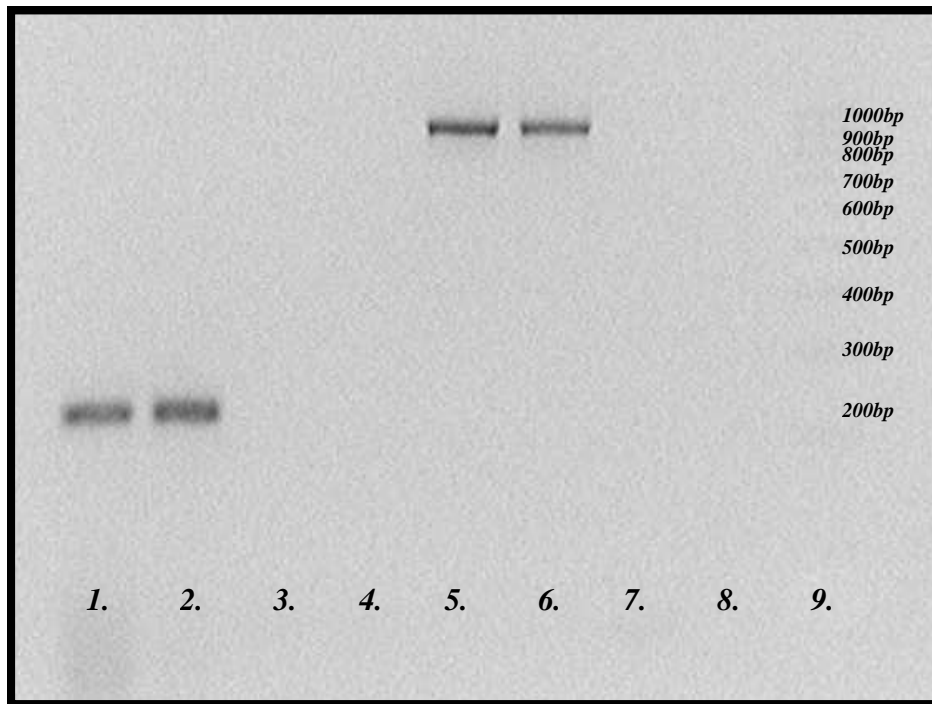


Figure 3.44

PCR gel for MOP3+1 primers with SH-SY5Y gDNA and cDNA as template. Lane 1 SH-SY5Y cDNA RT+, lane 2 SH-SY5Y cDNA RT+, lane 3 SH-SY5Y cDNA RT-, lane 4 SH-SY5Y cDNA RT-, lane 5 CEMx174 gDNA, lane 6 CEMx174 gDNA, lanes 7-8 water. Ladder lane 9. Amplicons of 207 base pairs are seen in lanes 1+2 relating to cDNA, while amplicons of 980 base pairs are seen in lanes 5+6 (gDNA). The weight ladder in lane 9 ranges from 1000 base pairs to 200 base pairs in 100 base pair increments.

Below in **Figure 3.45** another gel of MOP3+1 primers used in PCR against cDNA from SH-SY5Y cells confirms this, with a cDNA band at 207bp for the RT+ species, and a faint gDNA band for one of the RT- species.

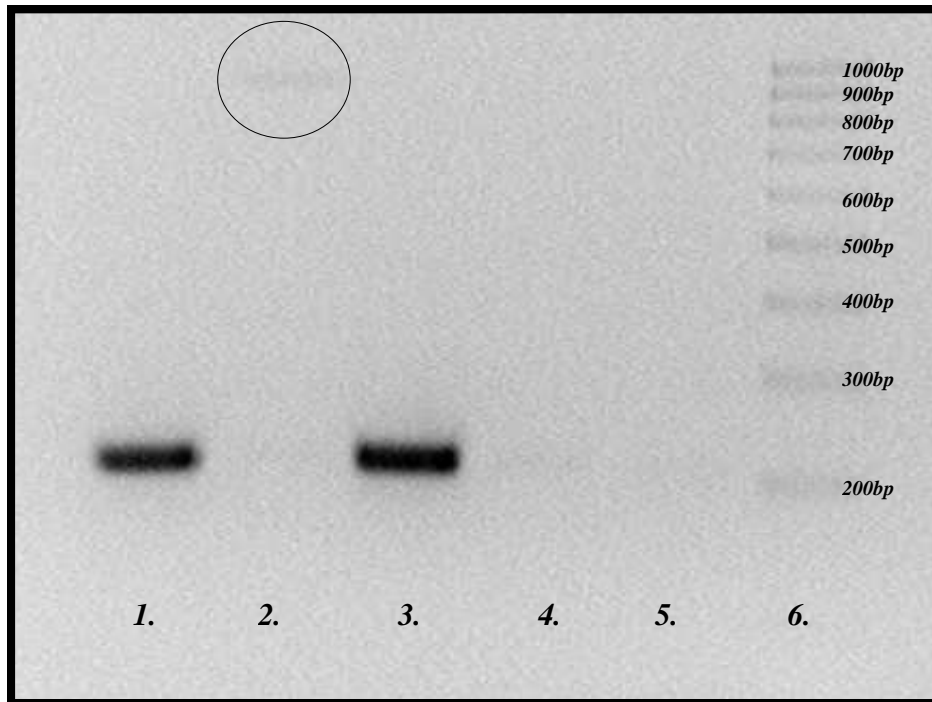


Figure 3.45

PCR gel for MOP3+1 primers with SH-SY5Y cDNA as template reverse transcribed (RT+) and non-reverse transcribed (RT-). Lane 1 SH-SY5Y cDNA RT+, lane 2 SH-SY5Y cDNA RT-, lane 3 SH-SY5Y cDNA RT+, lane 4 SH-SY5Y cDNA RT-, lane 5 water. Ladder lane 6. Amplicons of 207 base pairs are seen in lanes 1+3 relating to cDNA, while a faint amplicon (circled) of 980 base pairs is seen in lane 2 (gDNA). The weight ladder in lane 6 ranges from 1000 base pairs to 200 base pairs in 100 base pair increments.

A faint genomic DNA band is seen in lane 2, while cDNA bands are observed in 1 and 3. The MOP3+1 primer combination confirmed the presence of cDNA for the MOP receptor in SH-SY5Y cells (as shown above) and CHO_{hMOP} cells, **Figure 3.46** below. Interestingly the DNA for the MOP receptor transfected into CHO_{hMOP} cells does not contain any introns i.e. cDNA has been added to the genome of these cells and not gDNA. They therefore do not display genomic type MOP3+1 amplicons at 980bp, but just 207bp amplicons regardless of whether reverse transcription has been performed or not. All immunocompetent cells showed amplicons of length 980bp indicative of genomic DNA, but none showed amplicons at 207bp. This indicates that they are not producing the mRNA, which would encode for the receptor.

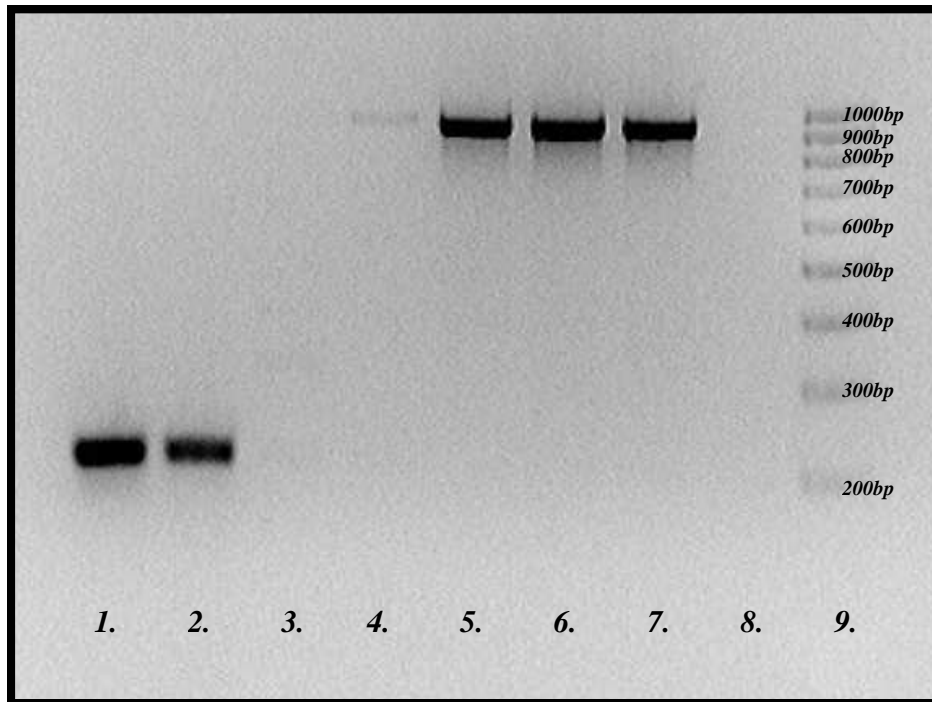


Figure 3.46

PCR gel for MOP3+1 primers with a variety of different templates both reverse transcribed (RT+) and non-reverse transcribed (RT-). Lane 1 CHO_{hMOP} cDNA RT+, lane 2 CHO_{hMOP} cDNA RT-, lane 3 PBMC cDNA RT+, lane 4 PBMC cDNA RT-, lane 5 CEM gDNA, lane 6 PBMC gDNA, lane 7 PBMC gDNA, lane 8 water. Ladder lane 9. Amplicons of 207 base pairs are seen in lanes 1+2 relating to cDNA. Note that hMOP cDNA has been transcribed into CHO_{hMOP} cells and not gDNA hence both RT+ and RT- CHO_{hMOP} cells give an amplicon at 207 base pairs. 980 base pairs products are seen in lanes 4-7 (gDNA). The weight ladder in lane 9 ranges from 1000 base pairs to 200 base pairs in 100 base pair increments.

In **Figure 3.46** CHO_{hMOP} cDNA and gDNA (i.e lane 2 with no reverse transcription step) gave bands at the same base pair length. PBMC cDNA has no band lane 3, but the gDNA from this species has a faint band in lane 4 at 980bp. Lane 5,6 and 7 are all from genomic templates and show bands at 980bp which is indicative of the gDNA for the MOP receptor.

PBMCs separated from the venous blood of 10 healthy male Caucasian volunteers age range 23-41, were also investigated for the presence of RNA encoding for the MOP receptor using the MOP3+1 primer combination. While all of these individuals showed evidence of the genomic message for the receptor none displayed the cDNA corresponding to the RNA message as shown in **Figure 3.47** below.

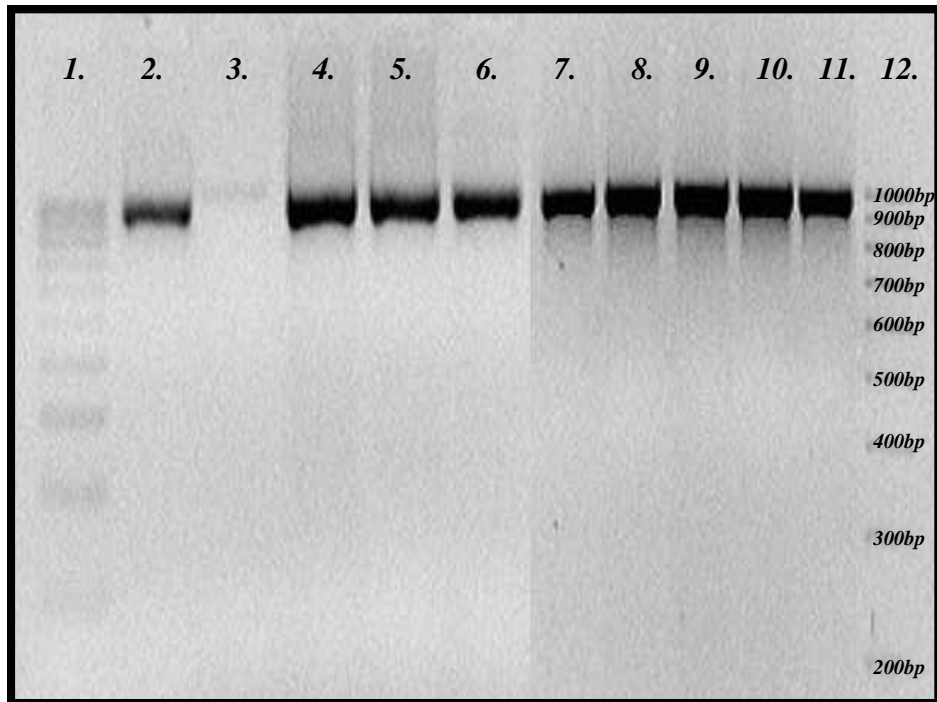


Figure 3.47

PCR from two gels for MOP3+1 primers cDNA from the PBMCs of ten healthy male volunteers. Lane 1+12 ladder. Lanes 2-11 cDNA from PBMCs. 980 base pairs products are seen in lanes 2-11 indicative of gDNA (lane 3 shows a faint but present band at 980 base pairs also). No cDNA product is seen. The weight ladder in lanes 1+12 ranges from 1000 base pairs to 200 base pairs in 100 base pair increments.

Formaldehyde integrity gels run in accordance with **Protocol 2.8**, did however provide evidence for good quality RNA extraction from the PBMCs of the ten healthy male volunteers **Figure 3.48**.

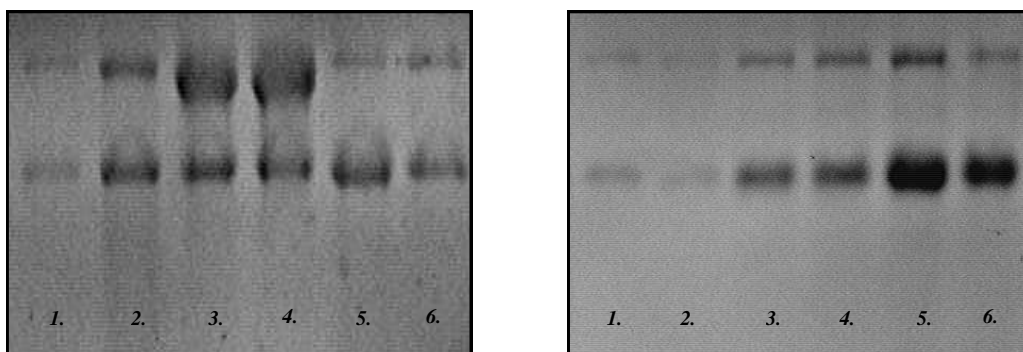


Figure 3.48. RNA integrity gel for the RNA extracted from the PBMCs of 10 healthy volunteers lanes 2-6, lane 1 shows atrial human RNA (*Ambion*) as control in each plate, five individuals are shown in each panel.

3.4.2 Results: Quantitative polymerase chain reactions

Quantitative PCR experiments using CHO_{hMOP} cDNA with *TaqMan*® probes (Hs00168570_m1) gave amplification plots indicative of the presence of human MOP receptor, as expected, with C_T values around 22 amplification cycles **Figure 3.49**. These results provided evidence that this technique could be used as a means of investigating for human MOP mRNA. However this method using *TaqMan*® primer/probe combinations when repeated for venous blood and PBMCs gave results supporting the findings from standard endpoint PCR, immunofluorescent labelling and radioligand binding, that there was no evidence for the expression of the classical MOP opioid receptor mRNA in **Figure 3.49 & 3.50**.

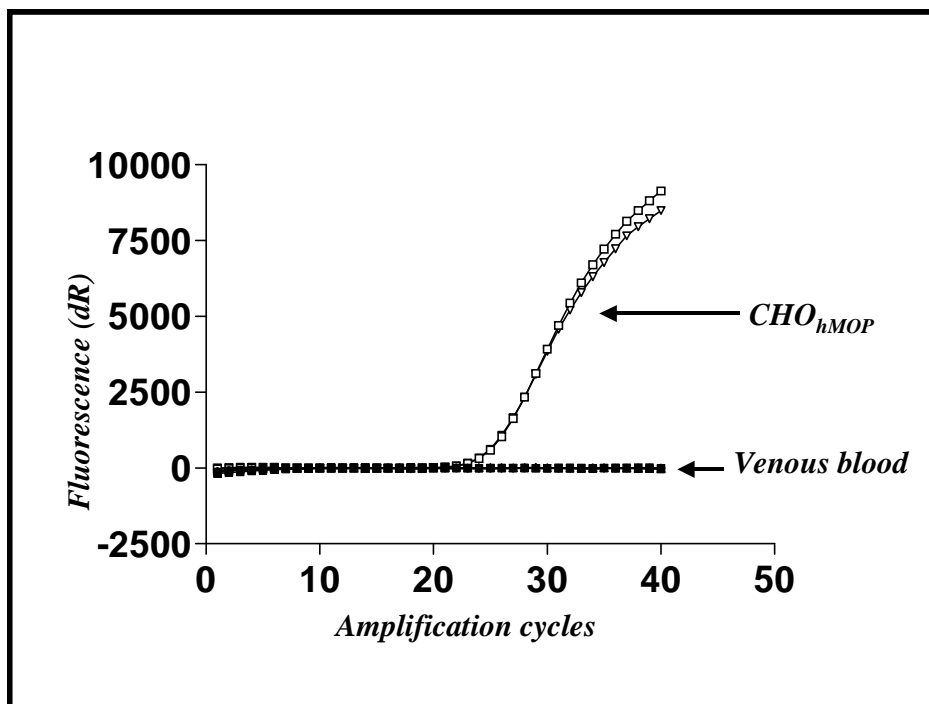


Figure 3.49. QPCR using *TaqMan*® Gene expression assay for MOP receptor with cDNA from CHO_{hMOP} cells as positive control, and with cDNA from whole venous blood. Example of five replicates of a total of five venous blood samples, with two CHO_{hMOP} positive controls. Venous blood shows no deflection of the curve, while CHO_{hMOP} cDNA shows deflection at 22 cycles.

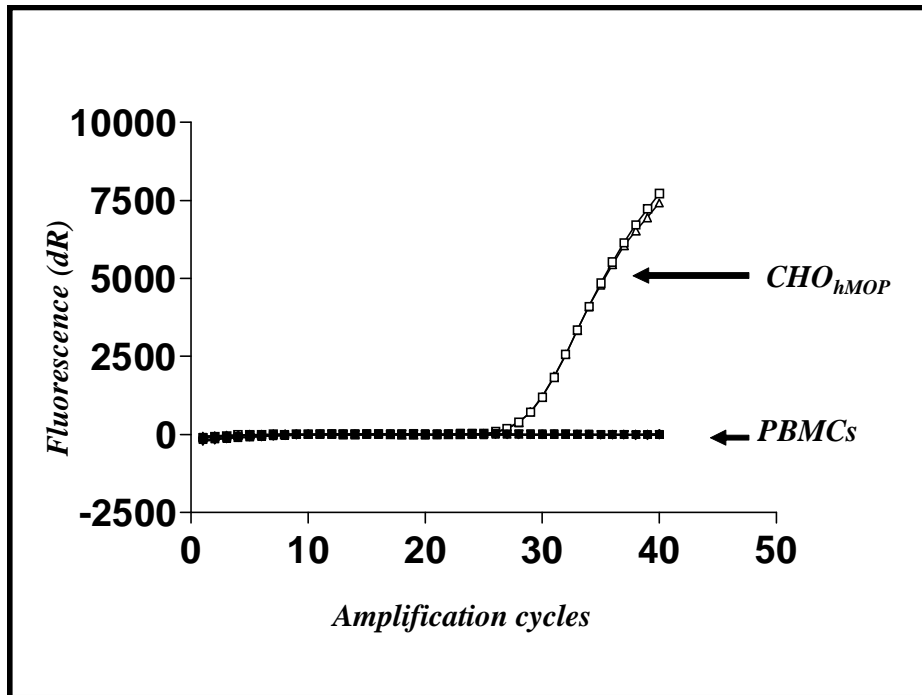


Figure 3.50. QPCR using *TaqMan*® Gene expression assay for MOP receptor with cDNA from *CHO_{hMOP}* cells as positive control curve, and with cDNA from PBMCs. Example of five replicates of a total of ten PBMC samples, with two *CHO_{hMOP}* positive controls. PBMCs show no deflection of the curve (labeled PBMC above), while *CHO_{hMOP}* cDNA shows deflection at 26 cycles.

3.4.3 Results: Stimulated upregulation of MOP gene expression

Standard gel based PCR imaging using a 3% agarose gel viewed under a UV light gave no indication of clear identifiable up-regulation in expression of the gene encoding for the human MOP receptor in Raji cells, following administration of 100-200pg/ml of TNF α to the cell culture 20 hours prior to harvesting. **Figure 3.51**. This procedure was repeated four times and on no occasion was there a band suggestive of up-regulation of mRNA encoding for the MOP receptor. In order to confirm that the TNF/cycloheximide mixture was active U937 cells were incubated in the presence of 30pg/ml of TNF α and 1 μ g/ml cycloheximide at 37°C, 5% CO₂ for twenty-four hours in RPMI. This combination would be expected to decrease cell viability (*Dong et al 1998*). Cells were then stained with trypan blue and viewed with a haemocytometer to confirm cell number and viability. **Figure 3.52** clearly shows increased U937 cell death after twenty-four hours incubation in TNF and cycloheximide. This suggests that this mixture was working as an active pro-inflammatory agent.

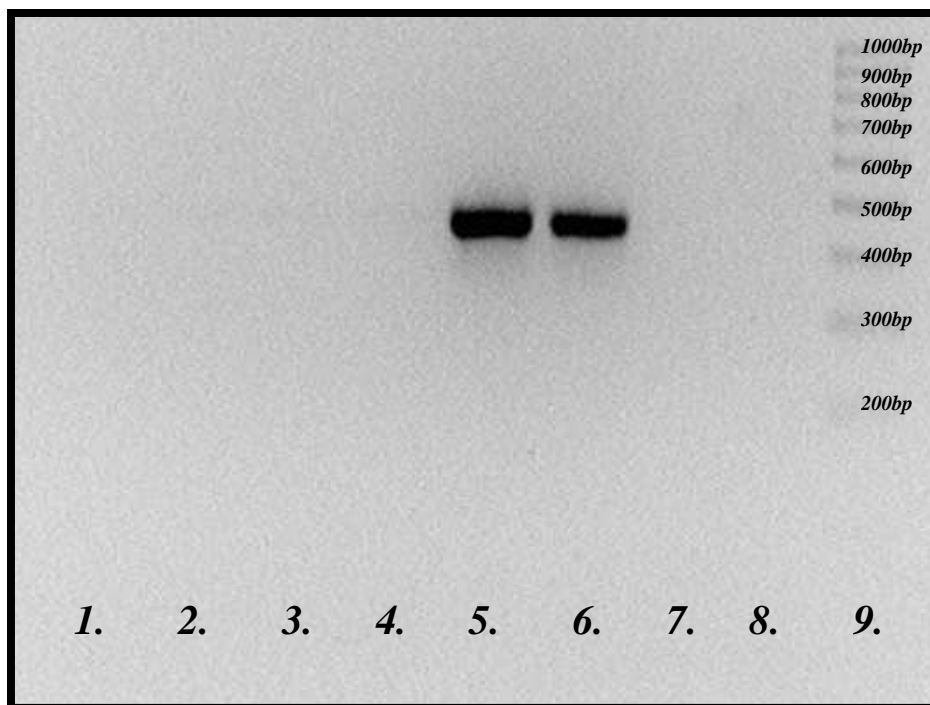


Figure 3.51. MOP2 primers with cDNA from the Raji cells treated and not treated with 100 pg/ml of TNF α . Lane 1 Raji TNF/CHX+ RT+, lane 2 Raji TNF/CHX+ RT-, lane 3 Raji TNF/CHX- RT+, lane 4 Raji TNF/CHX- RT-, lane 5 SH-SY5Y cDNA, lane 6 CEM gDNA, lane 7 RPMI control, lane 8 H₂O control, lane 9 ladder. There is no band either with or without addition

of TNF α in Raji cells. The weight ladder to the far right, ranges from 1000 base pairs to 100 base pairs in 200 base pair increments (values are shown to the left of the ladder).

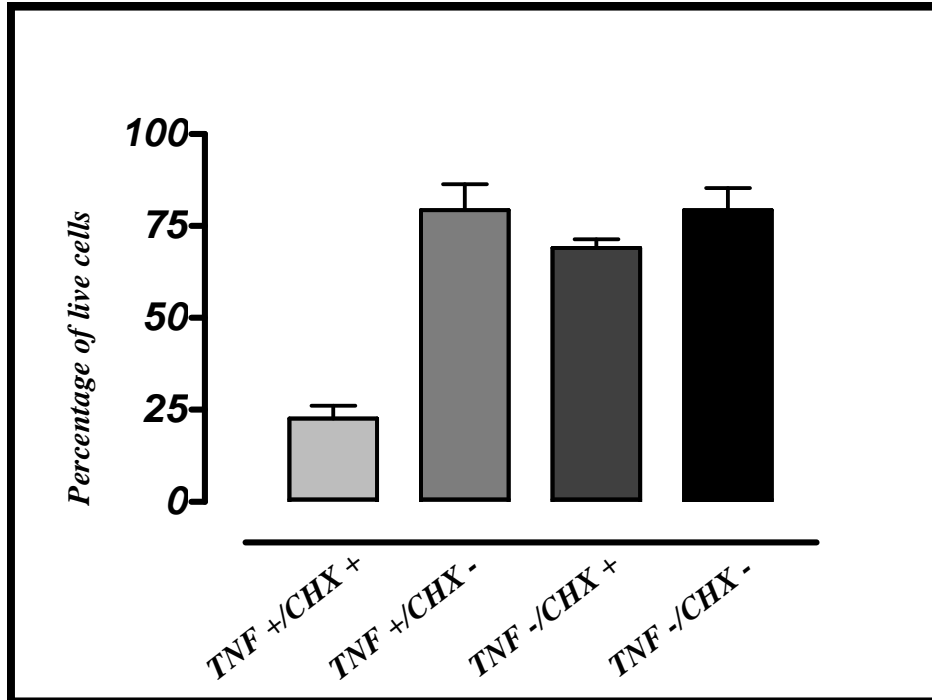


Figure 3.52. Survival of U937 cells treated and not treated with 30 pg/ml of TNF α and 1 μ g of cycloheximide after twenty-four hours. Error bars show SEM (n=3).

3.5 Discussion

In this series of experiments utilising a range of complimentary techniques we have failed to provide evidence for the presence of MOP receptors on peripheral blood mononuclear cells. Radioligand binding experiments with [³H]-Diprenorphine showed binding to CHO_{hMOP} cells, but no binding to any of the immune cell lines could be detected. There was some increase in specific binding at higher concentrations of [³H]-Diprenorphine, but this was thought to be due to additional penetrance of the cell membrane in a non-specific manner by the lipid soluble label at these higher concentrations.

In a series of immunofluorescent staining experiments utilising direct fluorescent microscopy, confocal microscopy and flow cytometry as imaging techniques, both of the commercially available MOP receptor primary antibodies proved to be ineffective at specific staining of the MOP receptor in CHO_{hMOP} cells (the positive control for all of these experiments). As would be expected therefore these primary antibodies also provided no specific MOP receptor staining when used with immunocompetent cells or immunocompetent cell lines. The primary antibody provided by *Professor Cote* of the University of Bethesda (1414) did however specifically stain for MOP receptors on CHO_{hMOP} cells, suggesting that this primary antibody is a useful probe for detection of the receptor, no staining was seen with immunocompetent cells providing further support for the view that MOP receptors are not present on peripheral immunocompetent cells.

A fifth fluorescent probe used to image MOP receptors was fluorescent-naloxone, a fluorescent analogue of the non-specific opioid antagonist naloxone. Radioligand competition binding experiments showed that though fluorescent-naloxone had different binding characteristics to its parent compound it could still be used as a fluorescent probe directed against opioid receptors, however like its parent compound it displays affinity for MOP, DOP and KOP receptors. Initial studies with CHO_{hMOP} cells, fluorescent-naloxone and flow cytometry displayed dose dependent binding to the MOP receptor.

The inability to find MOP receptors themselves on PBMCs led us to employ polymerase chain techniques in an attempt to locate the RNA message encoding for the protein. As discussed above however the presence of the RNA message only implies the transcription of receptor and does not guarantee its expression. Again a variety of DNA and RNA probes were used in the form of primer pairs. Finally a combination of two primers

originally used with different pairings was employed, which enabled the distinction of genomic DNA from complimentary DNA. When used with CHO_{hMOP} cells or human neural cell lines known to display MOP receptors, bands consistent with the presence of MOP receptor were imaged on agarose gels. However immunocompetent cells showed no such bands, strongly suggesting that the RNA message for the MOP receptor is not produced in these cells or the MOP receptor itself.

Collectively these experiments provide good evidence that peripheral blood mononuclear cells do not express the classical MOP receptor or its RNA message. These findings are however at odds with much of the literature produced within this area. As early as 1983 researchers (*Mehrishi et al 1983*) were reporting radioligand binding to peripheral blood mononuclear cells and other immunocytes separated from as little as 20 mls of human blood donated by healthy volunteers, in our laboratories we found these results impossible to reproduce.

Beck and *Caldioli* have previously used immunofluorescent and direct fluorescent staining with primary anti-MOP receptor antibodies and fluorescent opioid receptor antagonists respectively to study MOP receptors on peripheral blood mononuclear cells taken from human volunteers (*Beck et al 2002, Caldioli et al 1999*). The primary antibody NHQLENLEAETAPLP raised against the intracellular carboxyl terminal of the human MOP receptor was used in most cases. In these experiments phosphate buffered saline was used as a negative control and not normal rabbit serum in which the antibody was raised and suspended. These experiments therefore cannot rule out the possibility of some reaction with another portion of the cell distinct to antibody binding to the MOP receptor.

Chuang using the techniques of reverse transcription polymerase chain reactions has described the expression of the mRNA encoding for the MOP receptor in immunocompetent cells and cell lines of humans and other primates (*Chuang et al 1995b, Suzuki et al 2000*). The primer pairs used in these experiments have however been directed to regions of the genetic code located within one exon and so raise the possibility of amplification of genomic DNA rather than complimentary DNA produced from the reverse transcription of RNA encoding for the MOP receptor. In our experiments a primer pair was chosen, which could amplify both genomic DNA and complimentary

DNA but which would give differing amplicon weights dependent upon which original template was amplified. Using this technique we were unable to isolate RNA encoding for the MOP receptor in peripheral immunocompetent cells.

Despite these findings others have regularly shown an immunomodulatory effect of opioids both *in vitro* and *in vivo* (Manfredi et al 1993, Mellon et al 1998 & 1999, Philippe et al 2003, Yeagar et al 1991 & 1995). Following the observation, by researchers, that opiate abusers are more prone to opportunistic infections (bacterial, fungal and viral in nature) than non-addicts, it has long been suggested that morphine and its addictive analogues may produce detrimental effects on the immune system. Though initially this increased risk was attributed to dirty needles and the poorer nutritional standard of drug abusers, an increased infection rate seems to persist even in the absence of these circumstances (Cabral 2006, Friedman et al 2003, Spittal et al 2003). *In vivo* and *in vitro* laboratory models also suggest that opioids can exert deleterious effects upon the immune system. When administered *in vivo* to rodent models or human volunteers, opioids have been shown to precipitate profound changes in immune cell function encompassing a range of immunocompetent cells and causing alterations in their specific immunological roles (Mellon et al 1998 & 1999, Philippe et al 2003, Sacerdote et al 2001, Wang et al 2005, Yeager et al 1991 & 1995). Furthermore *in vitro* addition of opioids has been shown to alter a number of immunological parameters (Manfredi et al 1993, Morgan 1996, Saurer et al 2004). Natural killer cell activity, lymphocyte proliferation and antibody production are all affected by the addition of opioids to cell suspensions of immunocompetent cells, while the cytokine production profile of immune cells is affected by the addition of opioid analgesic agents (Murphy 2003, Roy et al 2001, Wetzel et al 2000).

Evidence exists within the literature to indicate that MOP agonists can exert an effect upon a central neuroimmune axis, possibly via classical MOP receptors and the hypothalamic-pituitary-adrenal axis, with immunomodulatory consequences (Mellon et al 1998). This physiological axis could explain the immunosuppressive results of the administration of opioids in man and whole animal studies. However the finding that immune cells do not display MOP receptors suggests, that though numerous studies describe alterations in immune cell function after opioids are added to cell suspensions of

immune cells, this functional effect of MOP agonists cannot be directed via interaction with the classical MOP receptor at a cellular level within the periphery. A number of different theories could explain how opioids influence immune cell function in the absence of MOP receptors. Most simply it is possible that opioid agonists may act at immune cells via a non-classical MOP receptor. *Cadet* has postulated a μ_3 receptor capable of interaction with classical MOP agonists but displaying a different DNA and protein sequence, this type of receptor has not been sequenced (*Cadet et al 2001, 2002 & 2003*). A second explanation is the expression of the MOP receptor only following exposure of immune cells to a variety of cytokines and proinflammatory compounds. The group of *Hollt* has found evidence for MOP receptor expression on immune cells after administration of tumour necrosis factor- α , **Figure 3.53** (*Kraus et al 2001 & 2003*). This expression was found to increase with time up to 24 hours, following the administration of TNF- α , **Figure 3.54**. However RNA transcripts were found in very low number requiring multiple PCR amplification cycles to show evidence of amplification product and so casting some doubt on these findings. In a series of experiments using TNF- α and cycloheximide stimulation of Raji cells we found no such up-regulation of MOP receptors at 40 amplification cycles. However if after repeated PCR cycles these experiments correctly point to the presence of MOP receptor RNA following immune cell exposure to TNF- α , the physiological and cellular significance of such low levels of transcript and hence protein expression requires further investigation.

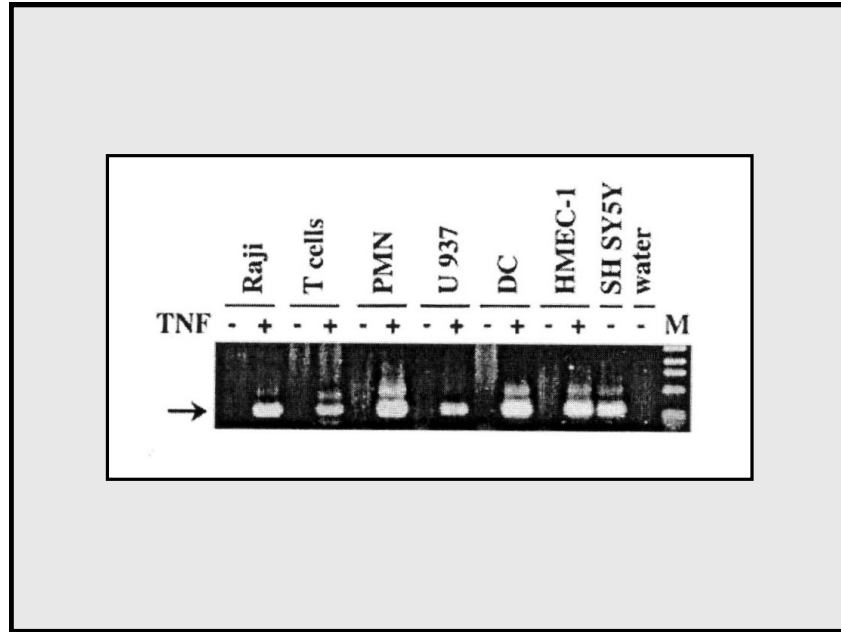


Figure 3.53. The above image shows agarose gel PCR analysis, shows bands corresponding to cDNA for the MOP receptor only after administration of TNF- α in the immunocompetent cell lines but in the basal state for the neuroblastoma cell line SH-SY5Y. From Kraus *et al* (2003) *Mol Pharmacol* 64: 876-84

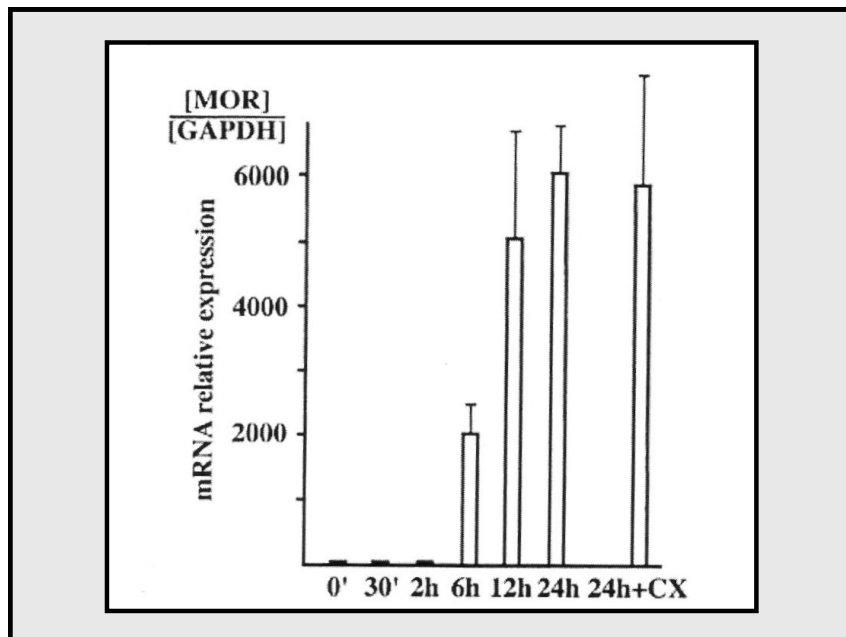


Figure 3.54. Quantitative PCR shows a relative increase in the expression of the MOP receptor in Raji cells compared to the housekeeping gene GAPDH. This relative increase is dependent upon the time from TNF- α administration, with the greatest increase at 24 hours. From Kraus *et al* (2003) *Mol Pharmacol* 64: 876-84

During episodes of traumatic injury it has been shown that there may be an inappropriate increase in the differentiation of naïve CD₄⁺ cells to T_H 2 lymphocytes, rather than T_H 1 CD₄⁺ cells. This preferential differentiation to T_H 2 cells favours immunological reactions capable of countering allergens and helminth infestation, while production of T_H 1 cells enhances the immune systems ability to deal with microbial infections. Some studies have suggested that MOP agonists may, like traumatic injury, promote T_H 2 lymphocyte production, and so reduce the immunological response to bacterial infection hence rendering a patient immunocompromised following opioid administration (*Roy et al 2001*).

When considering the organism as a whole each of the theories introduced above could provide an explanation for the effects opioid analgesic have on that organisms ability to cope with infection. However none of these models adequately and simultaneously explain the *in vitro* effects on individual cell lines and the *in vivo* effects of opioids on the body as a whole.

Chapter 4:

DOP & KOP Opioid Receptor Expression in Peripheral Immune Cells

4.1 Background

The DOP and KOP receptors were, respectively, the first and second opioid receptors to be cloned (*Evans et al 1992, Kieffer et al 1992, Kieffer 1995, McDonald et al 2005, Satoh et al 1995*). DOP agonists have been shown to produce both anti-nociceptive and analgesic effects when administered spinally and supra-spinally. Observations have also suggested that DOP agonists can produce respiratory depression and a reduction in gastrointestinal motility in a similar, though less marked manner to MOP receptor agonists. It is also thought that DOP agonists may be associated with mood regulation, with the limbic system showing a high density of DOP receptors (*McDonald et al 2005*). Similar to MOP and DOP receptor agonists, KOP receptor agonists also have an analgesic effect. However these compounds may also produce an anti-analgesic response if administered concurrently with MOP agonists via a mechanism located within the nucleus raphe magnus. KOP agonists have been shown to produce a more limited degree of respiratory depression when compared to MOP and DOP agonists, but unlike agonists at these two opioid receptor subtypes KOP agonists may also produce dysphoria (*McDonald et al 2005*). Despite findings that both DOP and KOP agonists are capable of eliciting analgesia and anti-nociception, opioid based analgesic agents used in clinical practice are almost universally MOP agonists, testifying to the greater efficacy and clinical utility of these compounds at controlling pain.

In the preceding chapter a series of experiments examining the expression of MOP receptors on a range of immune cell lines and PBMCs isolated from the blood of healthy volunteers were undertaken. In these experiments [³H]-Diprenorphine was used as a radiolabelled probe to investigate for the presence of MOP receptors. Despite convincing and reproducible binding of [³H]-Diprenorphine to CHO_{hMOP}, these studies suggest that PBMCs do not express MOP opioid receptors or that these receptors are in low abundance if present. The lack of any convincing binding of the non-specific opioid receptor antagonist, [³H]-Diprenorphine, also implies that these cells express none of the

classical opioid receptors (MOP, DOP or KOP), or that they are again in too low an abundance for this technique to find them.

Chapter 3 also describes the use of fluorescent-naloxone to look for the expression of MOP on PBMCs. Competition binding assays with fluorescent-naloxone and [³H]-Naloxone suggested that fluorescent-naloxone could be used as a fluorescent probe at opioid receptors. As with [³H]-Diprenorphine, fluorescent-naloxone consistently provided evidence for the presence of opioid receptors on the CHO_{hMOP}. Again however this result was not reproducible in any of the immunocompetent cells investigated. Naloxone is analogous to [³H]-Diprenorphine in being a non-specific classical opioid receptor antagonist, and though radioligand competition binding assays were only undertaken with fluorescent-naloxone / [³H]-Naloxone combinations, it seems likely that fluorescent-naloxone has activity at all three classical opioid receptors in a similar manner to its parent compound naloxone. Therefore a lack of binding of fluorescent-naloxone to immune cells would also indicate that none of the classical opioid receptors (MOP, DOP or KOP) are present on immune cells.

Following the failure of the two experimental approaches described above to show any evidence of classical opioid receptor-ligand binding on the surface of peripheral blood mononuclear cells, DOP and KOP receptor transcripts were measured.

The aims of this chapter are therefore:

- To investigate in detail whether whole venous blood, or PBMCs of healthy male volunteers, expresses either DOP or KOP receptors under basal 'resting' conditions. To accomplish this a series of standard gel based endpoint PCR and quantitative PCR experiments were performed.

4.2 Polymerase Chain Reaction

Chinese hamster ovary cells, transfected with and stably expressing human DOP (CHO_{hDOP}) or KOP (CHO_{hKOP}), were used to optimize polymerase chain reaction techniques for DOP and KOP receptor RNA expression prior to investigations using the RNA extracted from Raji cell lines grown in culture, PBMCs extracted from volunteers venous blood and whole blood.

The literature provides many examples of primer pairs that have been used to investigate both DOP and KOP receptor gene expression (*Chuang et al 1994 & 1995a, Gaveriaux et al 1995, Gaveriaux-Ruff et al 1997, Sharp 2006, Sharp et al 2000, Suzuki et al 2001*). Two of these primer pairs from the literature, the DOP2 pairing and KOP1 pairings described below, were initially chosen to investigate extracted RNA for DOP and KOP receptor gene expression. However during investigations it became clear that additional primers needed to be developed either to provide a means of differentiating genomic from complimentary DNA in the case of the KOP receptor or to provide an amplicon sufficiently small to be of use in subsequent quantitative PCR reactions. This led to the design and synthesis of two supplementary primer pairs, DOP1 and KOP2.

Though the DOP2 primer pair sat on two different exons and therefore made differentiation of genomic from complementary DNA possible, it produced an amplicon of 356 base pairs in length (not suitable for QPCR techniques). It was therefore decided to design a second primer pair, DOP1, which would produce a smaller amplicon at 92 base pairs in length. As can be seen from **Table 4.1** this primer pair encodes for a portion of the DOP genomic message on exon 4, rendering differentiation of genomic from complementary DNA difficult.

KOP1 primer pairs in contrast to the DOP2 pairing sat on the same exon, exon 3. This led to the development of a second primer pair to allow the differentiation of KOP RNA transcripts from genomic DNA. This primer pair was labeled KOP2 and produced an amplicon of 210 base pairs in length by the action of primers on exon 2 and 3 of the KOP receptor gene. These primer pairings are displayed in **Tables 4.1** and **4.2** for DOP and KOP pairings respectively.

4.2.1 Results: DOP primers, Endpoint PCR

A variety of cell lines were used to optimise PCR reaction conditions for DOP1 and DOP2 primers prior to use in human immune cells extracted from volunteers. Methods of RNA extraction utilised a TRI reagent/chloroform technique as described previously in **Chapter 2**, following the extraction of PBMCs from venous blood, **Protocol 2.1**. **Protocols 2.4-2.6** were followed for RNA extraction and reverse transcription respectively, while **Protocol 2.7** was used for the polymerase chain reaction itself. Amplicons were imaged under UV illumination after running for approximately 45 minutes on a 3% agarose gel made in 1% TAE buffer containing 5µl/100ml of ethidium bromide.

Primer	Sequence	mRNA Position	Amplicon size
DOP1F	5'- TGGACACCGAGATGTTGA-3' (<i>Exon 4</i>)	1649-1672	92
DOP1R	5'- AGTTAGAAACCGAAGCTGTCTCAAGG-3' (<i>Exon 4</i>)	1713-1741	92
DOP2F	5' -TAGAAGTGCGAGTGGTACTAC- 3' (<i>Exon 3</i>)	648-669	356
DOP2R	5'-CGGTCCTTCTCCTTGGA-3' (<i>Exon 4</i>)	986-1004	356

Table 4.1 Primer pairings used in standard gel based PCR for DOP transcripts.

It was thought that the 92 base pair DOP1 primer amplicon could be of use in subsequent quantitative PCR reactions, where shorter amplicons are advantageous. This amplicon would not be capable of differentiating genomic from complimentary DNA, as the sequence for both the forward and reverse primers are situated on exon 4 of the mRNA encoding for the DOP receptor. Unfortunately both of the DOP1 primer pairs, though sitting on the fourth exon of the mRNA encoding for the DOP receptor, actually corresponds to a region, which is not translated into protein. This region of the mRNA code had therefore not been incorporated into the genetic material transfected into the Chinese hamster cell line used in these experiments. This means that the DOP1 primer pairs are of limited use as a probe in this cell line. **Figure 4.1** shows an annealing gradient for the DOP1 primer pair using cDNA from CHO_{hDOP} cells as template. Though bands can be seen at the lower annealing temperatures of around 600, 400 and 250 base

pairs no product is seen at 92 base pairs, which would correspond to the amplicon of interest. The larger weight bands at lower temperatures are artifactual products.

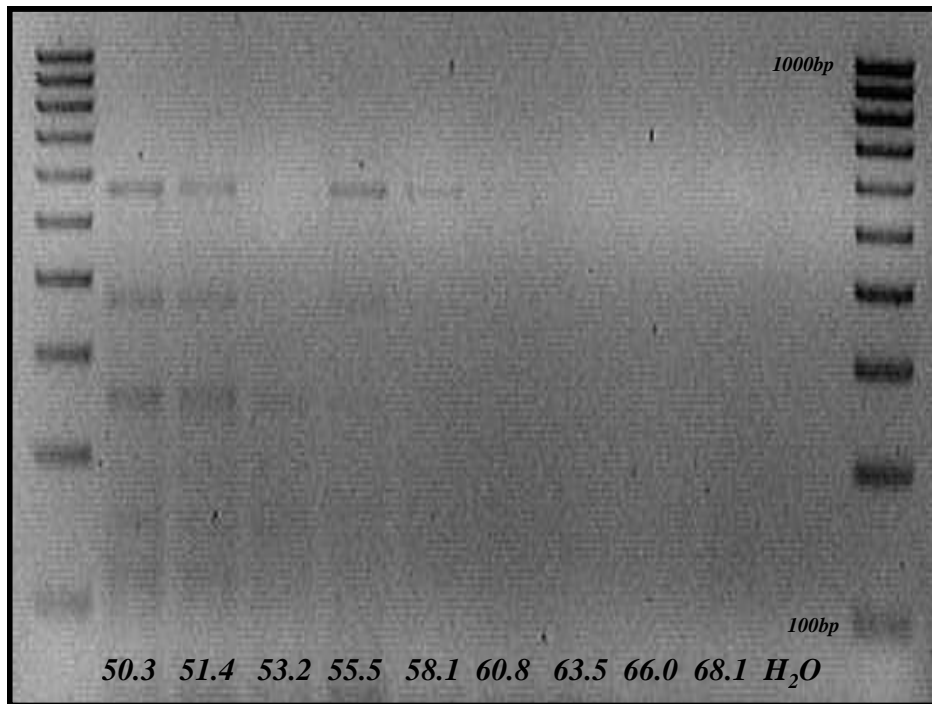


Figure 4.1. Annealing gradient for DOP1 primers used with cDNA from CHO_{hDOP} cells. All temperatures shown along the lower border are in degrees centigrade. No product is seen at the expected amplicon length of 92 base pairs. The weight ladders to the far left and right range from 1000 base pairs to 100 base pairs in 100 base pair increments.

However as the primer pair only recognises sequences on one exon, it was possible to use genomic DNA extracted from whole human blood and from the CEMx174 cell line, to perform a series of experiments to find the optimum annealing temperature. These experiments gave clear bands at 92 base pairs with all annealing temperatures used within the range. **Figure 4.2 and 4.3** Despite using a consistent quantity of cDNA as template in all of these reactions amplicons produced at 68.1 and 69.5°C were always fainter, while amplicons at an annealing temperature of 70.5°C were again more obvious.

It was however decided not to use the DOP1 primer pair in future experiments examining the DOP receptor due to its inability to differentiate genomic from complimentary DNA.

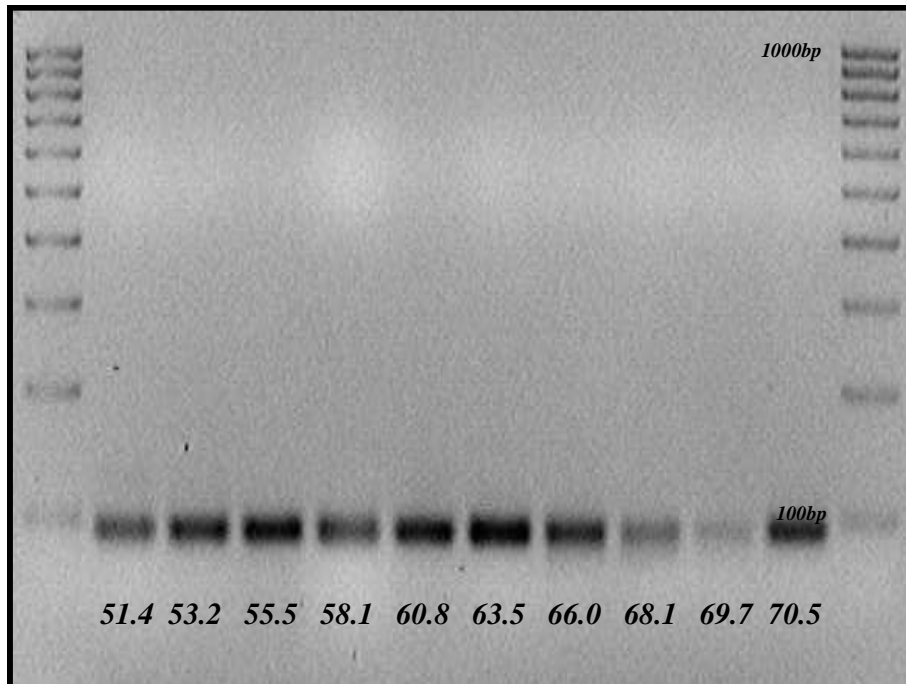


Figure 4.2. Annealing gradient for DOP1 primers used with gDNA from venous blood cells. All temperatures shown along the lower border are in degrees centigrade. All products give the expected amplicon length of 92 base pairs. The weight ladders to the far left and right range from 1000 base pairs to 100 base pairs in 100 base pair increments.

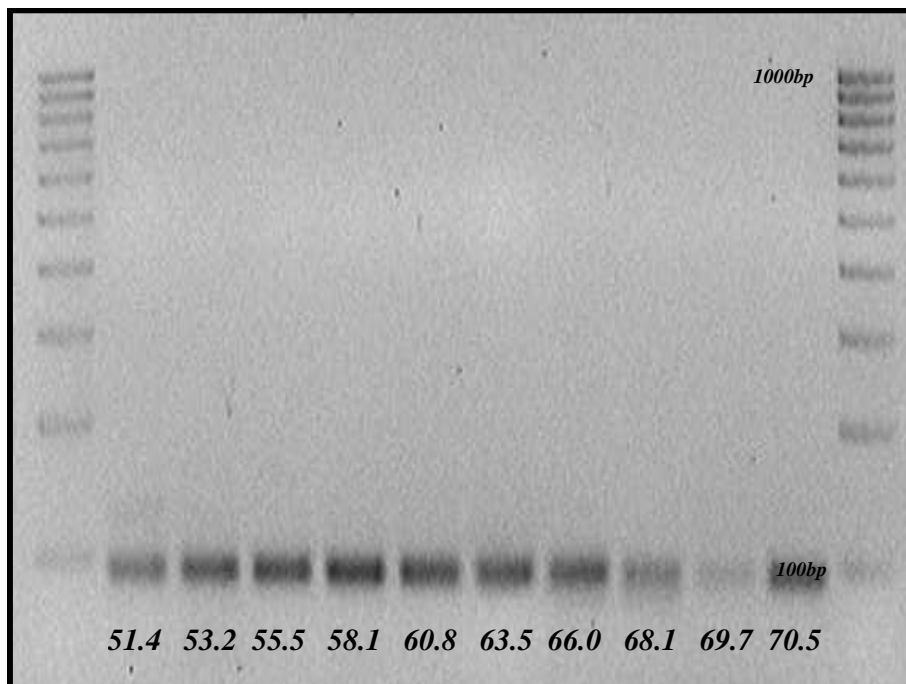


Figure 4.3. Annealing gradient for DOP1 primers used with gDNA CEMx174 cells. All temperatures shown along the lower border are in degrees centigrade. All products give the expected amplicon length of 92 base pairs. The weight ladders to the far left and right range from 1000 base pairs to 100 base pairs in 100 base pair increments.

The DOP2 primer pair was also optimised using RNA extracted from CHO_{hDOP} cells. This primer pair has an advantage over the DOP1 primers, in that not only are forward and reverse primers located on different exons so allowing for easier recognition of genomic from complimentary DNA, but also both primers are located at a portion of the genome, which is translated into protein. This meant that the CHO cells, which are transfected with only the minimal additional sequence that encodes the DOP receptor protein, could be used as a positive control. Optimisation experiments with this primer pair and CHO_{hDOP} cDNA gave an optimal annealing temperature of 58.1 °C **Figure 4.4**

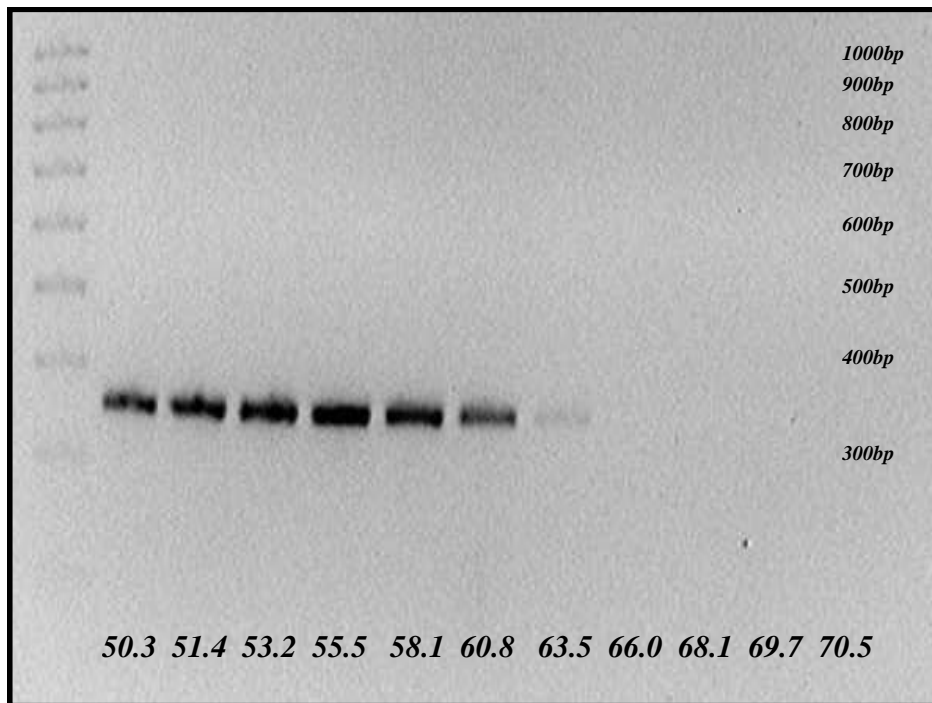


Figure 4.4. Annealing gradient for DOP2 primers used with cDNA from CHO_{hDOP} cells used as template. All temperatures shown along the lower border are in degrees centigrade. Clear products are seen of the expected amplicon length of 356 base pairs at the lowest 6 temperatures with a faint band at 63.5°C. The weight ladder to the far left, ranges from 1000 base pairs to 300 base pairs in 100 base pair increments (values are shown far right).

Whilst it can be seen from **Figure 4.4**, temperatures between 50.3 and 60.8 degrees centigrade yielded good quality amplicon images, a higher annealing temperature was chosen for further investigations as it was thought most likely to be specific for the cDNA of interest. The DOP2 primer pair was used in subsequent PCR experiments with CHO_{hDOP} cDNA as a positive control at this annealing temperature, 60.8 °C. **Figure 4.5**

below shows an agarose gel image of amplification of cDNA extracted from Raji cells. There are no bands seen at the 356 base pair weight for the lanes using cDNA from Raji cells as template, but a clear 356 base pair amplicon if CHO_{hDOP} cDNA is used. This implies there is no DOP receptor gene expression within Raji cells.

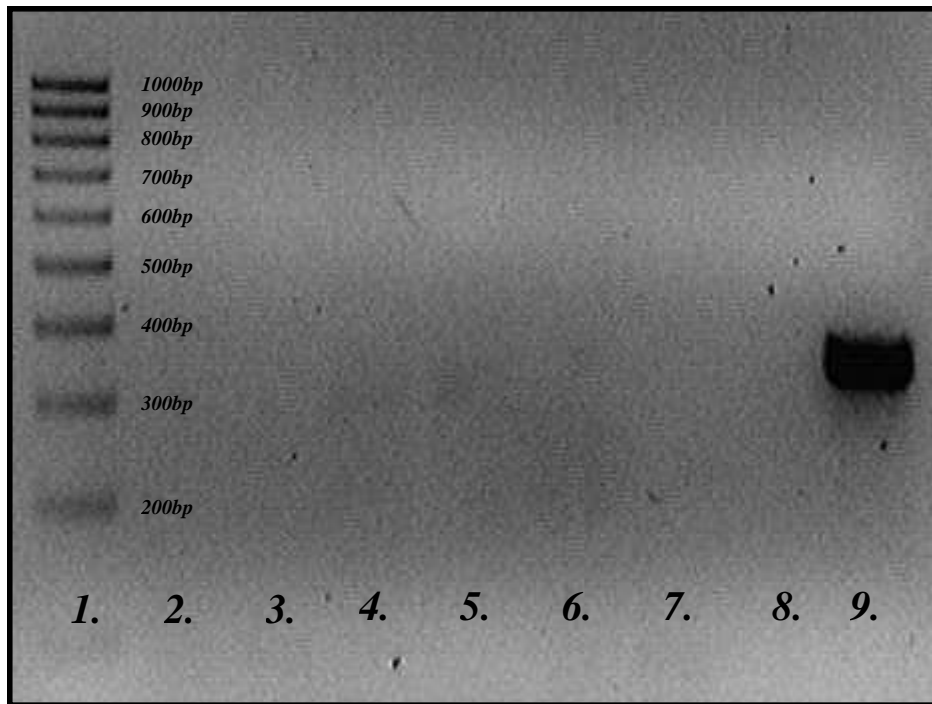


Figure 4.5. DOP2 primers with cDNA from Raji cells (lanes 2-8) or CHO_{hDOP} (lane 9). Only cDNA from CHO_{hDOP} cells gives a 356bp amplicon. The weight ladder to the far left, ranges from 1000 base pairs to 100 base pairs in 200 base pair increments (values are shown to right of ladder).

This experiment was repeated again using CHO_{hDOP} cells as a positive control, but with the cDNA produced from the peripheral blood mononuclear cells of ten healthy male volunteers, **Figure 4.6**. Again no amplicon indicative of the expression of the DOP receptor gene was found, with only a 356 base pair amplicon being seen for the Chinese hamster cells transfected with the DOP receptor.

RNA was also extracted from the whole blood of five healthy volunteers. A similar protocol to **Protocol 2.4** was employed utilising 0.75ml of TRI BD per 0.25ml of blood. This RNA was then reverse transcribed to cDNA and used as template in a standard PCR reaction. Again no cDNA encoding for the DOP receptor was found **Figure 4.7**.

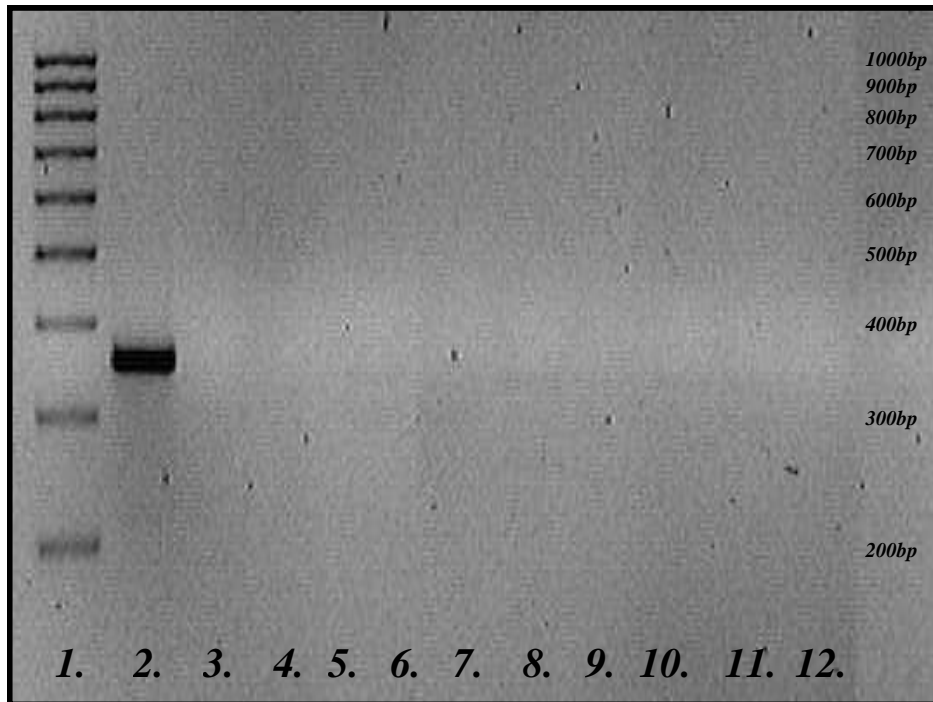


Figure 4.6. DOP2 primers with cDNA from PBMCs (lanes 3-12) or CHO_{hDOP} (lane 2). Only cDNA from CHO_{hDOP} cells gives a 356bp amplicon. Weight ladder to the far left 1000-200bp.

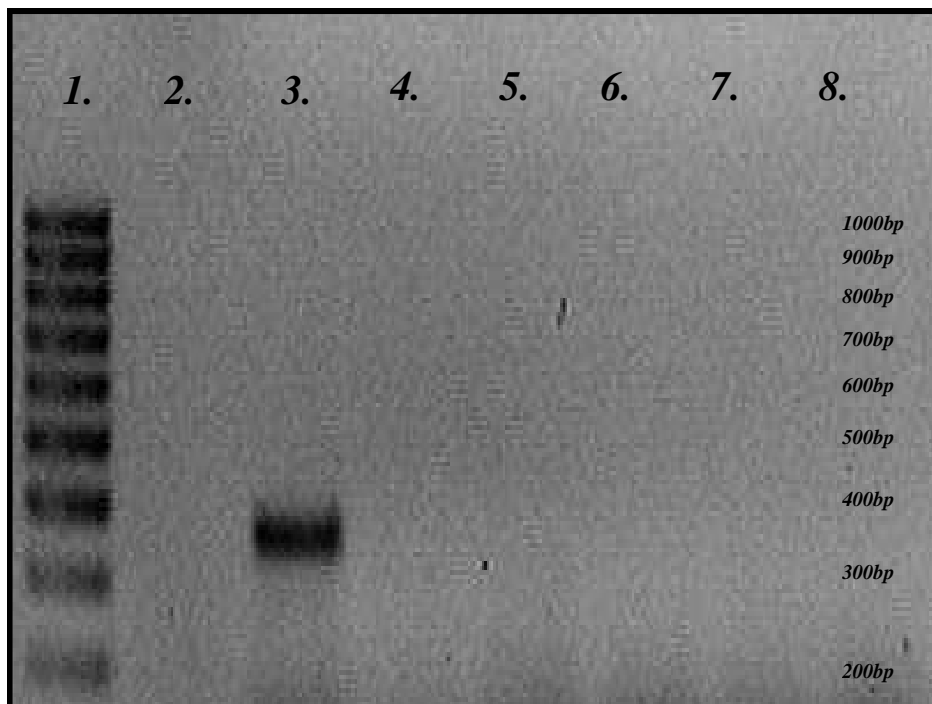


Figure 4.7. DOP2 primers with cDNA from whole venous blood (lanes 4-8), CHO_{hDOP} (lane 3) or water (lane 2). Only cDNA from CHO_{hDOP} cells gives a 356bp amplicon. Weight ladder to left.

4.2.2 Results: DOP Primers, Quantitative PCR

With this inability to find evidence that the mRNA encoding for DOP receptors are expressed by immune cells, further quantitative real time PCR (QPCR) reactions were run using commercially available *TaqMan*[®] Gene expression assays from Applied Biosystems for the DOP receptor (Hs00538331_m1), on the PBMC samples from healthy volunteers. Assays were capable of differentiating gDNA from cDNA and CHO_{hDOP} cDNA was used as a positive control. **Figure 4.8**. This experiment was repeated using cDNA extracted from the whole blood of five healthy volunteers **Figure 4.9**, and again using CHO_{hDOP} cDNA as a positive control. Neither of these templates extracted from the venous blood of healthy volunteers showed evidence of the RNA message encoding for the DOP receptor, though the positive control of CHO_{hDOP} cells did display QPCR data consistent with the presence of the transcript.

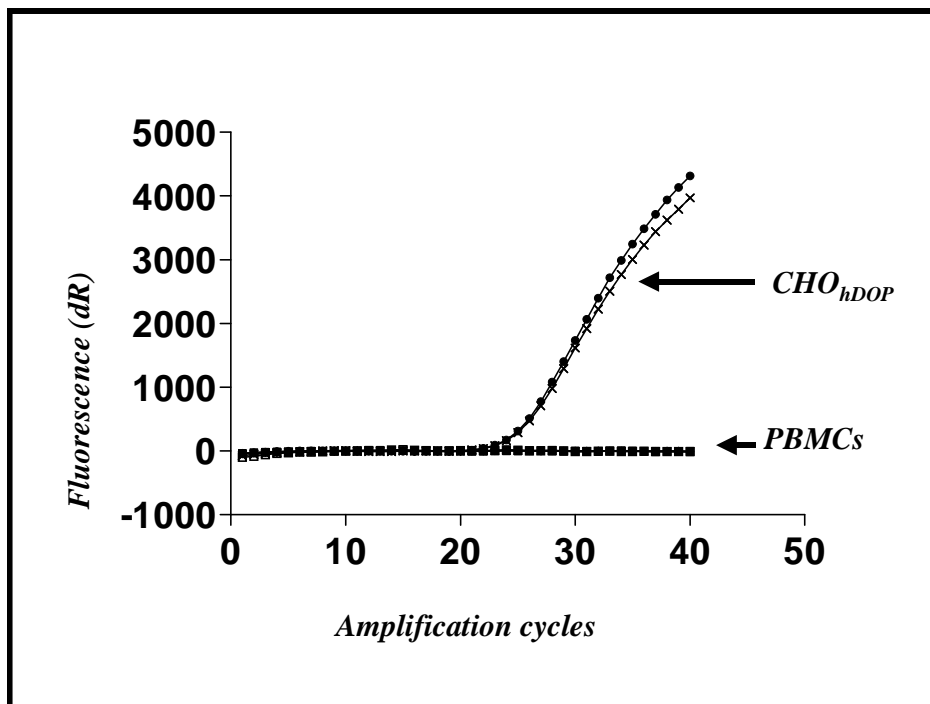


Figure 4.8 QPCR using *TaqMan*[®] Gene expression assay for DOP receptor with cDNA from CHO_{hDOP} cells as positive control curve, and with cDNA from PBMCs. Water was used as a negative control. Example of five replicates of a total of ten PBMC samples, with two CHO_{hDOP} positive controls. Both PBMCs and water show no deflection of the curve (labelled PBMCs), while CHO_{hDOP} cDNA shows amplification at 22 cycles.

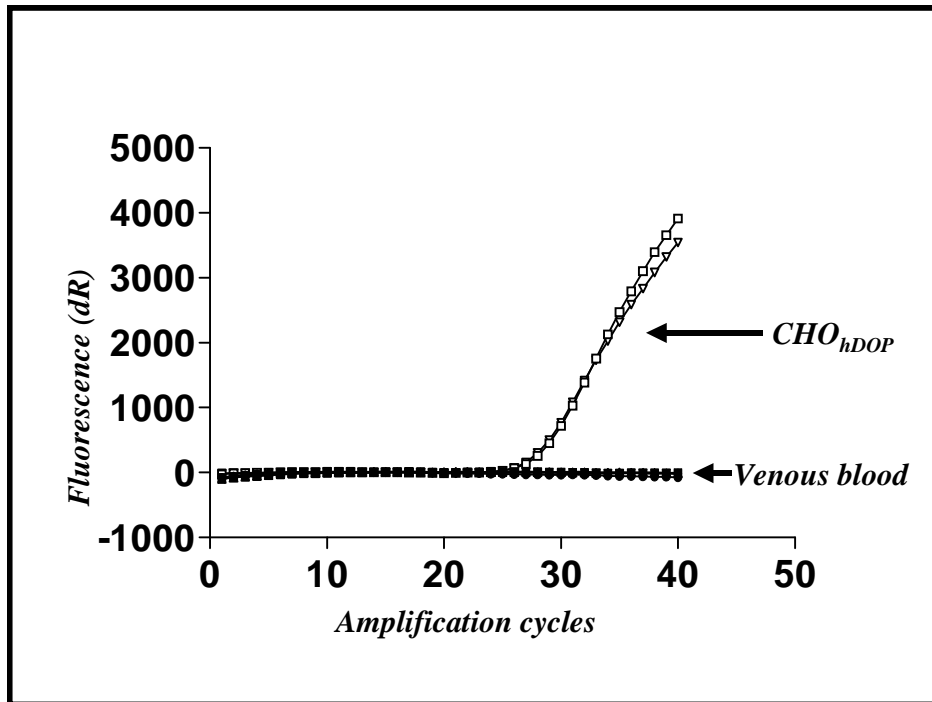


Figure 4.9 QPCR using *TaqMan*® Gene expression assay for DOP receptor with cDNA from CHO_{hDOP} cells as positive control, and with cDNA from whole venous blood. Water as a negative control. Example of five replicates of a total of five venous blood samples, with two CHO_{hDOP} positive controls. Both venous blood and water show no deflection of the curve (labeled Venous blood), while CHO_{hDOP} cDNA shows amplification at 24 cycles.

4.2.3 Results: KOP Primers, Endpoint PCR

As described above for the DOP receptor a number of different cell lines were used to optimise reaction conditions and annealing temperatures for the two KOP primer pairs used to investigate for the presence of the receptor in immune cells. **Protocols 2.4-2.7** were followed for production of cDNA and subsequent PCR amplification. Products were run on a 3% agarose gel imaged under UV illumination following staining with ethidium bromide in concentrations previously discussed.

KOP1 primers were initially used to probe for the presence of the KOP receptor. KOP1 forward and reverse primers both anneal to the same exon of the receptors genetic code. For this reason a second set of KOP primers were designed, KOP2. This primer pair gave a slightly larger amplicon at 210 base pairs in length, but importantly it allowed for identification of RNA message. CHO_{hKOP} cells could also act as a positive control as both forward and reverse KOP2 primers bounded a region of the genetic code that translates into protein. Primer pairs for KOP RNA, their position and the size of amplicon produced are shown in **Table 4.2**.

Primer	Sequence	mRNA Position	Amplicon size
KOP1F	5'-CGTCTCAAGAGCGTCCG-3' (<i>Exon 3</i>)	767-784	123
KOP1R	5'-TATGTGAATGGGAGTCCAGC-3' (<i>Exon 3</i>)	869-890	123
KOP2F	5'-TCACCAGCATCTTCACCTTG-3' (<i>Exon 2</i>)	441-460	210
KOP2R	5'-TGCAAGGAGCACTCAATGAC-3' (<i>Exon 3</i>)	632-651	210

Table 4.2 Primer pairings used in standard gel based PCR for DOP transcripts.

Polymerase chain reactions incorporating an annealing temperature gradient for the KOP1 primer pair were performed, **Figure 4.10**, and from this an optimum annealing temperature of 61.0°C was found. Though across a wide range of temperatures there were good amplicon bands on agarose gel analysis, which corresponded to the expected amplicon length of 123 base pairs, the band at 61.0°C was bright and at a high temperature. As both reverse and forward primers of the KOP1 pairing annealed to exon

3 of the genetic code and so were deemed inappropriate for further analysis of KOP mRNA production.

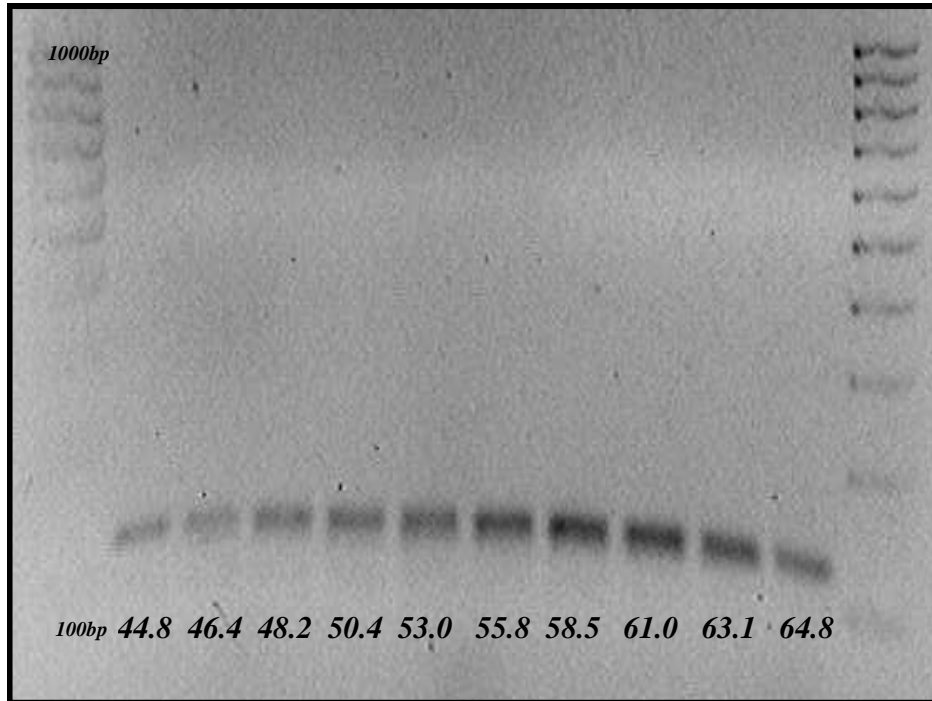


Figure 4.10. Annealing gradient for KOP1 primers used with cDNA from CHO_{hKOP} cells used as template. All temperatures shown along the lower border are in degrees centigrade. Clear products are seen of the expected amplicon length of 123 base pairs at all temperatures. The weight ladder to the far left and right, ranges from 1000 base pairs to 100 base pairs in 100 base pair increments (values for 1000bp and 100bp are shown to the left).

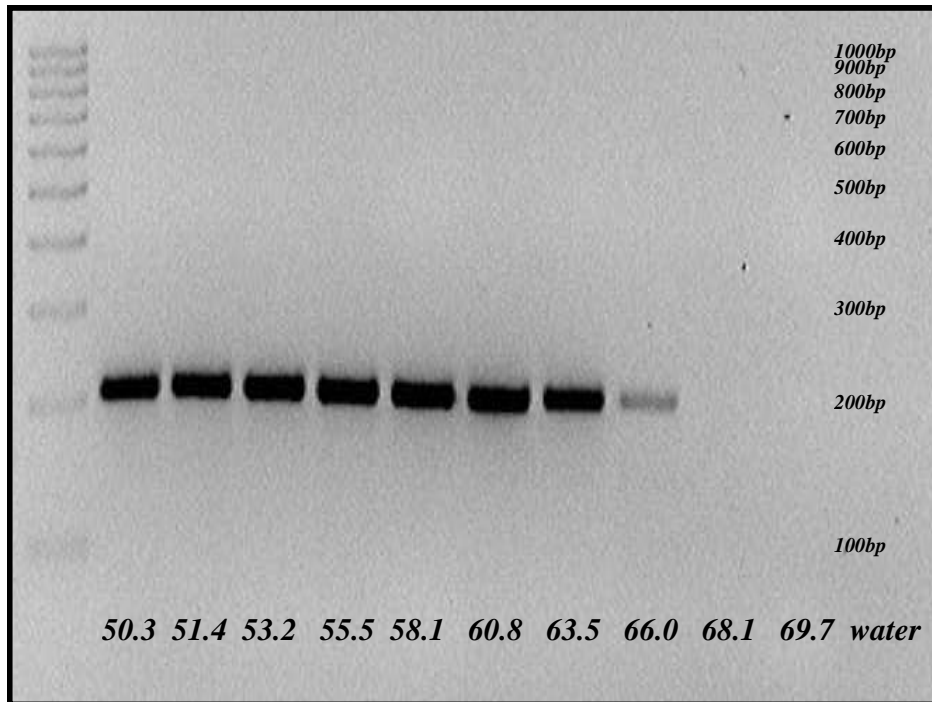


Figure 4.11. Annealing gradient for KOP2 primers used with cDNA from CHO_{hKOP} cells as template. All temperatures shown along the lower border are in degrees centigrade. Clear products are seen of the expected amplicon length of 210 base pairs at temperatures between 50.3°C and 66.0°C. The weight ladder to the far left, ranges from 1000 base pairs to 100 base pairs in 100 base pair increments (values are shown to the right).

Following this the KOP2 primer pair was used, in which the forward and reverse primers sit on exons 2 and 3 respectively. This primer pair was expected to give an amplicon of 210 base pairs in length. Again cDNA derived from CHO_{hKOP} cells were used to optimise the system with an initial annealing temperature experiment performed **Figure 4.11**. This temperature gradient experiment showed that the optimal annealing temperature for this primer pair was 60.8°C with amplicons at 210 base pairs not present above 66°C. These experimental conditions were then reproduced and used with cDNA from Raji cells and PBMCs from healthy male volunteers **Figures 4.12 & 4.13**. Unfortunately none of these investigations provided evidence for the expression of the KOP receptor gene in either the B cell lymphocytic line (Raji cells), or in PBMCs. This series of extractions and amplifications was therefore repeated for cDNA extracted from the whole blood of five healthy male volunteers. Again this yielded no products indicative of KOP receptor transcripts, **Figure 4.14**.

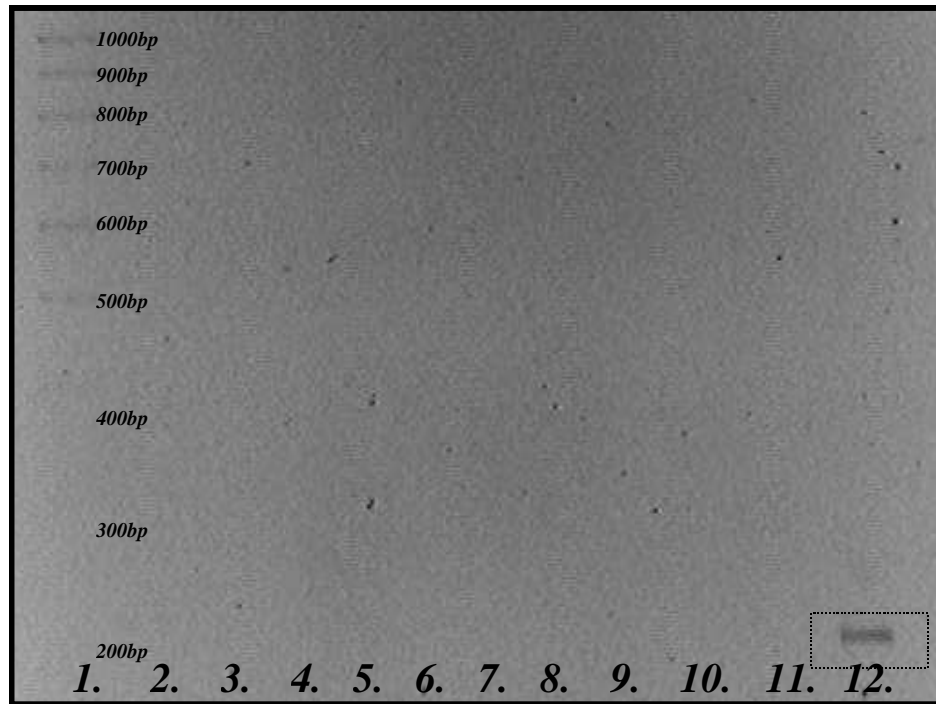


Figure 4.12. KOP2 primers with cDNA from Raji cells (lanes 2-11), CHO_{hKOP} (lane 12). Only cDNA from CHO_{hKOP} cells gives a 210 bp amplicon, in dashed box. Weight ladder 1000-200bp.

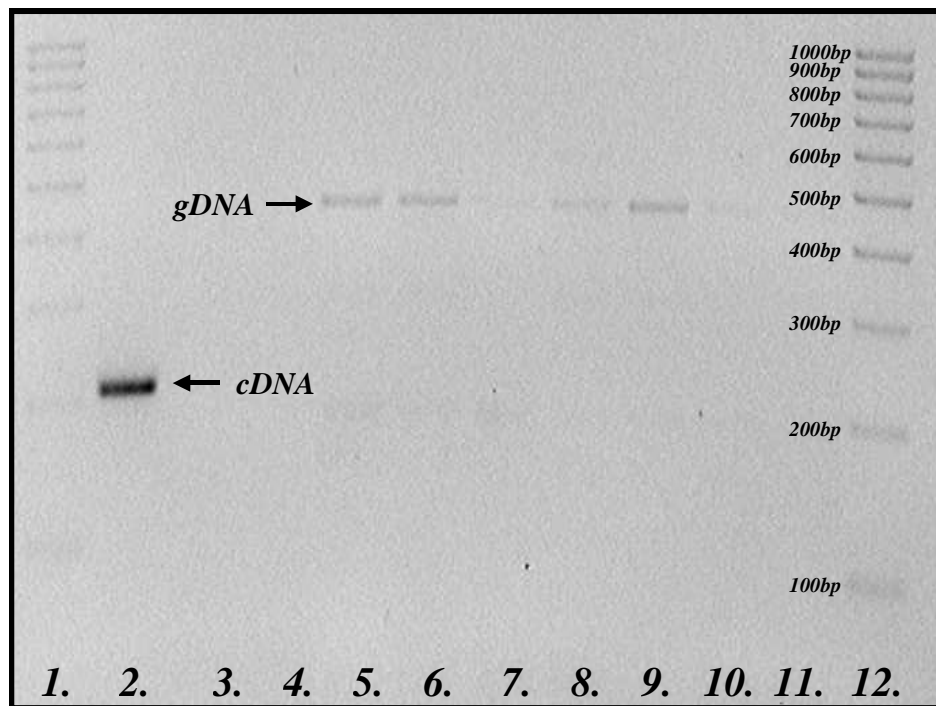


Figure 4.13. KOP2 primers, cDNA from PBMCs (lanes 3-11), CHO_{hKOP} (lane 2). Only cDNA from CHO_{hKOP} cells gives a 210bp amplicon. Weight ladder 1000-100bp, right. Both gDNA and cDNA amplicons are labelled.

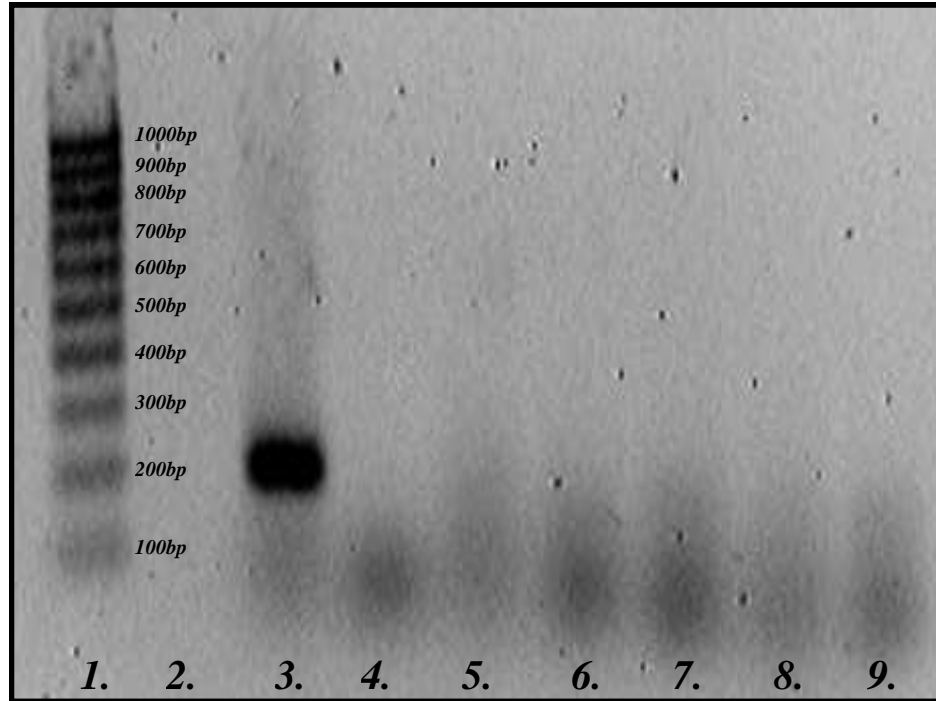


Figure 4.14. KOP2 primers with cDNA from whole venous blood (lanes 3-9), water (lane2) and CHO_{hKOP} (lane 3). Only cDNA from CHO_{hKOP} cells gives a 210bp amplicon. The weight ladder to the far left, ranges from 1000 base pairs to 100 base pairs in 100 base pair increments (values for 1000bp and 100bp are shown to the right of the ladder).

4.2.4 Results: KOP Primers, Quantitative PCR

As with previous searches for MOP and DOP receptors, a series of quantitative PCR experiments utilising CHO_{hKOP} cDNA as a positive control with TaqMan® Gene expression assays (Applied Biosystems Hs00175127_M1) directed at the KOP receptor were undertaken. Again these experiments utilized the protocols described in chapter 2 for the use of quantitative PCR, **Protocols 2.4-2.6 & 2.9**. Quantitative amplification with a KOP assay probe and cDNA extracted from the PBMCs of healthy volunteers was first undertaken. CHO_{hKOP} cell cDNA was used as a positive control and as expected this cell line gave increasing fluorescence with increasing amplification cycle indicative of KOP receptor gene transcripts. There was however no indication of the expression of the KOP receptor gene in PBMCs. **Figure 4.15**

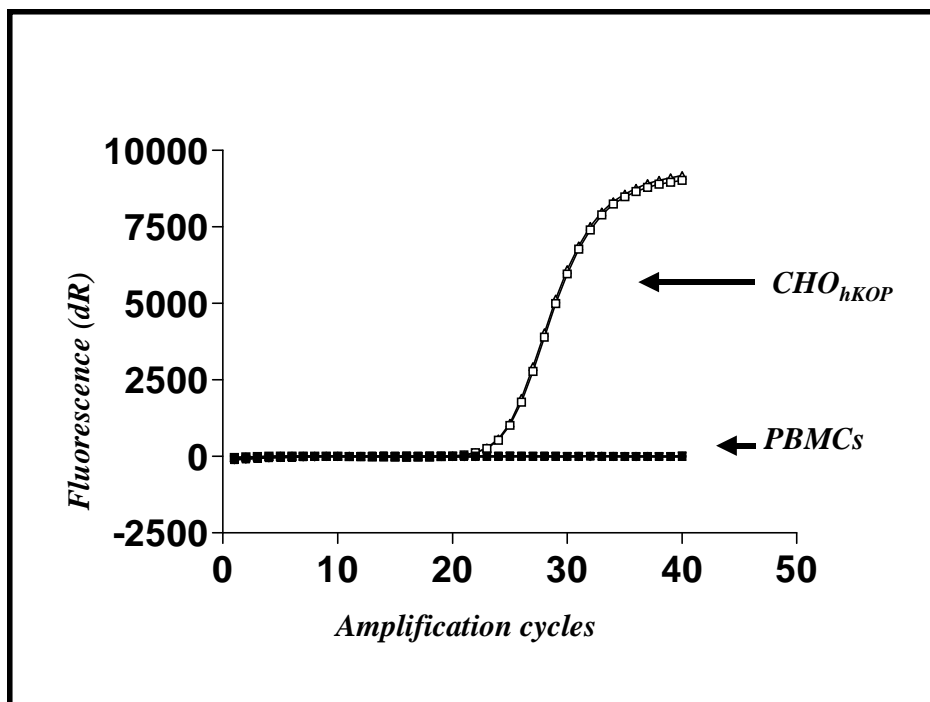


Figure 4.15 QPCR using TaqMan® Gene expression assay for KOP receptor with cDNA from CHO_{hKOP} cells as positive control, with cDNA from PBMCs. Water as a negative control. Example of five replicates of a total of ten PBMC samples, with two CHO_{hKOP} positive controls. Both PBMCs and water show no deflection of the curve (labeled PBMC above), while CHO_{hKOP} cDNA shows amplification at 22 cycles.

Investigations therefore showed no evidence for the mRNA for the KOP receptor being expressed in PBMCs. When this experiment was repeated in whole blood there is some suggestion at high amplification that the KOP receptor gene may be expressed in the

RNA extracted from these cells **Figure 4.16**. This finding was seen in all five replicates of cDNA extracted from whole blood. This observation was however only seen at the very highest amplifications of original template material, in excess of 35 cycles, and is not replicated in the standard PCR gel analysis preparations as described above. These findings would however indicate that some cellular fraction of whole blood could be expressing KOP receptor gene transcripts. In all of these experiments quantitative PCR undertaken with CHO_{hKOP} cells as a positive control consistently gave cumulative fluorescence emission data compatible with the presence of the expected KOP receptor amplicon.

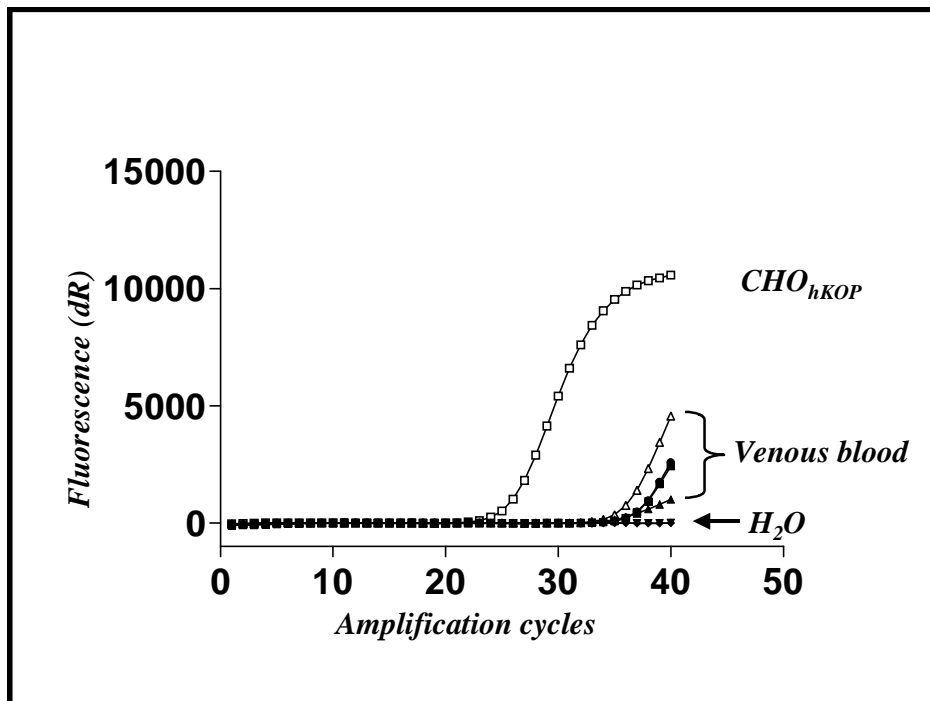


Figure 4.16. QPCR using *TaqMan*[®] Gene expression assay for KOP receptor with cDNA from CHO_{hKOP} cells as positive control, and cDNA from whole blood. Water as a negative control. Example of five replicates from five whole blood samples, with CHO_{hKOP} as positive control. CHO_{hKOP} cDNA shows amplification at 22 cycles while all five whole blood replicates show increases in fluorescence only after thirty amplification cycles.

4.3 Discussion

A number of experimental paradigms (radioligand binding, fluorescent binding (*Chapter 3*) and polymerase chain reaction techniques (*Chapter 4*)) have failed to show the presence of the two classical opioid receptors DOP and KOP in PBMCs or cultured B cell lymphocytes. These experimental techniques have proved robust and reproducible when used with CHO_{hDOP} and CHO_{hKOP} cell lines, the standard positive control used in these experiments. However though the experimental techniques provided no evidence to suggest that peripheral blood mononuclear cells or whole blood cells express DOP opioid receptors or synthesise the RNA, which encodes for it under basal conditions, there is some suggestion that KOP receptor gene transcripts may be expressed in very low abundance by whole venous blood. This finding was only seen in quantitative polymerase chain reactions at high cycle numbers and was not supported by any other experimental technique used, notably standard gel based PCR analysis.

Though there is no universal consensus as to the presence of DOP and KOP receptors on immune cells the above conclusions are at variance with the findings of some groups (*Bidlack et al 2006, Lawrence et al 1995 & 1997, Sharp et al 2000 & 2001*). However there is little doubt that if either DOP or KOP receptors are expressed on the surface of peripheral blood mononuclear cells then their expression must be in extremely low abundance. This is illustrated by the fact that as in the above experiments most groups have been unable to find evidence that DOP or KOP receptors are present on immunocytes, using a range of techniques.

Previous groups have suggested, through the use of fluorescently labelled DOP and KOP ligands coupled with flow cytometric analysis, that these receptors may be displayed on the surface of peripheral blood mononuclear cells (*Lawrence et al 1995, Sharp et al 2000, Suzuki et al 2001*). These studies have generally used high concentrations of fluorescently labelled receptor ligands and even higher concentrations of unlabelled antagonists to calculate non-specific binding. These compounds have frequently been utilised in concentrations far in excess of their K_i 's. By utilising such high concentrations of a fluorescent probe it is possible that there may be an additional penetrance of the cell membrane in a non-specific manner by the lipid soluble probe.

The papers purporting to describe fluorescent DOP and KOP ligands binding to their respective opioid receptors on immune cells do not present classical dose-response data or discuss the IC_{50} or B_{MAX} for ligand membrane systems, as we have done with PBMCs/CHO_{hMOP} and fluorescent-naloxone above.

Previously *Kraus* has shown the up regulation of MOP receptors in immunocytes following addition of TNF α , a mediator of inflammation, such that MOP transcripts can be found with quantitative PCR techniques (*Kraus et al 2001 & 2003*). Analogous to this, DOP receptor expression has been observed on T-lymphocytes following stimulation for 48 hours with phyto-haemagglutinin, another inflammatory mediator (*Sharp et al 2001*). These studies again relied upon fluorescent staining techniques with high concentrations of fluorescent moiety and only suggested DOP to be displayed on less than half the T-lymphocytes studied after stimulation. However these studies do raise the possibility that peripheral immune cells do have the ability at least *in vitro* to express opioid receptors under certain conditions.

Following an inability to find DOP and KOP receptors on the surface of PBMCs and a range of immunocompetent cells, cells were investigated for the expression of the RNA encoding for DOP and KOP receptors. Research groups have suggested that both DOP and KOP mRNA could be extracted from immune cells, however these experiments have frequently used primer pairs sitting on just one exon, and none had used molecular probes such as the *TaqMan*[®] Gene expression system in conjunction with quantitative PCR techniques to address this question (*Chuang et al 1994 & 1995a*). Investigations described in this chapter looking at RNA expression of DOP and KOP receptors have used primer pairs, with the capacity to differentiate genomic from complimentary DNA. In all instances these primer pairs, whether of classical design or *TaqMan*[®] Gene expression probes, have been verified using Chinese hamster cells transfected with the opioid receptor in question. Using this method we have been unable to find any evidence that the gene encoding for the DOP receptor is manufactured in naïve PBMCs, whole blood or Raji cells. In a similar fashion RNA encoding for the KOP receptor could not be found in PBMCs or Raji cells. However at high amplification there was an indication that KOP receptor RNA may be present at very low transcript numbers in whole blood cells.

Chapter 5:

NOP Opioid Receptor Expression in Peripheral Immune Cells

5.1 Background

Opium and its derivatives have been used for many thousands of years. Friedrich Serturmer was the first to isolate morphine as the major analgesic component of opium in 1779. However, the three classical opioid receptors DOP, KOP and MOP were only cloned between 1992 and 1993. Following this advance in opiate pharmacology a previously uncharacterised receptor was cloned in 1994 and using reverse pharmacology, its ligand identified (*Bunzow et al 1994, Mollereau et al 1994*). The receptor was named ORL₁ (opioid like receptor 1), and shortly after its discovery two groups identified a 17-amino acid neuropeptide, simultaneously, as its endogenous ligand (*Meunier et al 1995, Reinscheid et al 1995*). The names initially given to the ligand by the two groups were nociceptin and orphanin FQ. This system, though initially described by a number of different names is now known today as the NOP receptor/nociceptin (N/OFQ) ligand system. The NOP receptor possesses many similarities to the classical opiate receptors and substantial sequence conservation between species. Differences in its pharmacology, namely naloxone insensitivity, have however led IUPHAR to classify NOP as “a non-opioid branch of the OP family of receptors” (*IUPHAR. Opioid receptors: Introduction 2007*).

Investigations described in the previous two chapters have failed to provide convincing evidence for the presence of any of the three classical opioid receptors, MOP, DOP or KOP, in peripheral blood mononuclear cells or in venous blood. QPCR experiments in **Chapter 4** using *TaqMan*® probes directed at the KOP receptor did show amplification products at cycles greater than 30 when cDNA extracted from venous blood was used as template. This receptor shares around 80% homology with the NOP receptor. In addition, of all the opioid receptor systems so far described in the literature, the NOP/N/OFQ system has been most persistently implicated in immuno-modulation at a cellular level (*Hom et al 1999, Peluso et al 2001, Serhan et al 2001*). For these reasons this chapter documents studies searching for the presence of the NOP receptor on peripheral blood immune cells. In this series of experiments Chinese hamster ovary cells transfected with

the human NOP receptor were used as a positive control. However the human neuroblastoma cell line SH-SY5Y is also known to express NOP receptors but in much lower densities than CHO_{hNOP} cells, and was therefore used as a low expression positive control (*Cannarsa et al 2008, Connor et al 1996, Peluso et al 2001*). A series of experiments were also undertaken with human Raji cells, grown in culture as a source of immunocompetent cells. By culturing these cell lines *in vitro* a far greater mass of cells could be obtained than for the PBMCs, which could only be harvested from human volunteers via venesection hence limiting the amount of cellular material available for analysis.

The aims of this chapter were therefore:

- To investigate in detail whether whole venous blood, or PBMCs isolated from the blood, of healthy male volunteers, express NOP receptors under basal ‘resting’ conditions. To accomplish this a series of standard gel based endpoint PCR and quantitative PCR experiments was performed.
- A series of GTP γ [³⁵S] binding assays was also undertaken with PBMCs and Raji cells, to investigate whether a functional response to ligand binding at a putative NOP receptor could be detected in immune cells.
- To investigate whether stimulation of immune cells by a variety of cytokines could upregulate NOP expression. Endpoint PCR was employed in order to accomplish this.

5.2 Radioligand Binding Studies

In a manner similar to that described above in *Chapters 3 & 4* for MOP, DOP and KOP receptors, radioligand binding experiments were used to probe for expression of the NOP receptor in a variety of cells and cell lines.

5.2.1 Results: Saturation binding experiments

CHO_{hNOP} cells bound [³H]-N/OFQ in a concentration-dependent and saturable manner, *Figure 5.1*. Note that with this peptide radioligand NSB was low, typically less than 1% of the radioligand K_d.

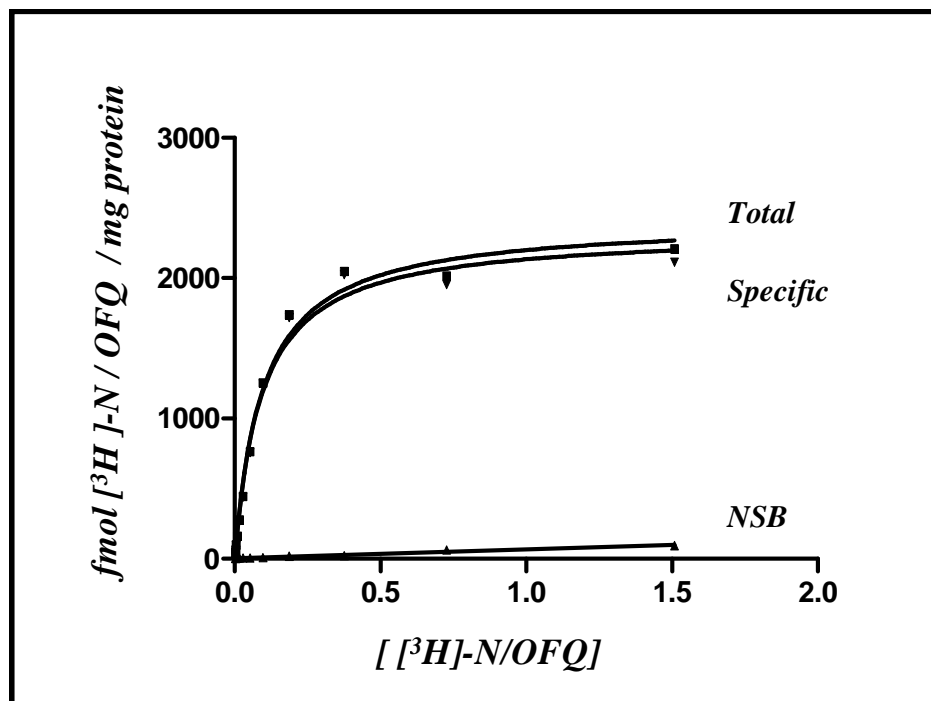


Figure 5.1. Binding of [³H]-N/OFQ to CHO_{hNOP} cells (example of one n=3)

When the log of [³H]-N/OFQ is plotted against fmol/mg protein a typical sigmoid curve is produced, *Figure 5.2*. from which a pK_D and B_{max} of 9.92 ± 0.11 (SEM) and 2082 ± 62.3 (SEM) fmol/mg protein can be estimated.

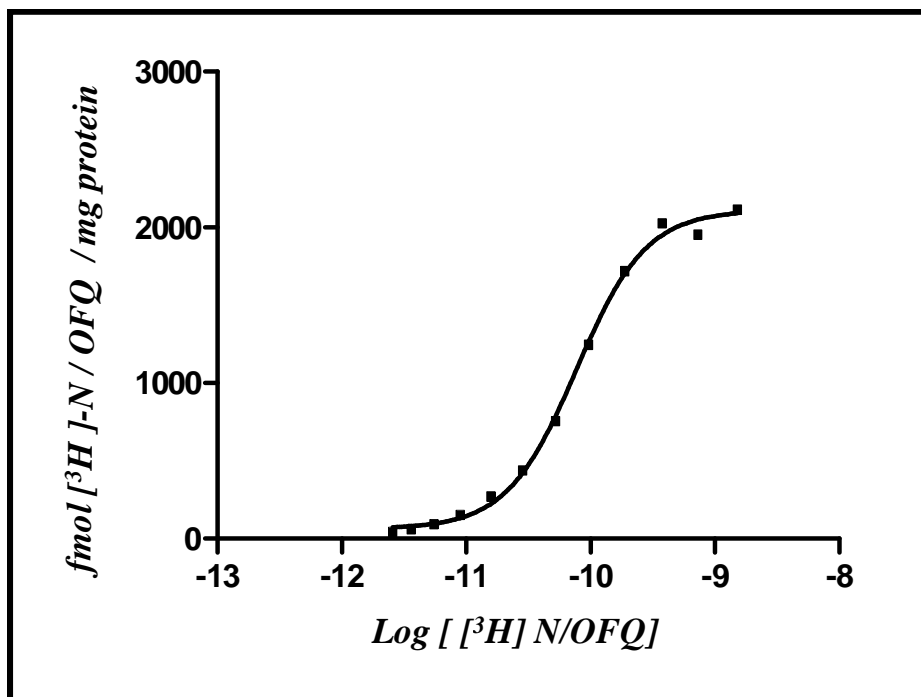


Figure 5.2. Semi-logarithmic plot [³H]-N/OFQ vs specific binding in CHO_{hNOP} cells

These saturation binding assays were repeated in a range of immunocompetent cells both harvested from the blood of healthy volunteers or grown as cell lines in culture. None of these experiments produced binding isotherms suggestive of the presence of the NOP receptor on these cells. **Figure 5.3** below shows an example of [³H]-N/OFQ binding to PBMC membranes. In this instance the data is expressed as the concentration of [³H]-N/OFQ per milligram of protein, rather than raw radioactive activity (DPM). However unlike **Figure 5.1** there was no increase in specific binding. From **Figure 5.3** it can also clearly be seen that non-specific binding rises throughout the concentration range, and that it also constitutes a significant part of total binding. It should also be noted that while the B_{MAX} for CHO_{hNOP} cells is 2082 ± 62.3 (SEM), for PBMCs binding does not saturate and absolute values are low despite using a high mass of cellular protein.

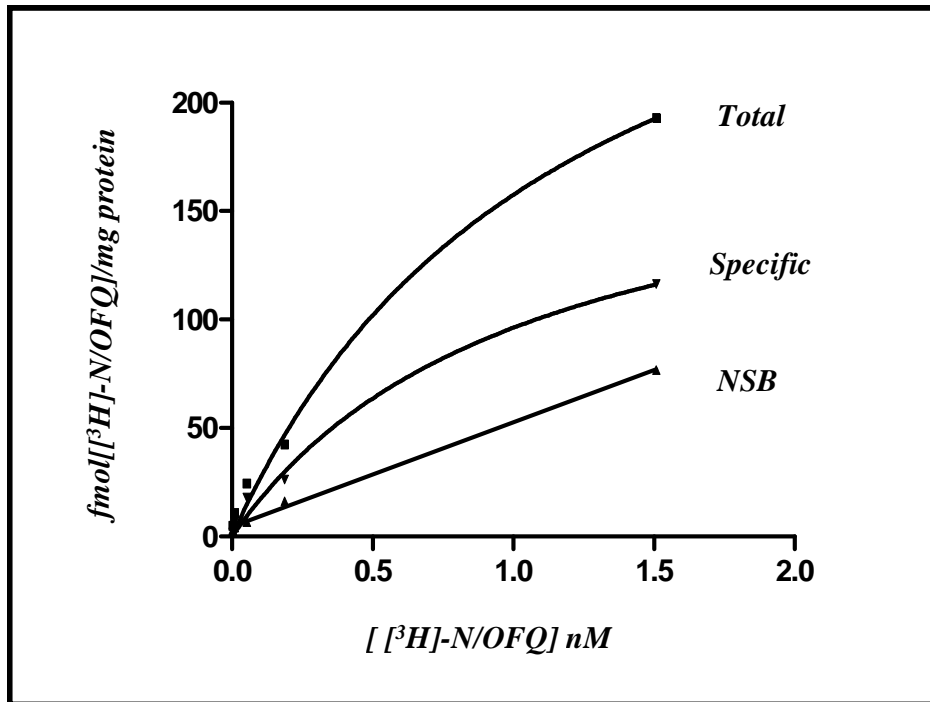


Figure 5.3. $[^3\text{H}]\text{-N/OFQ}$ vs radioactive decay expressed as mass of protein in PBMCs. (representative from $n=3$)

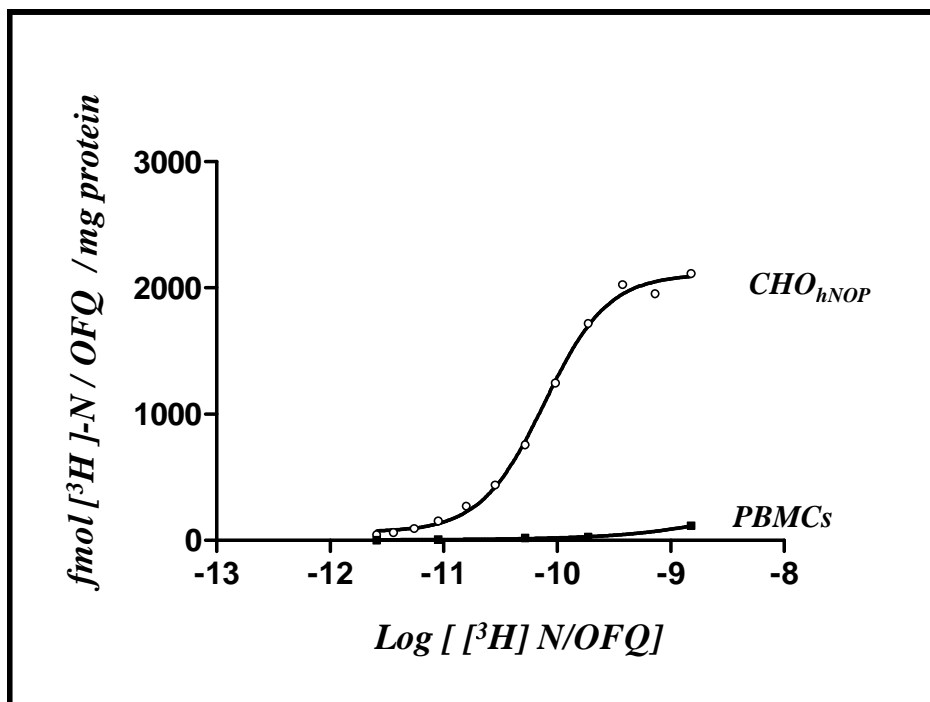


Figure 5.4. $\text{Log } [^3\text{H}]\text{-N/OFQ}$ vs specific binding in PBMCs (\bullet) ($n=3$) and CHO_{hNOP} binding for comparison (\circ), example of one plot.

If this data is expressed as a semi-logarithmic plot of $\log [{}^3\text{H}\text{-N/OFQ}]$ against specific binding expressed as fmol/mg protein, again there is no suggestion of NOP receptor binding, **Figure 5.4.**

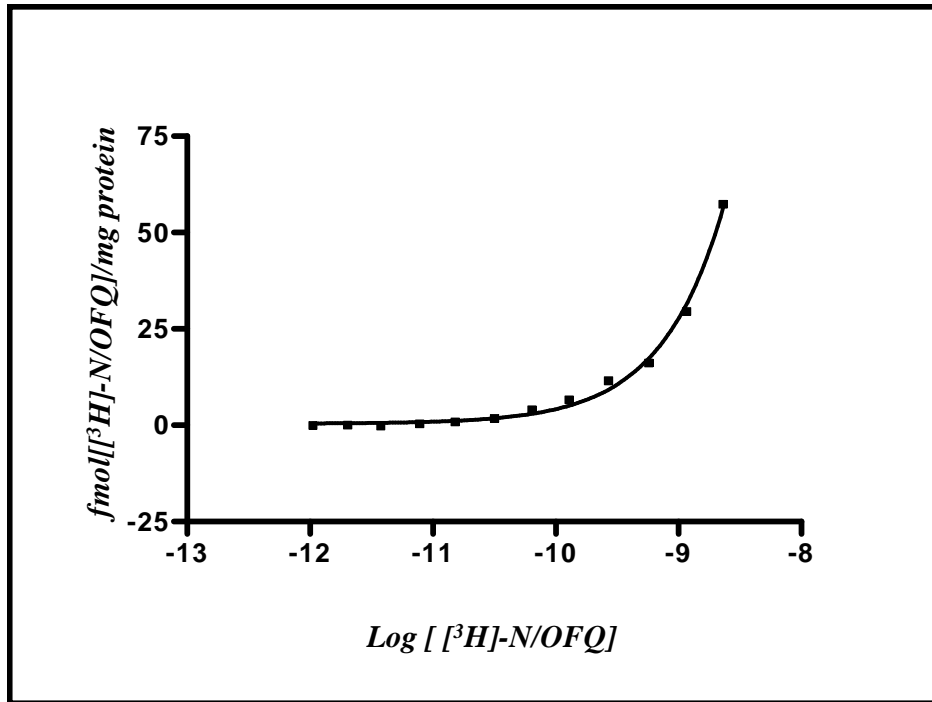


Figure 5.5. $\log [{}^3\text{H}\text{-N/OFQ}]$ vs radioactive decay expressed as binding per mass of protein in Raji cells. (representative from n=3)

Radioligand binding experiments undertaken with Raji cells also showed no concentration dependent or saturable binding over the range encompassing NOP pK_D . **Figure 5.5.**

5.2.2 Results: $GTP\gamma[^{35}S]$ binding assays

In CHO_{hNOP} cells the binding of $GTP\gamma[^{35}S]$ was stimulated by N/OFQ in a concentration dependent and saturable manner **Figure 5.8**.

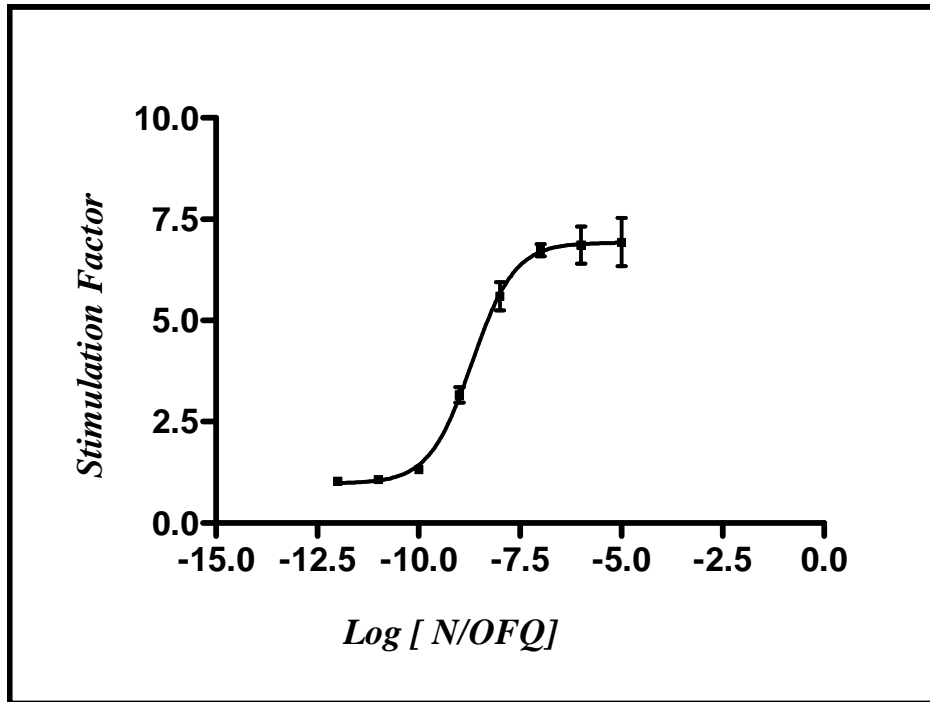


Figure 5.8. Semi-logarithmic plot log [N/OFQ] vs stimulation factor in CHO_{hNOP} cells (representative from n=3), $GTP\gamma[^{35}S]$ binding assay.

Analysis of these data gave a pEC_{50} and stimulation factor of 8.68 ± 0.01 and 6.92 ± 0.17 respectively. Similar experiments performed with the Raji cell line were equivocal. Of a total of seven experiments five produced a concentration dependent increase in $GTP\gamma[^{35}S]$ binding, while in the remaining two experiments there was no stimulation of $GTP\gamma[^{35}S]$ binding. If the five sets of “positive data” are analysed a pEC_{50} of 8.17 ± 0.30 SEM and stimulation factor of 1.058 ± 0.005 can be calculated **Figure 5.9**.

Membranes prepared from PBMC cells showed no evidence of the presence of functional NOP receptors **Figure 5.10**.

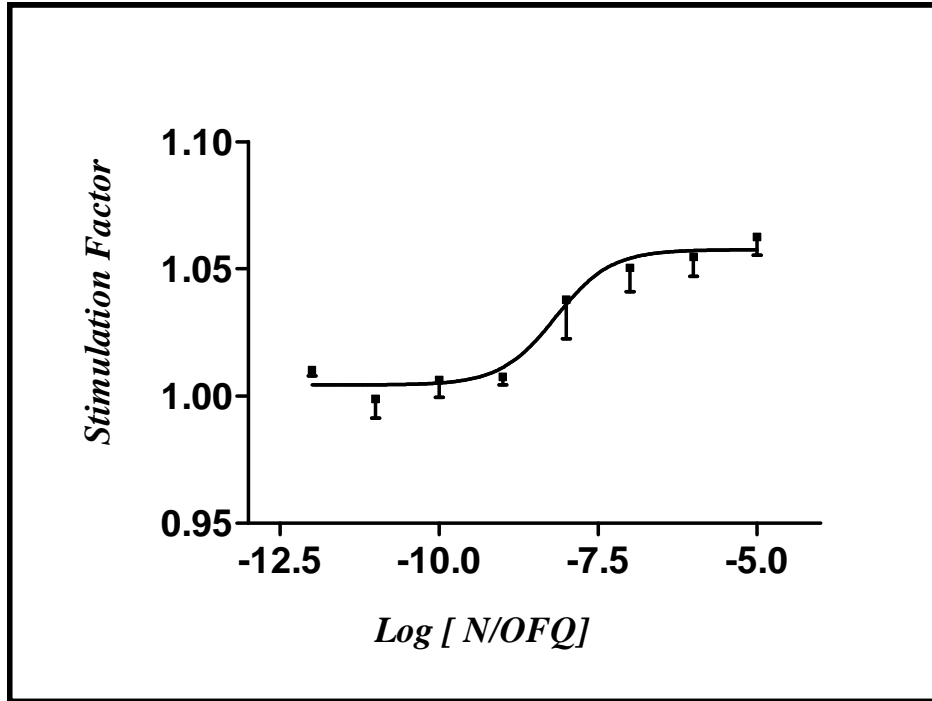


Figure 5.9. Semi-logarithmic plot log [N/OFQ] vs DPM in Raji cells, $GTP\gamma$ [^{35}S] binding assay. Data are mean \pm SEM (n=5).

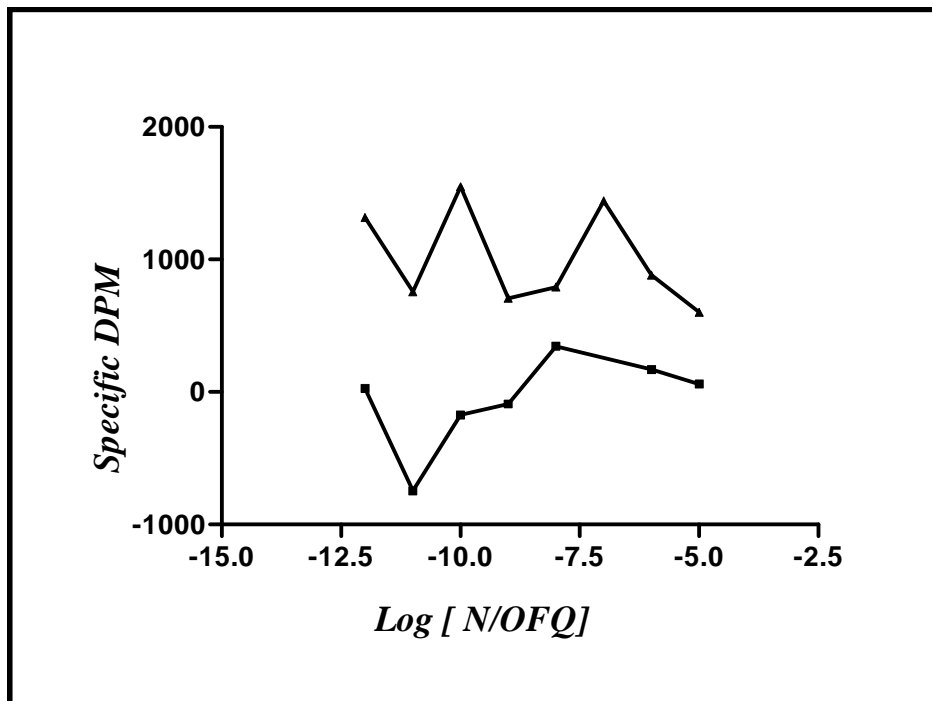


Figure 5.10. Semi-logarithmic plot log [N/OFQ] vs DPM in PBMC cells, $GTP\gamma$ [^{35}S] binding assay (n=2, each line representing one experiment)

5.3 Polymerase Chain Reaction

With the inability to find NOP receptors on PBMCs and other immunocompetent cells using radiolabelled saturation-binding techniques and with inconsistent results using GTP γ [^{35}S] in Raji cells, experimental protocols developed in the previous two chapters were used to investigate for the presence of RNA encoding for the NOP receptor. Chinese hamster ovary cells, transfected with and stably expressing the receptor of interest, in this case the human NOP receptor (CHO_{hNOP}) were used in conjunction with PBMCs to optimize polymerase chain reaction techniques, which would then be employed with immunocompetent cells. The SH-SY5Y cell line is also known to express NOP receptors in a lower density than CHO_{hNOP} cells; therefore it was used as a low expression comparator. Raji cells were also used as a readily available source of human immune cells, which could easily be grown in large volumes *in vitro*. A search of the literature relating to polymerase chain reaction amplification of the genetic code for the human receptor provided a number of possible primer pairs (Arjomand *et al* 2002, Fiset *et al* 2003, Pampusch *et al* 2000, Peluso *et al* 1998). One of these primer pairs, the NOP1 pairing described below (NOP1 F+R), was chosen to investigate extracted RNA for NOP receptor gene expression. This primer pair was chosen as it had the ability to differentiate genomic DNA from complimentary DNA, as reverse and forward primers annealed to different exons of the genetic code. A *TaqMan*[®] Gene expression assay from Applied Biosystems (Hs00173471_m1) was also used to provide probes for use in quantitative PCR reactions. This system could then be used to more accurately track changes in RNA expression over time and in different physiological or pharmacological environments.

Primer pairs were also found which corresponded to the genetic sequence encoding for prepronociceptin (NOPP1 F+R), the precursor of the endogenous agonist, N/OFQ, and 'putative physiological' NOP antagonist, nocistatin. However this primer pair when used in PCR yields an amplicon 546 base pairs in length, too long for QPCR. A second primer pair (NOPP2) was therefore developed for this purpose, which again bounded an intron and so allowed for differentiation of genomic DNA from mRNA. They were used with a SYBR green fluorescent dye labeling system and were not *TaqMan*[®] probes. Their design and reaction optimization is described in greater detail in the following chapter

with the description of the design of a range of primers for housekeeping genes. The NOPP2 primers were used as primer pairs in reactions in quantitative polymerase chain reactions in which the cDNA extracted from the blood of healthy volunteers was used as template *Table 5.1*.

Primer	Sequence	mRNA Position	Amplicon size
NOP1F	5'-GCCGTTCTGGGAGGTTATCTAC-3' (<i>Exon 1</i>)	21-42	563
NOP1R	5'-AGGAGCTGGACACGGCTCG-3' (<i>Exon 2</i>)	566-584	
NOPP1F	5'-CCTGCACCATGAAAGTCCTG-3' (<i>Exon 1</i>)	204-223	546
NOPP1R	5'-CCTTCCGGCTACACATTACC-3' (<i>Exon 2</i>)	731-750	
NOPP2F	5'-CCTGCACCAGAATGGTAATG-3' (<i>Exon 2</i>)	718-737	106
NOPP2R	5'-GCTGAGCACATGCTGTTTG-3' (<i>Exon 3</i>)	807-824	

Table 5.1 Primers are shown in the left hand column, NOP1F & 1R encoding for the receptor, while NOPP encodes for prepronociceptin the precursor for both N/OFQ and nocistatin. F and R signify forward and reverse primers respectively Primer sequence and position of the primer on the RNA code are also shown, note that all primer pairs sit across an exon-exon boundary. The right hand column shows amplicon size produced with each primer pair

5.3.1 Results: Endpoint PCR

Experimental conditions for the optimization of NOP receptor and peptide primers used cDNA from CHO_{hNOP}, PBMCs or whole blood. Images of gel electrophoresis for these reactions are shown in **Figures 5.11-5.13**.

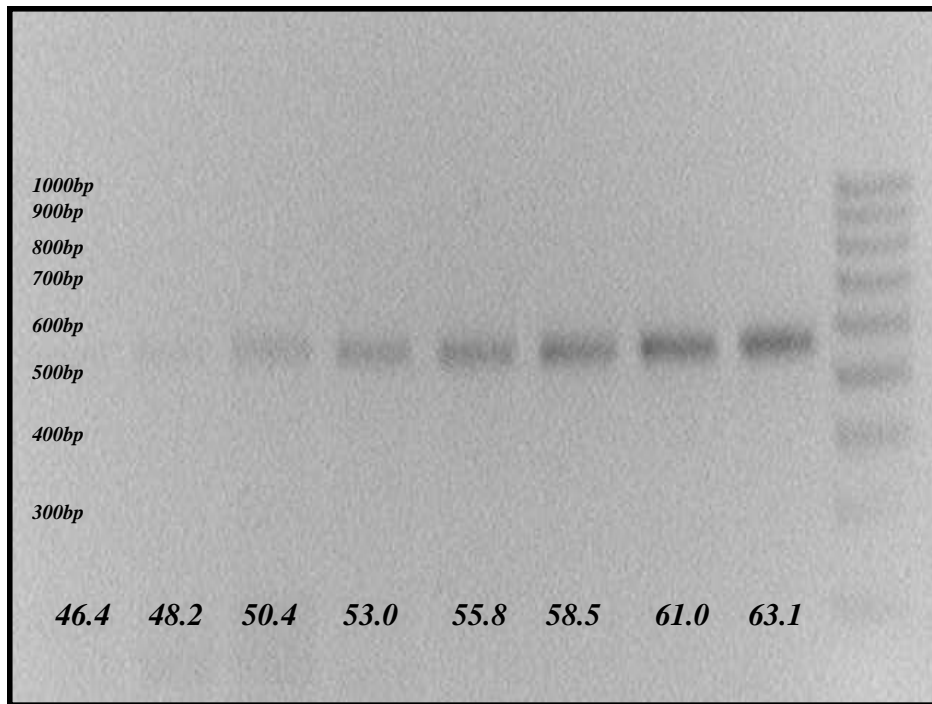


Figure 5.11. Annealing gradient for NOP1 receptor primers using cDNA from PBMCs. All temperatures along the lower border are shown in °C. The weight ladder to the far right ranges from 1000 base pairs to 300 base pairs in 100 base pair increments. Clear bands are seen at 563bp at 53.0–63.1°C.

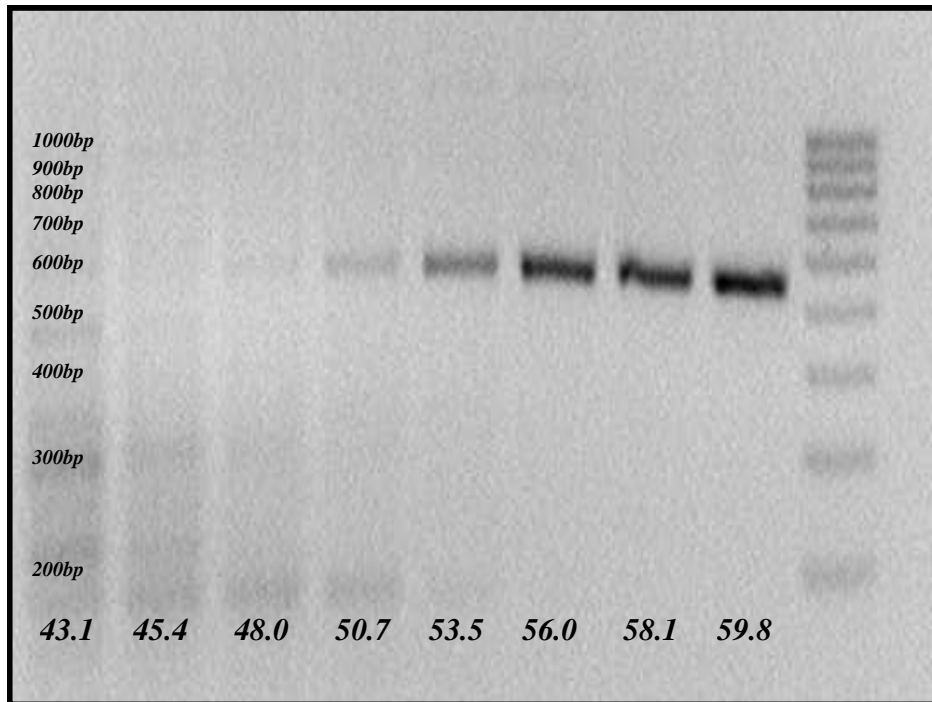


Figure 5.12. Temperature annealing gradient for NOPP1, cDNA from PBMCs. Temperatures along the lower border are in °C. Weight ladder ranges from 1000-200 bp. Clear bands are seen at 546bp at 53.5 – 59.8°C.

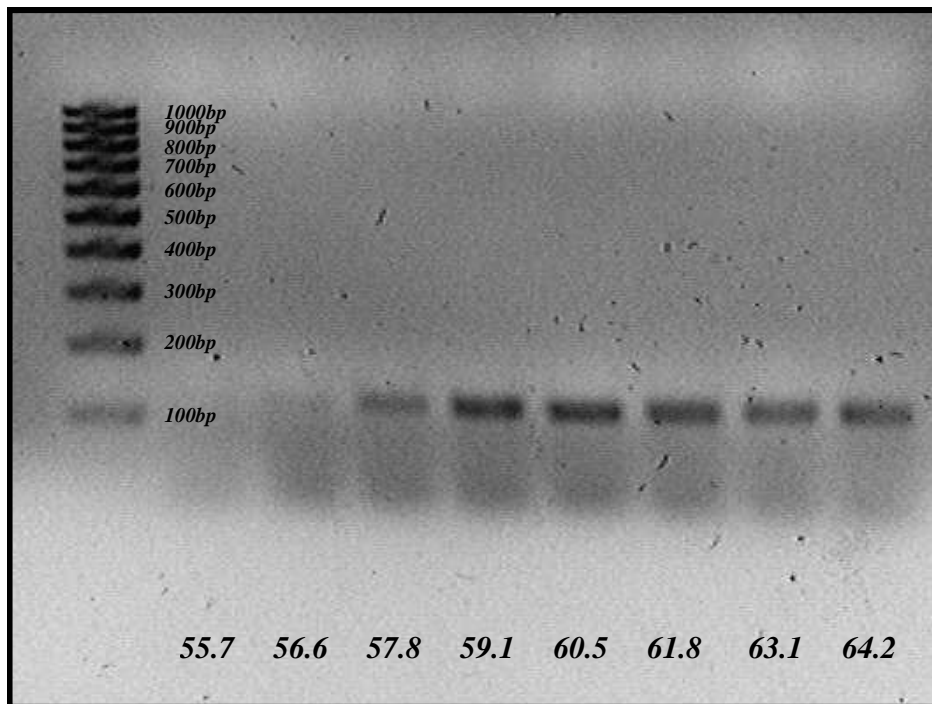


Figure 5.13. Temperature annealing gradient for NOPP2, cDNA from venous blood. Temperatures along the lower border in °C. The weight ladder ranges from 1000 to 100 base pairs in 100 base pair increments. Clear bands are seen at 106bp at 57.8 – 64.2°C.

From these reactions optimal annealing temperatures were 63.1 °C for the NOP receptor primers, 59.8 °C for NOPP1 and 60.5°C for the NOPP2 primer pair as shown in **Table 5.2** below.

Gene	Primer pair	Amplicon size	Annealing Temperature
NOP receptor	NOP1	563	63.1°C
Prepronociceptin	NOPP1	546	59.8°C
Prepronociceptin	NOPP2	106	60.5°C

Table 5.2 Calculated NOP receptor and prepronociceptin primer pair combinations, optimized annealing temperatures and amplicon sizes.

PCR with cDNA from PBMCs, Raji cells, SH-SY5Y cells and CHO_{hNOP} cells all gave images on electrophoretic analysis consistent with the presence of RNA encoding for the human NOP receptor. **Figures 5.14-5.15.**

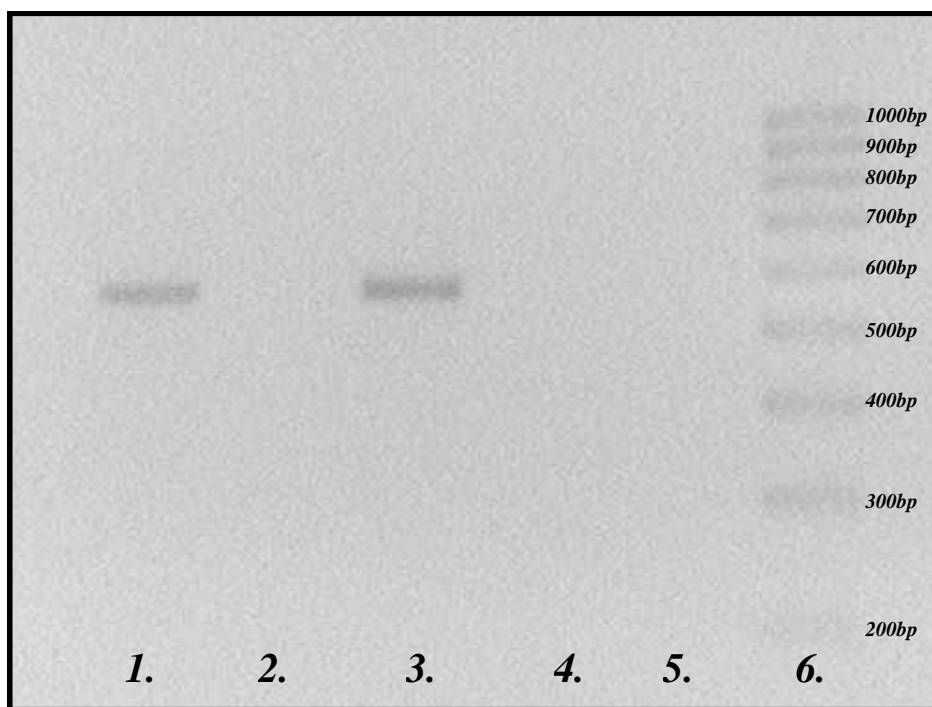


Figure 5.14. NOP1 primers with cDNA from SH-SY5Y cells (lanes 1-4). SH-SY5Y RT+ lane 1, SH-SY5Y RT- lane 2, SHSY5Y RT+lane 3, SH-SY5Y RT- lane4, water lane 5. Only cDNA from reverse transcribed cells gives a 563 bp amplicon. The weight ladder to the far right, ranges from 1000 base pairs to 200 base pairs in 100 base pair increments (values to the right of the ladder).

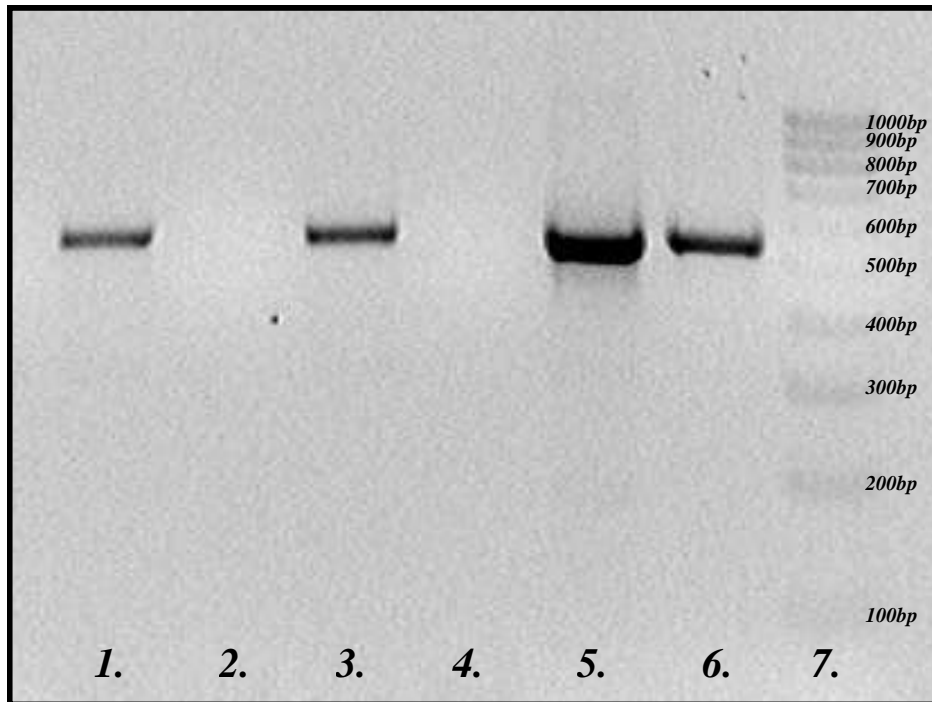
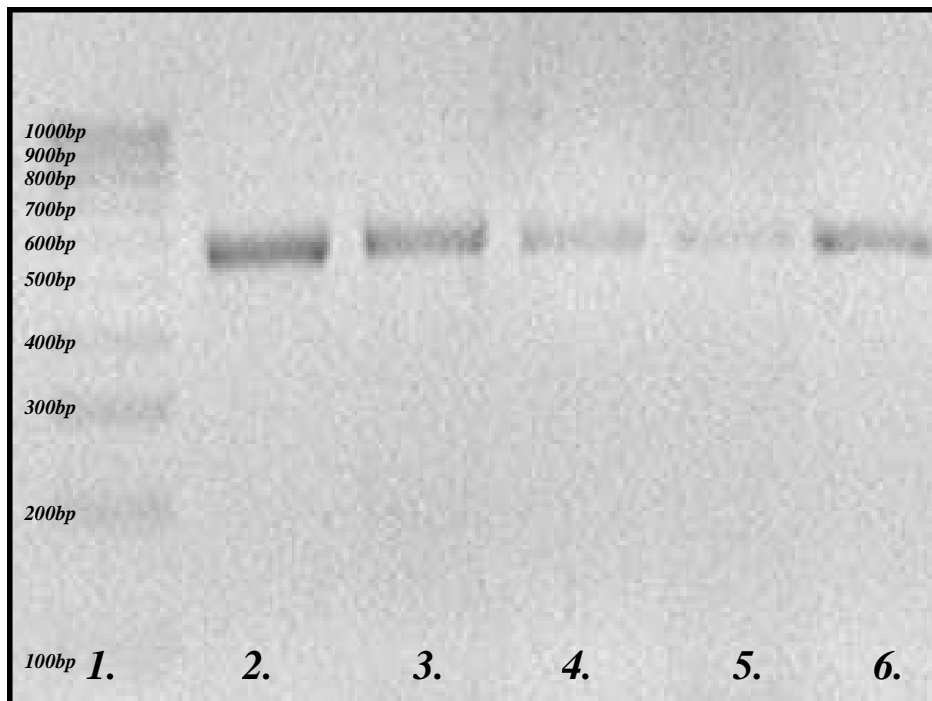
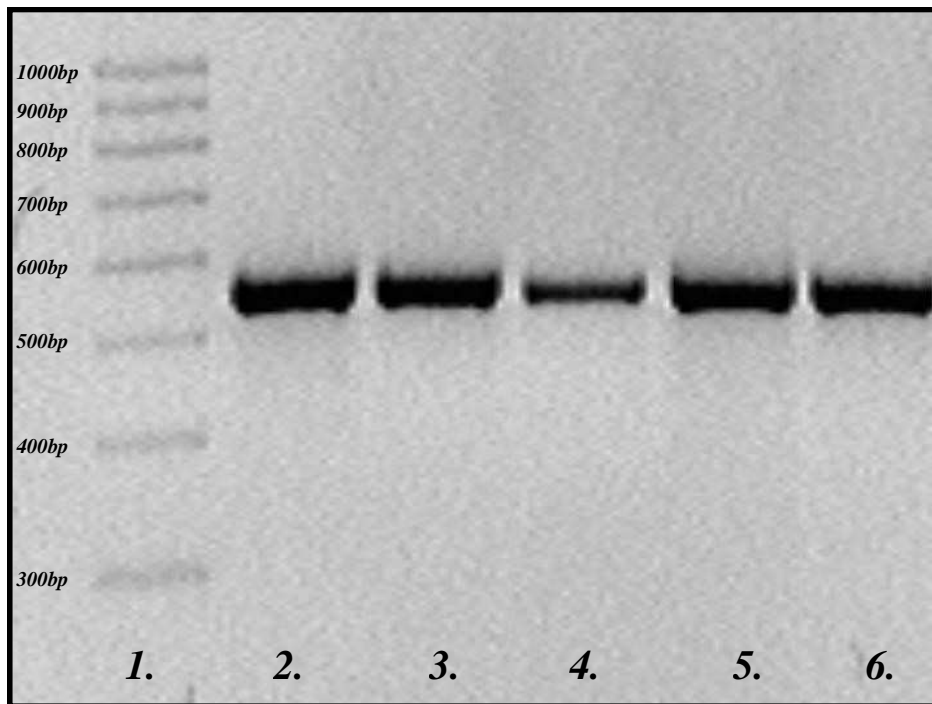


Figure 5.15. NOP1 primers with cDNA from Raji and CHO_{hNOP} cells. Raji RT+ lane 1, Raji RT- lane 2, Raji RT+ lane 3, Raji RT- lane 4, CHO_{hNOP} RT+ lane 5, CHO_{hNOP} RT- lane 6, ladder lane 7. cDNA from Raji reverse transcribed cells gives a 563 bp amplicon. cDNA from Raji non-reverse transcribed cells gives no 563 bp amplicon. Reverse transcribed and non-reverse transcribed material from CHO_{hNOP} cells give amplicons at 563bp. The weight ladder to the far right, ranges from 1000 to 100 base pairs in 100 base pair increments (values to the right of the ladder).

Figure 5.15 shows bands for Raji RNA which has been reverse transcribed into cDNA while RNA extracted but not reverse transcribed (Raji RT-) shows no bands. CHO_{hNOP} cells however show bands whether reverse transcription has taken place or not. This is indicative of the fact that the cDNA encoding for the NOP receptor has been transfected into the Chinese hamster ovary cells and not genomic DNA, hence both reverse transcribed cells and non-reverse transcribed cells produce amplicons at 563bp.

Figure 5.16 shows PCR products following standard end point PCR with cDNA extracted from the PBMC component of healthy volunteer blood with NOP1 receptor primers. All of the samples show clear bands at 563 base pairs indicative of the presence of the RNA encoding for the NOP receptor. Similar results were found with the cDNA extracted from the whole blood of healthy male volunteers, **Figure 5.17**. In this image SH-SY5Y cells were used as a low expression positive control.



Figures 5.16. NOP1 primers with cDNA from PBMCs from ten healthy volunteers five in upper and five in lower image with ladder in both instances at far left. In each panel lane 1 ladder, lanes 2-6 PBMCs. All PBMCs give a 563 bp amplicon. The weight ladder to the far left, ranges from 1000 to 100 base pairs in 100 base pair increments (values are shown to the left of the ladder). Differences in imaging led to differences in band intensity between the two gels.

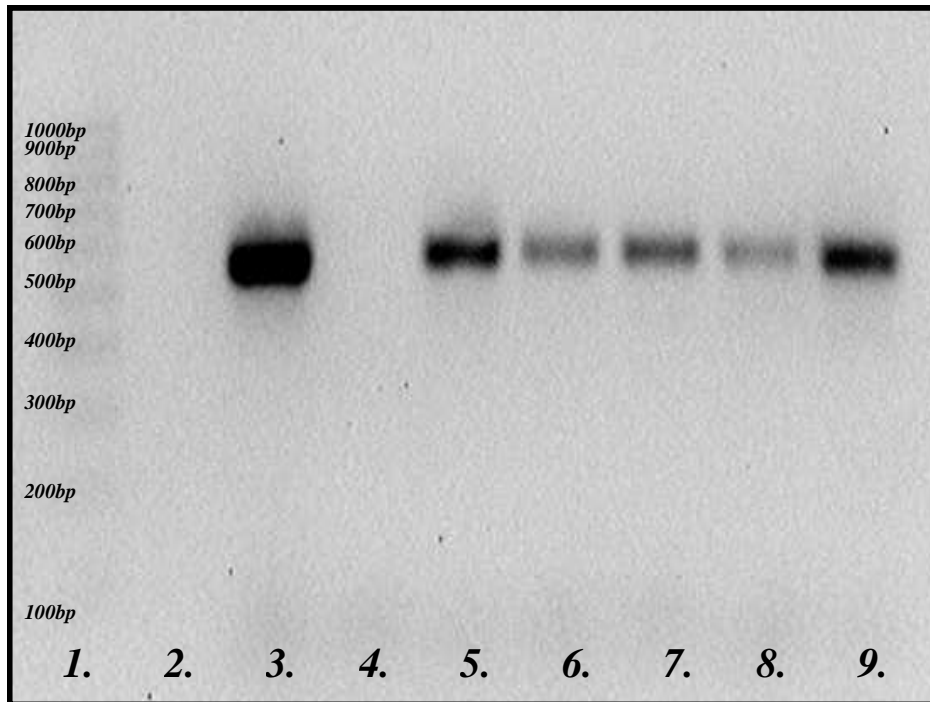


Figure 5.17. NOP1 primers with cDNA from the venous blood of five healthy volunteers, SH-SY5Y cDNA is used as a positive control. Lane 1 ladder, lane 2 water, lane 3 SH-SY5Y, lane 4 water, lanes 5-9 venous blood. SH-SY5Y control and all venous blood samples give a clear amplicon at 563 bp. The weight ladder to the far left, ranges from 1000 base pairs to 100 base pairs in 100 base pair increments (values are shown to the left of the ladder).

Figure 5.18 shows results for cDNA produced following the extraction of RNA from the PBMCs of ten healthy male volunteers following PCR with prepronociceptin primers, the precursor for both the NOP agonist (N/OFQ) and physiological antagonist (nocistatin). All ten individuals clearly show bands on gel electrophoresis after PCR indicative of the presence of prepronociceptin mRNA. Raji cells were also shown to display the RNA encoding for prepronociceptin as shown in **Figure 5.19**. However despite displaying evidence for the NOP receptor the neuroblastoma cell line SH-SY5Y showed no evidence of prepronociceptin RNA expression **Figure 5.20**. As would be expected CHO_{hNOP} cells, the cell line used as a positive control in the investigation for the presence of the human NOP receptor, consistently showed no evidence for the existence of RNA encoding for prepronociceptin (not shown).

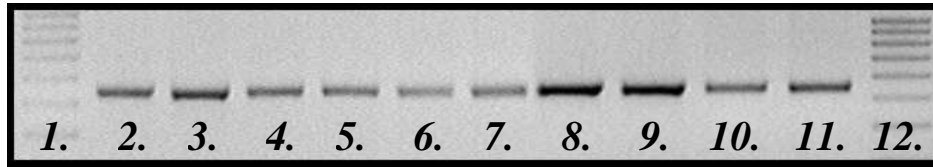


Figure 5.18. Prepronociceptin primers, NOPP1, with cDNA from the PBMCs of ten healthy volunteers. Lane 1 + 12 ladder, lane 2-11 PBMCs. All PBMC blood samples give a clear amplicon at 546 bp. The weight ladder to the far left and right, ranges from 1000 base pairs to 400 base pairs in 100 base pair increments.

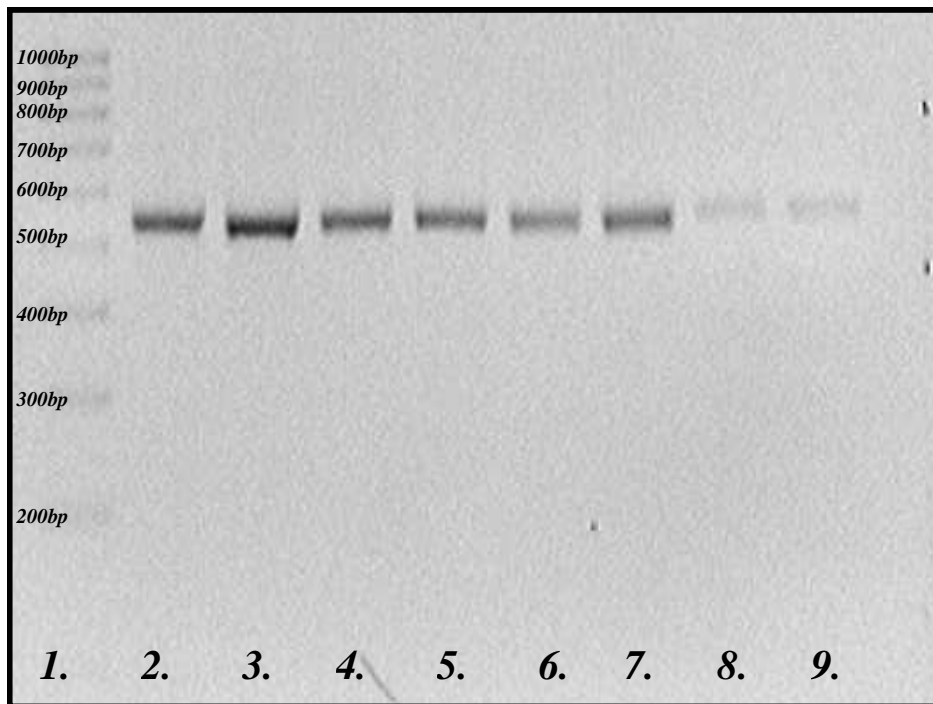


Figure 5.19. NOPP1 primers with cDNA from the PBMCs of six healthy volunteers and Raji cells all reverse transcribed. Lane 1 ladder, lane 2-7 PBMCs, lane 8 + 9 Raji. All samples give a clear amplicons at 546 bp. Weight ladder ranges from 1000-200 base pairs in 100 base pair increments.

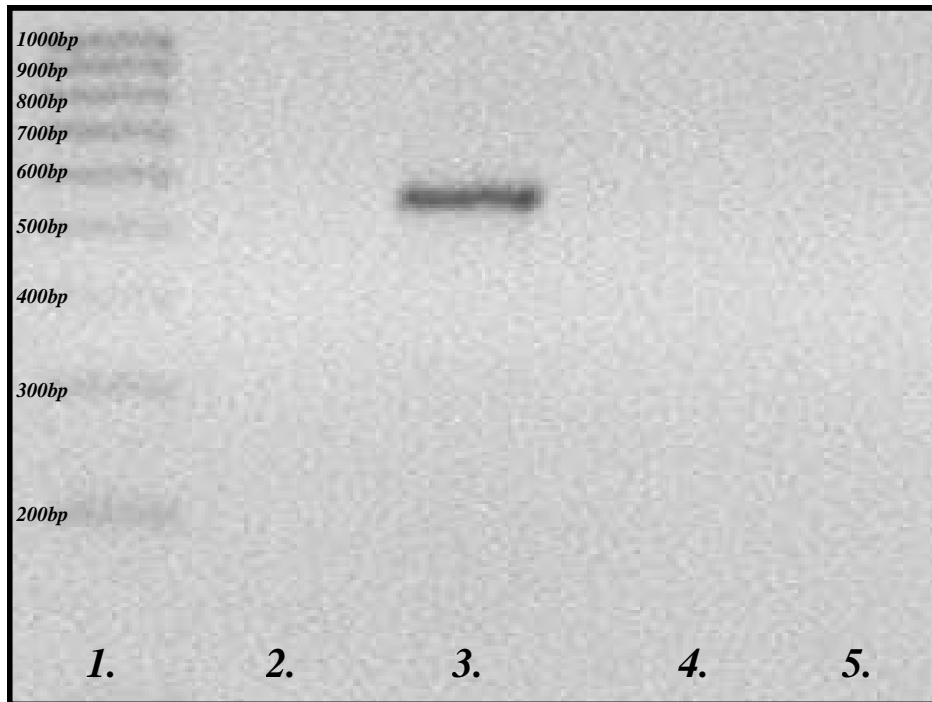


Figure 5.20. NOPP1 primers with cDNA from the Raji and SHSY5Y cells all reverse transcribed. Lane 1 ladder, lane 2 water, lane 3 Raji, lanes 4-5 SH-SY5Y. Only Raji cells give amplicons at 546 bp, no amplicons are seen with SH-SY5Y cDNA. The weight ladder to the far left, ranges from 1000 to 200 base pairs in 100 base pair increments (values are shown to the left of the ladder).

5.3.2 Results: Quantitative PCR

Quantitative PCR reactions showed increasing fluorescence with increasing cycle number for cDNA from PBMCs when used in conjunction with *TaqMan*[®] Gene expression probes directed at the NOP receptor **Figure 5.21**. These findings were mirrored when cDNA from whole blood was used as template **Figure 5.22**. Both of these sets of results suggest that the RNA encoding for the receptor is expressed in PBMCs and whole blood. These results support the standard gel based PCR analysis techniques described above.

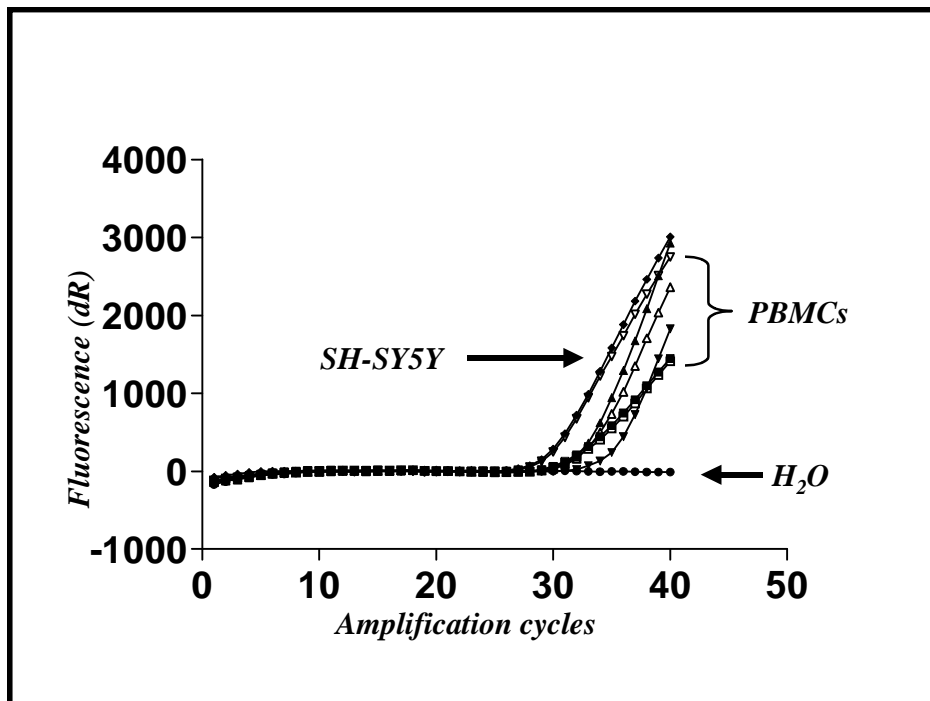


Figure 5.21. QPCR using *TaqMan*[®] Gene expression assay for NOP receptor with cDNA from SH-SY5Y cells as a low expression positive control curve, and with cDNA from PBMCs. Water was used as a negative control. Example of five replicates of a total of ten PBMC samples, with two SH-SY5Y positive controls. Water shows no deflection of the curve, while SH-SY5Y cDNA shows amplification at 28, PBMCs show amplification around 30 cycles.

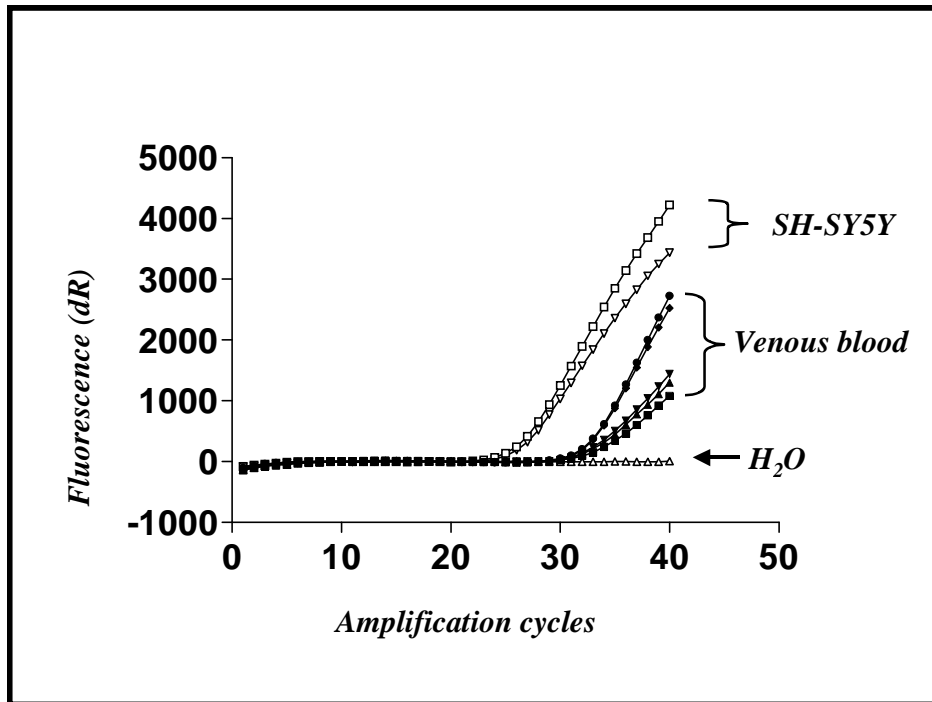


Figure 5.22. QPCR using *TaqMan*[®] Gene expression assay for NOP receptor with cDNA from SHSY5Y cells as a low expression positive control, and with cDNA from venous blood. Water was used as a negative control. Example of five replicates of a total of five venous blood samples, with two SH-SY5Y positive controls. Water shows no deflection of the curve, while SH-SY5Y cDNA shows amplification at 24, venous blood show amplification around 30 cycles. Note the C_t value for the SH-SY5Y cDNA is the same even though the maximal fluorescence achieved differs between the two samples.

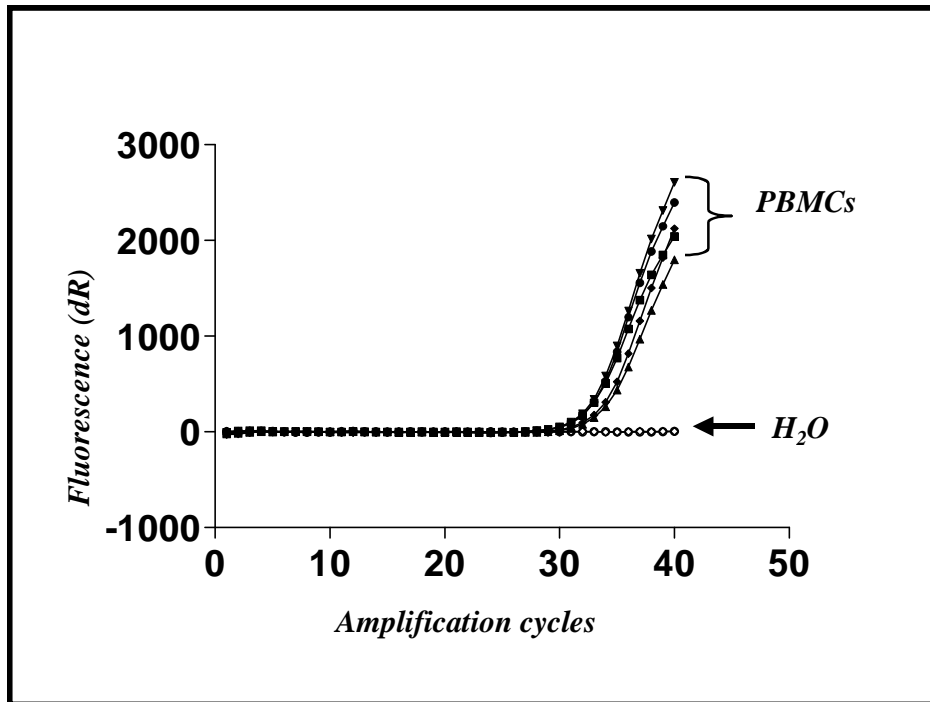


Figure 5.23. QPCR using SYBR green expression assay for N/OFQ (NOPP2) with cDNA from PBMCs. No positive control was available. Water was used as a negative control. Example of five replicates of a total of five PBMC samples. Water shows no deflection of the curve, while venous blood samples show amplification around 30 cycles.

Quantitative PCR reactions using SYBR green fluorescent labeling and the NOPP2 primer pair showed increasing fluorescence with increasing cycle number for cDNA from PBMCs **Figure 5.23**. These results correlate with the standard gel based PCR analysis techniques described above.

5.4 Stimulated Upregulation of NOP Receptor Gene Expression

The standard gel based PCR analysis and quantitative PCR techniques described above provided good evidence to suggest that peripheral blood mononuclear cells, whole blood cDNA, Raji cells and SH-SY5Y cells express the RNA encoding for the NOP receptor. Previous studies have indicated that the RNA encoding for MOP receptors might be expressed in peripheral immune cells, when cultured in the presence of TNF α and cycloheximide, experimental conditions mimicking an inflammatory environment. As described above in **Chapter 3** looking for the presence of the MOP receptor on PBMCs, this is a finding we were unable to replicate. However a similar experimental approach was used to examine upregulation of NOP receptor message with Raji cells utilizing standard gel based PCR technology. This technique was not repeated with PBMCs due to the limited number of *ex vivo* cells available from healthy volunteers for this type of assay.

5.4.1 Results: Stimulated Expression of NOP

Standard gel based PCR imaging using a 3% agarose gel viewed under a UV light gave no indication of clear identifiable upregulation in expression of the gene encoding for the human NOP receptor in Raji cells **Figure 5.24**. This was regardless of whether 100 pg/ml or 200pg/ml of TNF α was added to the culture 20 hours prior to harvesting.

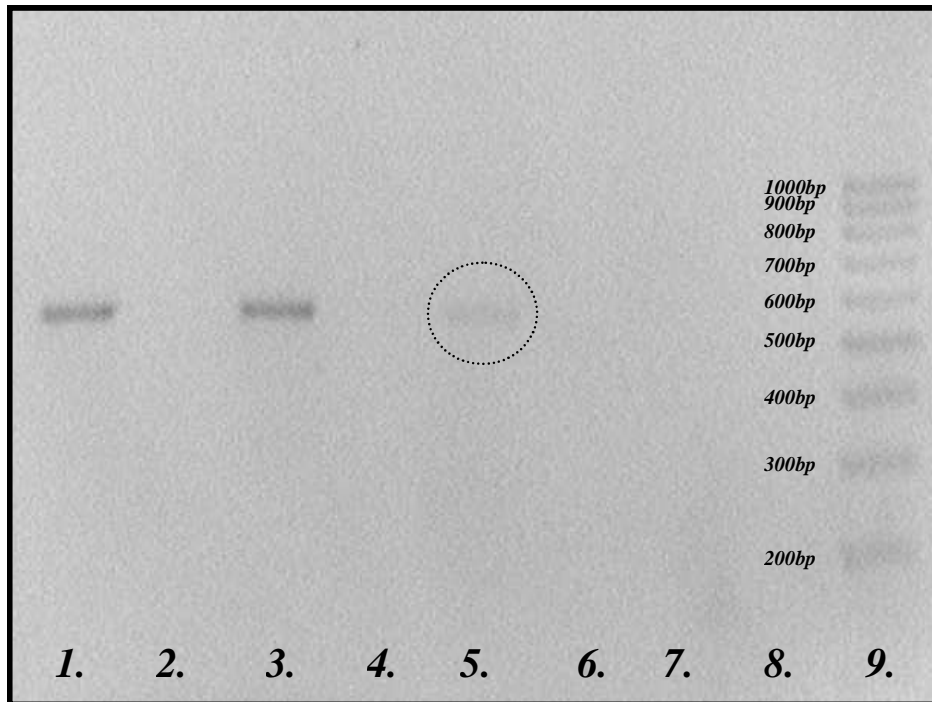


Figure 5.24. NOP1 primers with cDNA from the Raji, SH-SY5Y reverse transcribed and not reverse transcribed and CEM gDNA. Raji cells grown in the presence or absence of TNF α . Lane 1 Raji TNF+ RT+, lane 2 Raji TNF+ RT-, lane 3 Raji TNF- RT+, lane 4 Raji TNF- RT-, lane 5 SH-SY5Y RT+ (within circle), lane 6 SH-SY5Y RT-, lane 7 CEM gDNA, lane 8 water and lane 9 ladder. Reverse transcribed Raji and SH-SY5Y cells give amplicons at 563 bp, no amplicons are seen with non-reverse transcribed entities, CEM gDNA or water. There is no difference in band density with or without addition of TNF α in Raji cells. The weight ladder to the far right, ranges from 1000 base pairs to 200 base pairs in 100 base pair increments (values are shown to the left of the ladder). CEM and SH-SY5Y cDNA were used as positive controls in these experiments and to aid the differentiation of genomic from complimentary DNA if required.

5.5 Discussion

In the series of experiments described above saturation binding assays utilizing [³H]-N/OFQ failed to show the presence of the NOP receptor on peripheral blood mononuclear cells and the Raji cell line, even when a large mass (125 - 400µg of crude membrane per assay) of cultured cells was analysed.

Chinese hamster ovary cells transfected with the human receptor however did consistently display [³H]-N/OFQ binding, providing evidence that this type of investigation could be used effectively to determine NOP expression on cellular material. It should be noted however that [³H]-N/OFQ is a low specific activity radiolabel and may therefore not be adequate to detect receptors if in low abundance. The neuroblastoma cell line, SH-SY5Y also expresses NOP receptors but in a density too low to be found using [³H]-N/OFQ as a radiolabelled probe. It is possible to use [¹²⁵I]-N/OFQ as a probe to measure this expression. Using this technique it can be estimated that SH-SY5Y cells express approximately 10 fmol.mg⁻¹ of NOP protein using this high specific activity radiolabel (unpublished data). This however was not undertaken for immune cells in this series of experiments, as it proved prohibitively expensive.

Amplified functional GTPγ[³⁵S] assays similarly gave no suggestion that PBMCs express the NOP receptor, however with the Raji cell line the results were inconsistent. While 5 out of 7 experimental replicates gave some indication of a concentration dependent increase in binding indicative of GDP exchange for GTP (i.e., receptor activation), two further experiments showed no such increase. If analyzed in isolation the five replicates suggestive of receptor binding, provide a concentration dependent increase in binding with a pEC₅₀ of 8.16 ± 0.30 (SEM), a value that correlates well with the values obtained when CHO_{hNOP} cells are used as a positive control (pEC₅₀ = 8.681 ± 0.01 SEM). We have previously used this system to report densities of NOP protein to around 25 fmol.mg⁻¹ in inducible cell systems and dog brain extracts (*Johnson et al 2004, McDonald et al 2003*). These results provide evidence of the presence of NOP receptors on the β lymphocytic cell line (Raji cells), however the absolute values for conversion of GDP to GTPγ[³⁵S] are low and the calculated stimulation factors are also similarly low. For these reasons any

inference from this series of GTP γ [³⁵S] binding assays as to the presence of NOP receptors on Raji cells needs to be treated with some caution.

Transcripts of the gene encoding for the NOP receptor were found using PCR techniques in Raji cells, PBMCs and whole blood cDNA, with RNA extracted from CHO_{hNOP} and SH-SY5Y used as positive controls. Interestingly the cDNA extracted from the Chinese hamster ovary cells transfected with NOP DNA gave similar bands on PCR to its genomic DNA as shown in **Figure 5.15**. This implies that only the coding portion of the genetic code was transfected into this cell line with no introns. Quantitative PCR using *TaqMan*[®] Gene expression assays from Applied Biosystems supported these findings with clear evidence that NOP receptor transcripts are expressed in PBMCs and whole blood. If we assume equal starting template of PBMC and SH-SY5Y in QPCR and comparable reaction conditions, then it is not unreasonable to suggest that PBMCs express less NOP RNA than SH-SY5Y cells (less than 10 fmol.mg⁻¹ protein NOP). This level would be below the detection limit of the [³H] binding protocols discussed above.

The precursor to the endogenous ligands at the NOP receptor (N/OFQ and nocistatin) was also found in immune cells using endpoint polymerase chain techniques. PCR experiments with Raji cells, PBMCs from healthy volunteers and whole blood cDNA, from a similar population, when used in tandem with NOPP1 primers, indicated that prepronociceptin transcripts are expressed in these cell lines. Unsurprisingly quantitative PCR using a SYBR green fluorescent probe supported the finding that peripheral blood mononuclear cells also contains transcripts for prepronociceptin. At face value, the lack of [³H]-N/OFQ binding in PBMCs is not consistent with clear identification of NOP mRNA in PCR. However, we feel that receptor expression is likely to be very low, rendering [³H]-N/OFQ radioligand binding ineffectual at providing data suggestive of NOP expression.

At this point it seems reasonable to postulate that as PBMCs express NOP receptor RNA and display the ability to produce prepronociceptin then some form of autoregulation of function may occur. In inflammation classical opioid receptors are upregulated on peripheral nerves and white blood cells attracted to these sites release classical opioid peptides to provide a degree of endogenous analgesia via a 'neuro-immune axis' (*Mousa*

et al 2000, 2002 & 2004, Stein et al 2000 & 2003). Based on our data and that of others it is not unreasonable to add the NOP-N/OFQ system to this axis.

Chapter 6:

Opioid Signalling in Peripheral Immune Cells During Sepsis

6.1 Background

The results from experiments described in *Chapters 3&4* have suggested that MOP, DOP and KOP receptors are not expressed on the surface of peripheral blood mononuclear cells. Moreover their transcripts, expressed as a component of the messenger RNA manufactured within these cells in their naïve state, are also absent. In *Chapter 5*, NOP receptor RNA transcripts were shown to be synthesized by peripheral blood mononuclear cells in this state and there was some evidence from GTP γ [³⁵S] binding assays to suggest that the receptor itself may also be expressed in Raji cells. Various studies have also implicated the administration of commonly used opioid analgesic agents with derangements in immune cell function, both in *in vitro* and *in vivo* environments (*Hashiba et al 2003, Manfredi et al 1993, Mellon et al 1998 & 1999, Philippe et al 2003, Yeagar et al 1991 & 1995*). Previous investigators have also suggested a deleterious effect of opioid analgesics on survival in models of sepsis (*Greenelch et al 2004, Hess et al 1981, Malcolm et al 1988, Spink et al 1967, Roy et al 1998 & 1999*).

The normal response to inflammation comprises a number of common features; raised body temperature, heart and respiratory rate and an increase or decrease in the white cell count from normal. This response is termed a systemic inflammatory response. Sepsis is the clinical syndrome displaying these features and is characterized by the presence of a clinically significant blood borne infection (*American College of Chest Physicians/Society of Critical Care Medicine Consensus Conference 1992, Levy et al 2001*).

In 2001 The International Sepsis Definitions Conference defined sepsis as, the presence of the systemic inflammatory response syndrome (SIRS) plus an identifiable infection, where SIRS is classified by the existence of two or more of the following:

- Body temperature $> 38^{\circ}\text{C}$ or $< 36^{\circ}\text{C}$
- Heart rate > 90 beats/min
- Respiratory rate $> 20/\text{min}$ or $\text{PaCO}_2 < 4.3$ kPa, or the need for mechanical ventilation for a non-respiratory cause
- White cell count $>12,000$ cells/ mm^3 , $<4,000$ cells/ mm^3 or $>10\%$ immature neutrophils

This may cause widespread release of inflammatory mediators, immunological derangement and alterations in the coagulative properties of the blood. The alterations described may in turn lead to organ dysfunction. If sepsis is accompanied by marked organ dysfunction it is termed severe sepsis. Currently the incidence of severe sepsis is estimated to be 3 cases per 1000 population and 2.26 cases per 100 hospital discharges. Though severe sepsis can occur in any age group, it is more common in the elderly with an incidence of 0.2 per 1000 in children and 26.2 per 1000 in those aged over 85. Mortality from severe sepsis is approximately 30% overall, and increased in the elderly. Recent estimates suggest that there are over 200,000 deaths in the United States annually from sepsis (*Angus et al 2001*).

Investigators have suggested that MOP receptor gene transcripts may be expressed following *in vitro* cellular stimulation by inflammatory mediators, such as those involved in sepsis and the physiological response to sepsis (*Borner 2002 & 2004, Kraus et al 2001 & 2003*). However using an inflammatory surrogate of $\text{TNF}\alpha$ no such up-regulation of mRNA was identifiable for MOP or NOP receptors *in vitro* in a B-lymphocytic cell line (*Chapters 3 & 5*). Small animal models however have shown a role for the nociceptin system in the local control of blood pressure with appreciable drops in mean arterial pressure and increases in vessel diameter following the administration of N/OFQ to anaesthetized animals (unpublished data *Williams JP*).

The aims of this chapter were therefore:

- To follow any changes in mRNA expression of the three classical opioid receptors, the NOP receptor and prepronociceptin within the blood of patients suffering from a significant septic insult, during their stay on the Leicester Royal Infirmary Adult Intensive Care Unit. The technique of quantitative PCR was used to attempt to accurately map changes in gene expression during this time frame.
- To quantify changes in serum N/OFQ concentration using radioimmunoassay techniques.
- It was hoped that by studying changes in opioid receptor expression and endogenous NOP receptor ligand concentration a better understanding of their role in the septic response and of their involvement in a neuroimmune axis could be achieved.

6.2 Primer Design and Optimisation

In previous chapters quantitative PCR and standard end point PCR have been used to look for mRNA transcripts, which encode for the NOP receptor, classical opioid receptors and prepronociceptin. These experiments have provided an ‘all or nothing’ comment on expression. This chapter however is concerned with observing a variation in mRNA expression. This requires that any observed change in gene expression be judged against a standardised, consistent and constant measure. A number of approaches have been used in the literature to tackle this problem of measuring a change in expression (*Bustin 2000, Pfaffl et al 2004, Vandesompele et al 2002*). One commonly used method is to look at the cycle threshold (C_t) value for a particular threshold fluorescence, standardised to the starting number of cells or RNA extracted. Accurate enumeration of cells is possible with whole blood samples drawn from blood. At the same time as blood is taken for RNA extraction, blood for full blood count can also be drawn and analysed. However this still assumes that the mRNA extracted is of a uniformly good quality between individuals and at individual time points. In addition this analysis either requires that mRNA be purified from the total RNA, or that the ratios of rRNA (the predominant RNA fraction) to mRNA be constant. These drawbacks clearly limit the usefulness of this approach. Another commonly used approach to normalisation described in the literature is to use an internal control or housekeeping gene (*Bustin 2000*). This technique requires that along with the gene of interest a second stably expressed gene be analysed. It is assumed that as this second gene is unchanging in its expression it can be used as a constant to which the gene of interest can be normalised, hence variations in the gene of interest can be deduced over a range of conditions while expression of the housekeeping gene remains steady. One obvious limitation of this technique is the requirement for a stably expressed internal control. A variety of housekeeping genes are described within the literature dependent upon the tissue of interest. These genes are usually chosen to reflect functional aspects of cellular mechanisms which themselves are consistent over time and pathological states. Unfortunately close analysis of the constancy of internal controls has often suggested that no gene when analysed in isolation can be relied upon to be invariant and that housekeeping gene expression may vary considerably. *In vivo*, sepsis is accompanied by highly dynamic changes in the leucocyte fraction. Increased

activity in the haemopoetic regions of the body leads to an increased production in immature white cells and a destruction of older cells. The cellular actions and mechanisms of existing cells also change, with immunocompetent cells directing their energies to countering microbiological pathogens. These cellular changes will be mirrored by alterations in gene expression within cells. Finding one individual internal control to use as a housekeeping gene against this backdrop of dynamic cellular change is a difficult if not impossible task. *Vandesompele et al* described a strategy using a number of housekeeping genes, which would allow calculation of the most stably expressed genes in any given system under investigation (*Vandesompele et al 2002*). Variations in expression of these genes relative to each other could then be compared and a normalisation factor calculated to provide a more consistent internal control for subsequent analysis of any genes of interest. This type of analysis should limit the errors frequently encountered with the use of just one housekeeper. It was hoped that this system, using a number of housekeeping genes, could be employed in this study to track changes in the genes of interest during a septic episode. A search of the literature provided a number of housekeeping genes that had been used previously in white blood cells. These investigations looked at changes in gene expression in inflammatory conditions or at rest, but none were specifically concerned with sepsis. Genes that had been used in more than one study showing good consistency or housekeepers from studies in inflammatory processes were chosen in preference to be internal controls (*Boeuf et al 2005, Dheda et al 2004, Nadkarni et al 2002, Pachot et al 2004, Vandesompele et al 2002, Zhang et al 2005*). From this literature search six housekeeping genes were identified (B2M, EF1A, HPRT, PPIB, UBC and YWHAZ). Primer pairs were designed for these genes using *Primer 3* and *Operon* freeware to minimise primer dimer formation. Blast software was used to confirm primer annealing and reduce the possibility of adherence to anything other than the gene of interest (in this case the housekeeping gene). Primer pairs were designed to rely on SYBR green fluorescent imaging and so were chosen to sit across exon-exon boundaries to help distinguish cDNA from gDNA as described previously. Amplicon products were designed to be around 100 base pairs in length to facilitate the use of QPCR. A primer pair for HPRT was already

available in house and had been used to good effect previously. This primer pair was therefore used unchanged in the following studies.

For the genes of interest ready optimized *TaqMan*® gene expression assays (*Applied Biosystems*) were used to follow changes in DOP, KOP, MOP and NOP gene expression, while the NOPP2 primer pair (*Chapter 5*) was used to follow changes in prepronociceptin, the gene encoding for the precursor molecule to N/OFQ and nocistatin. Housekeeper and NOPP2 primer sequences, the genes to which they anneal and the size of amplicon they produce are shown in *Table 6.1*, while the function of each of these genes is outlined in *Table 6.2*.

Gene	Forward primer	Reverse Primer	Prod. size
B2M	5'- TCGCGCTACTCTCTCTTTCTG-3'	5'- ACTTCCATTCTCTGCTGGATG-3'	90
EF1A	5'- AGCCCATGTGTGTTGAGAGC-3'	5'- CTCTGTCCACTGCTTTGATG-3'	110
HPRT	5'-GCAGACTTTGCTTTCCTTGGTCAG-3'	5'- GTCTGGCTTATATCCAACACTTCGTG- 3'	103
PPIB	5'- GGCTCCCAGTTCTTCATCAC-3'	5'- TCTTGGTGCTCTCCACCTTC-3'	115
UBC	5'- GTCGCAGTTCTTGTGTTGTGG-3'	5'- TCGAGGGTGATGGTCTTACC-3'	90
YWHAZ	5'- TGAAGCCATTGCTGAAGTTG-3'	5'- CTCCTGGGTATCCGATGTC-3'	113
NOPP2	5'- CCTGCACCAGAATGGTAATG-3'	5'- GCTGAGCACATGCTGTTTG-3'	108

Table 6.1. Genes, forward and reverse primers with the size of amplicon that they produce.

Gene	Gene Function
B2M	Beta-2-microglobulin is a component of the major histocompatibility complex (MHC) class I heavy chain found on the surface of nearly all nucleated cells.
EF1A	Involved in the binding of aminoacyl-tRNAs to 80S ribosomes and the hydrolysis of GTP into GDP.
HPRT	Hypoxanthine-guanine-phosphoribosyltransferase (HPRT) is a ubiquitous enzyme, which if absent causes Lesch-Nyhan syndrome an X-linked disease.
PPIB	PPIB (cyclophilin B) catalyses the isomerization of peptide bonds from trans to cis at proline residues, helping proteins to fold.
UBC	Ubiquitin is a protein that occurs in all eukaryotic cells. Its main role is to mark other proteins for destruction.
YWHAZ	YWHAZ (Tyrosine 3-monooxygenase activation protein) has been shown to be involved in the protein kinase C signaling pathway.
NOPP2	Encodes for the precursor to both N/OFQ and nocistatin, prepronociceptin. These peptides are agonist and physiological antagonist at the NOP receptor respectively.

Table 6.2. Gene and function.

6.2.1 Methods: Housekeeping Primer Optimisation

Before using the housekeeping genes as internal controls in quantitative PCR reactions, a series of optimisation studies were required. These experiments ensured that the primer pairs work efficiently and accurately to amplify the housekeeping genes of interest. The first investigation performed in this series was a standard gel based PCR experiment for each of the primer pairs at a range of annealing temperatures. This ensured that the primers produced a single amplicon around the 100 base pair size and that they would anneal at around 57°C, the temperature used in the Stratagene Mx4000 (used for qPCR). cDNA from healthy volunteer blood was used as template for all of the optimisation experiments. As described in **Chapter 2** RNA was extracted from the whole blood of healthy volunteers **Protocol 2.4**.

Following standard PCR analysis quantitative PCR was undertaken with a range of concentrations for both forward and reverse primers (100-300nM). This allowed for the combination of forward and reverse primers, which yielded the lowest C_t value to be found. Plots of reaction efficiency for varying amounts of initial template were also made. At the same time a dissociation curve for the amplicon products was produced. This plot produces a melting curve for the QPCR amplification product at one distinct temperature if only one size amplicon is produced, as expected, during the QPCR reaction. These investigations provided confidence that the primer pairs not only produced 100% amplification efficiency, but also that the reaction conditions were consistent over a range of template concentrations. Quantitative PCR experiments used SYBR green fluorescence for imaging **Protocol 2.10**. This required a different thermal profile to be used than employed previously for the *TaqMan*[®] Gene expression system **Protocol 2.9**. An identical set of optimisation studies were also completed for the NOPP2 primer pair.

6.2.2 Results: Housekeeping Primer Optimisation

Standard PCR gave clear bands for amplicons at around 100 base pairs in length and at 57°C for all of the primer pairs. Unfortunately the primer pair coupling for UBC also gave a number of associated products at higher amplicon sizes. **Figures 6.1-6.6.**

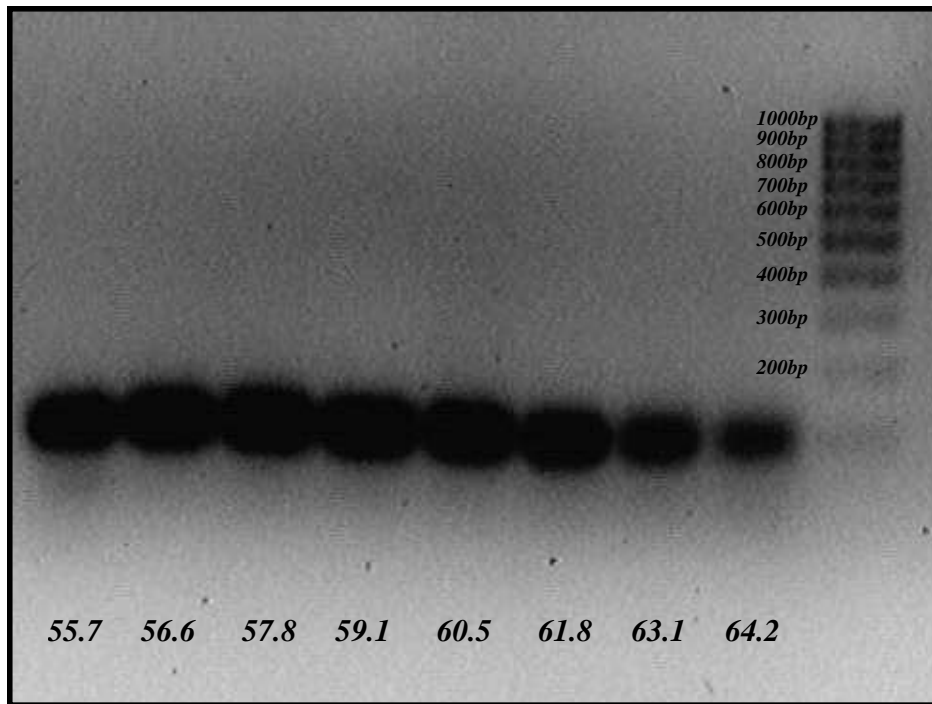


Figure 6.1. Annealing gradient for B2M primers used with cDNA from whole venous blood of healthy volunteers. All temperatures shown along the lower border are in degrees centigrade. All products give one amplicon at the expected length of 90 base pairs. The weight ladder to the right ranges from 1000 base pairs to 100 base pairs in 100 base pair increments, the 100bp label is obscured by the dark amplicon image at 64.2°C.

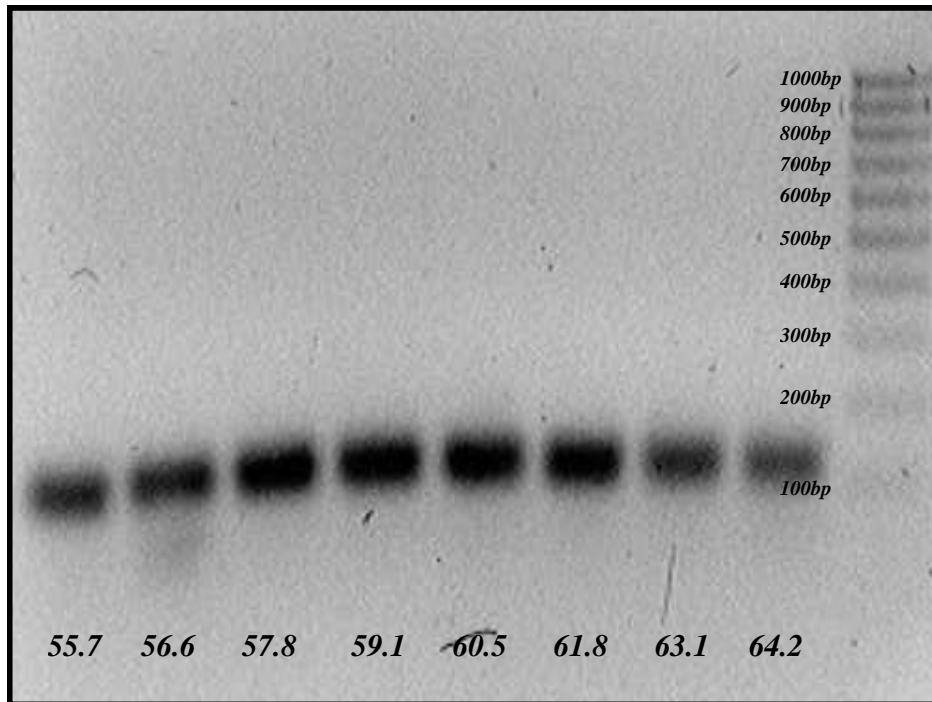


Figure 6.2. Annealing gradient for EF1A, cDNA from whole venous blood of healthy volunteers. Temp. in degrees centigrade. All products give an amplicon at 110 bp. Ladder 1000-100bp.

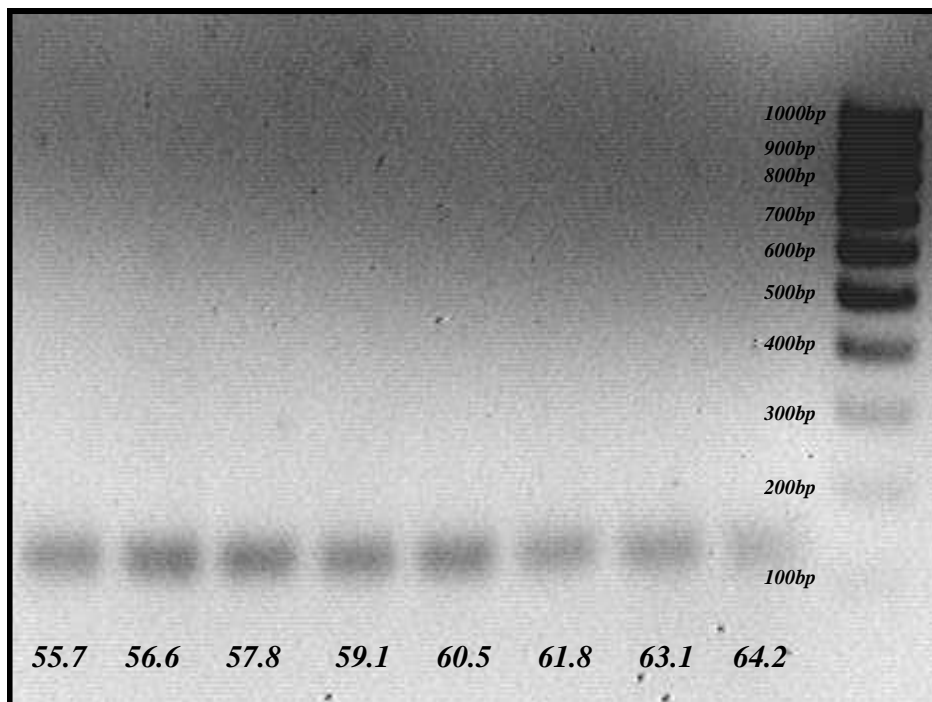


Figure 6.3. Annealing gradient for PPIB primers used with cDNA from whole venous blood of healthy volunteers. All temperatures in degrees centigrade. All products give one amplicon at the expected length of 115 base pairs. Weight ladder 1000-100bp

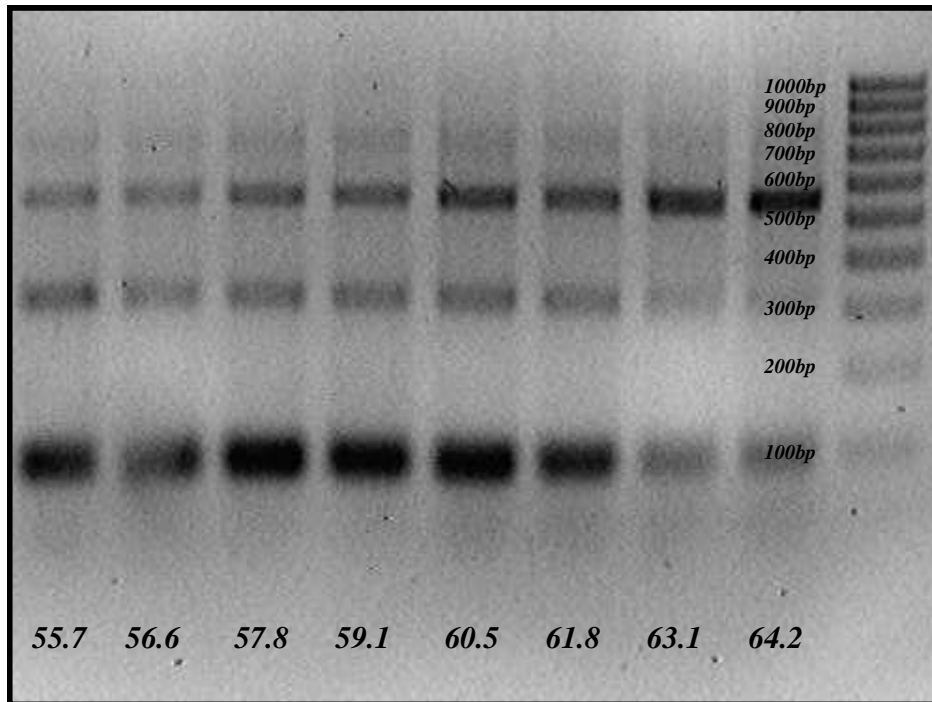


Figure 6.4. Annealing gradient for UBC primers, cDNA from whole venous blood of healthy volunteers. Temperatures in °C. All products give amplicon at 90 base pairs, but also additional amplicons at other sizes. Weight ladder 1000-100bp.

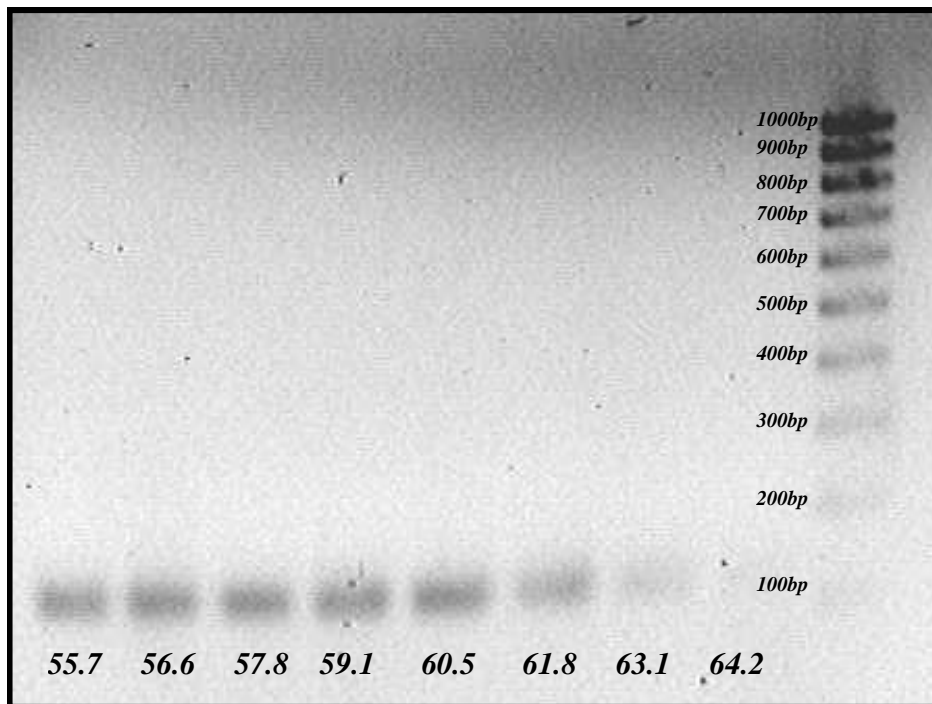


Figure 6.5. Annealing gradient for YWHAZ primers, cDNA from whole venous blood of healthy volunteers. Temperatures shown in °C. All products give one amplicon at 113 base pairs. Only a faint amplicon signal is seen at 63.1 and 64.2°C. Weight ladder 1000-100bp.

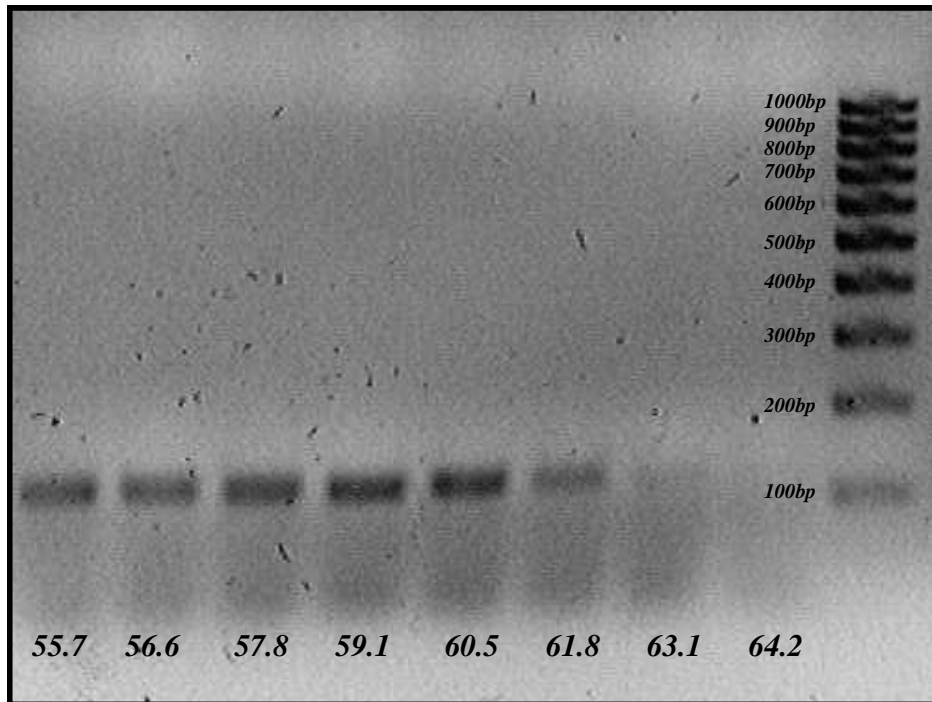
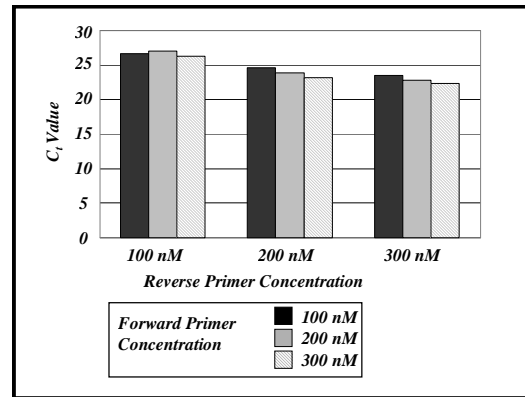
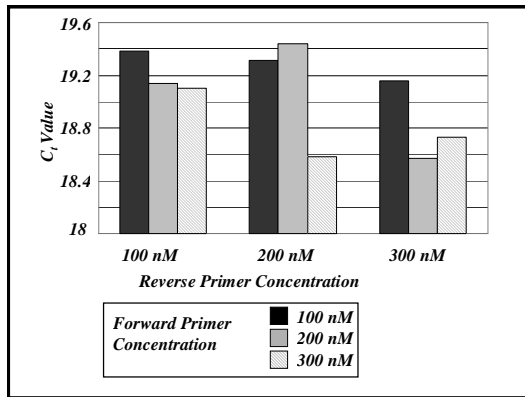


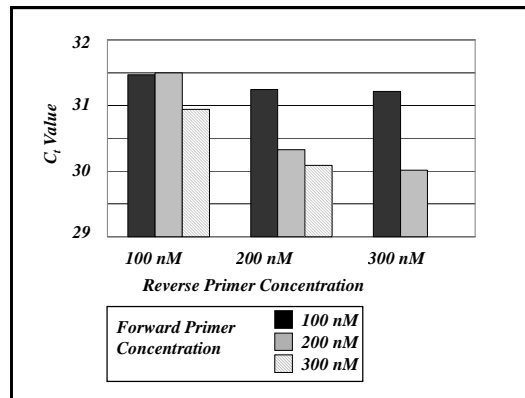
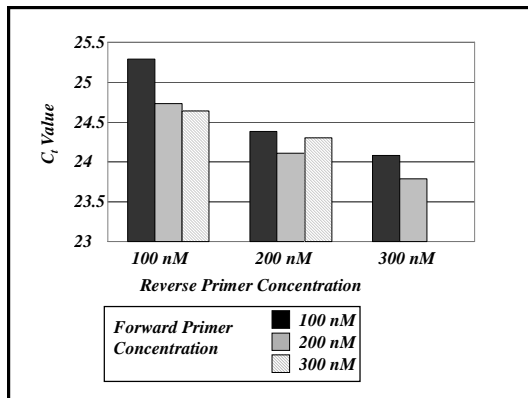
Figure 6.6. Annealing gradient for NOPP2 primers used with cDNA from whole venous blood of healthy volunteers. All temperatures shown along the lower border are in degrees centigrade. All products give one amplicon at the expected length of 108 base pairs. Only a faint amplicon signal is seen at 63.1 and 64.2°C. The weight ladder to the right ranges from 1000 base pairs to 100 base pairs in 100 base pair increments.

A standard PCR annealing experiment was not performed for the HPRT primer pair as it had been used to good effect for some time within our laboratories. In addition it was known that HPRT performed well at primer concentrations of 200nM for both forward and reverse primers, a series of experiments ensuring its efficiency over a range of template concentrations and a dissociation melt were undertaken. As the UBC primer pair gave multiple amplicons of differing length on standard PCR it was not used further as an internal control, therefore no additional optimisation experiments were performed. The B2M gene was found to be in high abundance in the cDNA produced from venous blood. Forward and reverse primer concentrations of 200nM provided conditions, which gave a low C_t in all instances. Therefore further primer concentration optimisation was not needed for the B2M gene. **Figure 6.7** shows the range of C_t values obtained with different forward and reverse primer concentrations. In all cases cDNA extracted from the venous whole blood of healthy individuals was used as template.



A. EF1A

B. PPIB

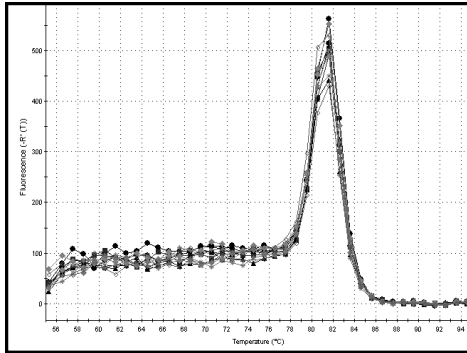


C. YWHAZ

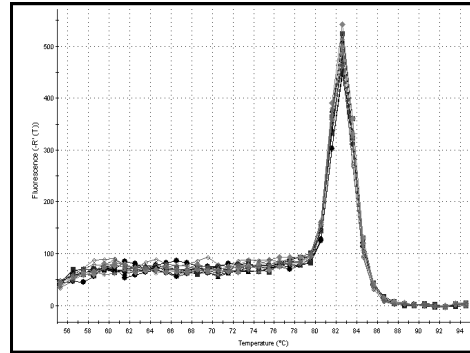
D. NOPP2

Figure 6.7. Shows C_t values for a range of forward and reverse primer concentration combinations between 100nM and 300nM for four target genes. The *y-axis* on each panel shows the cycle threshold at which fluorescence was greater than background. The *x-axis* shows the reverse primer concentrations (100-300nM), while the shaded histograms show the forward primer concentration used in combination with each reverse primer. Hence in Panel A the primer combination of 100nM reverse primer with 100nM forward primer (dark black histogram) has a C_t value of just less than 19.4.

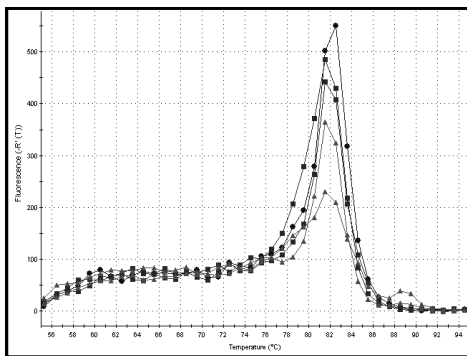
Panel A shows a minimal C_t value for EF1A primers of 18.6 with a 200nM/300nM combination. Panel B shows a minimal C_t value for PPIB primers of 23 with a 300nM/300nM combination. Panel C shows a minimal C_t value for YWHAZ primers of 23.75 with a 200nM/300nM combination. Panel D shows a minimal C_t value for NOPP2 primers of 30 with a 200nM/300nM combination. These primer combinations were therefore used in future experiments. An average of $n=2$ for all primer pairs are shown.



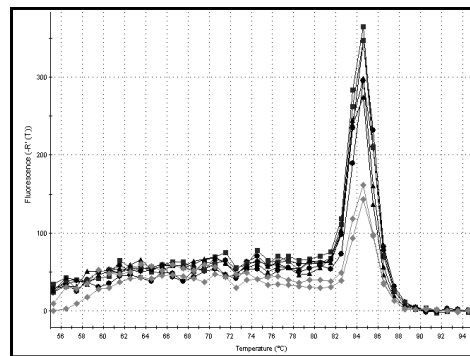
A. B2M



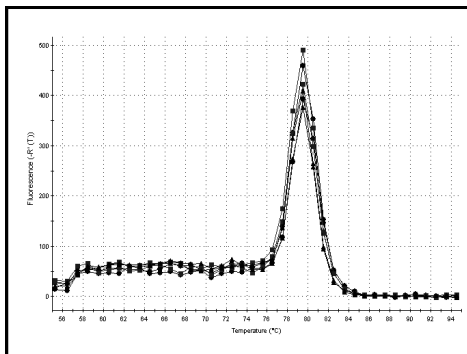
B. EF1A



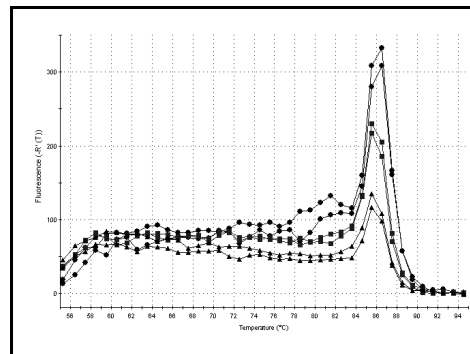
C. HPRT



D. PPIB



E. YWHAZ



F. NOPP2

Figure 6.8. Dissociation curves for B2M, EF1A, HPRT, PPIB, YWHAZ and NOPP2, show unique melting points for each, implying only one amplicon is produced for each primer pair. x-axis shows temperature, while the y-axis shows fluorescence (n=6).

Dissociation curves for all six primers (five housekeepers and NOPP2) showed a defined and unique melting point, implying that only one amplicon was produced following

QPCR for these primer combinations. Again cDNA extracted from the venous blood of healthy individuals was used as starting template. **Figure 6.8.**

Quantitative PCR experiments performed over a range of starting template concentrations showed that amplification was linear for all of the primer pairs used over a 100 to 1000 fold template variation, and around 100% efficiency for each primer pair **Table 6.3.** The optimised primer pair concentrations found above were used in these experiments **Figure 6.7.**

Primer	Amplification Eff. (%)	Linearity (R_{sq})
B2M	93.7	0.988
EF1A	95.4	0.994
HPRT	95.1	0.987
PPIB	103.9	0.994
YWHAZ	99.7	0.986
NOPP2	103	0.982

Table 6.3. Amplification efficiency for each primer pair and linearity of amplification over a 100-1000 fold initial template variation.

The above primer pairs were therefore deemed suitable for use as internal controls or, as in the case of NOPP2, as a probe to explore the expression of the genes of interest. DOP, KOP MOP and NOP *TaqMan*® probes came ready optimized and so did not require a similar series of optimization experiments.

6.3 Patient Selection and Tissue Collection

Patients admitted to Leicester Royal Infirmary Adult Intensive Care Unit with a diagnosis of severe sepsis, sepsis or SIRS (as defined by the American College of Chest Physicians/Society of Critical Care Medicine Consensus Conference, 1992) were eligible for inclusion in the study. Patients were excluded for the following reasons:

1. Patient refusal, either prospectively or retrospectively
2. Relatives refusal to give assent
3. Children aged <16 years

Approval for the study was obtained from Leicestershire Research Ethics Committee. Eligible patients were approached following the decision to admit them to the Intensive Care Unit (ICU), if their clinical condition confirmed the suspicion of sepsis/SIRS. An investigator then explained the study to them and gave them an information leaflet detailing the reasons behind the study and what it would entail. The patients were then given the opportunity to read this documentation and ask questions. If a patient agreed to take part in the study, written consent was obtained. **Appendix 3.**

Some patients were too ill to give informed consent on ICU admission, but were included in the study if their relatives assented at the time. These patients were approached during their recovery and consent was sought retrospectively. Upon admission to ICU patients' medical records were reviewed by one of the investigators in order to confirm the diagnosis (or otherwise) of severe sepsis/SIRS. Details of height, weight, current medication and past medical history were also recorded along with a range of other clinical laboratory investigations and physiological data. Clinical management was at the discretion of the critical care team, in accordance with the Surviving Sepsis Campaign guidelines (*Dellinger et al 2004*). As part of routine care all patients had an indwelling arterial cannula. Blood (10 mls) was drawn from this cannula for analysis to avoid repeated venepuncture for the purposes of the study. Blood was taken within 24 hours of ICU admission. Following treatment for sepsis/SIRS, usually with fluids and inotropic drugs, further 10 ml samples of blood were taken at subsequent intervals of 24, 48 and 72 hours. A final sample of blood was taken when the patient was considered fit for

discharge to the ward. In total this involved a maximum of 50 ml of blood being taken over a minimum of 4 days.

In parallel with this the patients Sequential Organ Failure Assessment score (SOFA score) was recorded on a daily basis (*Vincent et al 1996*). This scoring system allowed for an objective assessment of the patients clinical condition on a day-to-day basis. The SOFA score is a well-validated measure of organ function, which is in widespread use. Data is collected from six physiological fields, which include the respiratory, haematological, hepatic, cardiovascular, central neurological and renal systems. Each area is given a score of 0-4, where higher scores are indicative of greater organ dysfunction. Therefore at any moment in time a patient may have a SOFA score between 0 and 24. In this study SOFA scores were recorded at the time blood was taken for analysis and it was hoped that a correlation between physiological well being (namely SOFA score), classical opioid receptor gene expression (DOP, KOP and MOP), NOP receptor gene expression, N/OFQ peptide gene expression and plasma N/OFQ concentration could be found. **Table 6.4** shows the six physiological variables measured and the SOFA scores assigned to each.

	0	1	2	3	4
PaO₂ / FiO₂ (kPa)	> 52	≤ 52	≤ 40 ⁺	≤ 26 ⁺⁺	< 13
Platelets (10 ⁹ litre ⁻¹)	>150	150-100	99-50	49-20	<20
Bilirubin (μmol l ⁻¹)	<20	20-32	33-100	101-203	>203 ^{**}
CVS (mmHg or μgkg ⁻¹ min ⁻¹)	MAP>70 SBP> 90	MAP<70 SBP <90	Dop ≤ 5 Dobut (any dose)	Dop > 5 Adr ≤ 0.1 Norad ≤ 0.1	Dop > 15 Adr > 0.1 Norad > 0.1
GCS (Best approximation if sedated)	15	13-14	10-12	6-9	<6
Creatinine (μmol l ⁻¹)	<106	106-168	169-300	301- 433 or urine less 500mld ⁻¹	434 or urine less 200mld ⁻¹ *

Table 6.4. SOFA scores for various physiological parameters. Scores are between 0-4 for each area, with a maximum total score of 24.

Higher scores are indicative of greater physiological dysfunction.

MAP = Mean arterial pressure
P_aO₂ = Arterial partial O₂ pressure
GCS = Glasgow coma score
Dobut = Dobutamine
Norad = Noradrenaline

SBP = Systolic blood pressure
F_iO₂ = Fractional inspired O₂
Dop = Dopamine
Adr = Adrenaline

⁺ Criteria for acute lung injury, ⁺⁺ Criteria for acute respiratory distress syndrome, * Or in the presence of renal replacement therapy, ** Or in the presence of liver dialysis (Molecular Adsorbents Recirculation System) support.

6.4 Plasma and RNA Preparation from blood

Blood was aspirated from the indwelling arterial cannula into a 10 ml Monovette tube (Sarstedt, Leicester, UK) pre-filled with EDTA to stop coagulation. Aprotinin, (Calbiochem, UK) 0.6 TIU ml^{-1} , was then added. Tubes were then mixed thoroughly and immediately placed on ice. Within ten minutes these samples were split into two aliquots of 4ml and 6ml sample volumes. The 4ml sample was used for RNA extraction, while the plasma fraction of the whole blood was isolated from the remaining 6mls.

6.4.1 RNA extraction:

It was intended that RNA would be extracted from the peripheral blood monocytes cell fraction of the blood of the septic patients in a manner similar to that described in the preceding chapters. The 4ml aliquot of blood set aside for this purpose was diluted with PBS and gently layered over Ficoll-Paque as described in **Chapter 2, Figure 2.1**. This mixture was then centrifuged at 1500g for 30 minutes and the PBMC layer removed prior to further clean up with PBS centrifugation. The PBMC cellular pellet was then used for RNA extraction using TRI reagent BD and chloroform as described in **Protocol 2.4**. Following drawing of blood from the first few patients recruited to the study it rapidly became clear that the lymphocyte counts of septic patients were lower than those of healthy volunteers. When the seventy individual blood samples from the twenty-one patients recruited to the study were analysed, it became clear that this trend was maintained throughout this septic population and during the septic episode. There are normally between $1.5\text{-}4.0 \times 10^9/\text{L}$ lymphocytes in the venous blood from a healthy individual (Kumar et al 2002). However in the patients recruited to this study the mean lymphocyte count was $0.85 \times 10^9/\text{L}$ with a standard error of 0.055. Throughout the course of the study the highest lymphocyte count recorded in any patient was $1.9 \times 10^9/\text{L}$ (note that the mean white cell count was $13.76 \pm 1.24 \times 10^9/\text{L}$). This technique was therefore unsuccessful in the blood of septic patients and so it was decided that RNA would be extracted from the whole blood component rather than the PBMC fraction. RNA was therefore extracted from 4ml of whole arterial blood in a similar manner to that described previously for venous blood **Protocol 2.4**. However following addition of TRIBD and 5N acetic acid the “blood” was stored at -70°C until RNA was extracted (mean = 147.9 days

SEM = 9.30). Upon thawing for 30 minutes at room temperature chloroform was added and allowed to stand for 5 minutes and **Protocol 2.4** followed. The RNA extracted was stored at -70°C until reverse transcription. RNA samples were coded to maintain anonymity. Unfortunately this meant that though plasma was isolated from all twenty-one patients within the study, whole blood RNA samples were only acquired from the last eleven patients recruited.

Following storage at -70°C RNA samples were cleaned to remove contaminating traces of genomic DNA prior to reverse transcription **Protocol 2.6**. Due to the possibility of genomic DNA interfering with the kinetics of subsequent QPCR, DNA eradication was thought necessary in these samples despite the use of primer pairs designed to bound exons-exon borders.

RNA samples both purified and not, were analysed via biophotometry. This allowed the mass of RNA extracted and left following purification to be quantified, but also gave a crude indication of RNA quality through the absorbance ratio at 260/280. A further analysis of RNA integrity was also undertaken by running a series of RNA integrity gels as described in **Protocol 2.8**. RNA was then reverse transcribed to cDNA, **Protocol 2.5**. cDNA produced was used as template for further quantitative polymerase chain reactions. **Protocol 2.10** was used for primers requiring SYBR green for fluorescent imaging (housekeeping genes and prepronociceptin), while **Protocol 2.9** was used for the quantification of opioid receptor genes using the *TaqMan*[®] Gene expression system.

6.4.2 Plasma Isolation and radioimmunoassay

The remaining 6mls of blood was centrifuged at 3000g for 10 minutes at 4°C to obtain the plasma fraction. Plasma samples were coded when they were taken to maintain anonymity, and stored at -70°C . Patients acted as their own controls when they had recovered from their episode of sepsis. N/OFQ was assayed in these samples according to the procedure described above (pages 37-38).

6.5 Results:

6.5.1 Patient characteristics

Patient characteristics are shown in **Table 6.5**. Four patients died within 30 days of ICU admission, while five were admitted following major gastrointestinal surgery (two following perforated upper abdominal viscus, two after perforated lower abdominal viscus and one after Ivor-Lewis oesophagostomy). There was no statistically significant differences between survivors and non-survivors of sepsis requiring ICU admission. Importantly there was no difference in the gender or age of these two groups and no significant differences in SOFA or APACHE II (*Knaus et al 1985*) scores at ICU admission or at any time during their ICU stay. There was also no statistical difference in the length of ICU stay.

	All	Survivors	Non-Survivors
n	21	17	4
Age	47 (20-75)	43 (20-75)	64 (40-67)
Gender M:F	12:9	9:8	3:1
APACHE II	18 (7-30)	18 (7-30)	20 (18-26)
ICU stay (days)	7 (1-30)	7 (1-30)	6 (1-10)
Sepsis Source (n)			
Abdominal	5	3	2
Urosepsis	2	1	1
Respiratory	12	10	2
CNS	1	1	0
Unknown	2	2	0
SOFA Score			
Day 1	7 (1-17)	7.5 (1-17)	6 (3-13)
Day 2	5.5 (0-16)	5.5 (0-16)	7 (5-10)
Day 3	5 (0-13)	5 (0-13)	6 (5-8)
Day 4	6 (0-16)	6 (0-16)	7 (6-8)

Table 6.5 Patient characteristics. Age, APACHE II, ICU stay and SOFA scores are quoted as median (range). n = number of patients. There were no significant differences between survivors and non-survivors in terms of age ($p = 0.23$), APACHE II ($p = 0.21$) or length of stay ($p = 0.48$).

6.5.2 RNA expression:

RNA was collected from eleven patients yielding 38 separate samples. These samples contained a mean of 6261ng of RNA (SEM =403) before eradication of genomic DNA. After DNA eradication the mean value of RNA per sample fell to 5333ng (SEM =325). Samples showed an $A_{260/280} = 1.92$ (SEM 0.04) prior to DNA eradication and 1.87 (SEM 0.4) after. DNA eradication therefore gave approximately a 15 percent reduction in RNA. There was also strong correlation between the RNA content before and after RNA cleanup $r^2 = 0.92$ **Figure 6.9**.

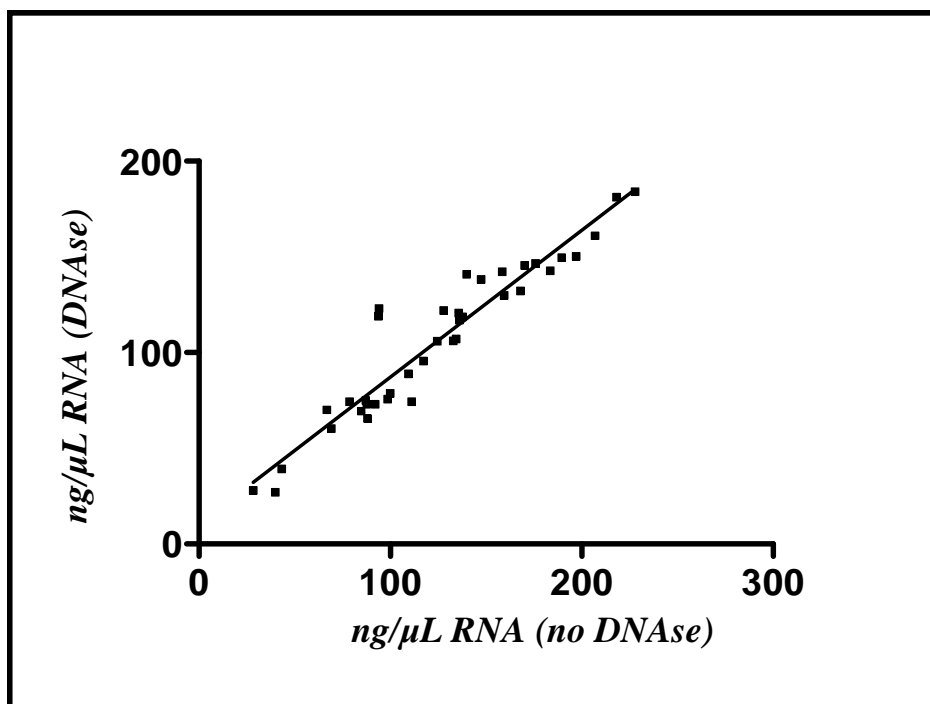


Figure 6.9. RNA before DNA eradication on x-axis, RNA after DNA eradication on y-axis. $r^2 = 0.92$, $p < 0.0001$.

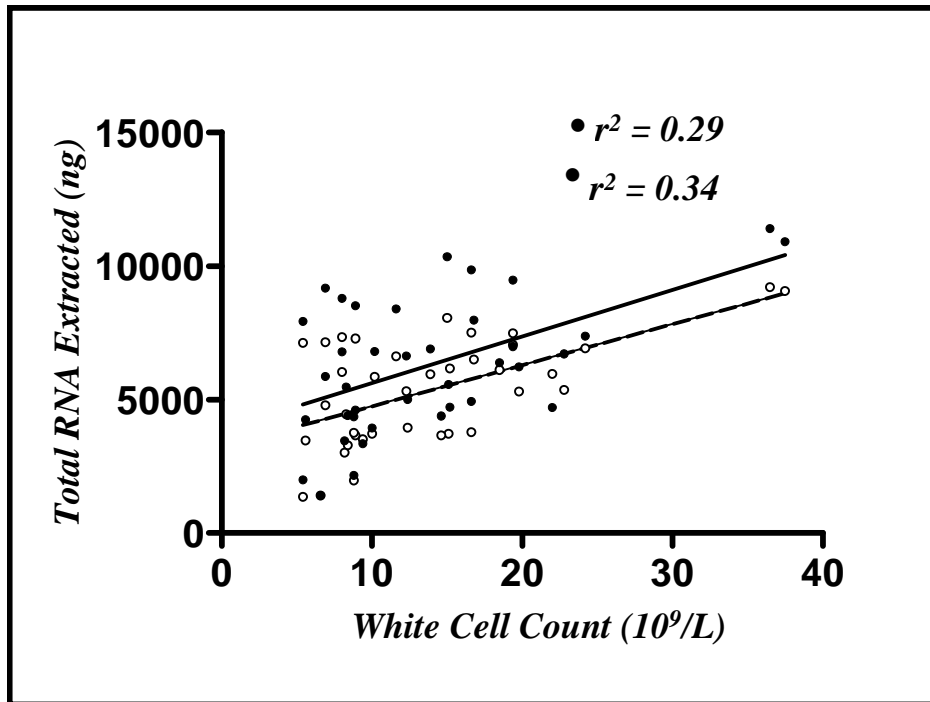


Figure 6.10. Correlation of RNA extracted from white cells and total white cell count, before DNA eradication (•) and after eradication (◊).

There was however some poor correlation between the quantity of RNA extracted from individual samples and the white cell count at the time of sampling. This correlation was more apparent after DNA eradication using the Ambion TurboDNase system ($r^2=0.29$, $p=0.0005$ before DNA eradication and after $r^2=0.34$, $p=0.0001$) **Figure 6.10**.

Despite the high $A_{260/280}$ absorbance ratios for these samples RNA integrity gels showed disappointing results with no clear ribosomal RNA bands. **Figure 6.11**. shows RNA integrity gels of RNA extracted from all 38 samples.

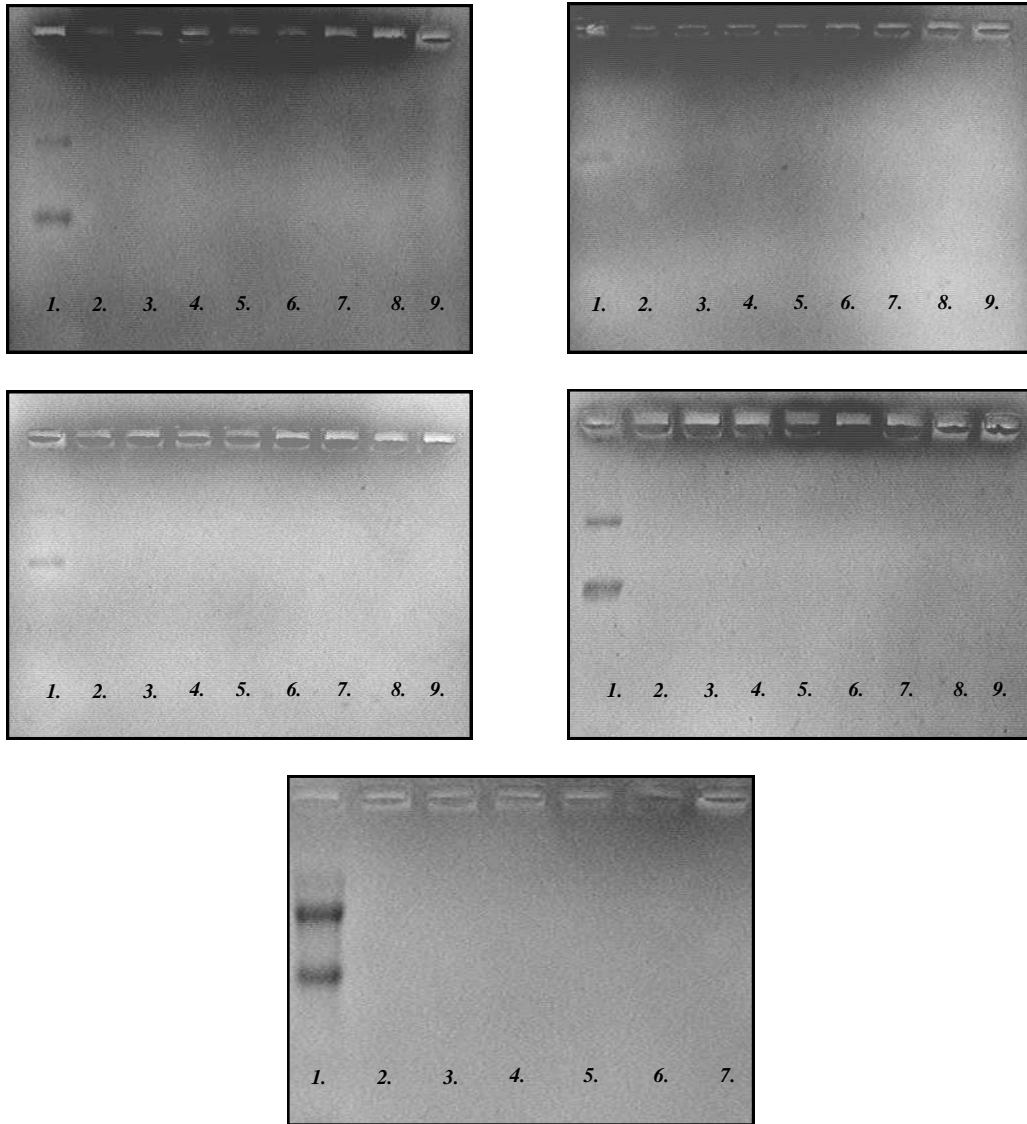


Figure 6.11. RNA integrity bands for septic blood samples. Lane 1 in each panel shows RNA from human atrial tissue (*Ambion*) as a control in all cases. No ribosomal bands were seen for any of the septic blood samples, despite clear control bands in all cases. Gels are RNA denaturing 1.2% formaldehyde agarose gels run at 100V for approximately 45 minutes.

These results contrast with the clear ribosomal bands found when RNA integrity gels are run for the RNA extracted from PBMCs of healthy volunteers **Figure 6.12** (also **Figure 3.48**).

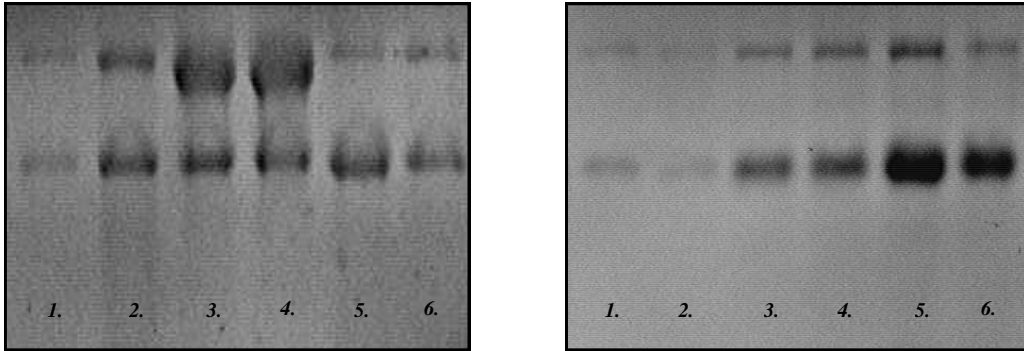


Figure 6.12. RNA integrity gel for the RNA extracted from the PBMCs of 10 healthy volunteers lanes 2-6, lane 1 shows atrial human RNA (*Ambion*) as control in each plate. Data from five individuals are shown in each panel. Gels are RNA denaturing 1.2% formaldehyde agarose gels run at 100V for approximately 45 minutes.

6.5.3 Quantitative PCR:

With the lack of good quality RNA it was understandable that QPCR also showed disappointing results when used to probe for housekeeping genes, opioid receptor genes or prepronociceptin, regardless of whether a SYBR green or *TaqMan*[®] Gene expression system was used. QPCR showed only limited evidence for the presence of cDNA encoding for any of the housekeeping genes. The two most abundant housekeeping genes, B2M and EF1A, had shown distinct bands on gel based PCR when cDNA extracted from whole venous blood of healthy volunteers was employed as a template, and in the case of EF1A fluorescence after only 18 cycles of QPCR, again with cDNA from whole blood. B2M transcripts were present in higher incidence than those for EF1A as judged by gel based PCR and so would be expected to show fluorescence at lower cycles in QPCR. Unfortunately QPCR amplification of the cDNA from septic samples only showed observable fluorescence for these two housekeeping genes at high amplification cycles above 30 **Figures 6.13-14**. The less abundant gene in venous whole blood YWHAZ showed no fluorescence over the entire 40 cycles of QPCR amplification **Figure 6.15**. In all of these experiments cDNA from SHSY5Y cells was chosen as a standard control. These standards displayed fluorescence at low cycle number indicative of the presence of the gene of interest, confirming that the probes and reaction conditions were working well.

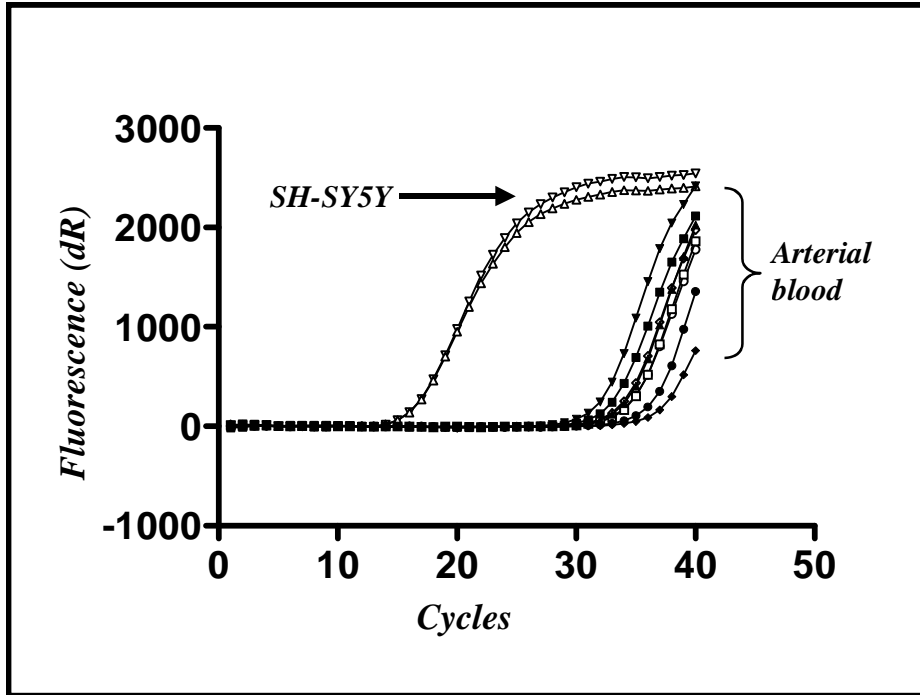


Figure 6.13. Shows increasing fluorescence with increasing cycle for the two control samples (SH-SY5Y cDNA) toward the left with B2M primers, while septic blood cDNA (n=8) shows only late increasing fluorescence with the same primer pairing. Example of 8 of 38 samples.

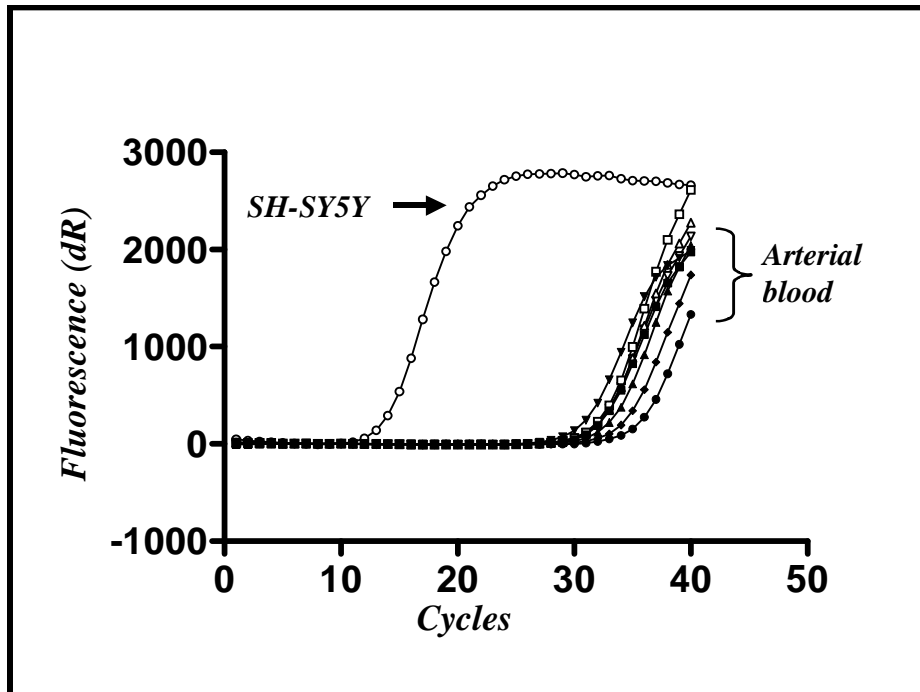


Figure 6.14. Shows increasing fluorescence with increasing cycle for control sample (SH-SY5Y cDNA) toward the left with EF1A primers, while septic blood cDNA (n=8) shows only late increasing fluorescence with the same primer pairing. Example of 8 of 38 samples.

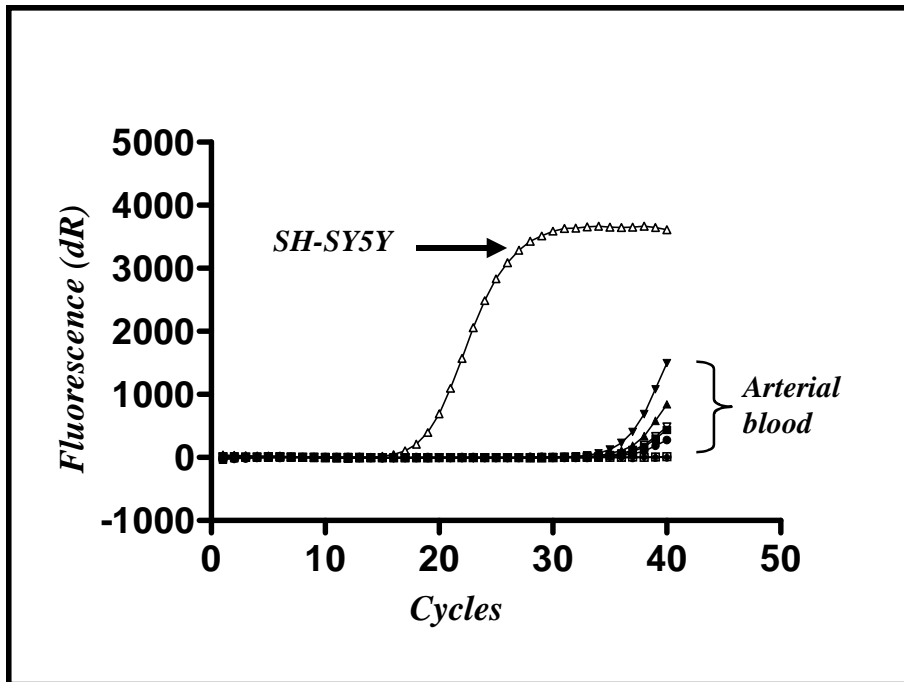


Figure 6.15. Shows increasing fluorescence with increasing cycle for the control sample (SH-SY5Y cDNA) toward the left with YWHAZ primers, while septic blood cDNA (n=8) shows only late increasing fluorescence with the same primer pairing. Example of 8 of 38 samples.

Quantitative PCR using cDNA from septic patients and *TaqMan*[®] probes directed at the opioid receptors also showed no evidence of RNA encoding for these targets, though in all instances there was good amplification of the standard control **Figures 6.16-19**.

The genes for prepronociceptin, HPRT and PPIB are expressed in lower concentration than those for B2M and EF1A therefore it was decided not to run QPCR experiments directed at looking for their presence after the failure to find transcripts encoding for any of the opioid receptors.

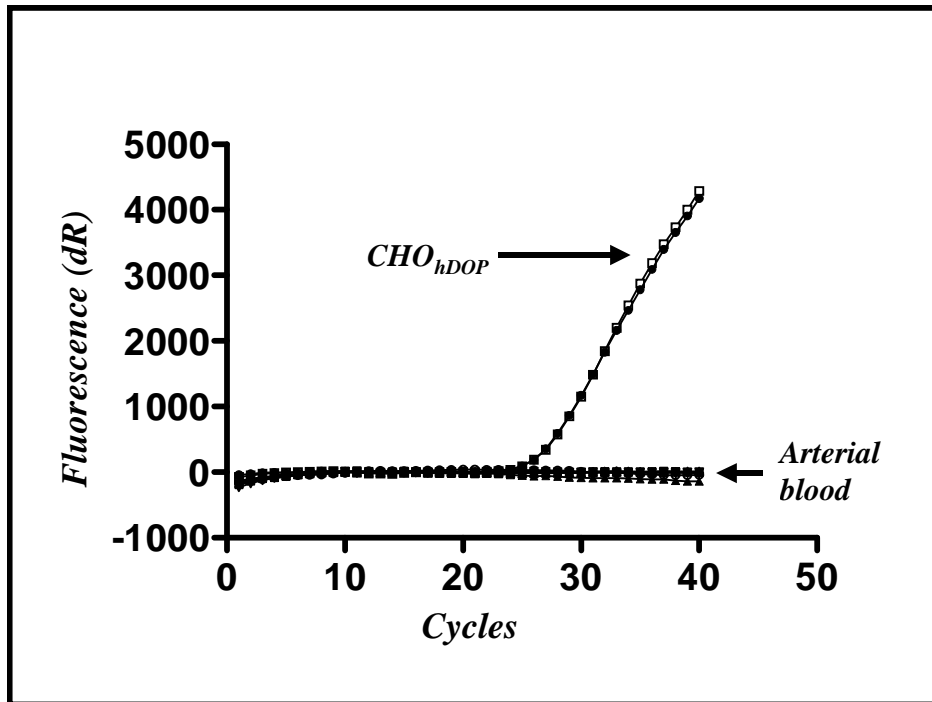


Figure 6.16. Shows increasing fluorescence with increasing cycle for the two control samples (CHO_{hDOP} cDNA) toward the left with *TaqMan*[®] DOP primers, while septic blood cDNA (n=8) shows no increasing fluorescence with the same primer pairing. Example of 8 of 38 samples.

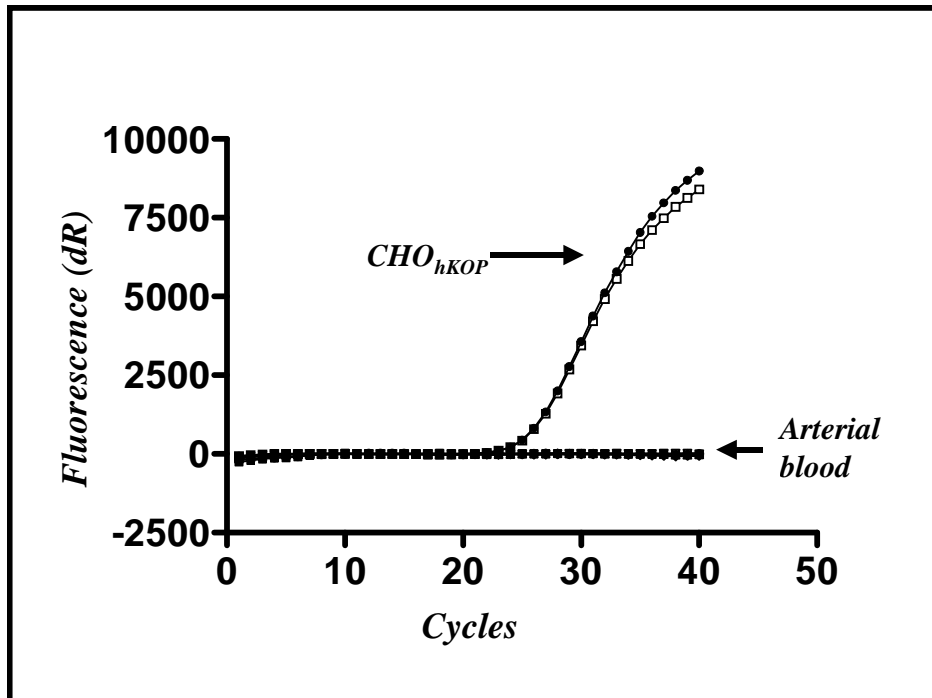


Figure 6.17. Shows increasing fluorescence with increasing cycle for the two control samples (CHO_{hKOP} cDNA) toward the left with *TaqMan*[®] KOP primers, while septic blood cDNA (n=8) shows no increasing fluorescence with the same primer pairing. Example of 8 of 38 samples.

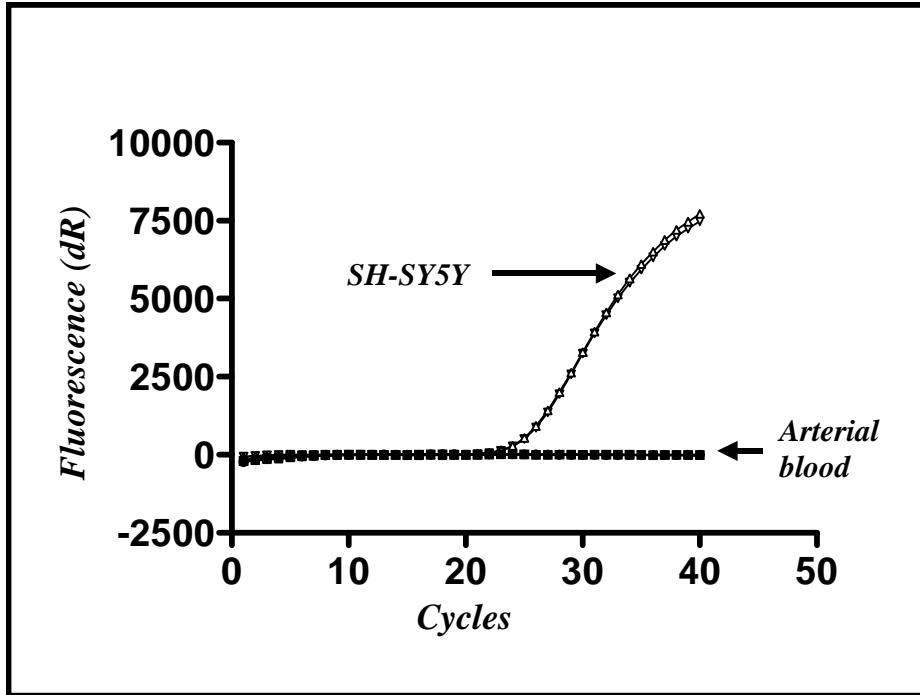


Figure 6.18. Shows increasing fluorescence with increasing cycle for the two control samples (SH-SY5Y cDNA) toward the left with *TaqMan*® MOP primers, while septic blood cDNA (n=8) shows no increasing fluorescence with the same primer pairing. Example of 8 of 38 samples.

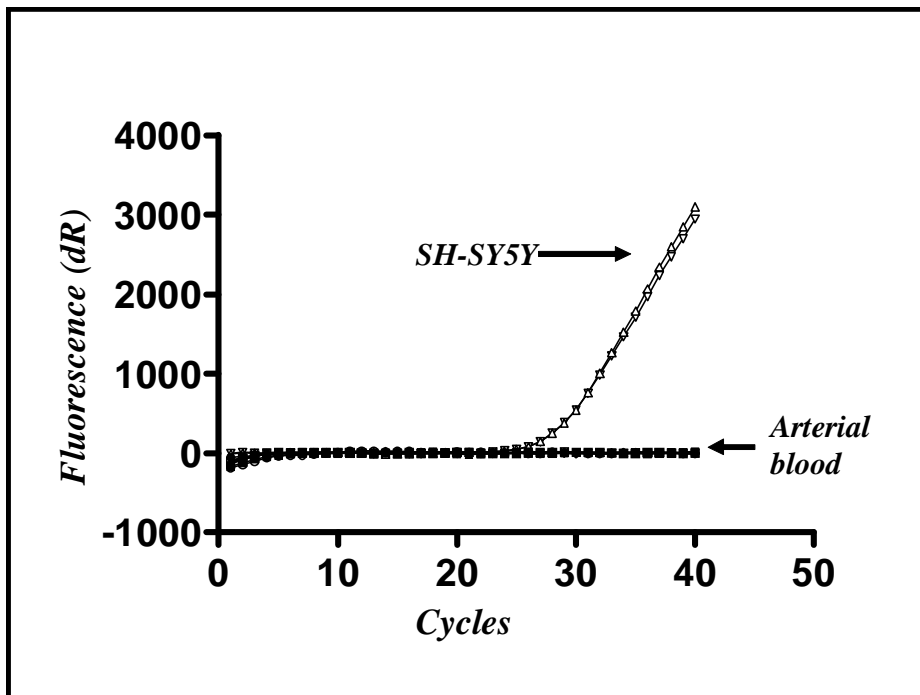


Figure 6.19. Shows increasing fluorescence with increasing cycle for the two control samples (SH-SY5Y cDNA) toward the left with *TaqMan*® NOP primers, while septic blood cDNA (n=8) shows no increasing fluorescence with the same primer pairing. Example of 8 of 38 samples.

6.5.4 Peptide radioimmunoassay:

In total 78 samples were collected from 21 patients during the course of the study. Fewer than 100 samples were collected due to the shortened duration of ICU stay in some patients. This was either due to rapid recovery or death within the four-day period in some patients. We also found collection of the recovery sample problematic in many patients because of early ICU discharge and removal of the arterial sampling line. This rendered acquisition of a recovery sample impossible in all but five patients. Clearly recovery samples were unavailable from the patients who died whilst in ICU.

Patient characteristics showed no statistically significant differences between survivors and non-survivors. There was also no clear association between N/OFQ concentration and illness severity, with no correlation between SOFA score and plasma N/OFQ concentration throughout the five-day period. Moreover there was no correlation between N/OFQ concentration and a range of markers of illness severity **Table 6.6**.

Figure 6.20. shows the standard curve obtained for radioimmunoassay with N/OFQ peptide. Analysis of this curve yielded a $\log IC_{50} = 10.57$.

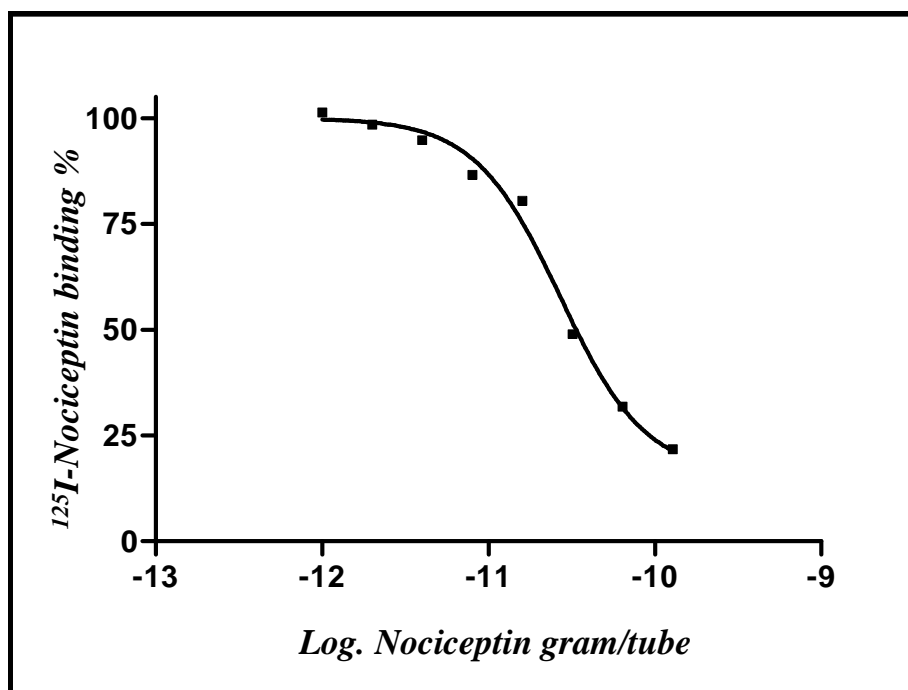


Figure 6.20. Standard curve for radioimmuno assay with N/OFQ peptide.

	<i>n</i>	<i>r</i>	<i>p</i>
Creatinine	21	+0.28	0.204
Bilirubin	20	0.00	0.995
WCC	21	+0.11	0.628
Platelets	21	-0.06	0.802
APACHE II	21	+0.30	0.182
SOFA Total	21	+0.09	0.689
SOFA Respiratory	21	+0.12	0.600
SOFA Cardiac	21	+0.35	0.125
SOFA Renal	21	+0.20	0.390

Table 6.6. Correlations of N/OFQ concentration with various markers of illness severity on day 1. *n* = number of patients, *r* = Spearman correlation coefficient. Note bilirubin accounts for SOFA hepatic, while platelets are incorporated in the SOFA scoring system as a marker of haematological well being.

Though N/OFQ concentrations appeared to be lower in the few recovery samples collected, there was no significant change in N/OFQ concentration and day of ICU admission when analysed using one-way ANOVA ($p=0.60$) **Table 6.7.**

Days	Non-survivors	Survivors
1	3.0 (2.5-5.0)	1.0 (1.0 - 2.5)
2	1.3 (1.0 - 3.3)	1.6 (1.0 - 3.0)
3	1.4 (1.0 - 2.7)	1.0 (1.0 - 3.4)
4	2.8 (1.5 - 3.2)	1.5 (1.0 - 3.0)

Table 6.7 Plasma concentrations of N/OFQ measured serially in critically ill patients with Sepsis/SIRS. Values are reported as median [IQR] pg ml^{-1} . Recovery day sample analysis not shown due to the small number of samples collected.

Whilst showing no statistical difference between survivors and non-survivors SOFA scores upon ICU admission did show a significant variation in trend between day 1 and day 2. All patients who died while in hospital showed an increase in SOFA score despite intensive therapy during the first 48 hours of ICU admission. Only one patient from sixteen who survived showed an increase in SOFA score during this time course. This difference was found to be statistically significant using Mann-Whitney ($p=0.002$).

Plasma N/OFQ concentrations were found to be higher upon ICU admission in patients who subsequently died while in hospital compared with survivors (3.0 [2.5 – 5.0] pg ml⁻¹ in those who died in hospital (n= 4) vs. 1.0 [1.0 – 2.5] pg ml⁻¹ in survivors (p=0.028) when analysed using the Mann-Whitney test, **Table 6.7 & Figure 6.21**. Plasma N/OFQ concentrations were also higher in patients who had undergone major abdominal surgery when compared to those who had not when analysed using a Mann-Whitney test, 2.9 [2.3 – 4.4] vs 1.0 [1.0 – 2.3] pg ml⁻¹ (p = 0.014), **Figure 6.22**. In total four patients died within 30 days of ICU admission. This resulted from multi-organ failure in 3 cases, and a pulmonary embolism in the remaining case. **Table 6.8**.

Patient	Initial diagnosis	Time from ICU admission to death	Mode of death
1	Faecal peritonitis	1 day	MOFS
2	Faecal peritonitis	5 days	MOFS
3	Pneumonia / urosepsis	7 days	MOFS
4	Pneumonia	14 days	PTE

Table 6.8. Patient outcome. Patients died in hospital within 30 days of ICU admission from likely sepsis-related causes. MOFS - multiple organ failure syndrome, PTE - pulmonary thromboembolism.

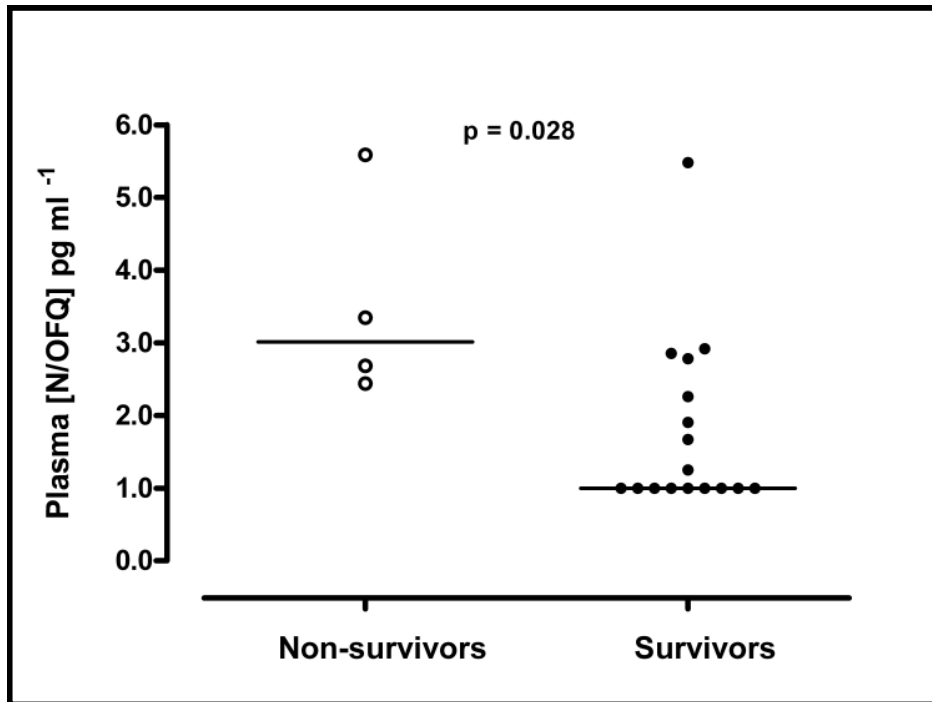


Figure 6.21. Plasma N/OFQ concentrations in critically ill patients with SIRS on admission to ICU n = 21, 4 non-survivors and 17 survivors. Data medians are indicated.

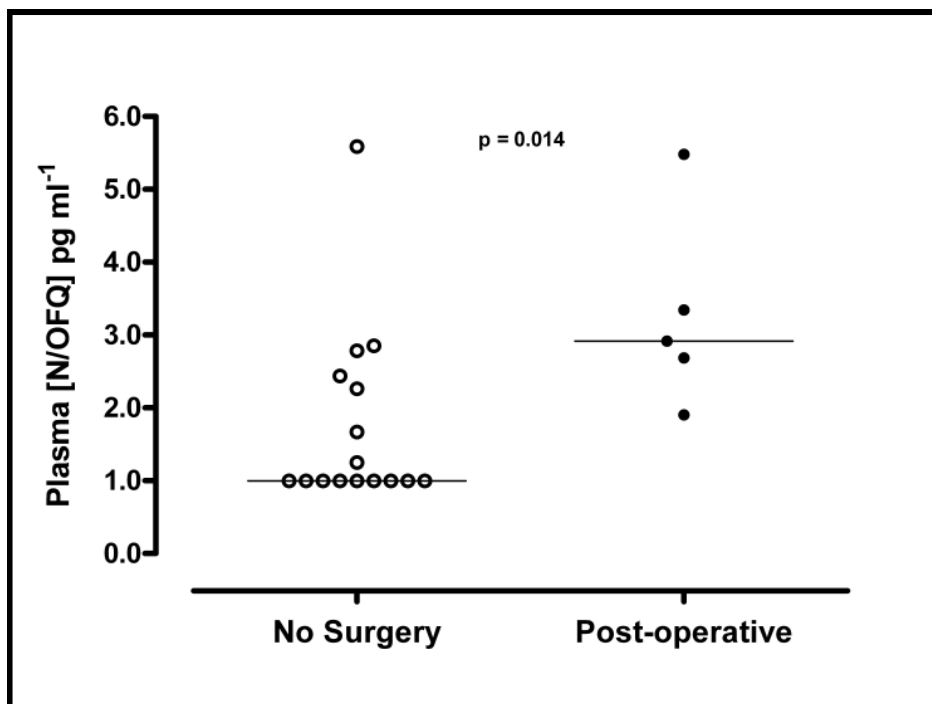


Figure 6.22. Plasma N/OFQ concentrations in major gastrointestinal post-operative patients and non-postoperative patients on ICU admission. n = 21, 5 post-operative and 16 non-postoperative. Data medians are indicated.

6.6 Discussion

The preceding chapters have provided strong evidence to support the view that none of the classical opioid receptors are expressed on peripheral blood mononuclear cells or in whole venous blood in the naïve state. Use of the same experimental paradigms supplies equally persuasive evidence to suggest that the NOP receptor and the precursor to its agonist and physiological antagonist, prepronociceptin, are present in naïve PBMCs and whole venous blood. Despite evidence against the presence of the classical opioid receptors in the naïve state, others have shown upregulation of MOP receptor transcripts in leukocytes after stimulation by mediators of inflammation (*Borner et al 2002, Kraus et al 2001 & 2003*). It was therefore thought that RNA extracted from the PBMCs of whole arterial blood of septic patients may well show transcripts encoding for the classical opioid receptors and changes in the expression of the NOP receptor and prepronociceptin. Sound evidence of opioid receptor expression in sepsis, particularly that of the MOP receptor, could have significant clinical importance, especially when the prevalent use of opioids as sedatives in intensive care is borne in mind.

The previous chapters have however largely looked at the classical opioid receptors and NOP in static un-stimulated immune cells. Investigations have also naturally focused on elucidating whether receptors are or are not present. Sepsis provides a cellular environment that is far more dynamic than encountered in cells cultured within the laboratory, an environment in which changes in RNA expression can be expected to occur. To follow these changes in RNA expression quantitative PCR techniques were chosen. This system required well validated housekeeping genes consistently expressed within such a dynamic setting to ensure the reproducibility and validity of any data obtained. A thorough search of the literature provided six possible candidates to be used as internal housekeeping controls for quantitative PCR analysis, in tandem with the calculation of a normalisation factor as described by Vandesompele (*Boeuf et al 2005, Dheda et al 2004, Nadkarni et al 2002, Pachot et al 2004, Vandesompele et al 2002, Zhang et al 2005*). Of these six housekeepers UBC was discarded due to the production of multiple amplification products following endpoint PCR. The five remaining housekeepers (B2M, EF1A, HPRT, PPIB and YWHAZ) all produced single amplification products at the temperature to be used in further QPCR experiments.

Primer pairs were chosen to give amplicons around 100 base pairs in length and to sit across exon-exon boundaries. Further primer optimisation elucidated the optimal primer concentrations to give minimal threshold cycles. A solitary peak on dissociation curves provided further confirmation of the presence of only one amplification product per primer pair. A similar process of optimisation was undertaken for the prepronociceptin primer pair. Following these investigations all six remaining primer pairs (five housekeepers and prepronociceptin) were judged sufficiently robust for use in QPCR analysis. *TaqMan*® gene expression assays were used to follow changes in expression of the classical opioid receptors (DOP, KOP and MOP) and the NOP receptor. These systems came ready optimized and therefore did not require further adjustment before use.

Subsequent extraction of blood and isolation of cellular fractions yielded markedly reduced amounts of PBMCs when compared to fractionation of blood from healthy individuals. A repeated search of the literature indicated that a lymphopaenia in parallel with a neutrophilia and raised total white cell count is a well documented and consistent response to a septic insult (*Wyllie et al 2004*). Therefore attempts to isolate sufficient quantities of PBMCs for RNA extraction from the first patients recruited to the study failed. It was therefore decided to extract RNA from whole blood rather than from an isolated fraction in the remaining eleven patients recruited. This seemed a reasonable compromise when data from whole venous blood also suggested the expression of the NOP receptor and prepronociceptin. Unfortunately however though biophotometry suggested that reasonable amounts and quality of RNA could be extracted from the whole blood of septic patients, RNA integrity gels showed that this RNA had been degraded at some point during the process of extraction and purification with no ribosomal bands evident on formaldehyde gel analysis. This degradation had occurred to such a degree that no ribosomal bands could be seen for any of the RNA samples from any of the septic patients.

Poor quality RNA extraction similarly affected subsequent QPCR investigations. Though the expression of a range of housekeeping genes was initially investigated in RNA from the blood of healthy volunteers, none of these transcripts were observed in comparable amounts in the septic bloods. EF1A along with B2M one of the most highly expressed

genes in blood in our control experiments, showed a C_t value of 18.6 in healthy venous blood. In the septic bloods however fluorescence was observed at around 32 amplification cycles or above, with a similar quantity of starting template. Similarly the B2M gene, which if anything is more abundant than EF1A in healthy blood, showed no or very little expression in the septic bloods. The remaining genes studied, both housekeepers and genes of interest, showed no expression. These results imply that either the extreme inflammatory conditions seen in sepsis produce a marked reduction in gene expression encompassing a wide range of essential cellular mechanisms, despite a generalised increased proliferation and number of white cells, or alternatively a reduced amount and quality of RNA had been extracted as indicated by formaldehyde gel analysis. The latter of these two suggestions seems the more likely.

Several factors may have contributed to the marked reduction in RNA yield from blood in patients with sepsis. Firstly blood was drawn from an arterial line as opposed to the venous blood collected in the volunteers. The arterial cannula in clinical practice is continually flushed with a crystalloid solution to ensure the patency of the line. Blood drawn directly from it will therefore to an extent be diluted by this solution. However in this study a 2-4 ml “dead space” was always first taken from the arterial line before any blood sample was acquired. This should therefore have ensured that the blood was not diluted and so have no bearing on the results of the study. It also seems unlikely that arterial and venous blood are of such differing cellular composition as to render the arterial blood essentially gene expression free. In addition it is not plausible that gene expression could be so radically altered in less than the time taken to completely circulate around the vascular bed from venous to arterial side (around 60 seconds).

The arterial bloods taken from patients with sepsis also differed from the healthy volunteer venous bloods in that 0.6TIU/mL of aprotinin was added to the samples. Aprotinin is a serine protease inhibitor frequently used in clinical practice as an anti fibrinolytic, in laboratory techniques it is more commonly used as a protease inhibitor so reducing protein degradation. It is not known to interfere with nucleic acids and is therefore unlikely to have lowered white cell RNA concentrations.

Another difference between the arterial and venous blood samples was the disparity in time before addition of TRI reagent to the two samples. Venous blood was commonly

taken within the laboratory into EDTA tubes, immediately placed on ice and TRI reagent BD was added within 5 minutes. The majority of the venous blood was then used for RNA extraction following this and from these samples consistently high quantities and quality of RNA were extracted. Venous blood was also stored at -70°C following addition of TRI BD and later converted to cDNA, again these samples also showed good RNA quantity and quality. Arterial blood was drawn from patients and placed on ice in a similar time frame but with the addition of 3TIU of aprotinin (a process taking 30-60 seconds). However there could be a 20-30 minute delay on ice prior to the addition of TRI reagent. This prolonged wait could possibly have contributed to a lowering of the amount and quality of RNA extracted. After adding TRI BD to the septic samples there was also an additional wait prior to RNA extraction and conversion to DNA. This involved storage at -70°C for 147.9 days (SEM 9.30) and could have resulted in a reduction in RNA quantity and quality. However similar samples of venous blood from healthy volunteers were likewise stored for prolonged periods prior to complete RNA extraction and these bloods consistently showed good RNA quality.

It seems most likely that a combination of the above factors has resulted in a degradation of the RNA extracted from the septic bloods. Some authorities advocate the use of a custom designed system such as the Paxgene blood collection vacutainers, which stabilise RNA immediately upon venesection (or arteriosection) and reduce variations in apparent gene expression caused by storage. This type of system may indeed have improved RNA yields.

Unlike the disappointing and inconclusive RNA data, radioimmunoassay of N/OFQ in the plasma derived from septic blood, did suggest that this peptide was raised in the patient subgroup that did not survive. Analysis showed that N/OFQ concentrations on ICU admission were statistically higher in patients subsequently found to be non-survivors compared to survivors. Admission plasma N/OFQ concentrations were 3.0 ($2.5 - 5.0$) pg ml^{-1} in those patients who died in hospital ($n= 4$) compared to 1.0 ($1.0 - 2.5$) pg ml^{-1} in survivors ($p=0.028$) when analysed using the Mann-Whitney test. This finding of a raised plasma N/OFQ concentration however was not consistently maintained over the time frame of the study, and though there was a trend toward lower N/OFQ concentrations with time from admission to the intensive care unit, this was again not

found to be statistically significant. Unsurprisingly an increase in SOFA score from day 1 to day 2 in the ICU despite maximal medical therapy was also found to be a good predictor of mortality. There was though no clear correlation between N/OFQ concentration and illness severity as judged by SOFA score. Moreover there was no correlation between heart rate, mean arterial pressure, inotropic requirement, SOFA_{cardiac} and N/OFQ. SOFA scores were fairly stable over the four-day ICU period analysed and showed no variation between groups. The lack of variation in SOFA scores may well be an indication of its limitations as a marker of sepsis, cytokine concentrations may act as a more accurate indicator of sepsis severity. There were however significantly higher plasma N/OFQ concentrations in patients immediately following major surgery, compared to those patients who had not undergone surgery; 2.9 [2.3 – 4.4] vs 1.0 [1.0 – 2.3] pg ml⁻¹ (p = 0.014). Numerical data are again presented as medians with interquartile range and analysed using the two-tailed Mann-Whitney test.

Though there is little published in the literature examining the interplay of N/OFQ and sepsis an Italian group has recently described an improvement in survival following administration of the NOP antagonist UFP-101 in the early stages of a small rodent model of sepsis (*personal communication Girolamo Calo*). A wealth of information regarding the cardiovascular effects of N/OFQ and its synthetic analogues has however been accumulated since the isolation of the NOP receptor and its endogenous ligand in the mid 1990's (*Malinowska et al 2002*). Localisation studies and investigations utilising the relatively recently manufactured synthetic antagonists to the NOP receptor have provided the catalyst for much of this work, with the last decade showing a growing understanding of the varied and widespread effects of N/OFQ on the cardiovascular system. While the majority of this knowledge has been derived from small animal and ex vivo tissue experiments, some work has been performed in patient populations (*Granata et al 2003, Malinowska et al 2002, Salis et al 2000*). Several groups have also previously provided laboratory evidence supporting the belief that nociceptin, along with the classical opioid receptors, plays a role in the modulation of immune responses at the cellular level (*Fiset et al 2003, Peluso et al 1998 & 2001, Serhan et al 2001, Waits et al 2004, Zhao 2002*).

The knowledge that plasma N/OFQ concentrations were elevated in septic intensive care patients who subsequently died, and an appreciation of the cardiovascular and immunological effects of N/OFQ raises a number of questions concerning the role of N/OFQ in sepsis. Small rodent models provide evidence to support the view that N/OFQ plays a part in the cardiovascular sequelae of sepsis, increasing vessel permeability and small arteriolar diameter (*Brookes et al 2007*). However in the septic patients studied, whilst N/OFQ concentrations were lower in survivors there was no correlation between a number of cardiovascular parameters and N/OFQ concentration. Nor was there any relationship found between SOFA_{cardiac} and N/OFQ concentration. This would suggest that though N/OFQ exerts a degree of influence over the cardiovascular system its effects are not overriding in sepsis. However it should also be noted that plasma N/OFQ concentration does not necessarily reflect peptide concentration in the local microvascular environment where its effects may be most marked. The finding of raised plasma levels in non-survivors upon admission is still intriguing. It could however be that in this instance N/OFQ is merely acting as a surrogate marker for more marked life threatening inflammatory responses at the microvascular level. What is clear is that whatever the true impact of N/OFQ on the cardiovascular and immune systems, further clinical studies need to be undertaken to fully understand its role.

Chapter 7:

Discussion

7.1 Summary of Main Findings.

The principle findings of this thesis are that MOP, DOP, KOP, and NOP receptor protein cannot be detected on human peripheral blood mononuclear cells. mRNA transcripts encoding NOP can however be demonstrated using polymerase chain reaction techniques. Of the classical opioid receptors, while mRNA transcripts for MOP and DOP are not expressed by peripheral blood mononuclear cells or in venous blood, KOP mRNA transcripts may be present in low abundance in whole venous blood. In addition the endogenous agonist to the NOP receptor, N/OFQ, was found to be elevated in patients admitted to the intensive care unit with SIRS/sepsis who died within 30 days of intensive care unit admission when compared to survivors within this time frame.

7.1.1 MOP Receptor Expression

Radioligand binding experiments with [³H]-Diprenorphine, a non-selective classical opioid ligand, show binding to CHO_{hMOP} cells in a dose dependent manner, but no evidence of binding to naïve PBMCs or a variety of immune cell lines even when a high mass (up to 1mg) of cellular material was used. Similarly fluorescent binding using either direct imaging or flow cytometry with a range of fluorescent labels provides evidence to suggest that CHO_{hMOP}, but not blood borne immune cells, express the MOP receptor. Furthermore endpoint and quantitative real-time PCR investigations suggest that immune cells do not express transcripts for MOP mRNA, while these are readily found for CHO_{hMOP}. This is the first study using a range of complimentary techniques to conclusively show the absence of MOP on PBMCs.

7.1.2 DOP/KOP Receptor Expression

Lack of binding of [³H]-Diprenorphine also implies that either none of the classical opioid receptors (MOP, DOP or KOP) are expressed by the immune cells investigated, or that this protein is in too low an abundance for this technique to be able to confirm its

presence. Staining with fluorescent-naloxone supports this finding. Endpoint and quantitative PCR reinforces the view that peripheral blood mononuclear cells in the naïve state produce neither DOP, nor KOP receptor transcripts. Quantitative PCR at high amplification, with C_t values in excess of 30, does however suggest that a low abundance of KOP transcripts may be present in whole venous blood.

7.1.3 NOP Receptor Expression

Saturation binding experiments and functional assays using [^3H]-N/OFQ and $\text{GTP}\gamma\text{-}[^{35}\text{S}]$ respectively, show no evidence of NOP receptor protein expression in peripheral blood mononuclear cells. There is some indication, from $\text{GTP}\gamma\text{-}[^{35}\text{S}]$ assays, that Raji cells may exhibit NOP receptor protein in low abundance. Endpoint and quantitative PCR support this finding, clearly indicating that NOP mRNA transcripts are present in some immune cell lines, venous blood and peripheral blood mononuclear cells. The mRNA transcript for prepronociceptin, the precursor of N/OFQ and nocistatin, is also expressed in peripheral blood mononuclear cells.

7.1.4 Opioid Signalling and Sepsis

Acquisition of cellular material from the arterial blood of individuals with SIRS/sepsis yielded poor quality RNA from which gene expression for opioid receptors, prepronociceptin and a range of housekeeping genes could not be found. Radioimmunoassay indicated that the admission plasma N/OFQ concentration was raised in individuals who died within thirty days of admission to the intensive care unit and in individuals post major abdominal surgery. No correlation was found between the severities of organ dysfunction, as measured by SOFA scores, and N/OFQ concentration.

7.2 MOP Receptor Expression.

Using an array of experimental techniques this thesis has failed to provide clear evidence to support the hypothesis that peripheral blood mononuclear cells display either the MOP receptor protein or that gene transcripts for MOP are present within these cells. Radioligand binding assays with [³H]-Diprenorphine and fluorescent staining techniques using five different fluorescent probes showed no evidence for MOP receptor protein expression. For two of the fluorescent probes discussed and [³H]-Diprenorphine MOP receptors were however found on the positive control, CHO_{hMOP} cells. End point and quantitative PCR was also unsuccessful in identifying gene transcripts for the MOP receptor, while transcripts were consistently found in positive controls (CHO_{hMOP} and SH-SY5Y). Though gene transcription is frequently, and erroneously, cited as evidence for protein production, its absence in this instance indicates more compellingly that MOP protein is not synthesised by PBMCs. These findings were replicated in whole venous blood.

The belief that PBMCs do not display MOP receptors is however not universally held. Fluorescent staining using either indirect antibody techniques, or labelled opioid antagonists (*Beck et al 2002, Caldrioli et al 1999, Lang et al 1995*) have previously suggested that MOP protein may be present on the surface of PBMCs. A lack of methodological rigour however weakens these claims. Polyclonal antibody based experiments have failed to utilise normal rabbit serum as a negative control, raising the possibility of non-specific binding, while fluorescent-antagonists have been used in elevated concentrations or without adequate controls, leading again to the possibility of a high degree of non-specific binding.

Similarly investigators have reported that MOP gene transcripts can be isolated in primate and human PBMCs and other immune cell lines (*Chuang et al 1995b, Kraus et al 2001 & 2003, Stefano et al 1998*). The use of primer pairs placed within one exon, with or without gDNA eradication, casts doubt over much of this research, raising the suspicion of gDNA amplification rather than the identification of genuine gene transcripts. Novel MOP receptors with genomic sequences at variance with that of the classical neural MOP receptor have also been quoted as evidence for peripheral MOP expression on immune cells. This type of receptor has not as yet been sequenced. Perhaps

more compelling is the theory that MOP expression is up regulated following exposure of immune cells to a variety of cytokines. *Kraus's* group however needed multiple amplification cycles with QPCR to find any MOP gene transcripts, with their results supporting the hypothesis that in the naive unstimulated state PBMCs and other blood borne immune cells do not express gene transcripts for MOP.

Despite a lack of persuasive data supporting the supposition that MOP receptors are expressed by PBMCs and other immune cells, there is strong clinical and laboratory evidence to indicate that MOP agonists exert effects on immune cell function, which in a clinical setting may be detrimental (*Caldrioli et al 1999, Eisenstein et al 2006, McCarthy et al 2001b, Mellon et al 1999, Philippe et al 2003, Roy et al 1998 & 2001, Sacerdote et al 2001, Yaegar et al 1995*).

A wealth of research suggests that when administered *in vitro* to cell lines opioids produce effects upon immune cell function. These effects encompass a range of cellular functions including, reductions in natural killer cell activity, inhibition of macrophage and neutrophil phagocytic function, inhibition of neutrophil and monocyte chemotaxis to complement derived factors, inhibition in antibody production, direction of T cells toward Th₂ differentiation, changes in cytokine production and changes in haematopoietic cell development (*McCarthy et al 2001a, Mellon et al 1999, Roy et al 2001, Sacerdote et al 2001, Wetzel et al 2000*). Findings between studies are however often conflicting. Conclusions are often difficult to draw, and are complicated by the fact that immune cell function *in vivo* requires an interplay and communication between different classes of immune cell not seen in the singular immortal cell lines normally used in *in vitro* investigations. Changes in immune function in the presence of opioids may not however necessarily require opioid receptors to be present on immune cells.

Clinical studies and observations in patients and volunteers also indicate that opioids have harmful effects upon immune function. Retrospective studies indicate that *i.v.* drug users have a higher incidence of opportunistic infections and HIV, with a more rapid progression to AIDS than non-users (*Cabral 2006, Friedman et al 2003, Spittal et al 2003*). A direct correlation between opioid abuse and depressed immune function is however difficult to draw. When considering populations of *i.v.* drug users, direct inoculation by pathogens from dirty needles and poor nutritional standards may also

depress immune function. Animal models have also shown opioid induced depression of immune function (*Cabral 2006, Friedman et al 2003*).

Taken together *in vivo* and clinical studies provide persuasive evidence to support the view that opioid agonists can exert an effect upon the immune system. This effect may however be a direct one upon the function of immune cells and cell systems or more probably an effect on the central neuroimmune axis, possibly via classical opioid receptors and the hypothalamic–pituitary–adrenal axis, with immunomodulatory consequences (*Mellon et al 1998 & 1999*). High dose *in vitro* and *in vivo* studies have been shown to cause a centrally orchestrated opioid mediated release of corticosteroids accompanied by activation of the sympathetic nervous system, resulting in thymic hypoplasia and a peripheral lymphopaenia, **Figure 7.1**.

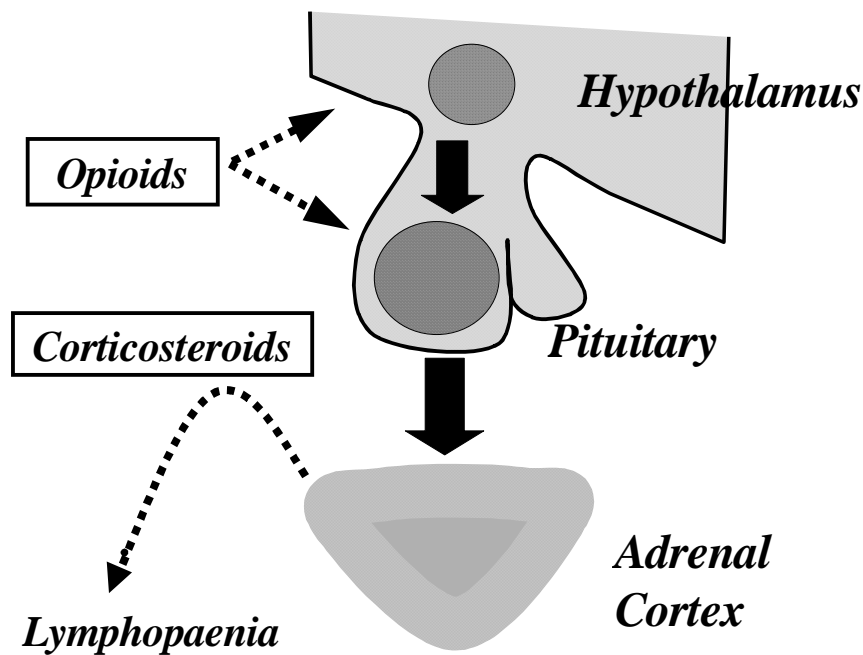


Figure 7.1

Opioid action on the HPA results in an increase in corticosteroid release from the adrenal cortex and lymphopaenia. Opioids also activate the sympathetic nervous system to induce immunosuppression.

The hypothalamic-pituitary-adrenal physiological axis could help explain opioid immuno-suppression in human and whole animal studies. It does not however fully explain the changes seen in immune cells cultured *in vitro* in the presence of opioids.

However, the finding that peripheral blood mononuclear cells do not display classical opioid receptors suggests this functional effect of opioids is unlikely to be via an interaction with classical receptors on PBMCs within the periphery.

A number of different theories could explain how opioids influence cellular function in the absence of MOP receptors. Most simply, it is possible that opioid agonists may act at PBMCs via a non-classical receptor. *Cadet et al.* have postulated a MOP₃ receptor capable of interaction with classical MOP agonists but displaying a different DNA and protein sequence. (*Cadet et al 2001, 2002 & 2003*). If this receptor type exists it would probably be amplified with the classical MOP primers.

As discussed above a second possibility is the expression of MOP receptors only after exposure of immune cells to a variety of cytokines and pro-inflammatory compounds. *Kraus et al.* have shown that MOP receptor expression on a range of immune cells including PBMCs is only seen after administration of tumour necrosis factor- α (TNF- α), or after the administration of the Th₂ specific cytokine, interleukin-4 (IL-4) or interleukin-2 (IL-2) (*Kraus et al 2001 & 2003, Madden et al 2001*). However RNA transcripts were found in very low number in both cases, requiring multiple PCR amplification cycles employing a nested PCR technique, in order to show evidence of PCR product. In this thesis expression of the MOP receptor was not observed following culture of a B-cell line with TNF- α and cycloheximide. Despite these limitations this general theory raises the fascinating prospect of a system in which immune cells are capable of delivering endogenous opioids to sites of inflammation, where newly synthesised MOP receptors have been trafficked along peripheral nerves (*Stein et al 2003*), while local inflammation elicits up-regulation of MOP receptors in activated immune cells, **Figure 7.2**.

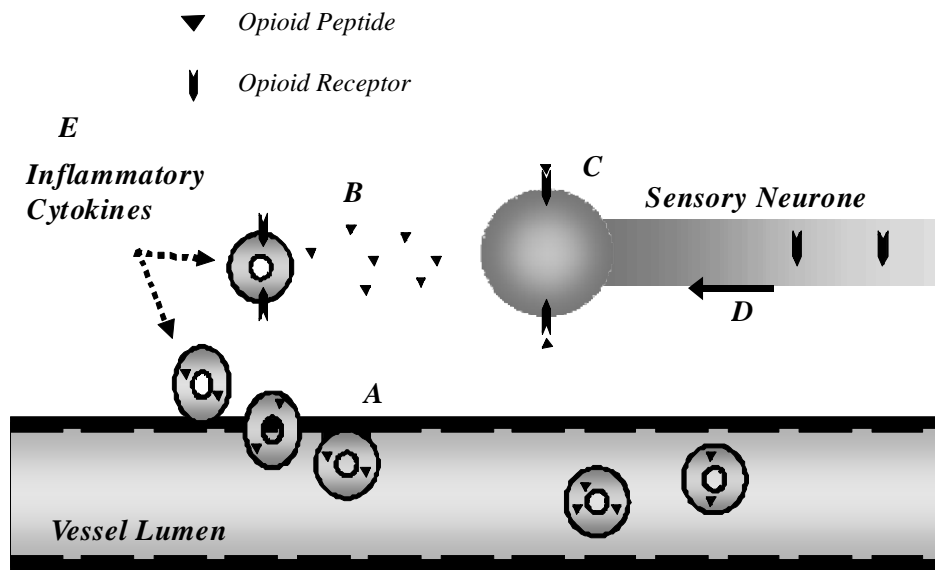


Figure 7.2

Mechanism of the peripheral action of endogenous opioids on peripheral receptors.

- A.** Adhesion molecules on both vascular endothelium and immune cells are up regulated, allowing passage of immune cells through the endothelium into the surrounding inflamed tissue. Immunocytes contain endogenous opioid peptides.
- B.** In response to sympathetic stimulation immune cells release endogenous opioid peptides into the inflamed tissue.
- C.** The released opioid peptides then bind to opioid receptors on peripheral sensory neurones.
- D.** Opioid receptors newly synthesised in the dorsal root ganglia in response to inflammation are trafficked to the periphery where they are presented at the neuronal membrane.
- E.** Inflammatory cytokines cause an upregulation of MOP receptors in immune cells attracted to the site of inflammation.

A less convoluted explanation of immune cell modulation by opioids may come from a direct and/or indirect antigenic activation of the peripheral immune system. T-lymphocytes usually only recognize processed proteins in the form of peptides presented to them by antigen presenting cells (APCs). For an immune reaction to occur APCs need to take up and process large antigens and present them to T-cells. Opioids used in common clinical practice therefore are unlikely to initiate this type of immune response. Antibodies however can recognize a range of compounds and almost any biological molecule (peptides, proteins, nucleic acids, polysaccharides, lipids and small chemicals) (Abbas & Lichtmann 2003). However small soluble molecules do not usually initiate humoral B-cell responses. This process may be circumvented by haptens, small

compounds, which may bind to a protein or peptide, altering the structure of the protein or peptide as it does so, and becoming an antigenic-conjugate capable of APC presentation to T-cells. This in turn can therefore lead to initiation of an immune response. Drug reactions (penicillin and halothane drug sensitivity reactions) have traditionally been ascribed in the past to this type of hapten reaction model, **Figure 7.3**. Hapten-protein complexes and haptens themselves in some instances may also directly interact with previously generated antibodies. It has also been suggested that drugs may form non-covalent bonds between APC and T-cell receptors on T-cells to initiate hypersensitivity reactions, which do not require initial antigen processing by an APC (Gerber *et al* 2006).

Clinically it is a quite common experience to observe a self-limiting immediate hypersensitivity reaction to *i.v.* administered opioids. Immunoglobulin-E binding to drug antigens causing mast cell degranulation is normally quoted as the cause for this reaction. IgE has been found in the serum of individuals who have experienced anaphylactic and allergic reactions following morphine administration. The reaction is mediated by histamine and other vasoactive compounds, and is not reversed or blocked by prior administration of an opioid receptor antagonist, such as naloxone (Blunk *et al* 2004, Sheen *et al* 2007).

It seems most likely that in the absence of MOP opioid receptors, MOP agonists may modulate immune function via a combination of effects upon the hypothalamic-pituitary-adrenal axis and via direct effects upon naïve peripheral immune cells as documented above. In conjunction with these pathways evidence from a number of researchers suggests that an inflammatory environment may provide the correct conditions for upregulated MOP expression on immune cells, and so for autoregulation of endogenous opioid delivery to peripheral nociceptive afferents.

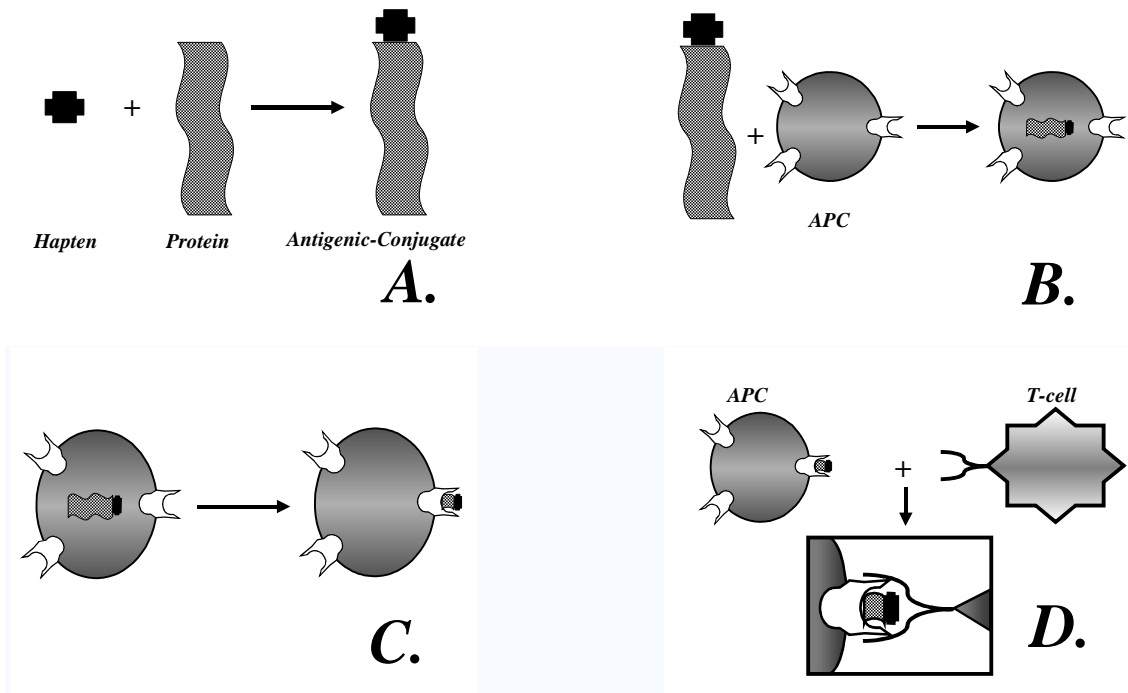


Figure 7.3

Mechanism of hapten initiation of an immune response.

A. Chemically reactive hapten binds to protein forming antigenic-conjugate

B. Conjugate is taken up by antigen presenting cell (APC)

C. Antigenic-conjugate is processed by APC and presented via major histocompatibility complex.

D. Presentation of antigen to T-cell and activation of immune response.

7.3 DOP/KOP Receptor Expression.

[³H]-Diprenorphine and naloxone are non-selective classical opioid antagonists, therefore the inability to find MOP receptor protein on the surface of PBMCs using these two techniques also indicates a lack of expression of DOP and KOP receptor protein on these cells.

Endpoint and quantitative PCR techniques using a number of primer pairs located on different exons encoding for the DOP gene gave no indication that DOP transcripts were expressed in the PBMCs of healthy male volunteers, a B-lymphocytic cell line or whole venous blood. Similarly no gene transcripts for the KOP receptor were found with PCR techniques with cDNA extracted from PBMCs and from a B-lymphocytic cell line. At high amplification cycles (in excess of 30 cycles) using quantitative PCR and *TaqMan*[®] Gene expression probes, there was a suggestion that KOP transcripts may be present in whole venous blood.

As with MOP receptors the belief that DOP and KOP are not expressed by PBMCs is not universally held. However others have previously used a combination of high concentrations of fluorescent probes and inadequate negative controls in fluorescent staining experiments, reducing the credibility of some of these conclusions. Moreover, PCR investigations have frequently used primer pairs confined to one exon raising the possibility of genomic contamination. *Gavériaux et al* present the clearest evidence for the expression of gene transcripts for KOP receptors in immune cells using robustly designed primer pairs placed on different exons of the genetic code (*Gavériaux et al 1995*). Interestingly however even with these well-designed primers, amplicons for KOP were only found in one out of three peripheral blood mononuclear cell samples harvested from volunteers, while three different Epstein-Barr virus transformed B-cell lines showed variable levels of expression of KOP. No other immune cell line investigated showed KOP gene transcripts. Another group show a decreasing level of KOP receptor protein expression during maturation of mouse lymphocytes using the less sensitive technique of immunofluorescent staining (*Ignatowski et al 1998 & 1999*).

There is clearly some evidence suggesting that selected immune cells may contain gene transcripts for KOP. A more thorough exploration of the association of KOP expression in a range of immortal *in vitro* immune cell lines could easily be undertaken and would

provide an additional insight into the prevalence and distribution of this classical opioid receptor. However more informative results would be obtained by gaining an understanding into the prevalence of KOP expression in *in vivo* human immune cells. An approximation to this could be arrived at by studying *ex vivo* immune cells separated into their respective classifications using fluorescence activated cell sorting (FACS) or magnetic activated cell sorting (MACS). Cluster differentiation marking using a variety of different fluorescent labels could be used to aid identification of distinct classes of cell. Once sorted RNA could be extracted from the cells as described previously and transcripts for KOP probed. There are a number of clear disadvantages with this technique however. Firstly a process of FACS or MACS would lengthen the period between venesection and RNA extraction, therefore increasing the likelihood of RNA degradation and derangement of its regulation. Secondly it would be difficult to observe *ex vivo* immune cells in an environment designed to mimic an inflammatory milieu unless cells were subsequently cultured. Though culture of *ex vivo* tissue is possible it would add additional complications to any study. Finally any investigation into individual classes of immune cell, whether *ex vivo* or immortal cell lines, ignores the fundamental requirement of the immune system to communicate across cell types to mount adequate responses.

7.4 NOP Receptor Expression.

While radioligand binding using [³H]-N/OFQ showed no evidence of NOP receptor protein expression on the surface of PBMCs or a B-cell line, a more sensitive downstream functional binding technique using GTPγ-[³⁵S] gave equivocal results. Using the GTPγ-[³⁵S] functional binding assay it could not be demonstrated that PBMCs express NOP protein, while results for a larger starting mass of Raji cells were less clear-cut. In some of the experiments performed no evidence of functional NOP protein was found; in the remaining studies data was suggestive of very low NOP expression. This laboratory has previously used GTPγ-[³⁵S] assays to report densities of NOP protein to around 25 fmol.mg⁻¹ in inducible cell systems and dog brain extracts (*Johnson et al 2004, McDonald et al 2003*). It therefore seems likely that Raji cells express NOP, but at a density lower than 25 fmol.mg⁻¹.

Both endpoint and quantitative PCR reliably identified gene transcripts for NOP in PBMCs, a B-cell line and whole venous blood. Gene transcripts for the endogenous precursor of N/OFQ and nocistatin, prepronociceptin, were found in PBMCs and a B-cell line, though no positive control was available. The findings of low expression of NOP receptors on a B-cell line and gene transcripts in B cells, PBMCs and venous blood broadly agree with the findings of other research teams, with one group finding a receptor density of less than 20 fmol.mg⁻¹ on a range of immortalised cell lines (*Arjomand et al 2002, Peluso et al 1998, Waits et al 2004*). Similarly others have indicated that not only are gene transcripts for prepronociceptin present in immune cells, but also that N/OFQ is secreted by neutrophils following degranulation (*Fiset et al 2003, Pampusch et al 1998*). Several groups have also previously provided laboratory evidence supporting the belief that NOP plays a role in the modulation of immune responses at the cellular level. *In vitro* experiments with T-lymphocytes stimulated by the presence of Staphylococcal enterotoxin B, show an up regulation of the cluster differentiation markers involved in T-cell activation following the addition of N/OFQ (10⁻¹²-10⁻¹⁴ M) (*Waits et al 2004*). It is believed that these effects are, at least in part, modulated via changes in prostaglandin synthesis within the cell in response to the administration of N/OFQ. Further *in vitro* studies have also indicated that N/OFQ can act as a potent chemotactic agent on monocytes, with less impressive results on neutrophils, where it may promote lysosomal

release (*Trombella et al 2005*). These effects can be mimicked by the addition of synthetic NOP receptor agonists and reversed by the addition of UFP-101, a synthetic NOP receptor antagonist. Additional studies have also found that N/OFQ is released by neutrophils in a time dependent manner in response to the inflammatory mediators fMLP and cytochalasin B (*Fiset et al 2003*). In addition our own studies have indicated that both the NOP receptor and N/OFQ are present in peripheral blood mononuclear cells. As a collection these studies provide strong evidence that N/OFQ can elicit functional changes in immunity at the cellular level, and that not only may immunocompetent cells respond to N/OFQ at a local level, but neutrophils in particular may well also have the mechanistic ability to synthesize N/OFQ. Thus, in a manner similar to the classical opioid systems, leucocytes may be involved in delivering N/OFQ to nervous tissues at sites of inflammation, experiencing paracrine immunomodulation and forming a 'nociceptin neuroimmune axis'. However with a NOP-N/OFQ system the machinery to manufacture N/OFQ peptide and a NOP receptor are already in place in naïve immune cells. Hence a feed back loop monitoring N/OFQ peptide concentration is available, requiring no further expression or up regulation of the system to become functional in the face of a septic insult, as may possibly be the case with the classical opioid receptors.

7.5 Opioid Signalling and Sepsis.

Both RNA integrity gels and quantitative PCR suggested that no, or extremely small amounts of RNA were isolated from the blood of individuals admitted to the intensive care unit with SIRS/sepsis. This poor yield contrasts with the consistently good quantities and quality of RNA extracted from cell lines, venous blood PBMCs and from whole venous blood of healthy volunteers. This difference in yield is probably due to a number of factors; length of time between vene/arteriosection and stabilisation, storage of blood samples, the septic insult, addition of aprotonin and analysis of arterial blood. The lack of consistent quality RNA samples in good amounts meant that variations in gene expression for opioid receptors, prepronociceptin and a range of housekeeping genes could not be investigated.

Radioimmunoassays did however show significant increases in plasma N/OFQ concentrations on the day of admission to the intensive care unit in individuals who subsequently died within thirty days. These increases were however not maintained throughout the intensive care stay. Additionally plasma N/OFQ was raised in patients who had undergone major abdominal surgery when compared with non-operative controls.

As discussed above there is a growing body of evidence implicating NOP and N/OFQ in the modulation of immune cell function, similarly several groups have in laboratory investigations shown an effect of the NOP/N/OFQ system on cardiovascular function. To date much of the basic research into the cardiovascular actions of N/OFQ has focused on its central effects. Repeatedly it has been shown that the NOP receptor and its transcripts can be found throughout the central nervous system (*Malinkowska et al 2002*). The receptor is particularly abundant in the hypothalamus and pons, two regions of the brain intimately involved with the autonomic control of cardiovascular responses. Injection of N/OFQ into the rostral ventrolateral medulla produces a parasympathetic response in the cardiovascular system, with a profound drop in heart rate and mean arterial blood pressure. These effects can be reversed by the administration of an N/OFQ antagonist (*Chu et al 1999*). Similar effects were seen following injection of N/OFQ into the nucleus tractus solitarius of rats and could be attenuated by bilateral vagotomy, reinforcing the

belief that the central cardiovascular properties of N/OFQ are parasympathetically mediated (*Shah et al 2003*).

Some investigations have also pointed to a peripheral action of N/OFQ upon the cardiovascular system. N/OFQ is a highly charged heptadecapeptide, which is therefore incapable of crossing the blood brain barrier, however intravenous injection of N/OFQ like central administration will produce a range of cardiovascular effects. *Champion* previously described a decrease in heart rate, mean arterial pressure, cardiac output and peripheral resistance following the administration of N/OFQ intrajugularly (*Champion et al 1997 & 1998*). In collaboration with the University of Sheffield we have independently shown that intravascular administration of N/OFQ to rats produces significant falls in mean arterial pressure and increases in arteriolar diameter (*unpublished data*). These studies provide an indication that in addition to its central effects, N/OFQ may also modulate cardiovascular responses in the periphery.

In conjunction with the laboratory evidence that NOP/N/OFQ affects immune and cardiovascular functions it is tempting to conclude that elevated N/OFQ concentrations may lead to a worsening of clinical outcome in patients suffering from SIRS/sepsis. *Petronilho et al* have shown that the NOP antagonist UFP-101 may ameliorate the inflammatory process as a result of a septic episode in rodents following caecal ligation (*personal communication*). The extension of this is that N/OFQ may have potential as a biochemical marker and predictor of survival in a septic patient population. N/OFQ did not however remain elevated beyond the day of admission in non-survivors or in the post surgical group. N/OFQ concentration also showed no correlation with SOFA_{cardiac}. It is possible that N/OFQ levels may be elevated in SIRS for a number of reasons and subsequent studies may show no significant correlation with outcome. However without further investigations in this challenging field no robust conclusions as to the exact influence N/OFQ has over sepsis can be drawn.

7.6 Concluding Statement.

This thesis has made a significant contribution to the understanding of opioids and the neuro-vascular-immune axis:

- A number of different experimental paradigms have shown that naïve human peripheral blood mononuclear cells do not express the classical opioid receptors
- Polymerase chain techniques have supported the view that naïve peripheral blood mononuclear cells express gene transcripts for the novel opioid receptor NOP and prepronociceptin (the precursor of its endogenous ligand), while functional assays have suggested that the NOP receptor itself may be expressed by B-cell lymphocytes, though in low abundance
- This thesis has reported for the first time an elevation in plasma N/OFQ in non-survivors of a septic insult requiring intensive care unit admission
- Similarly this thesis is the first to report an elevation in plasma N/OFQ concentrations following major abdominal surgery in septic patients
- We would like to suggest an amendment to the neuroimmune axis proposed by Stein and others to include the N/OFQ-NOP system.

Though our understanding of the role of opioids and immune cell function is growing, much of this knowledge stems from investigative work completed in a laboratory setting in cell cultures and small animal models. The next challenging phase is the translation of this evidence and theory into a clinical environment.

Appendix I: Protein Assay.

Modification of protein assay, after Lowry (*Lowry et al., 1951*)

Standards (0, 50, 100, 150, 200, and 250 $\mu\text{g}\cdot\text{ml}^{-1}$ BSA in 0.1 M NaOH) were used with samples simultaneously.

Samples were diluted as appropriate (1/5, 1/10, 1/20) in NaOH.

To 0.5ml standard or diluted sample, 2.5ml reducing solution was added, the whole mixed and incubated (10 min, room temperature).

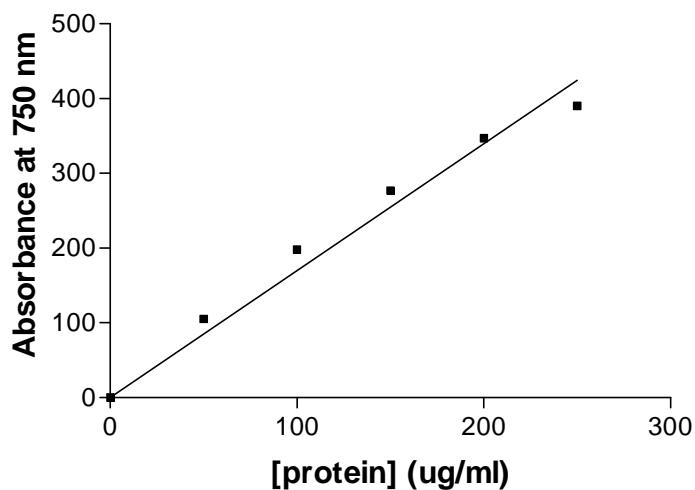
250 μl Folin and Ciocalteu's phenol reagent was added, the whole mixed and incubated (30 min, room temperature).

Absorbance was read in a spectrophotometer at 750nm and the results analysed using linear regression to produce standard curve with fixed origin. Valid results for each sample were averaged and used to analyse the binding results.

A typical standard curve for this assay is shown below.

Reducing solution comprised 100:1:1 solutions A:B:C (A – 2% Na_2CO_3 in 0.1M NaOH; B – 1% CuSO_4 in H_2O ; C – 2% Na/K tartrate in H_2O).

Folin and Ciocalteu's phenol reagent (stock diluted 1:3 in H_2O).



Typical standard curve for protein assay

Appendix II: Ethics Committee Approval 7218

University Hospitals of Leicester



DIRECTORATE OF RESEARCH AND DEVELOPMENT

Director: Professor D Rowbotham
Business Manager: Dr N J Seare
Service Manager: Mr M Roberts

NHS Trust

Leicester General Hospital

Co-ordinator: N Patel
Direct Dial: 0116 258 8246
Fax No: 0116 258 4226
email: natu.patel@uhl-tr.nhs.uk

Gwendolen Road
Leicester
LE5 4PW

Tel: 0116 249 0490
Fax: 0116 258 4666
Minicom: 0116 258 8188

24 February 2004

Dr John Williams
Senior Registrar/ Hon Lecturer
University Dept of Anaesthesia Critical Care and Pain Management,
LRI

Dear Dr Williams

**RE: UHL Ref. 9270 [Please quote this number in all correspondence]
Investigation into the presence of opioid receptors on human immune cells before and
after treatment in vitro with a variety of mediators of inflammation. Ethics Ref. 7218**

We have now been notified by the Ethics Committee that this project has been given a favourable opinion by the Ethics Committee (please see the attached letter from the Ethics Committee).

Since all other aspects of your UHL R+D notification are complete, I now have pleasure in confirming full approval of the project on behalf of University Hospitals of Leicester NHS Trust, Leicester Royal Infirmary Site.

This approval means that you are fully authorised to proceed with the project, using all the resources which you have declared in your notification form.

The project is also now covered by Trust Indemnity, except for those aspects already covered by external indemnity (e.g. ABPI in the case of most drug studies).

We will be requesting annual and final reports on the progress of this project, both on behalf of the Trust and on behalf of the Ethical Committee.

In the meantime, in order to keep our records up to date, could you please notify the Research Office if there are any significant changes to the start or end dates, protocol, funding or costs of the project.

I look forward to the opportunity of reading the published results of your study in due course.

Yours sincerely

Mr Michael Roberts
Service Manager for Research and Development



UHL 9270, Ethics ref: 7218

Leicestershire Local Research Ethics Committees

Lakeside House
4 Smith Way
Grove Park
Enderby
Leicester
LE19 1SS

Ethics Administration
Direct dial: 0116 295 7591/2

19 February 2004

7218 Please quote this number on all correspondence

Dr John P Williams
Honorary Lecturer in Anaesthesia
Dept. of Anaesthesia
LRI



Tel: 0116 295 7591/2
Fax: 0116 295 7582

Dear Dr Williams

Re: Investigation into the presence of opioid receptors on human immune cells before and after treatment in vitro with a variety of mediators of inflammation, ethics ref: 7218

The Chairman on behalf of the Leicestershire Local Research Ethics Committee (Committee One) has considered your response to the issues raised by the Committee at the first review of your application on 06 February 2004, as set out in our letter dated 13 April 2004. The documents considered were as follows:

Your letter, dated 18 February 2004
Amended Application form
Volunteer Information Sheet, Version 2, dated 16.02.04, uhl9270is-p040218
Patient Consent Form, Version 2, dated 16.02.04, uhl9720cf-p040218

'Please note that the box to initial next to point 3 on the consent form is missing'

The Chairman, acting under delegated authority, is satisfied that your response has fulfilled the requirements of the Committee. You are therefore given approval for your research on ethical grounds providing you comply with the conditions set out below.

Conditions of approval

- Where approval is given before receipt of CTX, please let the LREC have a copy of the CTX when it is available. If changes to the protocol are required by the MHRA (Medicines and Healthcare Products Regulatory Agency), the LREC approval will become void until those changes have been made and the revised protocol will need to be approved.
- You do not undertake this research in any NHS organisation until the relevant NHS management approval has been received.
- You do not deviate from, or make changes to, the protocol without the prior written approval of the LREC, except where this is necessary to eliminate immediate hazards to research participants or when the change involves only logistical or administrative aspects of the research. In such cases, the LREC

An advisory committee to Leicestershire, Northamptonshire and Rutland Strategic Health Authority

should be informed within seven days of the implementation of the change. Likewise, you should also seek the relevant NHS management approval for the amendment, or inform the NHS organisation of any logistical or administrative changes.

- You complete and return the standard progress report form to the LREC one year from the date of this letter and thereafter on an annual basis. This form should also be used to notify the Committee when your research is completed and should be sent to the REC within three months of completion. For a copy of the progress report please see www.corec.org.uk.
- If you decide to terminate this research prematurely, a progress report form should be sent to the LREC within 15 days, indicating the reason for the early termination. For a copy of the progress report please see www.corec.org.uk.
- You must advise the LREC of all Suspected Serious Adverse Reactions (SSARs) and all Suspected Unexpected Serious Adverse Reactions (SUSARs).
- You advise the LREC of any unusual or unexpected results that raise questions about the safety of the research.
- The project must be started within three years of the date of this letter.
- You should be able to assure the Ethics Committee that satisfactory arrangements have been made for the labelling, safe storage and dispensation of drugs and pharmaceutical staff are always willing to provide advice on this.

Your application has been given a unique reference number. Please use it on all correspondence with the LREC.

Yours sincerely



Dr PG Rabey
Chairman

Leicestershire Local Research Ethics Committee One

(N.B. All communications related to Leicestershire Research Ethics Committee must be sent to the LREC Office at Leicestershire, Northamptonshire and Rutland Health Authority. If, however, your original application was submitted through a Trust Research & Development Office, then any response or further correspondence must be submitted in the same way).

Volunteer information sheet

Version 3. 19.03.05

Study title

Investigation into the presence of opioid receptors on human white blood cells, before and after treatment, in vitro, with mediators of inflammation.

Principal investigator: Dr John Williams, Honorary Lecturer in Anaesthesia

You are being invited to take part in a research study. Before you decide it is important for you to understand why the research is being done and what it will involve. Please take time to read the following information carefully and discuss it with others if you wish. Ask us if there is anything that is not clear or if you would like more information. Take time to decide whether or not you wish to take part. This study will form part of the work contributing to my PhD studies.

What is the purpose of the study?

White blood cells are covered in a variety of proteins that react with substances present in the blood. One group of proteins that are present on the surface of cells are opiate receptors. Opiate receptors are also known to react with many commonly used painkillers to help reduce pain. The main objective of this study is to look for the presence of opiate receptors on white blood cells, **and other markers of inflammation**, before and after the administration (in a test tube) of a variety of compounds that can cause inflammation.

Why have I been chosen?

We are approaching fit healthy volunteers who work in the University Department of Anaesthesia. We plan to ask 10 volunteers to take part in this study. Volunteers suffering from problems with their immune system will not be included in the study.

Do I have to take part in the study?

It is up to you to decide whether or not to take part. If you do decide to take part you will be given this information sheet to keep and be asked to sign a consent form. If you decide to take part you are still free to withdraw at any time and without giving a reason. A decision to withdraw at any time, or a decision not to take part, will not affect the standard of care you receive.

What will happen to me if I take part?

If you agree, the proposed study will involve the analysis of 5-10 mls (about 1-2 teaspoons) of your blood for the presence protein receptors. The taking of blood involves a small pinprick in the arm, which may cause some mild discomfort. Following this, tests will be carried out on your blood at the University

Department of Anaesthesia, Leicester Royal Infirmary. You will not be asked to provide any further blood samples. Once blood has been taken from you the sample will be anonymised, and you will not be able to withdraw the sample from the study.

What are the possible disadvantages and risks of taking part?

The 5-10 mls of blood you donate will be taken from your arm; this involves a small pinprick and some discomfort. It is also possible that after the blood has been taken you may develop a bruise at the site. In very rare cases some local infection may develop. The investigators taking the blood are very experienced in this procedure, and will take all possible precautions to minimise the chances of these uncommon complications.

What are the possible benefits of taking part?

The results of this study may help us to find whether various proteins on the surface of white blood cells are important during infection and inflammation following the administration of pain killing drugs, and possibly allow new treatments to be developed.

What happens when the research stops?

At the end of the study all of the blood samples collected will be destroyed.

What if something goes wrong?

If you are harmed by taking part in this research project, there are no special compensation arrangements. If you are harmed due to someone's negligence, then you may have grounds for a legal action but you may have to pay for it. Regardless of this, if you wish to complain, or have any concerns about any aspect of the way you have been approached or treated during the course of this study, the normal National Health Service complaints mechanisms would be available to you.

Will my taking part in this study be kept confidential?

All information that is collected about you during the course of the research will be kept strictly confidential. Any information about you which leaves the hospital/surgery will have your name and address removed so that you cannot be recognised from it.

Who is organising and funding the research?

This study is being organised and paid for by the University of Leicester and the University Hospitals of Leicester NHS Trust.

Who has reviewed the study?

All research that involves NHS patients or staff, information from NHS medical records or uses NHS premises or facilities must be approved by an NHS Research Ethics Committee before it goes ahead. Approval does not guarantee that you will not come to any harm if you take part. However, approval means

that the committee is satisfied that your rights will be respected, that any risks have been reduced to a minimum and balanced against possible benefits and that you have been given sufficient information on which to make an informed decision.

How can I get more information?

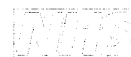
If you have any questions about this study please contact Dr John Williams, University Department of Anaesthesia, UHL NHS Trust, Leicester Royal Infirmary, Leicester LE1 5WW. Tel. 0116 2585291

If you have any questions about your rights as a participant in this research study, please contact the Research & Development Department Tel: 0116 2584109.

Thank you for reading this information sheet.

Appendix III: Ethics Committee Approval 7233

University Hospitals of Leicester



DIRECTORATE OF RESEARCH AND DEVELOPMENT

NHS Trust

Director: Professor D Rowbotham
Business Manager: Dr N J Seare
Service Manager: Mr M Roberts

Leicester General Hospital

Gwendolen Road
Leicester
LE5 4PW

Co-ordinator: N Patel
Direct Dial: 0116 258 8246
Fax No: 0116 258 4226
email: natu.patel@uhl-tr.nhs.uk

Tel: 0116 249 0490
Fax: 0116 258 4666
Minicom: 0116 258 8188

17 March 2004

Dr S Gold
University Department of Anaesthesia
Critical Care and Pain Management
LRI

Dear Dr Gold

RE: **UHL Ref. 9306** [Please quote this number in all correspondence]
Observational study of Urotensin II levels in patients with severe sepsis.
Ethics Ref. 7233

We have now been notified by the Ethics Committee that this project has been given a favourable opinion by the Ethics Committee (please see the attached letter from the Ethics Committee).

Since all other aspects of your UHL R+D notification are complete, I now have pleasure in confirming full approval of the project on behalf of University Hospitals of Leicester NHS Trust, Leicester Royal Infirmary Site.

This approval means that you are fully authorised to proceed with the project, using all the resources which you have declared in your notification form.

The project is also now covered by Trust Indemnity, except for those aspects already covered by external indemnity (e.g. ABPI in the case of most drug studies).

We will be requesting annual and final reports on the progress of this project, both on behalf of the Trust and on behalf of the Ethical Committee.

In the meantime, in order to keep our records up to date, could you please notify the Research Office if there are any significant changes to the start or end dates, protocol, funding or costs of the project.

I look forward to the opportunity of reading the published results of your study in due course.

Yours sincerely

Mr Michael Roberts
Service Manager for Research and Development



UHL 9306, Ethics ref: 7233

Leicestershire Local Research Ethics Committees

Lakeside House
4 Smith Way
Grove Park
Enderby
Leicester
LE19 1SS

Ethics Administration
Direct dial: 0116 295 7591/2

11 March 2004

7233 Please quote this number on all correspondence



Dr Stuart A Gold
Honorary Lecturer in Anaesthesia, Critical care and Pain management
University division of Anaesthesia, Critical care and Pain
LRI

Dear Dr Gold

**Re: Observational study of Urotensin II levels in patients with severe sepsis,
ethics ref: 7233**

The Chairman on behalf of the Leicestershire Local Research Ethics Committee (Committee Two) has considered your response to the issues raised by the Committee at the first review of your application on 19 February 2004, as set out in our letter dated 25 February 2004. The documents considered were as follows:

Your letter, dated 08 March 2004
Amended application form
PIS & CF, version 2, dated 8/3/2004, uhl9306is-p040308
RIS & AF, version 2, dated 8/3/2004, uhl9306is-pa040308

Thank you for your clear and comprehensive response

The Chairman, acting under delegated authority, is satisfied that your response has fulfilled the requirements of the Committee. You are therefore given approval for your research on ethical grounds providing you comply with the conditions set out below.

Conditions of approval

- Where approval is given before receipt of CTX, please let the LREC have a copy of the CTX when it is available. If changes to the protocol are required by the MHRA (Medicines and Healthcare Products Regulatory Agency), the LREC approval will become void until those changes have been made and the revised protocol will need to be approved.
- You do not undertake this research in any NHS organisation until the relevant NHS management approval has been received.
- You do not deviate from, or make changes to, the protocol without the prior written approval of the LREC, except where this is necessary to eliminate immediate hazards to research participants or when the change involves only logistical or administrative aspects of the research. In such cases, the LREC should be informed within seven days of the implementation of the change.

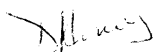
An advisory committee to Leicestershire, Northamptonshire and Rutland Strategic Health Authority

Likewise, you should also seek the relevant NHS management approval for the amendment, or inform the NHS organisation of any logistical or administrative changes.

- You complete and return the standard progress report form to the LREC one year from the date of this letter and thereafter on an annual basis. This form should also be used to notify the Committee when your research is completed and should be sent to the REC within three months of completion. For a copy of the progress report please see www.corec.org.uk.
- If you decide to terminate this research prematurely, a progress report form should be sent to the LREC within 15 days, indicating the reason for the early termination. For a copy of the progress report please see www.corec.org.uk.
- You must advise the LREC of all Suspected Serious Adverse Reactions (SSARs) and all Suspected Unexpected Serious Adverse Reactions (SUSARs).
- You advise the LREC of any unusual or unexpected results that raise questions about the safety of the research.
- The project must be started within three years of the date of this letter.
- You should be able to assure the Ethics Committee that satisfactory arrangements have been made for the labelling, safe storage and dispensation of drugs and pharmaceutical staff are always willing to provide advice on this.

Your application has been given a unique reference number. Please use it on all correspondence with the LREC.

Yours sincerely



Dr D Heney
Chairman
Leicestershire Local Research Ethics Committee Two

(N.B. All communications related to Leicestershire Research Ethics Committee must be sent to the LREC Office at Leicestershire, Northamptonshire and Rutland Health Authority. If, however, your original application was submitted through a Trust Research & Development Office, then any response or further correspondence must be submitted in the same way).



Relative information sheet and assent form

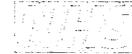
Study of urotensin II in severe infection

Principal Investigator: Dr Stuart Gold, Honorary Lecturer in Anaesthesia

You are being invited to allow your relative to take part in a research study. Before you decide it is important for you to understand why the research is being done and what it will involve. Please read the following information carefully and discuss it with others if you wish. Ask us if there is anything that is not clear or if you would like more information. We are asking you to confirm that you are not aware of any objection your relative would have to taking part in the study.

What is the purpose of this study?

Urotensin II is a newly discovered hormone that causes increases in blood pressure in animals. We wish to find out whether this hormone is affected by infection or inflammation causing low blood pressure (sepsis). Usually when you have infection or inflammation the blood vessels become more relaxed and get bigger, this can cause the blood pressure to fall. We would like to find out if this change in the blood vessel size is caused by changes in concentration of Urotensin II.



Why has your relative been chosen?

We are approaching all patients who are being admitted to Intensive care because of severe infection or inflammation. We plan to ask 25 patients to take part in this study in total. Your relative is too unwell at the moment to consent to take part in the study. Often in this situation we will ask their relatives to **ASSENT** to take part in the study. Only your relative can consent for themselves, however we are asking you to confirm that you are not aware of any objection your relative would have to taking part in the study. This is a very common situation in studies involving patients who are on Intensive Care.

Tel: 0116 2541414
Fax: 0116 2585631
Minicom: 0116 2586878

When your relative is well enough to have the study explained to them and allow them to consent if they wish. If your relative decides that they do not wish to take part in this research their samples will be destroyed.

Does my relative have to take part?

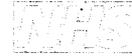
It is up to you to decide whether your relative would object to taking part or not. If you decide your relative would not object to taking part you will be given this information sheet to keep and be asked to sign an assent form. You, or your relative, are still free to withdraw at any time and without giving a reason. A decision to withdraw at any time, or a decision not to take part, will not affect the standard of care your relative will receive. If your relative decides, when they are well enough, that they do not wish to take part in this research their samples will be destroyed.

What will happen to my relative if they take part?

As part of your relatives care they will have a drip put into an artery, usually in the wrist. This is to monitor the blood pressure while they are in Intensive care, we can also take blood samples out of this drip without using any needles. The arterial drip will be put in whether you take part in the study or not.

If you agree to take part we will also take an extra 10 ml (two teaspoons) of blood when your relative is admitted to intensive care. While they are in intensive care a further 4 blood samples of 10 ml each (two teaspoons) will be taken over the next 4 days. If they leave Intensive care before this time then less blood samples will be taken.

The results of the tests will not affect your relatives care, and the results of the research will not be available until some time after they have left hospital. If your relative wants to know the results of the whole study once it is completed, please inform us and we will send them this information when it is available.



What are the blood tests for?

We will test the blood samples to measure the concentration of Urotensin II, a hormone which may be affected by having severe infection or inflammation. We will also look for the chemical that Urotensin II binds to, causing its effect (the Urotensin II receptor). As part of our research we will also look for other chemical and receptors, which may be altered during severe infection or inflammation. The tests will be performed at the University Department of Anaesthesia, Leicester Royal Infirmary.

Tel: 0116 2541414
Fax: 0116 2585631
Minicom: 0116 2586878

What are the possible disadvantages and risks of taking part?

The 50 ml of blood (10 teaspoons) will be taken from the drip in your relatives artery, which is part of their Intensive care monitoring. This means that the blood samples are taken without causing any extra pain or discomfort. The amount of blood being taken is very small and we do not anticipate any special risks from taking part in this study.

What if my relative is harmed by the study?

If your relative is harmed by taking part in this research project, there are no special compensation arrangements. If you are harmed due to someone's negligence, then you may have grounds for a legal action but you may have to pay for it. Regardless of this, if you wish to complain, or have any concerns about any aspect of the way you have been approached or treated during the course of this study, the normal National Health Service complaints mechanisms would be available to you.

What are the possible benefits to taking part?

The results of the tests may help us to find out whether this hormone is important during infection or inflammation causing low blood pressure, this may lead to improved understanding blood pressure control and allow new treatments to be developed.



Will my relatives taking part in this study be kept confidential?

All information collected about your relative during the course of this study will be kept strictly confidential. The samples we have taken will be coded, and any information about you which leaves the hospital will have your name and address removed so that you cannot be recognised from it. Your study doctor or nurse will give you a copy of this information sheet and your signed assent form to keep

Tel: 0116 2541414
Fax: 0116 2585631
Minicom: 0116 2586878

Who is organising and paying for the research?

This study is being organised and paid for by the University of Leicester and the University Hospitals of Leicester NHS Trust

How can I get more information?

If you have any questions about this study please contact Dr Stuart Gold or Dr Jonathan Thompson, University Dept of Anaesthesia, UHL NHS Trust, Leicester Royal Infirmary, Leicester LE1 5WW. Tel 0116 258 5291

If you have any questions about your rights as a participant in this research study, please contact the Research & Development Department on Tel: 0116 2584109.

Thank you for reading this information sheet.

Appendix IV: Ethics Committee Amendment 7233



School of Medicine

Stuart Gold
8 March 04

Dr D Heney
Chairman
Leicestershire Local Research Ethics Committee Two

Division of Anaesthesia, Critical Care &
Pain Management
Leicester Royal Infirmary
Leicester LE1 5WW, UK
Tel: +44 (0)116 258 5291
Fax: +44(0)116 285 4487
Email: anaec@le.ac.uk

Dear Dr Heney

**Re: Observational study of Urotensin II levels in patients with severe sepsis,
ethics ref: 7233**

Many thanks to you and the committee for considering the above study. I am grateful for the opportunity to amend my application with your suggestions. These documents are enclosed.

The committee raised the following ethical concerns:

1. The main concern arising from the review of this application was scientific validity. The committee requests clarification of the following issues:

(i) Will this project be part of a wider study? What is its context? Your aims are unclear.

(ii) Will there be a control group?

(iii) Will you be measuring other markers and parameters?

(i) This study is intended as a pilot study only. Research into Urotensin II is at quite an early stage. Other investigators in Leicester (Professor Ng) have studied the effects of Human systolic heart failure on Urotensin II and found it to be elevated. One interesting finding from the heart failure study is that Urotensin II is elevated in mild heart failure and this is independent of age and sex. It is possible that Urotensin II could be used in sepsis as an indicator of early heart failure.

In the heart failure study, brain natriuretic peptide, which is known to be elevated in heart failure was also measured and found to be elevated. Previous studies have shown that atrial and brain natriuretic peptide are elevated in septic shock. To our knowledge no one has measured Urotensin II in severe sepsis and septic shock. We are hypothesising that Urotensin II is also elevated in sepsis.

This study is intended to be part of a wider investigation into Urotensin II in health and disease. Other studies we are planning at the moment include; Urotensin II concentration following aortic cross-clamping during elective aortic aneurysm repair, Urotensin II concentration in smokers and non smokers, Urotensin II in patients with aortic aneurysms compared with matched controls and Urotensin II before, during and after cardiopulmonary bypass for elective coronary artery grafting.

The function in health and disease of Urotensin II has not been established and we aim to study a number of pathophysiological situations to try to gain some further insight into this recently discovered vasoactive peptide.

Leicester Warwick
Medical Schools



(ii) In this pilot study we plan to use each patient as their own control when they are in the recovery phase of their illness. The last sample of blood taken will be used as a control with patients off inotropes and no longer septic according to the consensus guidelines for diagnosis of sepsis and systemic inflammatory reaction. We realise that non-survivors in our population will weaken this study, however we would emphasise that this is a pilot study. Future studies in other disease states will include matched controls.

(iii) Initially we will measure Urotensin II only, as the diagnosis of sepsis and systemic inflammatory reaction is a clinical one and there is no “gold standard” test for sepsis. Following analysis of these results we may look for other inflammatory mediators. This has been included in our original LREC application and in the patient information leaflet.

The committee queried the following omissions/discrepancies:

1. Re: A15 on the application form - there is no need to notify the GP in this instance. Corec application form A 15. We will not notify patients GP's of their involvement in the study.

2. B41 states that blood samples will be anonymised and coded - please clarify. If they are anonymous, withdrawal from the study will not be possible, and patients should be informed of this (the PIL currently states that samples will be coded). Corec application form B 41. Blood samples will be coded with the patients initial and a number. All data will be stored on a computer where the data file is password protected

3. On both information leaflets:

Whilst it is laudable that you are willing to give individual patient results, the committee queries the value in this. The committee wondered if it would be better to give patients the opportunity to receive the study results rather than individual feedback.

This has been changed to “If you want to know the results of the whole study once it is completed, please inform us and we will send you this information when it is available.”

The first paragraph states 'take time to decide' but there will be little time in this patient group.

This has been removed from the information leaflets

(iii) Please remove the three bullet points from the first paragraph, as they are unnecessary.

This has been removed from the information leaflets

4. On the relative information leaflet:

(i) Rather than relatives giving 'permission' for the patient to take part, please word this in a way that the relative would feel more comfortable with, e.g. confirmation that they are not aware of any objection their relative would make.

This has been changed throughout the form

(ii) There is still reference to 'consent' rather than 'assent' - please amend. (e.g. last line of the paragraph headed 'Will my relatives taking part in this study be kept confidential'.

This has been changed

(iii) Relatives should be informed that should the patient not give consent, their samples will be destroyed.

This has been included

5. On the patient consent form:

Please remove reference to '[company name]' in point (3).

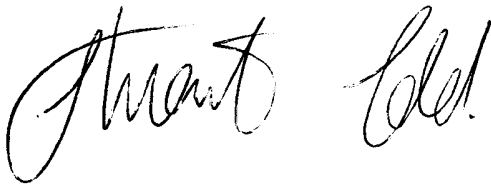
This has been removed

6. On the relative assent form:

(i) Please amend 'consent' to 'assent' (in the title and 'Name of Person taking consent').

This has been amended

Many thanks for your interest and help in this study,

A handwritten signature in black ink, appearing to read 'Stuart Gold'. The signature is written in a cursive, flowing style.

Stuart Gold
Honorary Lecturer
Anaesthesia, Critical Care and Pain Management

Bibliography

- Abbas AK, Lichtman AH. 2003. *Cellular and Molecular Immunology*. W B Saunders Co
- Alberts B, Johnson A, Lewis J, Raff M, Roberts K, Walter P. 2002. *Molecular Biology of the Cell*. Taylor & Francis.
- American College of Chest Physicians/Society of Critical Care Medicine Consensus Conference: definitions for sepsis and organ failure and guidelines for the use of innovative therapies in sepsis. *Crit Care Med*. 20:864-74.
- Angus DC, Linde-Zwirble WT, Lidicker J, Clermont G, Carcillo J, Pinsky MR. 2001. Epidemiology of severe sepsis in the United States: analysis of incidence, outcome, and associated costs of care. *Crit Care Med*. 29:1303-10.
- Arjomand J, Cole S, Evans CJ. 2002. Novel orphanin FQ/nociceptin transcripts are expressed in human immune cells. *J Neuroimmunol*. 130:100-8
- Beck M, Mirmohammadsadegh A, Franz B, Blanke J, Hengge UR. 2002. Opioid receptors on white blood cells: effect of HIV infection and methadone treatment. *Pain* 98: 187-94
- Berger H, Calo' G, Albrecht E, Guerrini R, Bienert M. 2000 [Nphe(1)]NC(1-13)NH(2) selectively antagonizes nociceptin/orphanin FQ-stimulated G-protein activation in rat brain. *J Pharmacol Exp Ther*. 294:428-33.
- Berne RM, Levy MN. 1996. *Principles of Physiology*. Mosby.
- Bidlack JM, Khimich M, Parkhill AL, Sumagin S, Sun B, Tipton CM. 2006. Opioid receptors and signaling on cells from the immune system. *J Neuroimmune Pharmacol*. 1:260-9.
- Bidlack JM. 2000. Detection and function of opioid receptors on cells from the immune system. *Clin Diagn Lab Immunol* 7: 719-23
- Binder W, Mousa SA, Sitte N, Kaiser M, Stein C, Schäfer M. 2004. Sympathetic activation triggers endogenous opioid release and analgesia within peripheral inflamed tissue. *Eur J Neurosci* 20: 92-100.
- Blunk JA, Schmelz M, Zeck S, Skov P, Likar R, Koppert W. 2004. Opioid-induced mast cell activation and vascular responses is not mediated by mu-opioid receptors: an in vivo microdialysis study in human skin. *Anesth Analg*. 98:364-70
- Boeuf P, Vigan-Womas I, Jublot D, Loizon S, Barale JC, Akanmori BD, Mercereau-Puijalon O, Behr C. 2005. CyProQuant-PCR: a real time RT-PCR technique for profiling human cytokines, based on external RNA standards, readily automatable for clinical use. *BMC Immunol*. 6:5
- Borgland SL. 2001. Acute opioid receptor desensitization and tolerance: is there a link? *Clin Exp Pharmacol Physiol* 28: 147-54
- Börner C, Höllt V, Kraus J. 2002. Involvement of activator protein-1 in transcriptional regulation of the human mu-opioid receptor gene. *Mol Pharmacol*. 61:800-5.

- Börner C, Kraus J, Schröder H, Ammer H, Höllt V. 2004. Transcriptional regulation of the human mu-opioid receptor gene by interleukin-6. *Mol Pharmacol*. 66:1719-26.
- Brack A, Rittner HL, Machelska H, Shaqura M, Mousa SA, Labuz D, Zöllner C, Schäfer M, Stein C. 2004. Endogenous peripheral antinociception in early inflammation is not limited by the number of opioid-containing leukocytes but by opioid receptor expression. *Pain*. 108:67-75.
- Brack A, Stein C. 2003. The role of the peripheral nervous system in immune cell recruitment. *Exp Neurol* 184: 44-9
- Brookes ZL, Stedman EN, Guerrini R, Lawton BK, Calo G, Lambert DG. 2007. Proinflammatory and vasodilator effects of nociceptin/orphanin FQ in the rat mesenteric microcirculation are mediated by histamine. *Am J Physiol Heart Circ Physiol*. 293:H2977-85.
- Bucher B. 1998. ORL1 receptor-mediated inhibition by nociceptin of noradrenaline release from perivascular sympathetic nerve endings of the rat tail artery. *Naunyn Schmiedebergs Arch Pharmacol* 358: 682-685
- Bunzow JR, Saez C, Mortrud M, Bouvier C, Williams JT, Low M, Grandy DK. 1994. Molecular cloning and tissue distribution of a putative member of the rat opioid receptor gene family that is not μ , δ or κ opioid receptor type. *FEBS Lett* 347: 284 – 288
- Bustin SA, Benes V, Nolan T, Pfaffl MW. 2005. Quantitative real-time RT-PCR--a perspective. *J Mol Endocrinol*. 34:597-601
- Bustin SA. 2000. Absolute quantification of mRNA using real-time reverse transcription polymerase chain reaction assays. *J Mol Endocrinol*. 25:169-93
- Bylund DB, Toews ML. 1993. Radioligand binding methods: practical guide and tips. *Am J Physiol*. 265: 421-9.
- Cabot PJ. 2001. Immune-derived opioids and peripheral antinociception. *Clin Exp Pharmacol Physiol*. 28:230-2.
- Cabral GA. 2006. Drugs of abuse, immune modulation, and AIDS. *J Neuroimmune Pharmacol*. 1:280-95.
- Cadet P, Mantione K, Bilfinger TV, Stefano GB. 2001. Real-time RT-PCR measurement of the modulation of Mu opiate receptor expression by nitric oxide in human mononuclear cells. *Med Sci Monit* 7: 1123-8
- Cadet P, Mantione KJ, Stefano GB. 2003. Molecular identification and functional expression of mu 3, a novel alternatively spliced variant of the human mu opiate receptor gene. *J Immunol*. 170:5118-23.
- Cadet P, Zhu W, Mantione KJ, Baggerman G, Stefano GB. 2002. Cold stress alters *Mytilus edulis* pedal ganglia expression of mu opiate receptor transcripts determined by real-time RT-PCR and morphine levels. *Brain Res Mol Brain Res*. 99(1):26-33.

- Caldirolì E, Leoni O, Cattaneo S, Rasini E, Marino V, et al. 1999. Neutrophil function and opioid receptor expression on leucocytes during chronic naltrexone treatment in humans. *Pharmacol Res* 40: 153-8
- Calo G, Guerrini R, Rizzi A, Salvadori S, Regoli D. 2000. Pharmacology of nociceptin and its receptor: a novel therapeutic target. *Br J Pharmacol* 129: 1261-83
- Calvey TN, Williams NE. 1997. *Principles and Practice of Pharmacology for Anaesthetists*. Blackwell Science.
- Cannarsa R, Landuzzi D, Cavina C, Candeletti S, Romualdi P. 2008. Kainic Acid Down-regulates NOP Receptor Density and Gene Expression in Human Neuroblastoma SH-SY5Y Cells. *J Mol Neurosci*. Feb 20
- Chalecka-Franaszek E, Weems HB, Crowder AT, Cox BM, Côté TE. 2000. Immunoprecipitation of high-affinity, guanine nucleotide-sensitive, solubilized mu-opioid receptors from rat brain: coimmunoprecipitation of the G proteins G(alpha o), G(alpha i1), and G(alpha i3). *J Neurochem*. 74:1068-78
- Champion HC, Bivalacqua TJ, Friedman DE, Zadina JE, Kastin AJ, et al. 1998. Nitric oxide release mediates vasodilator responses to endomorphin1 but not to nociceptin/OFQ in the hindquarters vascular bed of rats. *Peptides* 19: 1592-1602
- Champion HC, Czaplà MA, Kadowitz PJ. 1997. Nociceptin, an endogenous ligand for the ORL1 receptor, decreases cardiac output and total peripheral resistance in the rat. *Peptides* 18: 729-732
- Chen Y, Chang M, Wang ZZ, Chen LX, Yang Q, et al. 2002. [Nphe1]nociceptin(1-13)-NH2 antagonizes nociceptin-induced hypotension, bradycardia and hindquarters vasodilatation in the anesthetized rat. *Can J Physiol Pharmacol* 80: 31-35
- Cheng Y, Prusoff WH. 1973. Relationship between the inhibition constant (K₁) and the concentration of inhibitor which causes 50 per cent inhibition (I₅₀) of an enzymatic reaction. *Biochem Pharmacol*. 22: 3099-108
- Chomczynski P. 1993. A reagent for the single-step simultaneous isolation of RNA, DNA and proteins from cell and tissue samples. *Biotechniques*. 15:532-4, 536-7.
- Chu X, Xu N, Li P, Wang JQ. 1999. The nociceptin receptor-mediated inhibition of the rat rostral ventrolateral medulla neurons in vitro. *Eur J Pharmacol*. 364:49-53.
- Chuang LF, Chuang TK, Killam KF Jr, Chuang AJ, Kung HF, Yu L, Chuang RY. 1994. Delta opioid receptor gene expression in lymphocytes. *Biochem Biophys Res Commun*. 202:1291-9.
- Chuang LF, Chuang TK, Killam KF Jr, Qiu Q, Wang XR, Lin JJ, Kung HF, Sheng W, Chao C, Yu L, Chuang RY. 1995a. Expression of kappa opioid receptors in human and monkey lymphocytes. *Biochem Biophys Res Commun*. 209:1003-10.
- Chuang TK, Killam KF, Jr., Chuang LF, Kung HF, Sheng WS, et al. 1995b. Mu opioid receptor gene expression in immune cells. *Biochem Biophys Res Commun* 216: 922-30
- Collett BJ. 1998. Opioid tolerance: the clinical perspective. *Br J Anaesth* 81: 58-68
- Collett BJ. 2001. Chronic opioid therapy for non-cancer pain. *Br J Anaesth* 87: 133-43

- Connor M, Yeo A, Henderson G. 1996. The effect of nociceptin on Ca²⁺ channel current and intracellular Ca²⁺ in the SH-SY5Y human neuroblastoma cell line. *Br J Pharmacol.* 118:205-7.
- Corbett AD, Henderson G, McKnight AT, Paterson SJ. 2006. 75 years of opioid research: the exciting but vain quest for the Holy Grail. *British Journal of Pharmacology* 147:S153–S162
- Cowley E, Thompson JP, Sharpe P, Waugh J, Ali N, Lambert DG. 2005. Effects of pre-eclampsia on maternal plasma, cerebrospinal fluid, and umbilical cord urotensin II concentrations: a pilot study. *Br J Anaesth.* 95:495-9
- Cox BM, Chavkin C, Christie MJ, Civelli O, Evans C, Hamon MD, Hoellt V, Kiefer I, McKnight AT, Meunier JC, Portoghese PS. 2000. *Opioid receptors*. In The IUPHAR Compendium of Receptor Characterization. Ed. Gridlestone D. IUPHAR Media.
- Dellinger RP, Carlet JM, Masur H, Gerlach H, Calandra T, Cohen J, Gea-Banacloche J, Keh D, Marshall JC, Parker MM, Ramsay G, Zimmerman JL, Vincent JL, Levy MM. 2004. Surviving Sepsis Campaign Management Guidelines Committee. Surviving Sepsis Campaign guidelines for management of severe sepsis and septic shock. *Crit Care Med.* 32:858-73
- Despopoulos A, Silbernagl S. 2003. *Colour Atlas of Physiology*. New York, Thieme.
- Dheda K, Huggett JF, Bustin SA, Johnson MA, Rook G, Zumla A. 2004. Validation of housekeeping genes for normalizing RNA expression in real-time PCR. *Biotechniques.* 37:112-4, 116, 118-9
- Dong J, Naito M, Dan S, Tsuruo T. 1998. Establishment of a mutant from human monocytic leukaemia U937 that exhibits a genetically dominant resistance to TNF alpha-induced apoptosis. *Apoptosis.* 3:245-54
- Eguchi M. 2004. Recent advances in selective opioid receptor agonists and antagonists. *Med Res Rev* 24: 182-212
- Eisenstein TK, Rahim RT, Feng P, Thingalaya NK, Meissler JJ. 2006. Effects of opioid tolerance and withdrawal on the immune system. *J Neuroimmune Pharmacol.* 1:237-49.
- Evans, C., Keith, D., Morrison, H., Magendzo, K. and Edwards, R. 1992. Cloning of delta opioid receptor by functional expression. *Science* 258:1952 - 1955.
- Fiset ME, Gilbert C, Poubelle PE, Pouliot M. 2003. Human neutrophils as a source of nociceptin: a novel link between pain and inflammation. *Biochemistry* 42: 10498-505
- Florin S, Suaudeau C, Meunier JC, Costentin J. 1997. Orphan neuropeptide NocII, a putative pronociceptin maturation product, stimulates locomotion in mice. *Neuroreport.* 10:705-7.
- Friedman H, Newton C, Klein TW. 2003. Microbial infections, immunomodulation, and drugs of abuse. *Clin Microbiol Rev.* 16:209-19.
- Galley HF, Webster NR. 1999. A rough guide to molecular biology. *Br J Anaesth.* 83:675-81.
- Ganong WF. 2005. *Review of Medical Physiology*. McGraw-Hill Medical Paperback

- Gavériaux C, Peluso J, Simonin F, Laforet J, Kieffer B. 1995. Identification of kappa- and delta-opioid receptor transcripts in immune cells. *FEBS Lett.* 369:272-6.
- Gavériaux-Ruff C, Peluso J, Befort K, Simonin F, Zilliox C, Kieffer BL. 1997. Detection of opioid receptor mRNA by RT-PCR reveals alternative splicing for the delta- and kappa-opioid receptors. *Brain Res Mol Brain Res.* 48:298-304.
- Gerber BO, Pichler WJ. 2006. Noncovalent interactions of drugs with immune receptors may mediate drug-induced hypersensitivity reactions. *AAPS J.* 8:E160-5.
- Giuliani S, Tramontana M, Lecci A, Maggi CA. 1997. Effect of nociceptin on heart rate and blood pressure in anaesthetized rats. *Eur J Pharmacol* 333 (2-3): 177-179
- Granata F, Potenza RL, Fiori A, Strom R, Caronti B, Molinari P, Donsante S, Citro G, Iacovelli L, De Blasi A, Ngomba RT, Palladini G, Passarelli F. 2003. Expression of OP4 (ORL1, NOP1) receptors in vascular endothelium. *Eur J Pharmacol.* 482:17-23
- Greenelch KM, Haudenschild CC, Keegan AD, Shi Y. 2004. The opioid antagonist naltrexone blocks acute endotoxic shock by inhibiting tumor necrosis factor-alpha production. *Brain Behav Immun.* 18(5):476-84.
- Harrison C, Lambert DG. 2000. Opioid Pharmacology. *Anaesthesia, Pain and Intensive Care Medicine.* Ed. Gullo A. Springer.
- Harrison C, McNulty S, Smart D, Rowbotham DJ, Grandy DK, Devi LA, Lambert DG. 1999. The effects of endomorphin-1 and endomorphin-2 in CHO cells expressing recombinant mu-opioid receptors and SH-SY5Y cells. *Br J Pharmacol.* 128:472-8.
- Harrison LM, Kastin AJ, Zadina JE. 1998. Opiate tolerance and dependence: receptors, G-proteins, and antiopiates. *Peptides* 19: 1603-30
- Hashiba E, Hirota K, Kudo T, Calo G, Guerrini R, Matsuki A. 2003. Effects of nociceptin/orphanin FQ receptor ligands on blood pressure, heart rate and catecholamine release in guinea pigs. *Nauyn Schmiedebergs Arch Pharmacol* 367: 342-347
- Hess ML, Smith JM, Eaton LR, Kleinman W, Okabe E. 1981. Chronic opiate receptor occupation and increased lethality in endotoxemia. *Circ Shock.* 8:313-22.
- Hirota K, Okawa H, Appadu BL, Grandy DK, Lambert DG. 2000. Interaction of local anaesthetics with recombinant mu, kappa, and delta-opioid receptors expressed in Chinese hamster ovary cells. *Br J Anaesth.* 85:740-6.
- Hom JS, Goldberg I, Mathis J, Pan YX, Brooks AI, Ryan-Moro J, Scheinberg DA, Pasternak GW. 1999. [(125)I]orphanin FQ/nociceptin binding in Raji cells. *Synapse.* 34:187-91.
- Hoorfar J, Malorny B, Abdulmawjood A, Cook N, Wagner M, Fach P. 2004. Practical considerations in design of internal amplification controls for diagnostic PCR assays. *J Clin Microbiol.* 42:1863-8
- Ignatowski TA, Bidlack JM. 1998. Detection of kappa opioid receptors on mouse thymocyte phenotypic subpopulations as assessed by flow cytometry. *J Pharmacol Exp Ther.* 284:298-306.

- Ignatowski TA, Bidlack JM. 1999. Differential kappa-opioid receptor expression on mouse lymphocytes at varying stages of maturation and on mouse macrophages after selective elicitation. *J Pharmacol Exp Ther.* 290:63-70.
- Innis M, Gelfand DH, Sninsky JJ, White TJ. 1990. *PCR Protocols: A Guide to Methods and Applications*. Ed Innis M. Academic Press.
- IUPHAR. Opioid receptors: Introduction 2007. www.iuphar-db.org/GPCR/
- Jensen TS, Wilson PR, Rice ASC. 2003. Jensen TS & Gottrup H in *Assessment of neuropathic pain: Clinical Pain Management: Chronic Pain*. Arnold.
- Jessop DS, Richards LJ, Harbuz MS. 2002. Opioid peptides endomorphin-1 and endomorphin-2 in the immune system in humans and in a rodent model of inflammation. *Ann N Y Acad Sci.* 966:456-63.
- Johnson EE, McDonald J, Nicol B, Guerrini R, Lambert DG. 2004. Functional coupling of the nociceptin/orphanin FQ receptor in dog brain membranes. *Brain Res.* 1003:18-25.
- Kenakin TP. 2006. *A pharmacology primer. Theory, applications and methods*. Elsevier Academic Press.
- Kieffer, B. L. 1995. Recent advances in molecular recognition and signal transduction of active peptides. *Cell. Mol. Biol.* 15:615 - 635.
- Kieffer, B. L., Befort, K., Gaveriaux-Ruff, C. and Hirth, C. G. 1992. Delta-opioid receptor: isolation of a cDNA by expression cloning and pharmacological characterization. *Proc. Natl. Acad. Sci. U.S.A.* 89:12048 - 12052.
- Knaus WA, Draper EA, Wagner DP, Zimmerman JE. 1985. APACHE II: a severity of disease classification system. *Crit Care Med.* 13:818-29.
- Köhler G, Milstein C. 1975. Continuous cultures of fused cells secreting antibody of predefined specificity. *Nature.* 256:495-7.
- Kraus J, Borner C, Giannini E, Hickfang K, Braun H, Mayer P, Hoehe MR, Ambrosch A, König W, Hollt V. 2001. Regulation of mu-opioid receptor gene transcription by interleukin-4 and influence of an allelic variation within a STAT6 transcription factor binding site. *J Biol Chem* 276: 43901-8
- Kraus J, Borner C, Giannini E, Hollt V. 2003. The role of nuclear factor kappaB in tumor necrosis factor-regulated transcription of the human mu-opioid receptor gene. *Mol Pharmacol* 64: 876-84
- Kumar P, Clark M. 2002. *Clinical Medicine*. Saunders.
- Lang ME, Jour'd'Heuil D, Meddings JB, Swain MG. 1995. Increased opioid binding to peripheral white blood cells in a rat model of acute cholestasis. *Gastroenterology* 108: 1479-86
- Lawrence DM, el-Hamouly W, Archer S, Leary JF, Bidlack JM. 1995. Identification of kappa opioid receptors in the immune system by indirect immunofluorescence. *Proc Natl Acad Sci U S A.* 92:1062-6.

- Lawrence DM, Hutchinson I, Seyed-Mozaffari A, Archer S, Bidlack JM. 1997. Fluorescent staining of kappa opioid receptors using naltrexamine derivatives and phycoerythrin. *J Immunol Methods*. 28:173-81.
- Levy MM, Fink MP, Marshall JC, Abraham E, Angus D, Cook D, Cohen J, Opal SM, Vincent JL, Ramsay G; International Sepsis Definitions Conference. 2001. SCCM/ESICM/ACCP/ATS/SIS International Sepsis Definitions Conference. *Intensive Care Med*. 29:530-8.
- Likar R, Mousa SA, Philippitsch G, Steinkellner H, Koppert W, Stein C, Schäfer M. 2004. Increased numbers of opioid expressing inflammatory cells do not affect intra-articular morphine analgesia. *Br J Anaesth*. 93:75-80.
- Loeser JD, Butler SH, Chapman CR, Turk DC. 2001. Terman GW & Bonica JJ in *Spinal Mechanisms and Their Modulation: Bonica's Management of Pain*. Lippincott, Williams and Wilkins.
- Lowry OH, Rosebrough NJ, Lewis Farr A, Randall RJ. 1951. Protein measurement with the Folin phenol reagent. *J Biol Chem*. 193: 265-275
- Machelska H, Brack A, Mousa SA, Schopohl JK, Rittner HL, Schäfer M, Stein C. 2004. Selectins and integrins but not platelet-endothelial cell adhesion molecule-1 regulate opioid inhibition of inflammatory pain. *Br J Pharmacol*. 142:772-80.
- Machelska H, Cabot PJ, Mousa SA, Zhang Q, Stein C. 1998. Pain control in inflammation governed by selectins. *Nat Med*. 4:1425-8.
- Machelska H, Mousa SA, Brack A, Schopohl JK, Rittner HL, et al. 2002. Opioid control of inflammatory pain regulated by intercellular adhesion molecule-1. *J Neurosci* 22: 5588-96
- Madden JJ, Whaley WL, Ketelsen D, Donahoe RM. 2001. The morphine-binding site on human activated T-cells is not related to the mu opioid receptor. *Drug Alcohol Depend* 62:131-9
- Madeddu P, Salis MB, Millia AF, Emanuelli C, Geurrini R, et al. 1999. Cardiovascular effects of nociceptin in unanesthetized mice. *Hypertension* 33 (3): 914-919
- Malcolm DS, Zaloga GP, Willey SC, Amir S, Holaday JW. 1988. Naloxone potentiates epinephrine's pressor actions in endotoxemic rats. *Circ Shock*. 25:259-65.
- Malinowska B, Godlewski G, Schlicker E. 2002. Function of nociceptin and opioid OP4 receptors in the regulation of the cardiovascular system. *J Physiol Pharmacol*. 53:301-24.
- Manfredi B, Sacerdote P, Bianchi M, Locatelli L, Veljic-Radulovic J, Panerai AE. 1993. Evidence for an opioid inhibitory effect on T cell proliferation. *J Neuroimmunol* 44: 43-8
- McCarthy L, Szabo I, Nitsche JF, Pintar JE, Rogers TJ. 2001. Expression of functional mu-opioid receptors during T cell development. *J Neuroimmunol*. 114:173-80.
- McCarthy L, Wetzel M, Sliker JK, Eisenstein TK, Rogers TJ. 2001. Opioids, opioid receptors, and the immune response. *Drug Alcohol Depend* 62: 111-23
- McDonald J, Barnes TA, Okawa H, Williams J, Calo' G, Rowbotham DJ, Lambert DG. 2003. Partial agonist behaviour depends upon the level of nociceptin/orphanin FQ

- receptor expression: studies using the ecdysone-inducible mammalian expression system. *Br J Pharmacol.* 140:61-70
- McDonald J, Lambert DG. 2005. Opioid receptors. *Contin Educ Anaesth Crit Care Pain.* 5:22-25
- Mehrishi JN, Mills IH. 1983. Opiate receptors on lymphocytes and platelets in man. *Clin Immunol Immunopathol.* 27:240-9.
- Mellon RD, Bayer BM. 1998. Evidence for central opioid receptors in the immunomodulatory effects of morphine: review of potential mechanism(s) of action. *J Neuroimmunol* 83: 19-28
- Mellon RD, Bayer BM. 1999. The effects of morphine, nicotine and epibatidine on lymphocyte activity and hypothalamic-pituitary-adrenal axis responses. *J Pharmacol Exp Ther* 288: 635-42
- Melzak R, Wall PD. 1965. Pain mechanisms a new theory. *Science* 150: 971-9
- Meunier JC, Mollereau C, Toll L, Suaudeau C, Moisand C, Alvinerie P, Butour J. L, Guillemot JC, Ferrara P, Monsarrat B *et al.* 1995. Isolation and structure of the endogenous agonist of opioid receptor-like ORL-1 receptor. *Nature* 377: 532 - 535.
- Meunier JC. 1997. Nociceptin/orphanin FQ and the opioid receptor-like ORL1 receptor. *Eur J Pharmacol.* 340:1-15
- Meunier JC. 2000. The potential therapeutic value of nociceptin receptor agonists and antagonists. *Exp. Opin. Ther. Patents* 10:371-388
- Mollereau C, Parmentier M, Mailleu, P, Butour J L, Moisand C, Chalon P, Caput D, Vassart G, Meunier JC. 1994. ORL1, a novel member of the opioid receptor family. Cloning, functional expression and localization. *FEBS Lett.* 341: 33-38
- Morgan EL. 1996. Regulation of human B lymphocyte activation by opioid peptide hormones. Inhibition of IgG production by opioid receptor class (μ -, κ -, and δ -) selective agonists. *J Neuroimmunol* 65: 21-30
- Mousa SA, Machelska H, Schafer M, Stein C. 2000. Co-expression of beta-endorphin with adhesion molecules in a model of inflammatory pain. *J Neuroimmunol* 108: 160-70
- Mousa SA, Machelska H, Schäfer M, Stein C. 2002. Immunohistochemical localization of endomorphin-1 and endomorphin-2 in immune cells and spinal cord in a model of inflammatory pain. *J Neuroimmunol.* 126:5-15.
- Mousa SA, Shakibaei M, Sitte N, Schafer M, Stein C. 2004. Subcellular pathways of beta-endorphin synthesis, processing, and release from immunocytes in inflammatory pain. *Endocrinology* 145: 1331-41
- Mousa SA, Zhang Q, Sitte N, Ji R, Stein C. 2001. beta-Endorphin-containing memory-cells and μ -opioid receptors undergo transport to peripheral inflamed tissue. *J Neuroimmunol* 115: 71-8
- Murphy TJ. 2003. Simple nuclear factor kappaB-mediated μ -opioid receptor induction in immune cells. *Mol Pharmacol.* 64:796-7.

- Nadkarni MA, Martin FE, Jacques NA, Hunter N. 2002. Determination of bacterial load by real-time PCR using a broad-range (universal) probe and primers set. *Microbiology*. 148:257-66
- Okuda-Ashitaka E, Ito S. 2000. Nocistatin: a novel neuropeptide encoded by the gene for the nociceptin/orphanin FQ precursor. *Peptides*. 21:1101-9.
- Pachot A, Blond JL, Mouglin B, Miossec P. 2004. Peptidylpropyl isomerase B (PPIB): a suitable reference gene for mRNA quantification in peripheral whole blood. *J Biotechnol*. 114:121-4.
- Pampusch MS, Osinski MA, Brown DR, Murtaugh MP. 1998. The porcine mu opioid receptor: molecular cloning and mRNA distribution in lymphoid tissues. *J Neuroimmunol*. 90:192-8
- Pampusch MS, Serie JR, Osinski MA, Seybold VS, Murtaugh MP, Brown DR. 2000. Expression of nociceptin/OFQ receptor and prepro-nociceptin/OFQ in lymphoid tissues. *Peptides*. 21:1865-70.
- Pan Z, Hirakawa N, Fields HL. 2000. a cellular mechanism for the bi-directional pain-modulating actions of orphanin FQ/nociceptin. *Neuron* 26: 515-522
- Patrini G, Massi P, Ricevuti G, Mazzone A, Fossati G, Mazzucchelli I, Gori E, Parolaro D. 1996. Changes in opioid receptor density on murine splenocytes induced by in vivo treatment with morphine and methadone. *J Pharmacol Exp Ther*. 279:172-6.
- Peluso J, Gavériaux-Ruff C, Matthes HW, Filliol D, Kieffer BL. 2001. Orphanin FQ/nociceptin binds to functionally coupled ORL1 receptors on human immune cell lines and alters peripheral blood mononuclear cell proliferation. *Brain Res Bull*. 54:655-60.
- Peluso J, LaForge KS, Matthes HW, Kreek MJ, Kieffer BL, Gavériaux-Ruff C. 1998. Distribution of nociceptin/orphanin FQ receptor transcript in human central nervous system and immune cells. *J Neuroimmunol*. 81:184-92.
- Petronilho FC, Souza B, Machado R, Constantino L, Guerrini R, Calo G, Gavioli EC, Streck EL, Dal-Pizzol. 2008. Nociceptin/orphanin FQ-NOP receptor system as a mediator of sepsis progression. In Press
- Pfaffl MW, Tichopad A, Prgomet C, Neuvians TP. 2004. Determination of stable housekeeping genes, differentially regulated target genes and sample integrity: BestKeeper--Excel-based tool using pair-wise correlations. *Biotechnol Lett*. 26:509-15
- Philippe D, Dubuquoy L, Groux H, Brun V, Chuoï-Mariot MT, Gaveriaux-Ruff C, Colombel JF, Kieffer BL, Desreumaux P. 2003. Anti-inflammatory properties of the mu opioid receptor support its use in the treatment of colon inflammation. *J Clin Invest*. 111:1329-38.
- Prather PL, Tsai AW, Law PY. 1994. Mu and delta opioid receptor desensitization in undifferentiated human neuroblastoma SHSY5Y cells. *J Pharmacol Exp Ther* 270:177-84
- Rang HP, Dale MM, Ritter JM, Flower R. 2007. *Rang & Dale's Pharmacology*. Churchill Livingstone.

- Reinscheid RK, Nothacker HP, Bourson A, Ardati A, Henningsen RA, Bunzow JR, Grandy DK, Langen H, Monsma F J, Civelli O. 1995. Orphanin-FQ: a neuropeptide that activates an opioid-like G protein-coupled receptor. *Science* 270:792 - 794.
- Reinscheid RK, Nothacker H-P, Bourson A, Ardati A, Henningsen RA, et al. 1995. orphanin FQ; a neuropeptide that activates an opioid like G protein-coupled receptor. *Science* 270: 792-794
- Rittner HL, Brack A, Machelska H, Mousa SA, Bauer M, et al. 2001. Opioid peptide-expressing leukocytes: identification, recruitment, and simultaneously increasing inhibition of inflammatory pain. *Anesthesiology* 95: 500-8
- Roy S, Balasubramanian S, Sumandeeep S, Charboneau R, Wang J, et al. 2001. Morphine directs T cells toward T(H2) differentiation. *Surgery* 130: 304-9
- Roy S, Cain KJ, Charboneau RG, Barke RA.1998. Morphine accelerates the progression of sepsis in an experimental sepsis model. *Adv Exp Med Biol.* 437:21-31.
- Sacerdote P, Gaspani L, Rossoni G, Panerai AE, Bianchi M. 2001. Effect of the opioid remifentanyl on cellular immune response in the rat. *Int Immunopharmacol.* 1:713-9.
- Saiki RK, Bugawan TL, Horn GT, Mullis KB, Erlich HA. 1986. Analysis of enzymatically amplified beta-globin and HLA-DQ alpha DNA with allele-specific oligonucleotide probes. *Nature.* 324:163-6
- Salis MB, Emanuelli C, Milia AF, Guerrini R, Madeddu P. 2000. Studies of the cardiovascular effects of nociceptin and related peptides. *Peptides.* 21:985-93
- Satoh, M. and Minami, M. 1995. Molecular pharmacology of the opioid receptors. *Pharmacol. Ther.* 68:343 - 364.
- Saurer TB, Carrigan KA, Ijames SG, Lysle DT. 2004. Morphine-induced alterations of immune status are blocked by the dopamine D2-like receptor agonist 7-OH-DPAT. *J Neuroimmunol* 148: 54-62
- Serhan CN, Fierro IM, Chiang N, Pouliot M. 2001. Cutting edge: nociceptin stimulates neutrophil chemotaxis and recruitment: inhibition by aspirin-triggered-15-epi-lipoxin A4. *J Immunol.*15:3650-4.
- Shah N, Chitravanshi VC, Sapru HN. 2003. Cardiovascular responses to microinjections of nociceptin into a midline area in the commissural subnucleus of the nucleus tractus solitarius of the rat. *Brain Res.* 984:93-103
- Shapiro HM. 1995. *Practical flow cytometry.* Wiley-Liss, Inc.
- Shaqura MA, Zollner C, Mousa SA, Stein C, Schafer M. 2004. Characterization of mu opioid receptor binding and G protein coupling in rat hypothalamus, spinal cord, and primary afferent neurons during inflammatory pain. *J Pharmacol Exp Ther* 308: 712-8
- Sharp BM, Li MD, Matta SG, McAllen K, Shahabi NA. 2000. Expression of delta opioid receptors and transcripts by splenic T cells. *Ann N Y Acad Sci.* 917:764-70.

- Sharp BM, McAllen K, Gekker G, Shahabi NA, Peterson PK. 2001. Immunofluorescence detection of delta opioid receptors (DOR) on human peripheral blood CD4+ T cells and DOR-dependent suppression of HIV-1 expression. *J Immunol.* 167:1097-102.
- Sharp BM. 2006. Multiple opioid receptors on immune cells modulate intracellular signaling. *Brain Behav Immun.* 20:9-14.
- Sheen CH, Schleimer RP, Kulka M. 2007. Codeine induces human mast cell chemokine and cytokine production: involvement of G-protein activation. *Allergy.* 62:532-8.
- Spink WW, Starzecki B. 1967. Experimental canine endotoxin shock: failure to correlate outcome with persistent endotoxemia. *Proc Soc Exp Biol Med.* 126:574-6.
- Spittal PM, Bruneau J, Craib KJ, Miller C, Lamothe F, Weber AE, Li K, Tyndall MW, O'Shaughnessy MV, Schechter MT. 2003. Surviving the sex trade: a comparison of HIV risk behaviours among street-involved women in two Canadian cities who inject drugs. *AIDS Care.* 15:187-95.
- Stefano GB, Salzet B, Fricchione GL. 1998. Enkephalin and opioid peptide association in invertebrates and vertebrates: immune activation and pain. *Immunol Today* 19: 265-8
- Stein C, Schafer M, Machelska H. 2000. Why is morphine not the ultimate analgesic and what can be done to improve it? *J Pain* 1: 51-6
- Stein C, Schafer M, Machelska H. 2003. Attacking pain at its source: new perspectives on opioids. *Nat Med* 9: 1003-8
- Suzuki S, Chuang LF, Doi RH, Bidlack JM, Chuang RY. 2001. Kappa-opioid receptors on lymphocytes of a human lymphocytic cell line: morphine-induced up-regulation as evidenced by competitive RT-PCR and indirect immunofluorescence. *Int Immunopharmacol.* 1:1733-42.
- Suzuki S, Miyagi T, Chuang TK, Chuang LF, Doi RH, Chuang RY. 2000. Morphine upregulates mu opioid receptors of human and monkey lymphocytes. *Biochem Biophys Res Commun* 279: 621-8
- Trombella S, Vergura R, Falzarano S, Guerrini R, Calo G, Spisani S. 2005. Nociceptin/orphanin FQ stimulates human monocyte chemotaxis via NOP receptor activation. *Peptides.* 26:1497-502.
- Vandesompele J, De Preter K, Pattyn F, Poppe B, Van Roy N, De Paepe A, Speleman F. 2002. Accurate normalization of real-time quantitative RT-PCR data by geometric averaging of multiple internal control genes. *Genome Biol.* 18;3(7)
- Vidal EL, Patel NA, Wu G, Fiala M, Chang SL. 1998. Interleukin-1 induces the expression of mu opioid receptors in endothelial cells. *Immunopharmacology.* 38:261-6
- Vincent JL, Moreno R, Takala J, Willatts S, De Mendonça A, Bruining H, Reinhart CK, Suter PM, Thijs LG. 1996. The SOFA (Sepsis-related Organ Failure Assessment) score to describe organ dysfunction/failure. On behalf of the Working Group on Sepsis-Related Problems of the European Society of Intensive Care Medicine. *Intensive Care Med.* 22:707-10.

- Waits PS, Purcell WM, Fulford AJ, McLeod JD. 2004. Nociceptin/orphanin FQ modulates human T cell function in vitro. *J Neuroimmunol.* 149:110-20
- Wang J, Barke RA, Charboneau R, Roy S. 2005. Morphine impairs host innate immune response and increases susceptibility to *Streptococcus pneumoniae* lung infection. *J Immunol.* 174:426-34
- Wetzel MA, Steele AD, Eisenstein TK, Adler MW, Henderson EE, Rogers TJ. 2000. Mu-opioid induction of monocyte chemoattractant protein-1, RANTES, and IFN-gamma-inducible protein-10 expression in human peripheral blood mononuclear cells. *J Immunol.* 165:6519-24.
- Wyllie DH, Bowler IC, Peto TE. 2004. Relation between lymphopenia and bacteraemia in UK adults with medical emergencies. *J Clin Pathol.* 57:950-5
- Yeager MP, Colacchio TA, Yu CT, Hildebrandt L, Howell AL, et al. 1995. Morphine inhibits spontaneous and cytokine-enhanced natural killer cell cytotoxicity in volunteers. *Anesthesiology* 83: 500-8
- Yeager MP, Colacchio TA. 1991. Effect of morphine on growth of metastatic colon cancer in vivo. *Arch Surg.* 126:454-6.
- Zhang X, Ding L, Sandford AJ. 2005. Selection of reference genes for gene expression studies in human neutrophils by real-time PCR. *BMC Mol Biol.* 18:4.
- Zhao H, Wu GC, Cao XD. 2002. Immunomodulatory activity of orphanin FQ/nociceptin on traumatic rats. *Acta Pharmacol Sin.* 23:343-8
- Zollner C, Shaqura MA, Bopaiah CP, Mousa S, Stein C, Schafer M. 2003. Painful inflammation-induced increase in mu-opioid receptor binding and G-protein coupling in primary afferent neurons. *Mol Pharmacol* 64: 202-10